REPORT NO.
UCB/EERC-81/18
NOVEMBER 1981

EARTHQUAKE ENGINEERING RESEARCH CENTER

STUDIES ON EVALUATION OF SHAKING TABLE RESPONSE ANALYSIS PROCEDURES

by

J. MARCIAL BLONDET

Report to the National Science Foundation

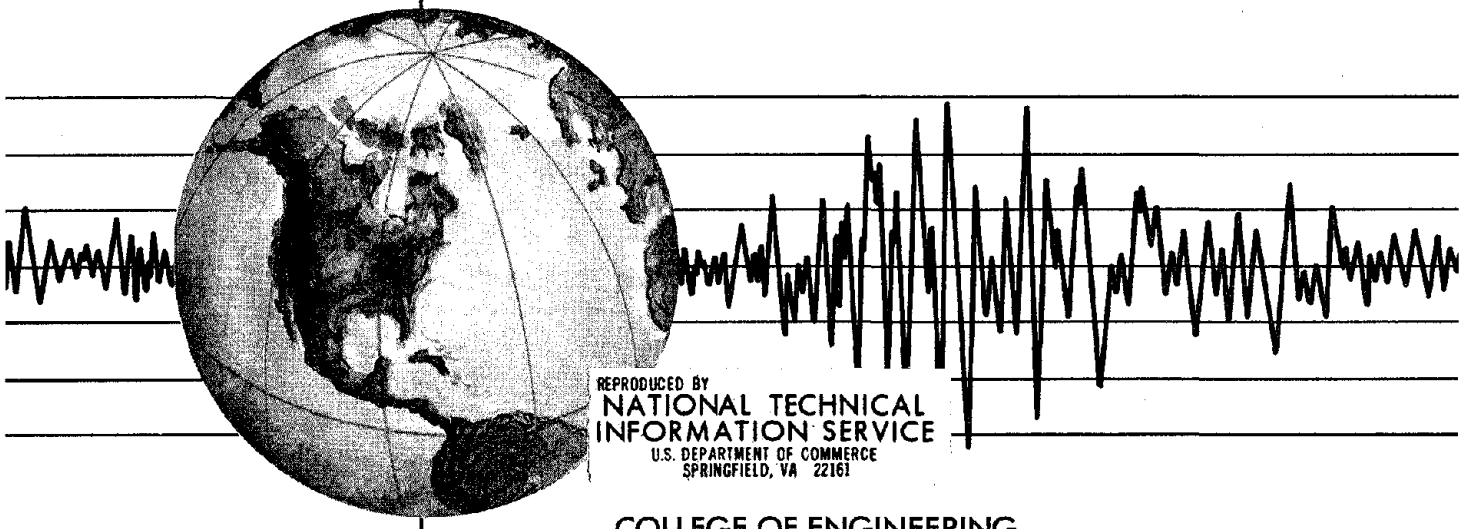

COLLEGE OF ENGINEERING

UNIVERSITY OF CALIFORNIA · Berkeley, California

For sale by the National Technical Information Service, U.S. Department of Commerce, Springfield, Virginia 22161.

See back of report for up to date listing of EERC reports.

50272-101

REPORT DOCUMENTATION PAGE	1. REPORT NO. NSF/CEE-81047	2.	3. Recipient's Accession No. PB82 197278
4. Title and Subtitle: Studies on Evaluation of Shaking Table Response Analysis Procedures			5. Report Date: November 1981 6.
7. Author(s): J. Marcial Blondet			8. Performing Organization Rept. No. UCB/EERC-81/18
9. Performing Organization Name and Address: Earthquake Engineering Research Center, University of California, Berkeley, 47th Street & Hoffman Blvd., Richmond, California 94804			10. Project/Task/Work Unit No. 11. Contract(C) or Grant(G) No. (C) (G) PFR-7908257
12. Sponsoring Organization Name and Address: National Science Foundation, 1800 G Street, N.W., Washington, D.C. 20550			13. Type of Report & Period Covered 14.

15. Supplementary Notes

16. Abstract (Limit: 200 words)

PART A: GLOBAL SEISMIC RESPONSE OF REINFORCED CONCRETE STRUCTURES

The evolution of the response of reinforced concrete frames to seismic ground motions is studied using experimental data from shaking table tests of a reinforced concrete model structure.

The structural response during shaking is analyzed and correlated with the input table motion. The response is characterized by means of the average vibration period and the effective acceleration; the ground motion by its pseudoacceleration response surface. The distribution of the energy supplied to the structure by the shaking table is also described.

PART B: SHAKING TABLE SIGNAL PROCESSING

In this part numerical methods for filtering shaking table and seismic signals are studied.

Two widely used techniques, namely the window method and the Ormsby filter, are examined and combined into a numerical scheme with greater flexibility in the specification of the filter parameters and in the numerical performance.

18. Availability Statement: Release Unlimited	19. Security Class (This Report)	21. No. of Pages: 216
	20. Security Class (This Page)	22. Price

STUDIES ON EVALUATION OF SHAKING TABLE RESPONSE ANALYSIS PROCEDURES

by

J. Marcial Blondet

A Report to the National Science Foundation

Report No. UCB/EERC-81/18

Earthquake Engineering Research Center
University of California
Berkeley, California

November 1981

ABSTRACT

PART A: GLOBAL SEISMIC RESPONSE
OF REINFORCED CONCRETE STRUCTURES

The evolution of the response of reinforced concrete frames to seismic ground motions is studied using experimental data from shaking table tests of a reinforced concrete model structure.

The structural response during shaking is analyzed and correlated with the input table motion. The response is characterized by means of the average vibration period and the effective acceleration; the ground motion by its pseudoacceleration response surface. The distribution of the energy supplied to the structure by the shaking table is also described.

PART B: SHAKING TABLE SIGNAL PROCESSING

In this part numerical methods for filtering shaking table and seismic signals are studied.

Two widely used techniques, namely the window method and the Ormsby filter, are examined and combined into a numerical scheme with greater flexibility in the specification of the filter parameters and in the numerical performance.

ACKNOWLEDGEMENTS

I would like to express my gratitude to the persons and institutions who made this work possible. The research program described in this report was financially sponsored by the National Science Foundation. The continuous support of the NSF to research in Earthquake Engineering using the Earthquake Simulator is gratefully acknowledged. I am grateful to the Catholic University of Peru for granting me a leave of absence to complete my doctoral studies at Berkeley and for their economic support during the first year.

The most rewarding experience during my stay at U. C. Berkeley has undoubtedly been to work for Professor Ray Clough under whose guidance my life has been enriched, both professionally and personally. The valuable suggestions and friendly advice of Professor Stephen Mahin, my academic adviser, is kindly appreciated. I would also like to thank Professor Bruce Bolt for reviewing this report as a member of my Dissertation Committee.

Many thanks are due to Gail Feazell and Gert Weil, from the Graphics Department of EERC, for their outstanding job in preparing the drawings. I am also indebted to Erico Crespo, who generously offered to handwrite the formulas,

which greatly enhance the presentation of this report and to Gianfranco Ottazzi who partially financed the microcomputer system in which this document was written. The Computer Center at UCB provided the indispensable computing and plotting facilities.

I am forever thankful to the Torrano family, who gave me a home during my last weeks at Berkeley. Finally, I would like to thank my wife, Caroline for her love and companionship during the course of this work.

TABLE OF CONTENTS

LIST OF TABLES

LIST OF FIGURES

1) INTRODUCTION

1.1 Preface

The initial purpose of this investigation was to explore the possibilities offered by the data measured during shaking table tests for understanding the seismic response of reinforced concrete structures. The main points of interest were how the structural characteristics changed during shaking, and the relationship of this change to the characteristics of the excitation.

During the research, questions arose regarding the quality of some of the measurements obtained during shaking table tests. These questions led to an investigation in the field of digital signal processing, especially to numerical data filtering procedures. The result of this digression was the development of a computer program to perform the most necessary chores on experimental data manipulation (and, of course, the verification of the quality of the data under question).

This thesis is therefore divided in two parts, treating quite dissimilar topics. Part A is devoted to the study of the global seismic response of a reinforced concrete frame, tested in the U.C.Berkeley Earthquake

Simulator Laboratory. Part B deals with the implementation of numerical techniques for the processing of shaking table data. The only link between the two parts is their raw material: numerical data measured during shaking table earthquake simulation tests, and their fundamental objectives: reliable shaking table experimentation.

1.2 Report Organization

Part A of this report is presented in Chapters Two through Six. Chapter Two exposes the motivation and the goals imposed for for this study. The RCF2 test program is briefly described in Chapter Three, which summarizes the main characteristics of the test specimen, the input table motions and the relevant experimental results. Chapter Four deals with a study of the variation of the fundamental vibration frequency of the test frame during shaking, and the utilization of these results to estimate the evolution of the lateral stiffness and displacement ductility. These results are then correlated in chapter Five with the characteristics of the table input motions by extending the concept of pseudoacceleration response spectrum, to include the effect of time. Finally, concluding remarks are made in Chapter Six; indicating the need for further research in the areas involved in this study.

Part B is developed in Chapters Seven to Ten. Chapter Seven introduces the need for filtering procedures in shaking table data processing. Some basic concepts of numerical filtering are described in Chapter Eight, concluding with the presentation of a combined method for digital filtering, implemented in a general purpose computer program developed for the processing of shaking table and seismic data. This computer program is briefly described in chapter Nine, where some application examples are also shown. Finally, chapter Ten concludes part B by pointing out the benefits and dangers of filtering experimental and seismic data.

The user manual for the program described in part B is given in the Appendix.

PART A

GLOBAL SEISMIC RESPONSE

OF REINFORCED CONCRETE STRUCTURES

2) MOTIVATION: DESCRIPTION OF SEISMIC INPUT AND STRUCTURAL RESPONSE

The study of the seismic response of reinforced concrete structures constitutes a great challenge: very complex mechanisms, most of them not fully understood, are involved. Shaking table tests provide a convenient way to undertake this study, since they can be designed as realistic simulations of seismic events during which the significant or interesting features of the behavior can be monitored and measured.

A very large amount of data has been obtained at the University of California at Berkeley, through an experimental program which involved the shaking table testing of five reinforced concrete frame models and the information collected from such tests proved to be very valuable for the interpretation of the response behavior of the test specimens.

The motivation for this study arose while performing an evaluation of the second reinforced concrete frame (RCF2) test program with the purpose to determine whether or not the experiments adequately simulated a typical, well built, reinforced concrete building subjected to strong seismic ground shaking [1].

During the course of the evaluation described above, the experimental data was reduced and presented in the "standard" way: the table input motions were characterized via their elastic response spectra and the time-histories of acceleration. The response of the structure was described by plotting selected forces and their corresponding deformation quantities as time-histories, and also these quantities were plotted against each other. Even though the most relevant characteristics of the the input and the response were apparent in these graphs, some important features of the seismic experience were not clearly portrayed. For example, the variation of the mechanical properties of the test specimen as damage spread and intensified during shaking, and the correlation of this evolving response with the seismic input were not explicit in the mentioned representations of the measured data.

The goal of this investigation was to explore different ways to process and display the experimental data gathered during the RCF2 test program, in order to gain insight into the complex interrelation between the seismic excitation and the unfolding of the response it causes on the structure. This report describes some attempts made towards this goal, their practical implications, and their significance as a basis for further research.

3) RCF2 EXPERIMENTAL PROGRAM

3.1 Preliminary Remarks

This chapter briefly describes the RCF2 test program: the main characteristics of the test structure and the input shaking table motions, and the most relevant features of the structural response, from a global point of view. The information presented here has been entirely obtained from References 1 and 2.

3.2 Test Structure

The design of RCF2 was conceived to simulate a typical reinforced concrete framed structure, having a predominantly flexural, ductile mode of behavior [3]. The test specimen was derived from the prototype two story office building shown in Fig. 3.1, by means of a scale reduction, followed by a number of modifications imposed by the shaking table capabilities, for economic reasons and for testing convenience. The major modifications on the scaled model were a reduction in the distance between longitudinal frames and the inclusion of concrete blocks to simulate the inertia of the deleted portions. A previous study [1] has shown that the global structural properties of the prototype were adequately simulated.

Figure 3.2 shows the test specimen, RCF2, and the shaking table arrangement. A detailed list of the instrumentation used is given in Reference 2. The reinforcement detailing is shown in Fig. 3.3; it complies with the requirements imposed by the UBC 1979 Code [4] for ductile moment-resisting space frames to be built in the most seismically active regions of the USA.

3.3 Testing Program

The objective of the RCF2 testing program was to study the response of an initially undamaged structure under strong seismic shaking. Based on experience gained with a previous frame model, RCF2 was tested with a sequence of three shaking table inputs (runs); it was then repaired with epoxy injection and the testing sequence was repeated. Finally a "destructive" static test was performed.

The basic dynamic input signal used throughout the experimental program was the N69W component of the ground acceleration recorded at Taft in 1952. The intensity of the shaking was controlled by scaling the amplitude of the original record; the time scale remained unchanged. As a consequence, the table motions simulated ground shakings which could have been induced under different conditions (distance to source and local geology and site characteristics) than those at Taft during the 1952 eartquake [1].

Table 3.1 summarizes the testing program. To assess the accuracy of the seismic ground motion simulation, the acceleration records for the specified Taft earthquake and the recorded shaking table motions for the first (unrepaired) testing sequence are shown in Fig. 3.4 a) through d). Figure 3.5 presents the pseudoacceleration response spectra for the Taft signal and selected table motions.

In addition to the shaking table tests, the lateral flexibility and vibration properties of the frame were measured before and after each test; these data are shown in Table 3.2.

3.4 Test Results

A summary describing the overall performance of RCF2 during the first testing sequence follows. The results presented here are based on observations made during the experimental phase and on the measured data, processed using "standard" methods.

3.4.1 Run W1

This mild shaking was performed with the aim of inducing in the virgin test structure a degree and distribution of cracking representative of normal service conditions. Before the test, some cracks had appeared

after the concrete blocks were added to the frame.

As expected, after the test the structure showed minor cracking (especially in the bottom story members) distributed in patterns characteristic of lateral loading. The effect of cracking was apparent in the approximately 18% reduction in the fundamental vibration frequency. This significant change is a clear indication of the loss of stiffness suffered by the structure in its transition from the uncracked to the cracked condition. The low strain amplitudes monitored at critical reinforcement locations indicate that the structure remained within expected service conditions throughout the test.

The response during shaking can be evaluated by studying plots of the horizontal floor displacements, relative to the table (Fig. 3.6) and the interstory shear-drift relationship developed by the structure (Figs. 3.7 and 3.8). The most relevant features shown in these figures are:

1) The motion of each floor can be described as a sinusoid with slowly varying amplitude and phase; this is characteristic of resonant systems subjected to excitations with a wide-band frequency spectrum.

2)Both stories oscillated in phase around the static equilibrium configuration, following similar displacement patterns. The response was thus primarily in the first vibration mode.

3)The frequency of the oscillations remained fairly stable throughout most of the shaking, which implies that most of the cracking occurred early in the test, and that afterwards the stiffness of the specimen remained basically constant. This effect can also be observed in Figs. 3.7 and 3.8.

4)The decaying nature of the oscillations after the shaking table motion ceased (at about 20.5 seconds) is characteristic of elastic, slightly damped systems.

5)The force-deformation relationship, although essentially linear, shows a mild hysteretic component due probably to the opening and closing of the concrete cracks during the oscillations. This effect was more important in the bottom story, where most of the cracking occurred.

In summary, during run W1 RCF2 responded in a global sense as a single degree of freedom elastic and underdamped system. The table shaking caused some cracking, especially on the first story members, but the structure was essentially undamaged after the test.

3.4.2 Run W2

In this case, the purpose of the test was to study the effect of a violent earthquake-induced ground shaking on a structure without significant previous seismic history. The shaking table input consisted of an amplified version of the Taft signal, with the aim of inducing in the structure a significant amount of damage.

The effect of the shaking on the structure was evident after the test was completed: many significant flexure cracks appeared at the end zones of the bottom story columns and longitudinal girders, and minor cracks could be seen at the base of the top columns and along the top zone of the first story slab.

The reduction of the fundamental vibration frequency in this case was about 35%. In addition, the steel reinforcement yielded near the end zones of the bottom story columns. It is evident that the structure suffered a noticeable degradation in its lateral stiffness and probably went through several cycles of inelastic deformation.

The relative floor displacement time-histories are shown in Fig. 3.9 and the bottom and top story lateral force-deformation relationship in Figs. 3.10 and 3.11. These figures show a very different type of response than

that observed during run W1. The most important characteristics of the response are:

1)As in run W1, both floors oscillated in phase. The test structure therefore behaved again, from a global point of view, as a single degree of freedom systemd.

2)The floors, however, did not oscillate with respect to a fixed equilibrium configuration. The center of the oscillations seemed to move quite erratically during the first half of the test. During the last part of the shaking, the structure oscillated with respect to a configuration which corresponded to a permanent lateral deformation of the first story. This indicates that significant nonlinear behavior occurred, particularly in the bottom story columns.

3)The frequency of the oscillations towards the end of the test was noticeably lower than at the beginning. Figure 3.9 is not, however, sufficient to determine how the frequency changes were produced during the test.

4)The extreme complexity of the response of reinforced concrete structures under severe seismic excitation is revealed in Figs. 3.10 and 3.11. The force-deformation curves follow intricate paths, showing the interaction of effects such as the yielding of the reinforcing steel,

severe concrete cracking, steel-concrete bond deterioration, anchorage zone slippage,etc.

Unfortunately, these plots conceal the evolutive nature of the response, since these effects did not take place simultaneously. An effective aproach to deal with this problem is to examine the response during succesive short duration intervals. Figures 3.12 and 3.13 a) through f) present the interstory shear-drift relationship developed by the bottom and top stories within succesive 5 second intervals. These plots provide the following information.

5)The structure suffered a considerable loss of lateral stiffness during the first ten seconds of shaking, caused by the occurrence of a few cycles of large inelastic deformation.

6)Afterwards, the force-deformation relationship became more regular (quasilinear) but with a "pinched" shape, as a result of phenomena like bond deterioration, and the opening and closing of the cracks in the concrete.

To summarize, this test caused an appreciable amount of structural damage in RCF2 which was manifested in the significant nonlinearities in the response. Most of the damage was confined to the bottom story members, in a

"soft-story" type of mechanism. As in run W1, the structure responded basically as a single degree of freedom system.

3.4.3 Run W3

In this case, a severe aftershock was simulated by exposing the already damaged test structure to a table input similar to that of run W2.

After the test was completed, it was possible to observe that the cracking patterns from run W2 were extended. In some regions, the influence of shear could now be noticed from the inclination of the cracks. In addition, some spalling and crushing of the concrete occurred near the base of the bottom story columns. The further reduction of the fundamental frequency was only about 7%, which indicated that in this case the stiffness degradation was not so dramatic.

The data acquired during the test is presented in the same form as for run W2. Figure 3.14 shows relative lateral displacement time-histories for both floors; the interstory shear-drift relationships are plotted in Figs. 3.15 (bottom) and 3.16 (top), for the whole test, and in succesive 5 second intervals in Figs. 3.17 and 3.18 a) through f).

In general, the response of RCF2 during run W3 had similar characteristics to that of the previous test. The structure behaved basically as a single degree of freedom system, suffered several cycles of significant inelastic deformation at the beginning of the test (again, mainly in the bottom story) followed by a more regular response. No permanent displacement of the first story was produced.

The force-deformation curves show a more pronounced "pinching" effect, indicating an increasing importance of shear deformation, bond deterioration and cracking on the response.

It is also worth emphasizing that the lateral stiffness degradation phenomenon was less important in this case, due probably to the circumstance that the test specimen was already damaged before the test, having in consequence less stiffness to lose.

3.5 Observations and Conclusions

This investigation was prompted basically from the following observations, made while processing the experimental results:

1) The occurrence of damage to the structure due to the simulated seismic ground shaking was not a uniform,

continuous process; on the contrary, it was an evolving phenomenon by which the system varied the nature of its response, to adapt its physical characteristics to a changing and extremely demanding environment.

2) The occurrence of structural damage is manifested in the structure as a combination of several nonlinear effects such as the development of a hysteretic, pinched force-deformation relationship and a noticeable stiffness degradation. Its overall effect on the response, however, appears to be characterized by a reduction of the natural vibration frequency (or, conversely, an increase of the vibration period).

3) It was possible to assign an average lateral stiffness to the test structure during any relatively short time interval, even in the cases when appreciable nonlinear behavior was present. This observation suggests that the system oscillated basically in a certain dominant frequency, which changed as the lateral stiffness changed.

4) The structure behaved globally as a single degree of freedom system, as demonstrated in the lateral floor displacement time-histories. Its displacement response can therefore be characterized by a single displacement component, and its vibration properties by the fundamental vibration period.

5)Most of the response nonlinearities, and thus the structural damage, occurred in the bottom story members.

In view of the preceding observations, it seemed reasonable, and feasible, to attempt to study the evolution of the response during shaking, by examining the variation of the predominant frequency (or period) on the bottom story displacement response. This study is described in the following chapter.

TEST STRUCTURE CONDITION	RUN NO.	SHAKING TABLE SPAN SETTING	PEAK ACCELERATION (g's.)	RUN IDENTIFICATION
WITH CONCRETE BLOCKS AND LATERAL BRACING	1	100	0.097	W1
	2	850	0.57	W2
	3	850	0.65	W3
REPAIRED, WITH CONCRETE BLOCKS AND LATERAL BRACING	4	50	0.07	R1
	5	850	0.78	R2
	6	850	0.82	R3

TABLE 3.1 EARTHQUAKE SIMULATOR TEST PROGRAM

TEST NO.	LAST RUN BEFORE TEST	NATURAL FREQUENCY (HZ.) FIRST MODE	NATURAL FREQUENCY (HZ.) SECOND MODE	DAMPING FACTOR (%CRIT.) FIRST MODE	DAMPING FACTOR (%CRIT.) SECOND MODE	LATERAL FLEXIBILITY MATRIX COEFFICIENTS (IN/KIP.) F BB	F BT	F TT
1	NONE *	6.58	20.58	1.55	2.09	.0138	.0161	.0305
2	NONE	3.80	9.80	1.28	1.59	.0148	.0167	.0393
3	W1	3.13	8.70	4.20	1.93	.0229	.0260	.0485
4	W2	2.03	6.50	5.77	2.99	.0563	.0678	.1235
5	W3	1.88	6.14	6.56	3.46	.0673	.0819	.1431
6	NONE	2.58	7.22	2.67	2.00	.0316	.0410	.0870
7	R1	2.31	6.45	3.52	2.00	.0394	.0455	.0960
8	R2	1.49	5.77	5.40	2.78	.0940	.1260	.2590
9	R3	1.28	4.38	7.10	3.10	.1528	.2090	.3830

TABLE 3.2 VARIATION OF NATURAL FREQUENCY, DAMPING FACTOR AND LATERAL FLEXIBILITY COEFFICIENTS BETWEEN TESTS

* No concrete blocks on structure.

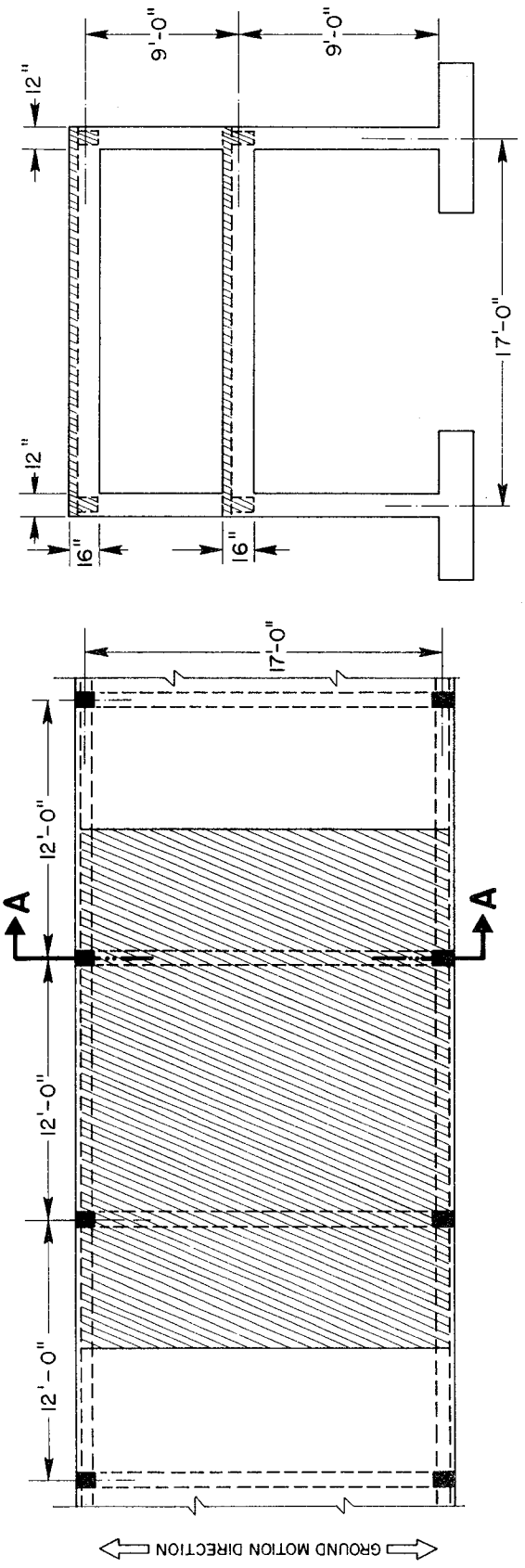

Fig. 3.1 PROTOTYPE STRUCTURE DIMENSIONS.

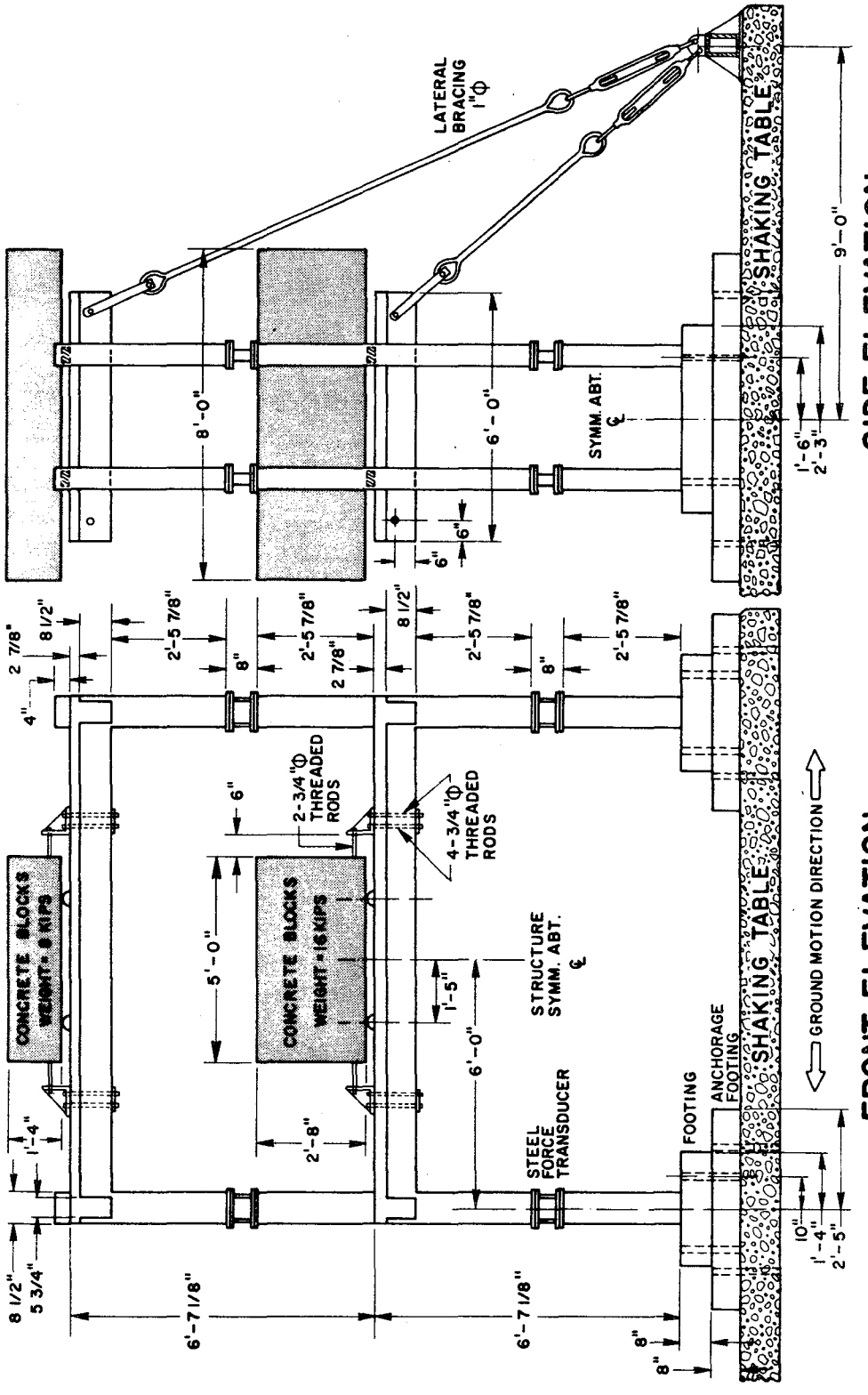

Fig. 3.2 TEST STRUCTURE AND SHAKING TABLE ARRANGEMENT.

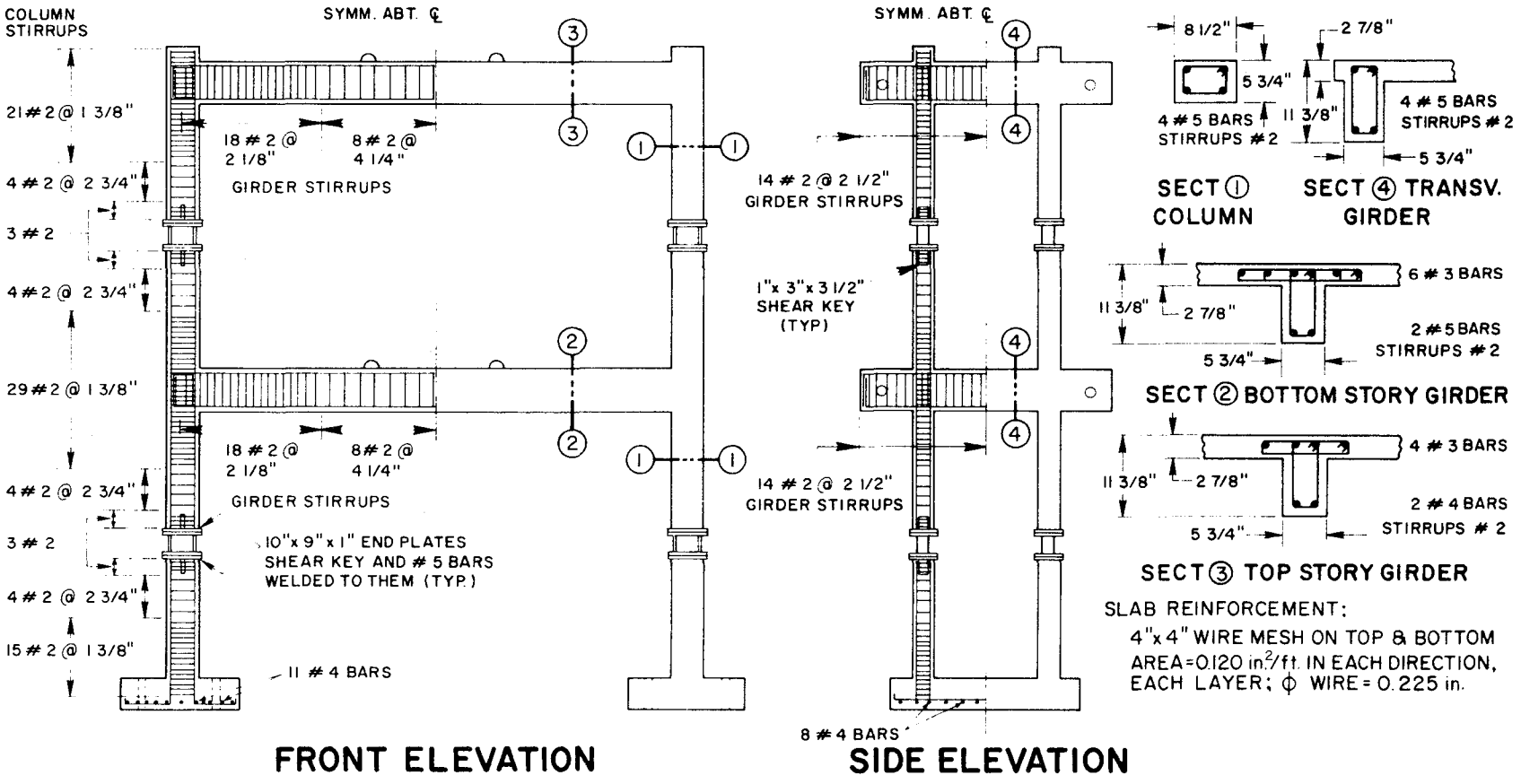

Fig. 3.3 TEST STRUCTURE - DETAILS OF REINFORCEMENT.

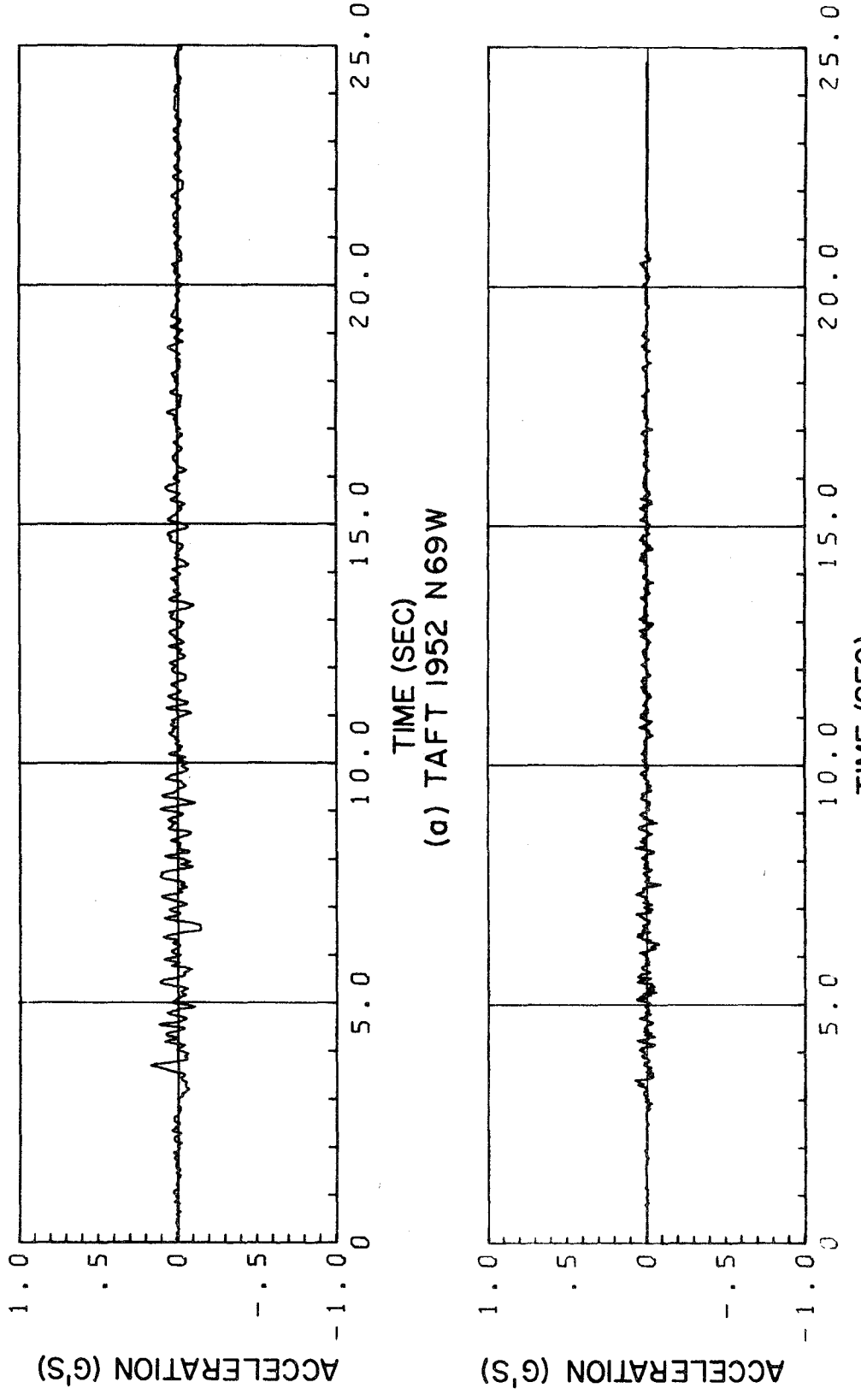

Fig. 3.4 TAFT 1952, N69W ACCELERDGRAM AND TABLE ACCELERATION RECORDS.

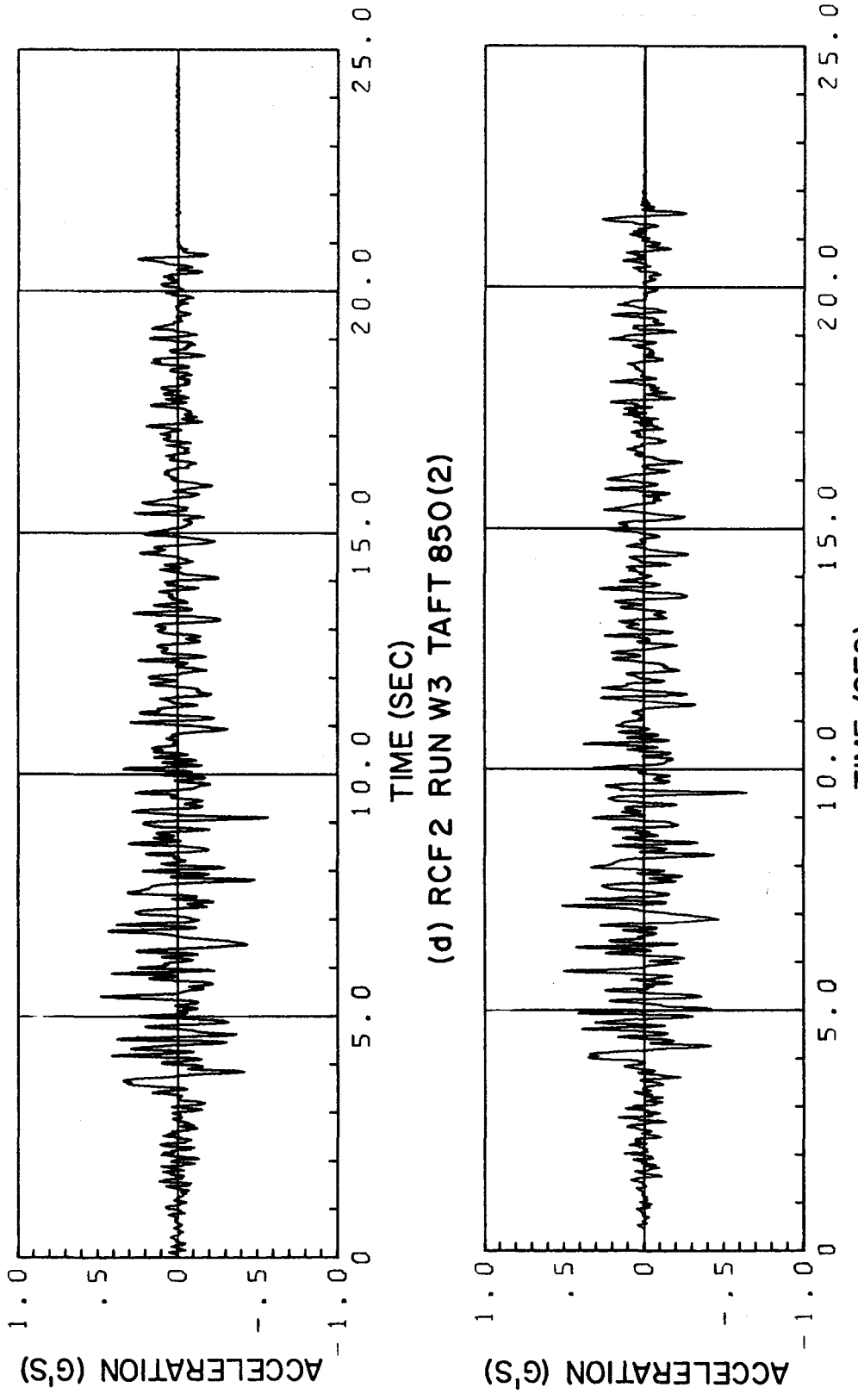

Fig. 3.4 TAFT 1952, N69W ACCELEROGRAM AND TABLE ACCELERATION RECORDS.

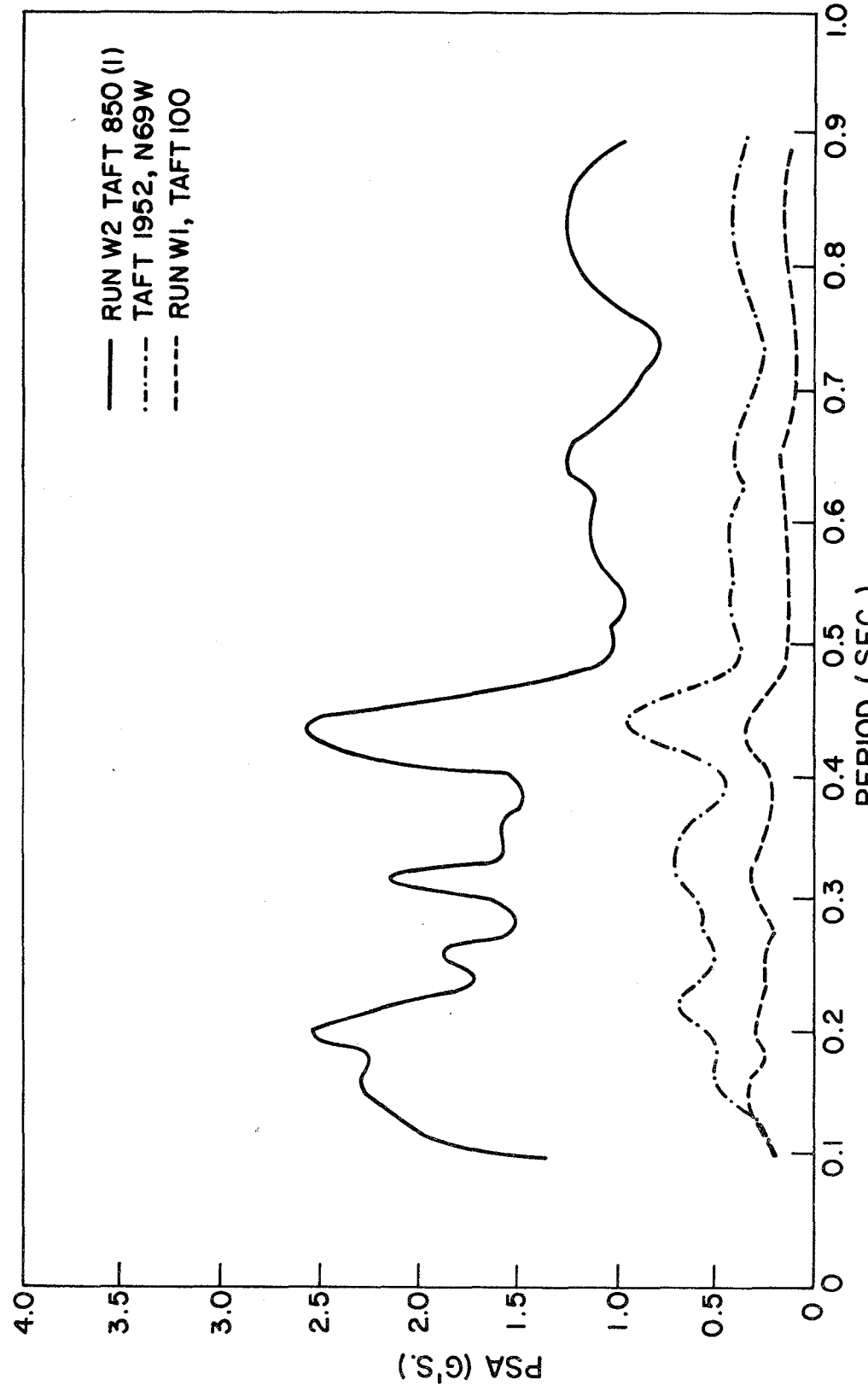

Fig. 3.5 PSEUDOACCELERATION RESPONSE SPECTRA OF TAFT SIGNAL AND RUNS W1 AND W2 (DAMPING: 2% CRIT.)

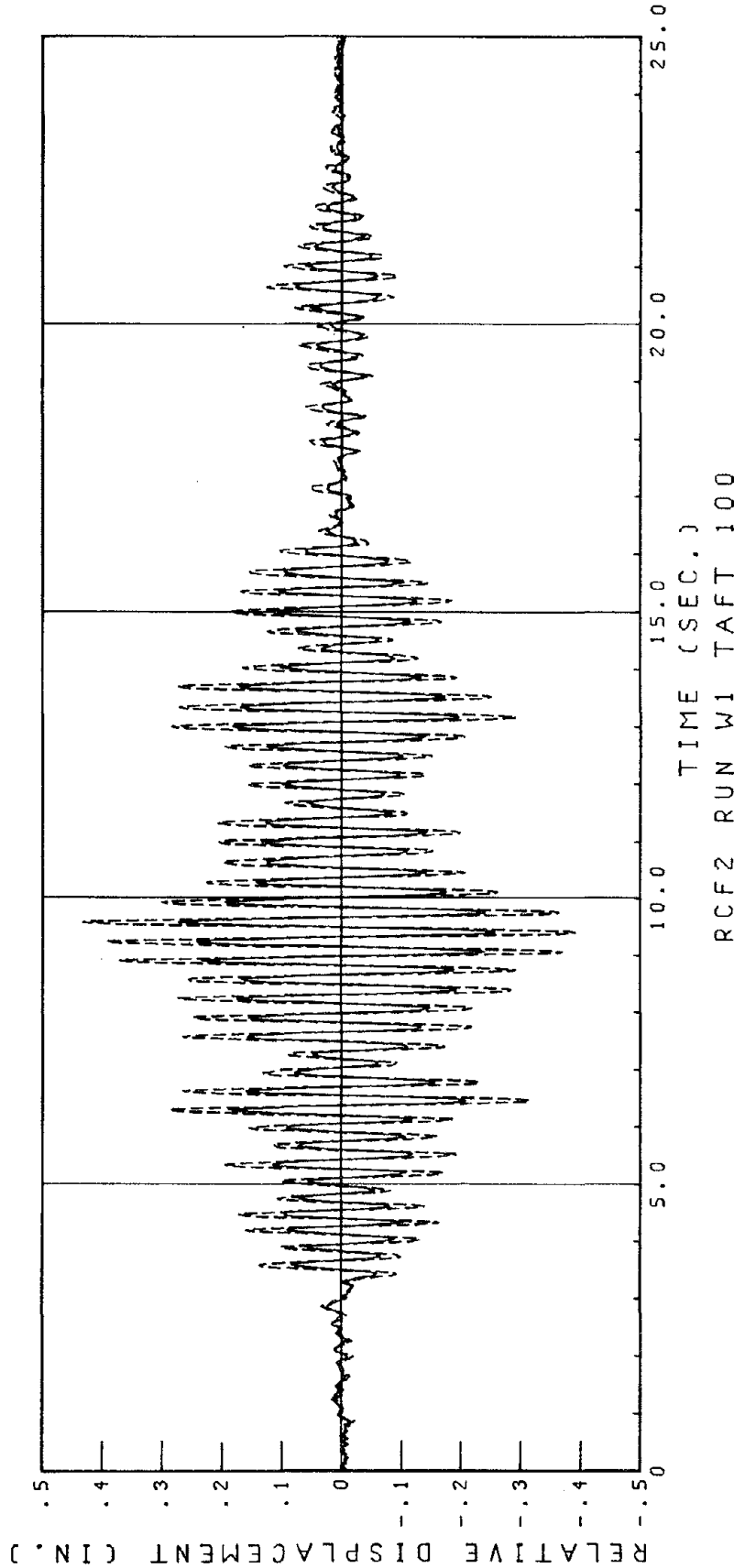

Fig. 3.6 DISPLACEMENT RESPONSE OF RCF2 DURING RUN W1.
SOLID LINE: FIRST FLOOR; DASHED LINE: SECOND FLOOR.
(RELATIVE TO TABLE)

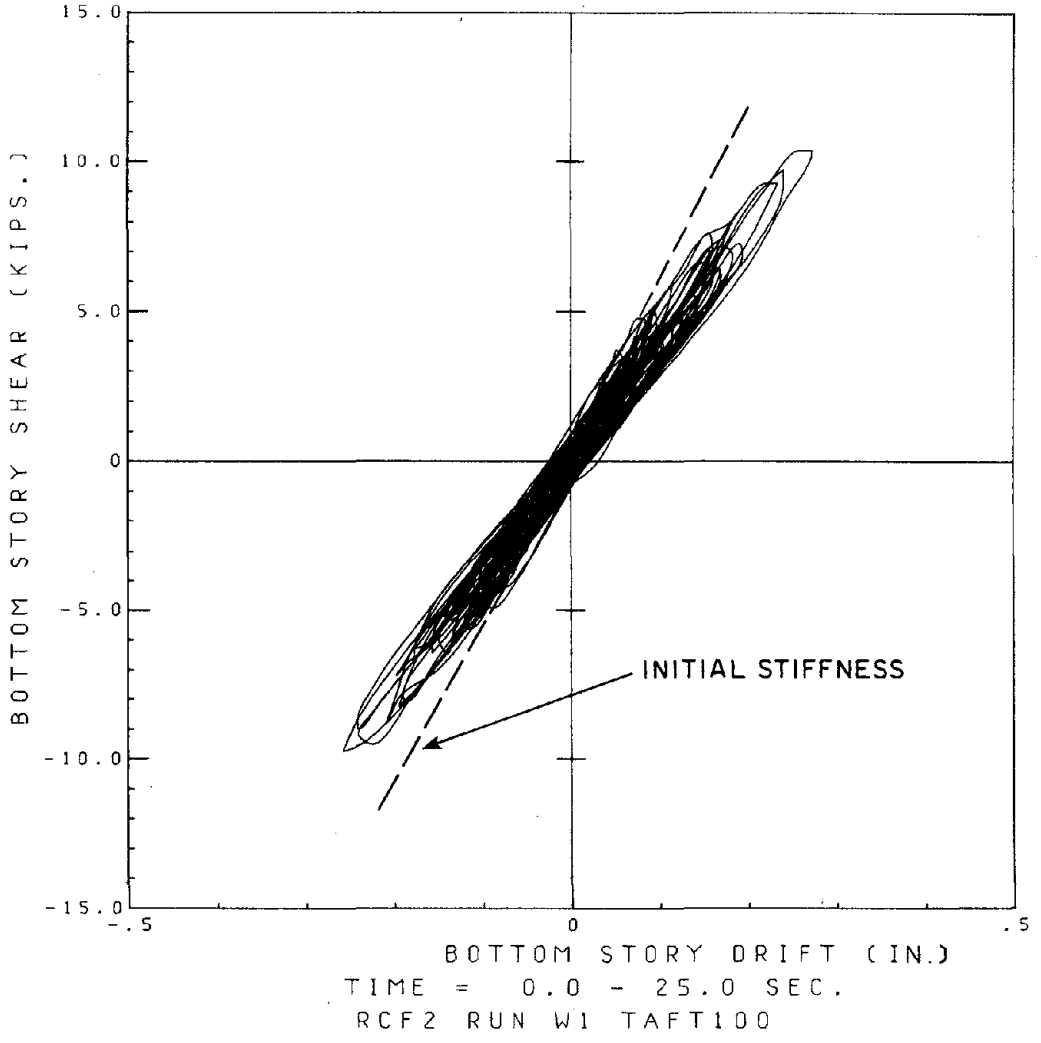

Fig. 3.7 BOTTOM STORY SHEAR - DRIFT RELATIONSHIP. RUN W1.

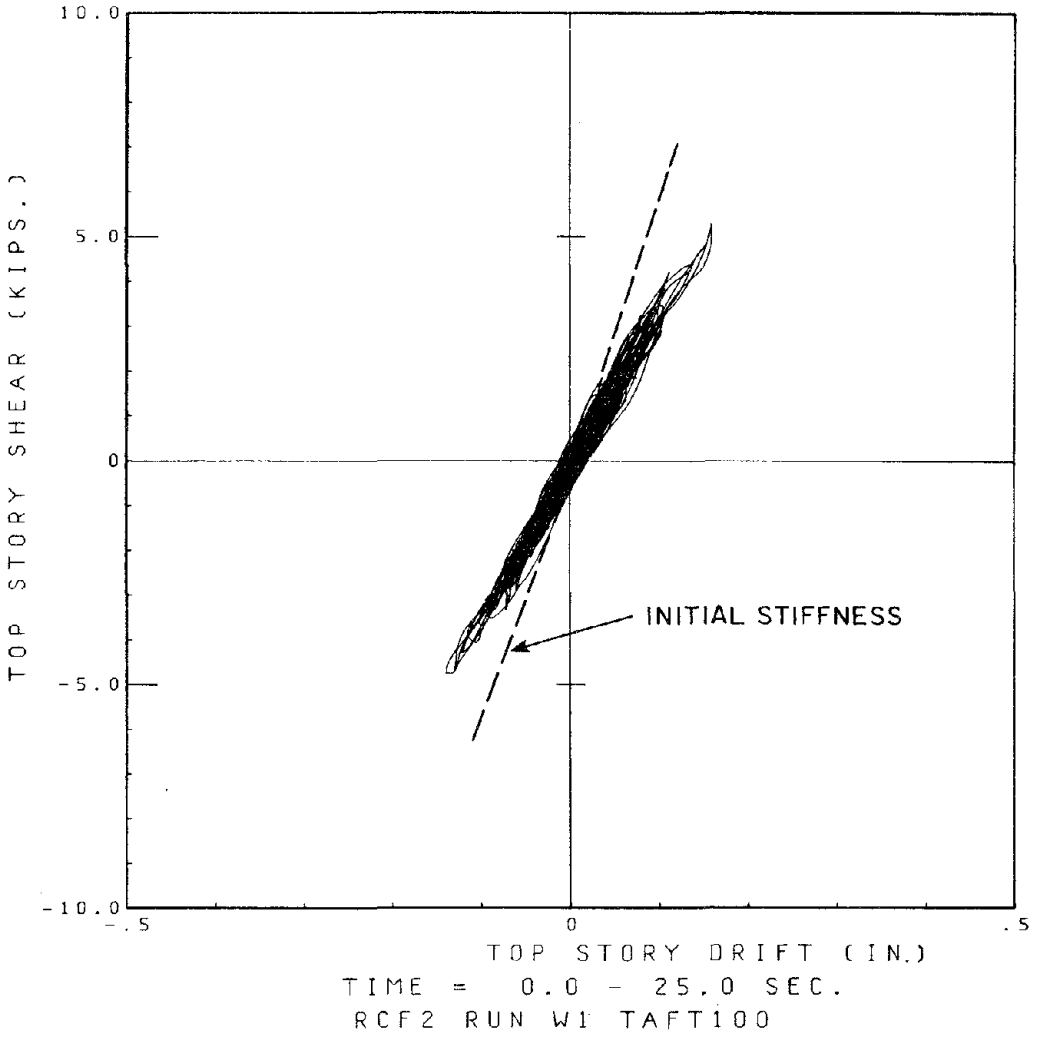

Fig. 3.8 TOP STORY SHEAR - DRIFT RELATIONSHIP. RUN W1.

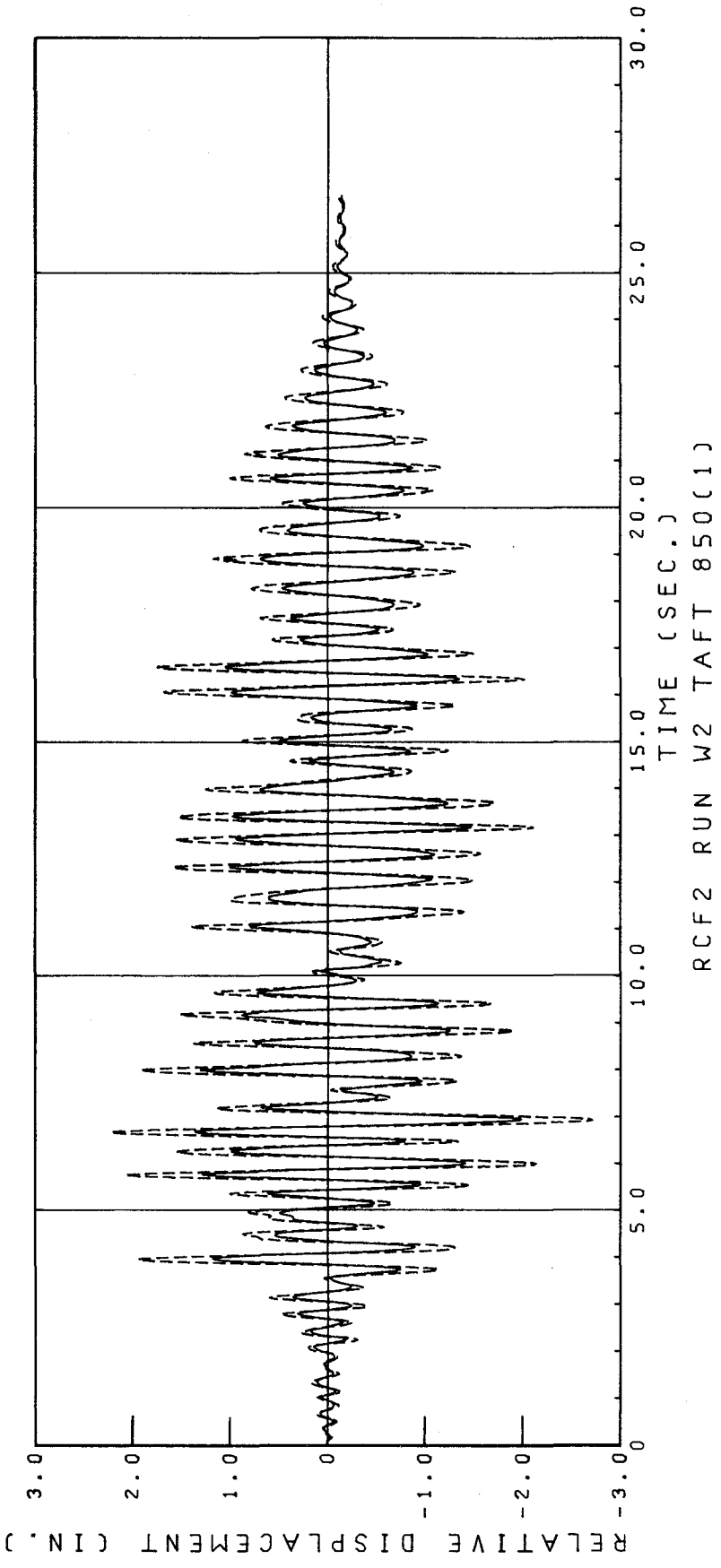

Fig. 3.9 DISPLACEMENT RESPONSE DURING RUN W2.
SOLID LINE:FIRST FLOOR; DASHED LINE: SECOND FLOOR.
(RELATIVE TO TABLE)

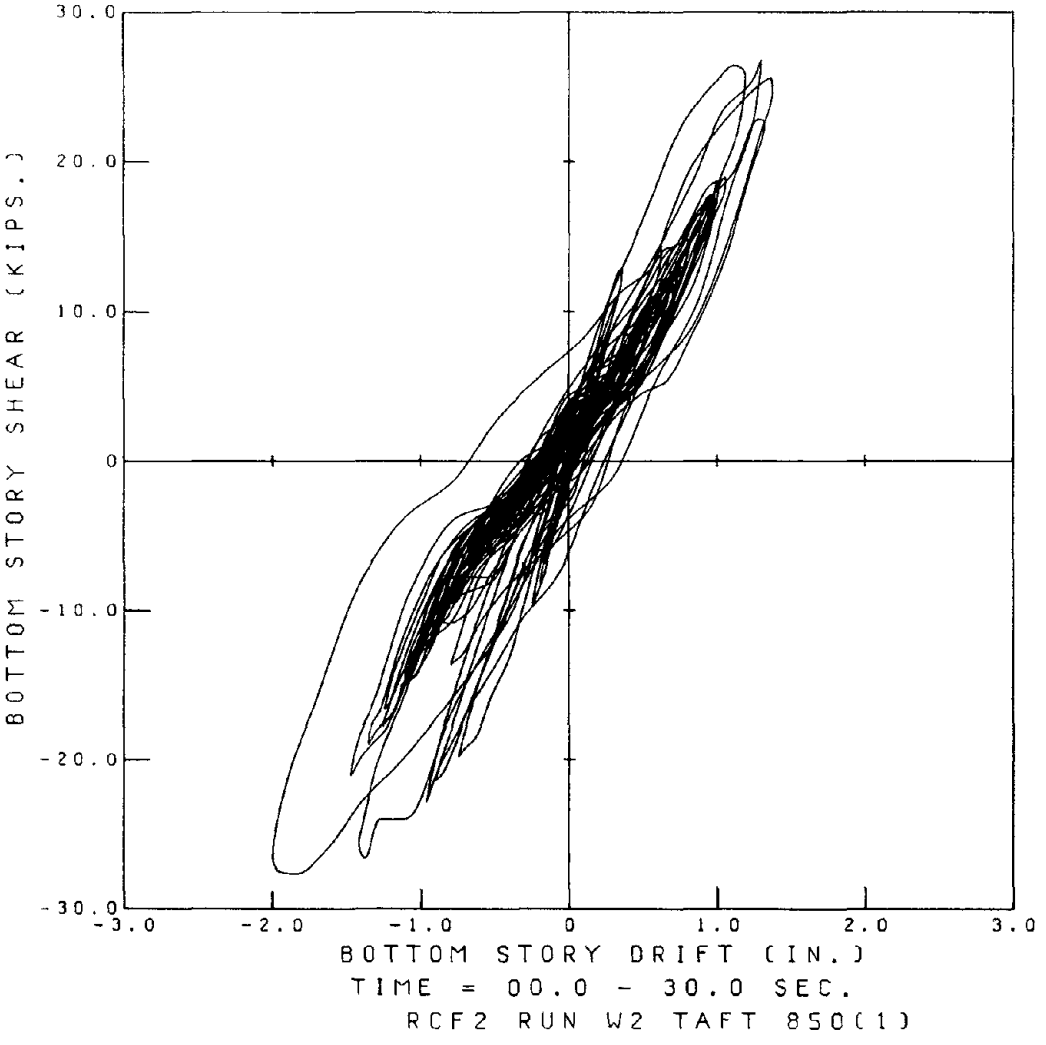

Fig. 3.10 BOTTOM STORY SHEAR - DRIFT RELATIONSHIP. RUN W2.

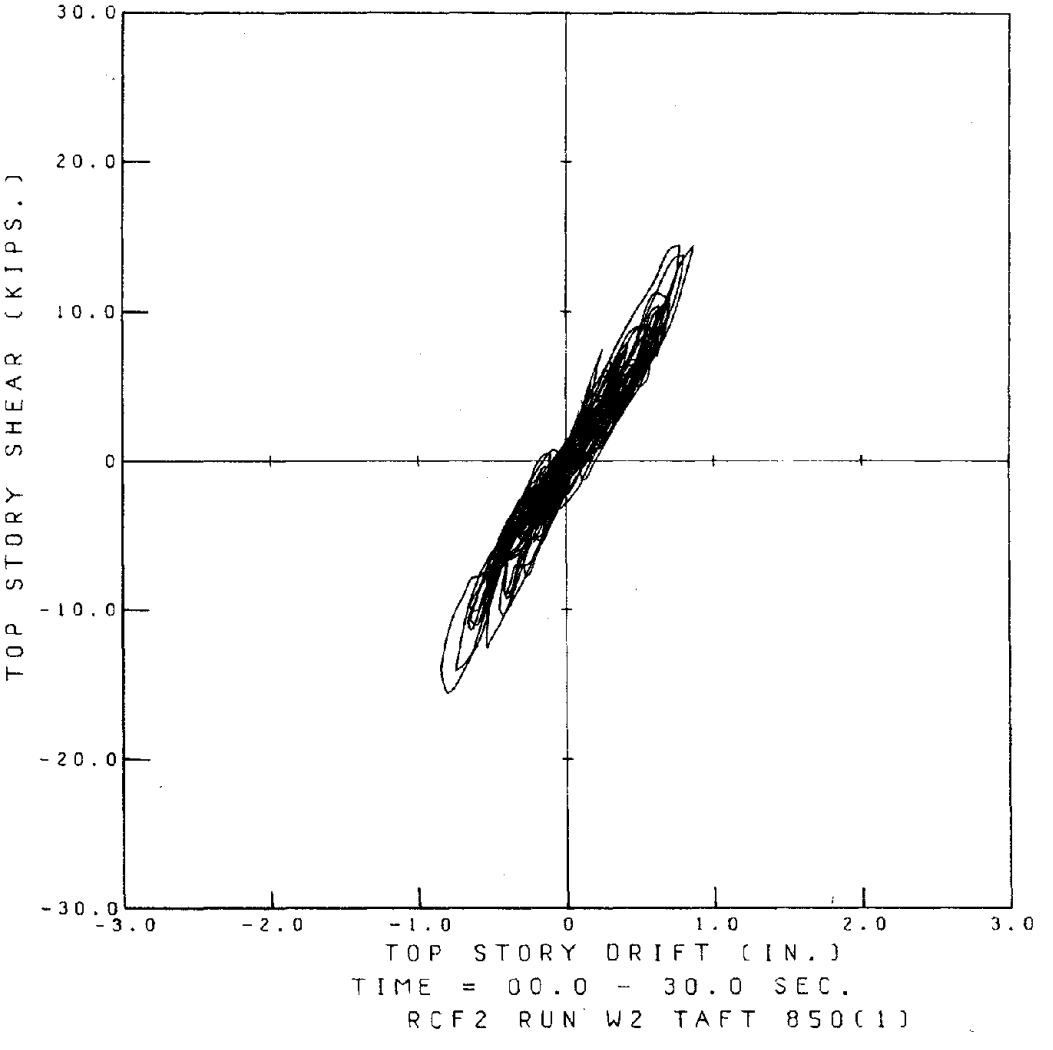

Fig.3.11 TOP STORY SHEAR - DRIFT RELATIONSHIP. RUN W2.

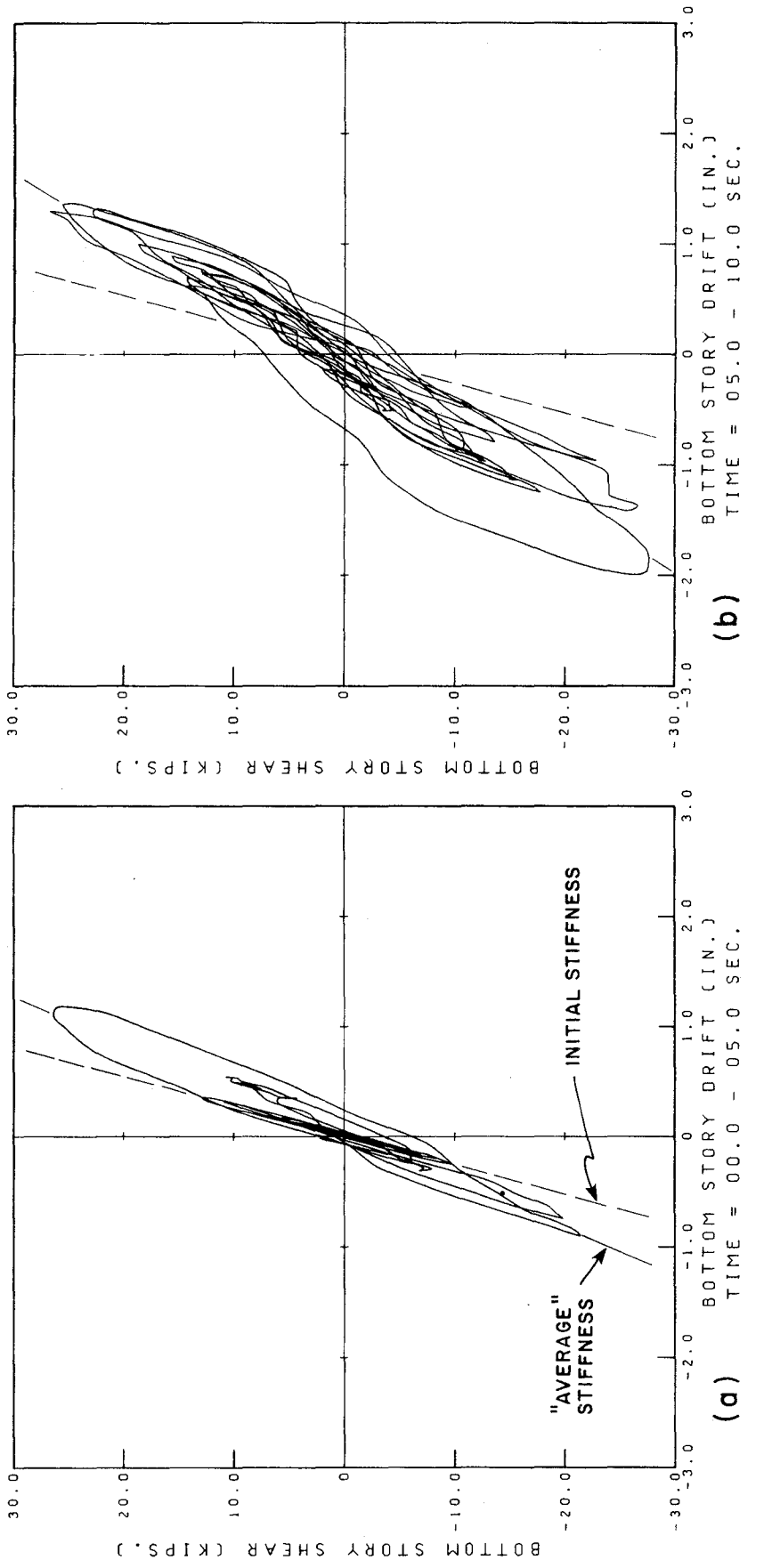

Fig. 3.12 BOTTOM STORY SHEAR - DRIFT RELATIONSHIP DURING 5 SEC. INTERVALS. RUN W2.

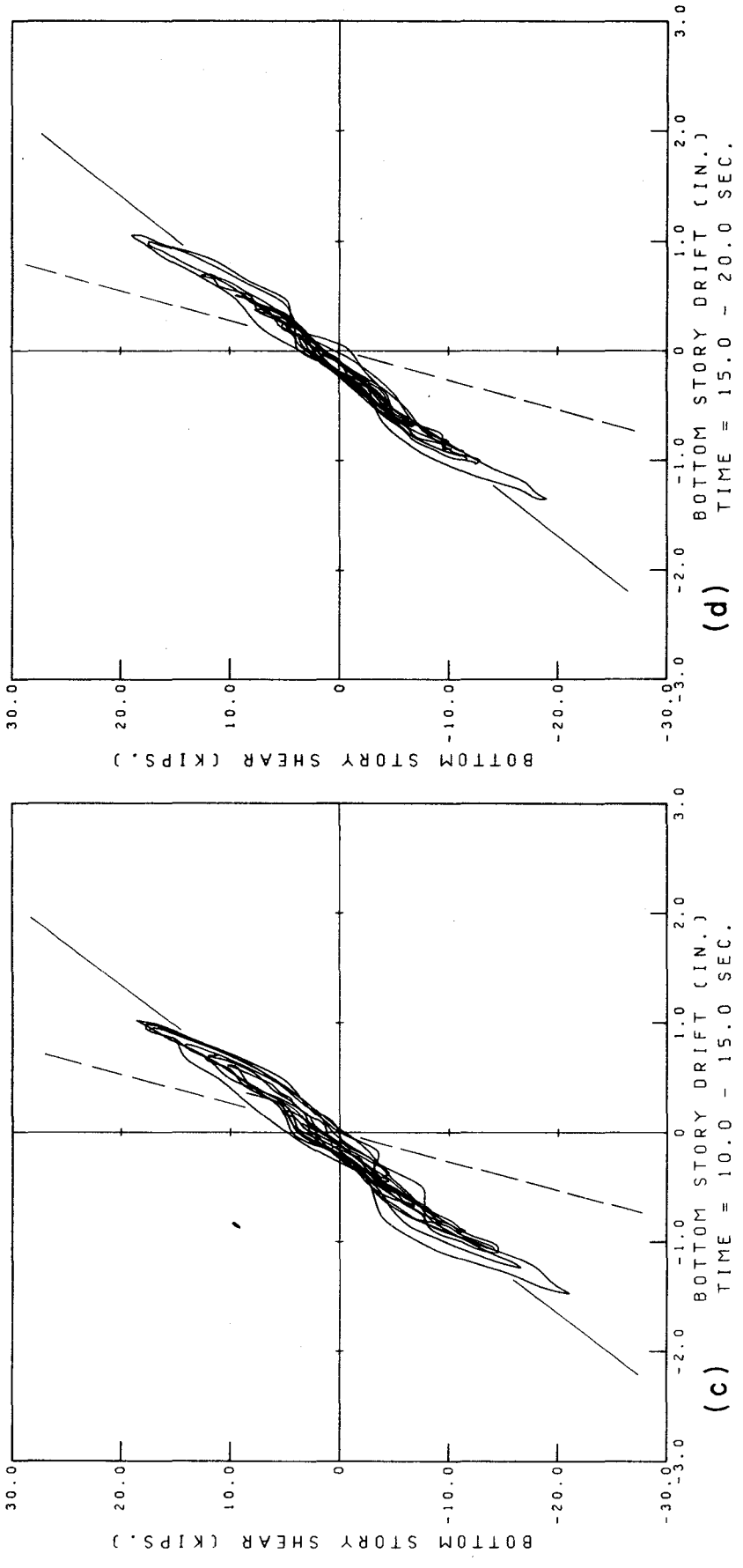
BOTTOM STORY SHEAR (KIPS.)
30.0
20.0
10.0
0
-10.0
-20.0
-30.0
-3.0
-2.0
-1.0
0
1.0
2.0
3.0
BOTTOM STORY DRIFT (IN.)
(c)
TIME = 10.0 - 15.0 SEC.
(d)
TIME = 15.0 - 20.0 SEC.
RCF2 RUN W2 TAFT 850(1)

Fig. 3.12 (CONT.)

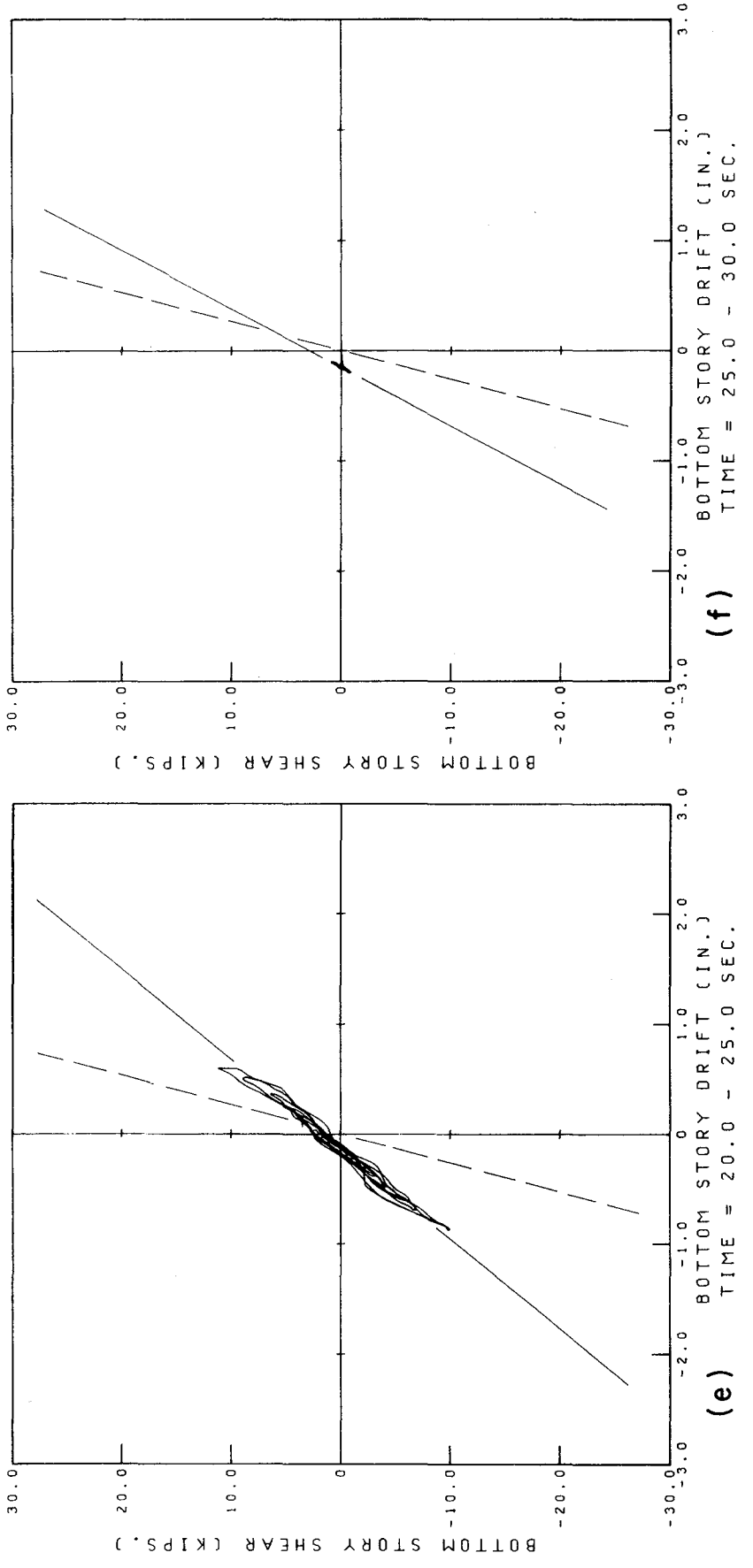

RCF2 RUN W2 TAFT 850(1)

Fig. 3.12 (CONT.)

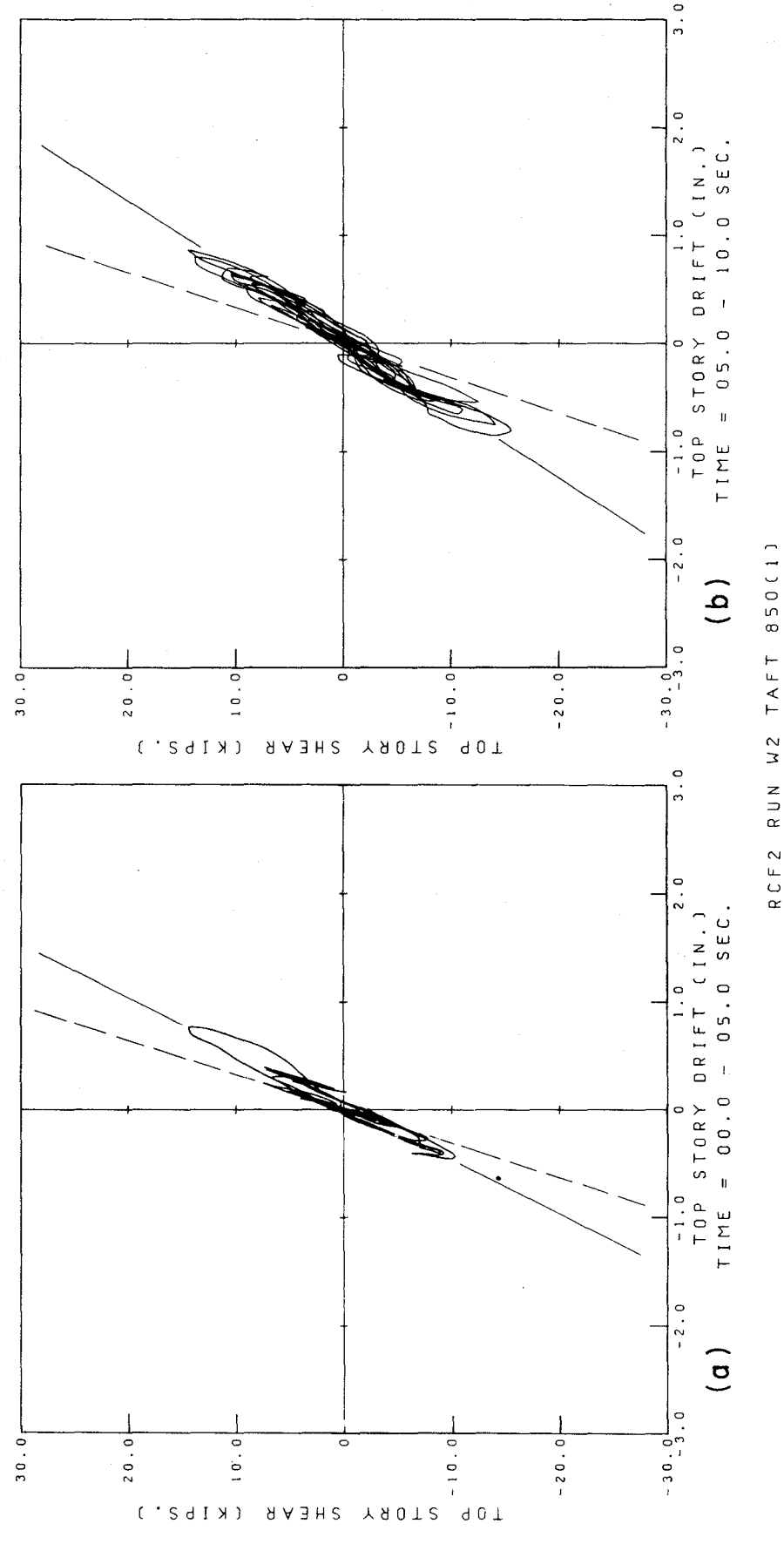

Fig. 3.13 TOP STORY SHEAR - DRIFT RELATIONSHIP DURING 5 SEC. INTERVALS. RUN W2

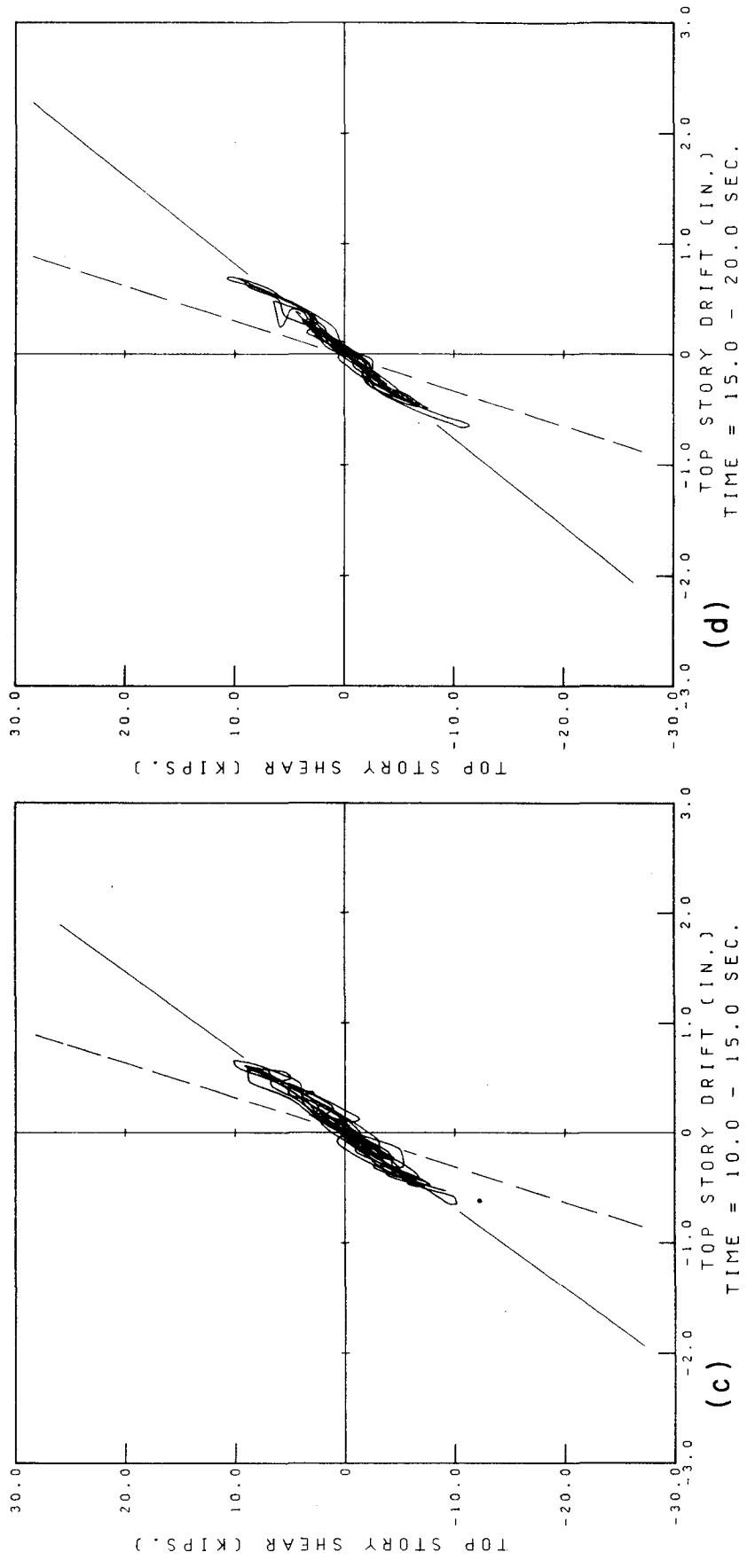
TOP STORY SHEAR (KIPS.)
30.0
20.0
10.0
0
-10.0
-20.0
-30.0
-3.0
-2.0
-1.0
0
1.0
2.0
3.0
TOP STORY DRIFT (IN.)
(c)
TIME = 10.0 - 15.0 SEC.
(d)
TIME = 15.0 - 20.0 SEC.
RCF2 RUN W2 TAFT 850(1)

Fig. 3.13 (CONT.)

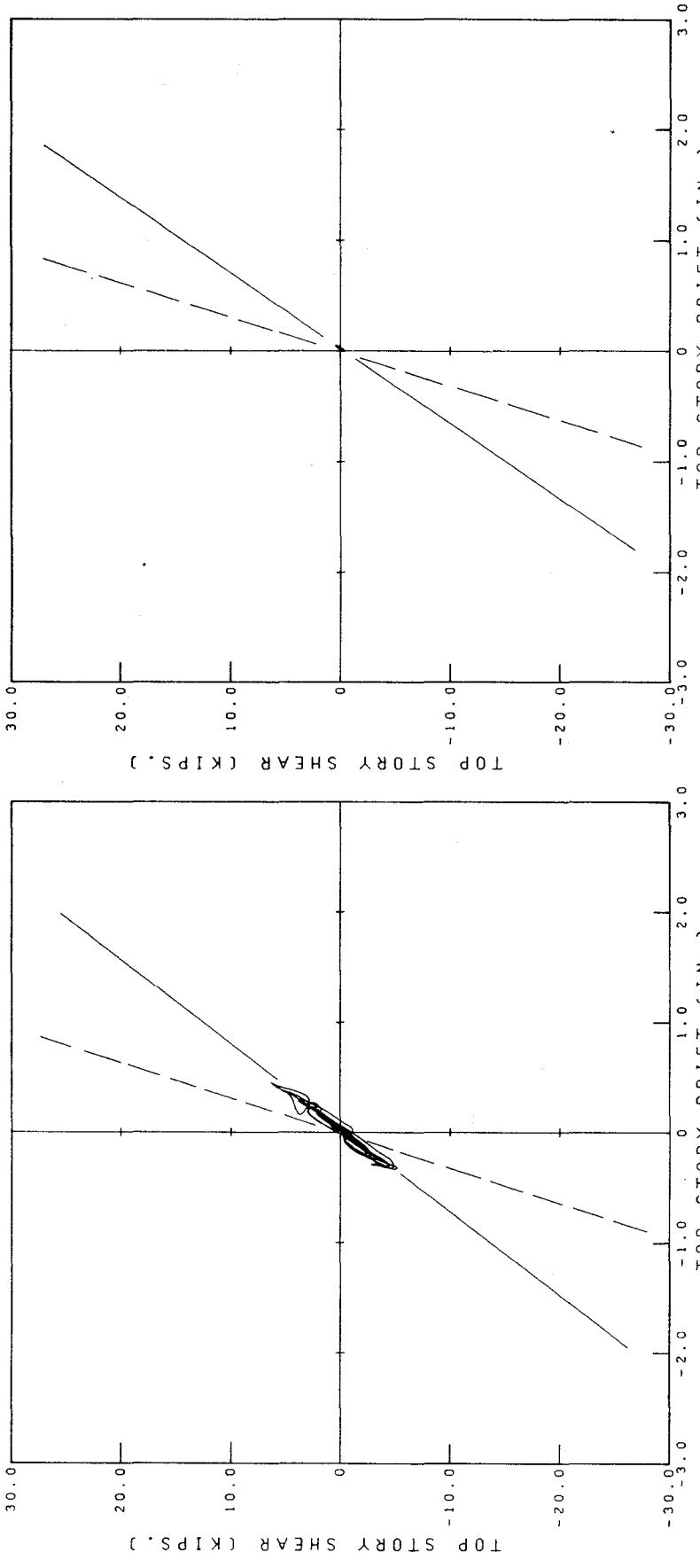
TOP STORY SHEAR (KIPS.)
30.0
20.0
10.0
0
-10.0
-20.0
-30.0
-3.0
-2.0
-1.0
0
1.0
2.0
3.0
TOP STORY DRIFT (IN.)
(e)
TIME = 20.0 - 25.0 SEC.
(f)
TIME = 25.0 - 30.0 SEC.
RCF2 RUN W2 TAFT 850(1)

Fig. 3.13 (CONT.)

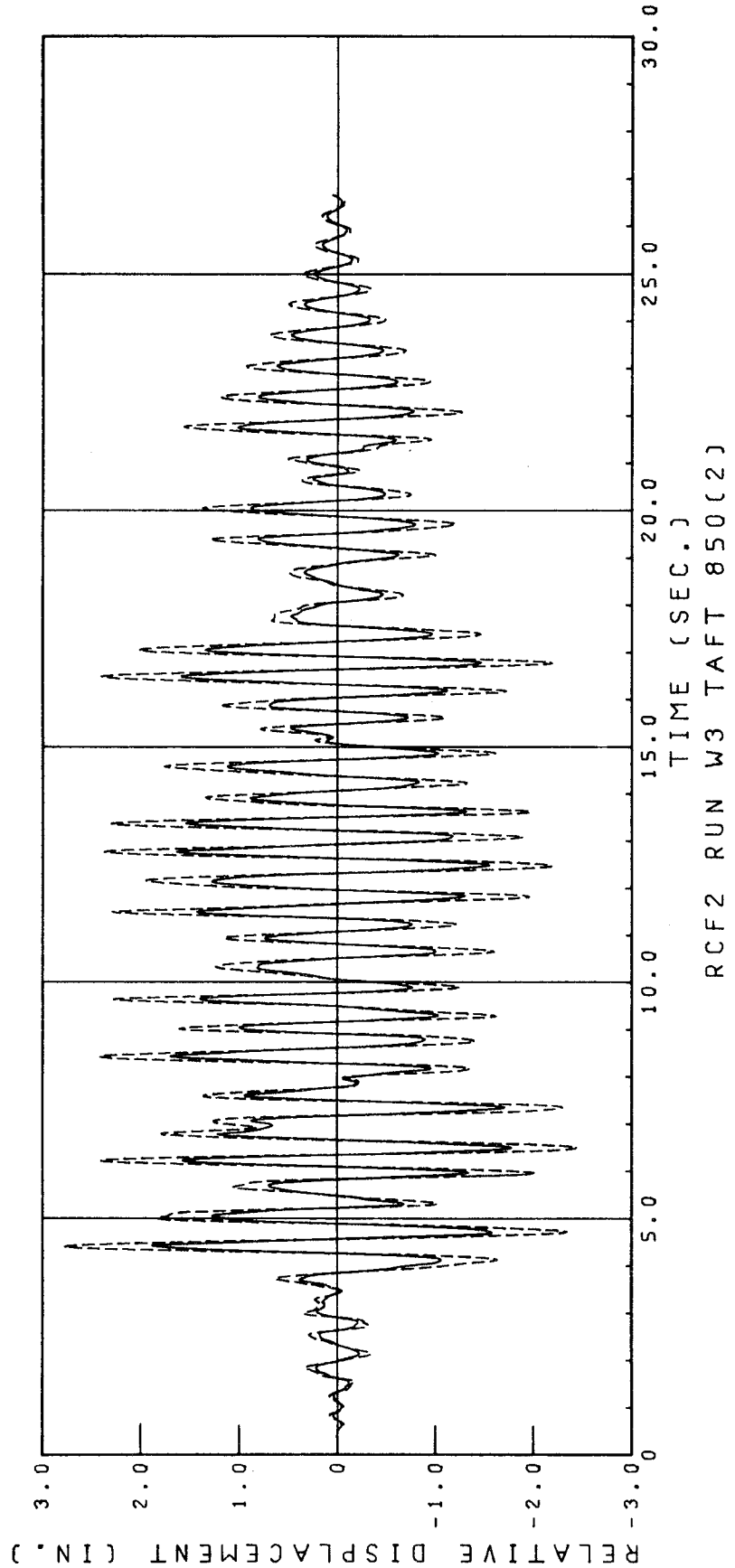

Fig 3.14 DISPLACEMENT RESPONSE DURING RUN W3.
SOLID LINE: FIRST FLOOR; DASHED LINE: SECOND FLOOR.
(RELATIVE TO TABLE)

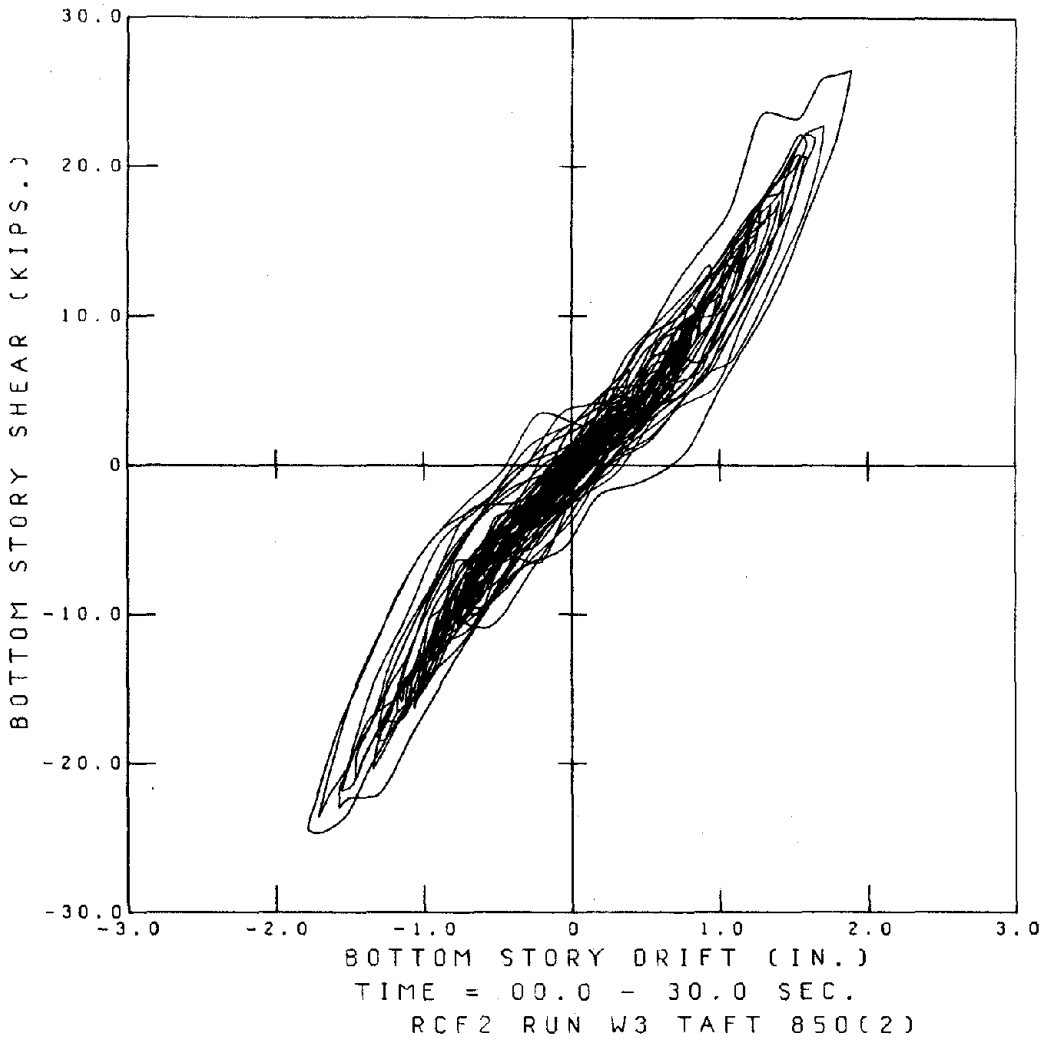

Fig.3.15 BOTTOM STORY SHEAR - DRIFT RELATIONSHIP. RUN W3.

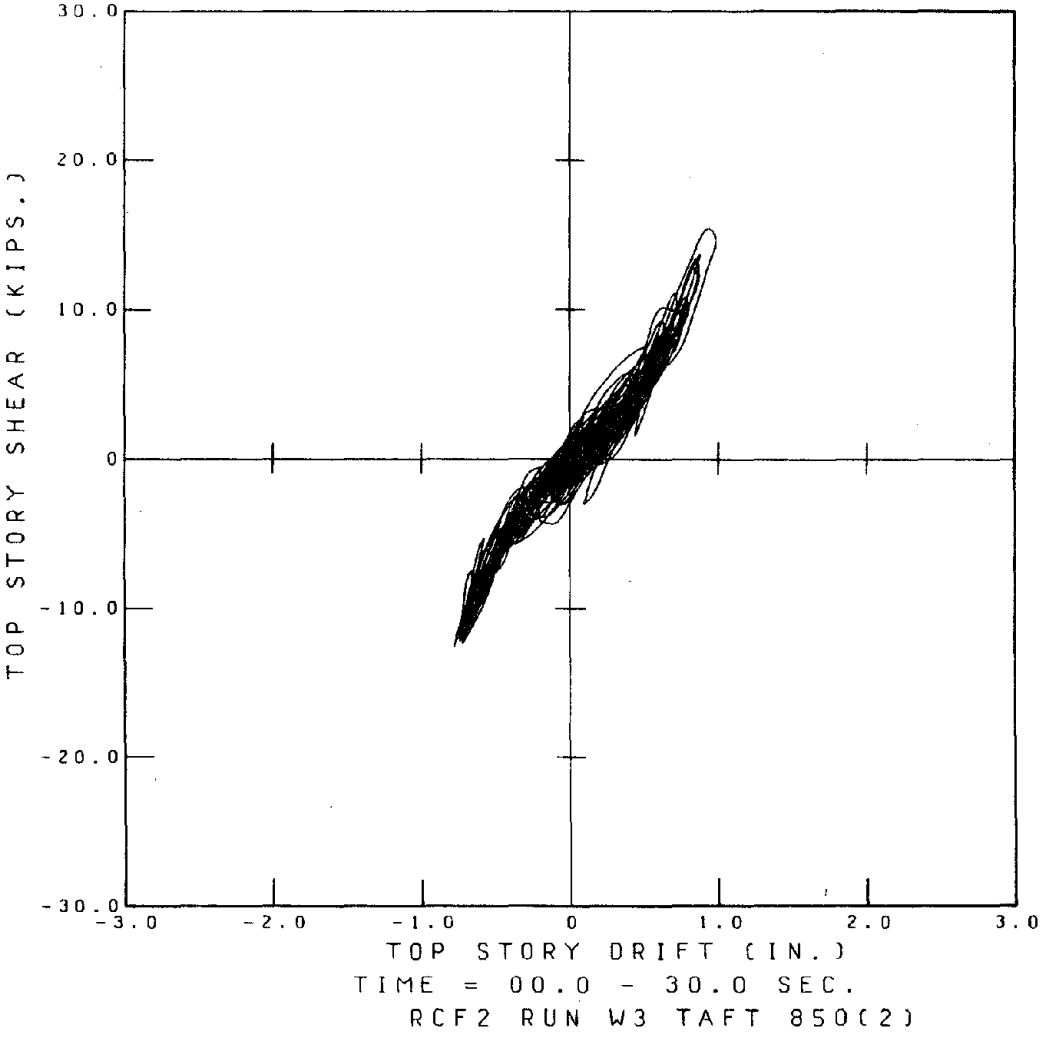

Fig.3.16 TOP STORY SHEAR - DRIFT RELATIONSHIP. RUN W3.

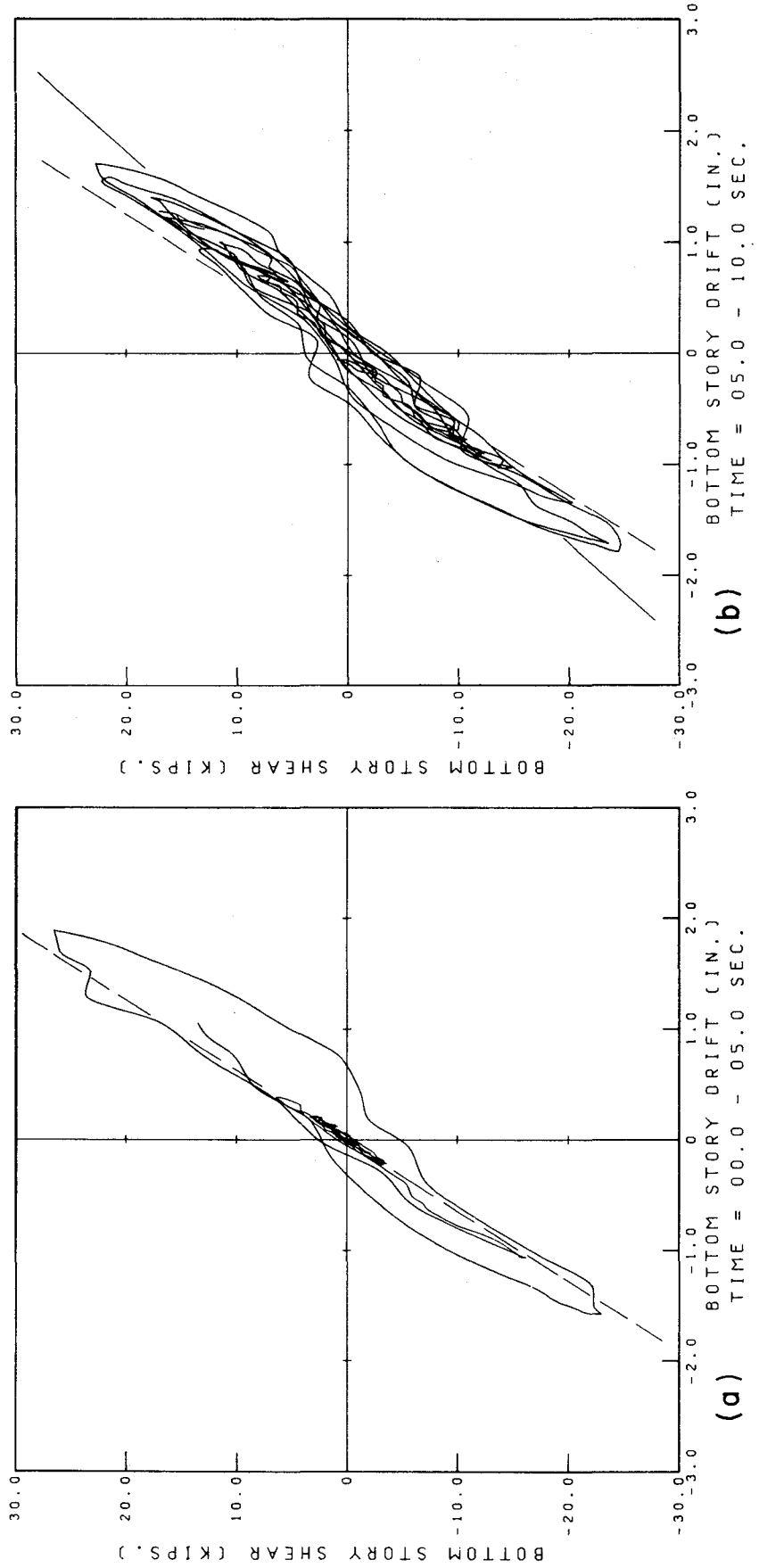

Fig. 3.17 BOTTOM STORY SHEAR - DRIFT RELATIONSHIP DURING 5 SEC. INTERVALS. RUN W3.

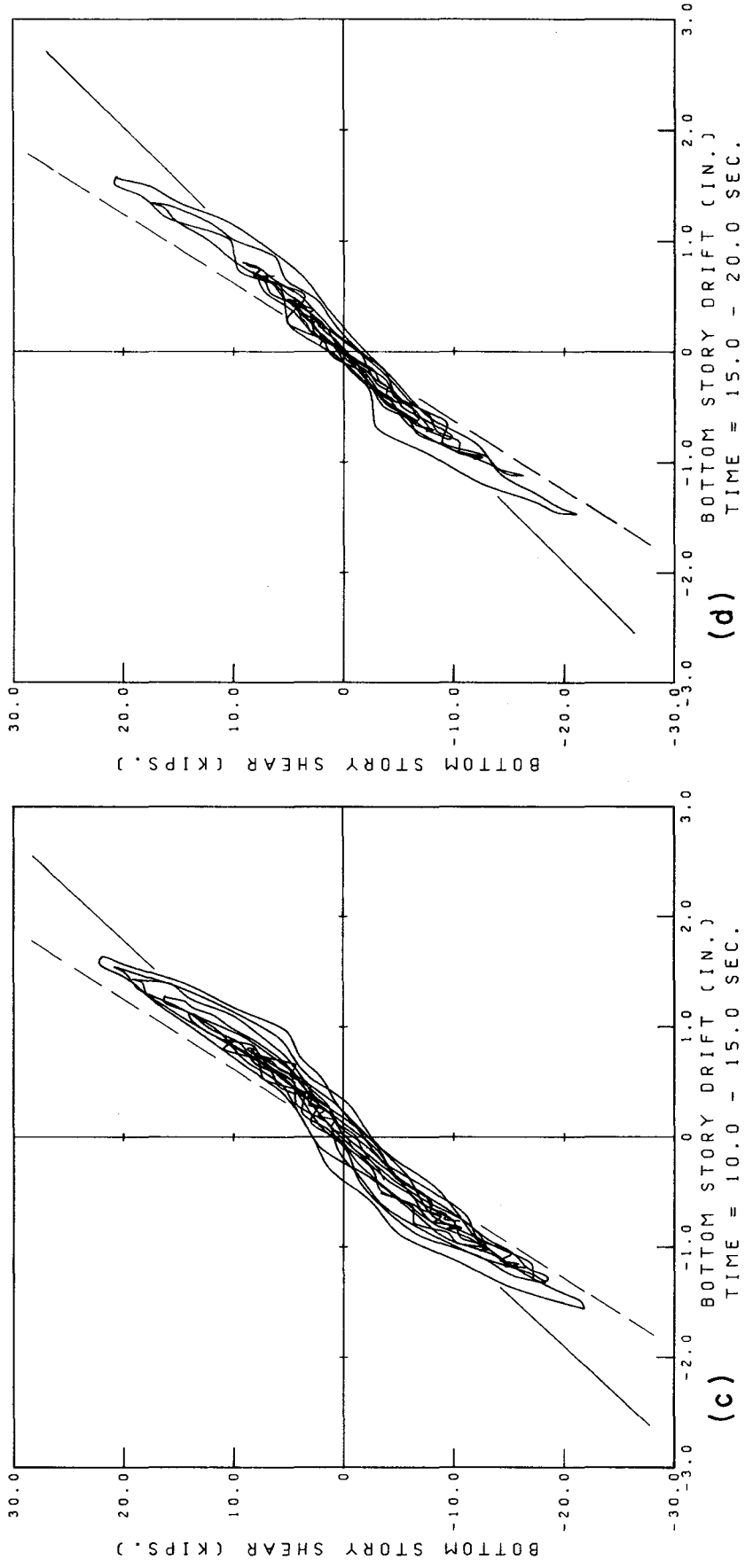

RCF2 RUN W3 TAFT 850(2)

Fig. 3.17 (CONT.)

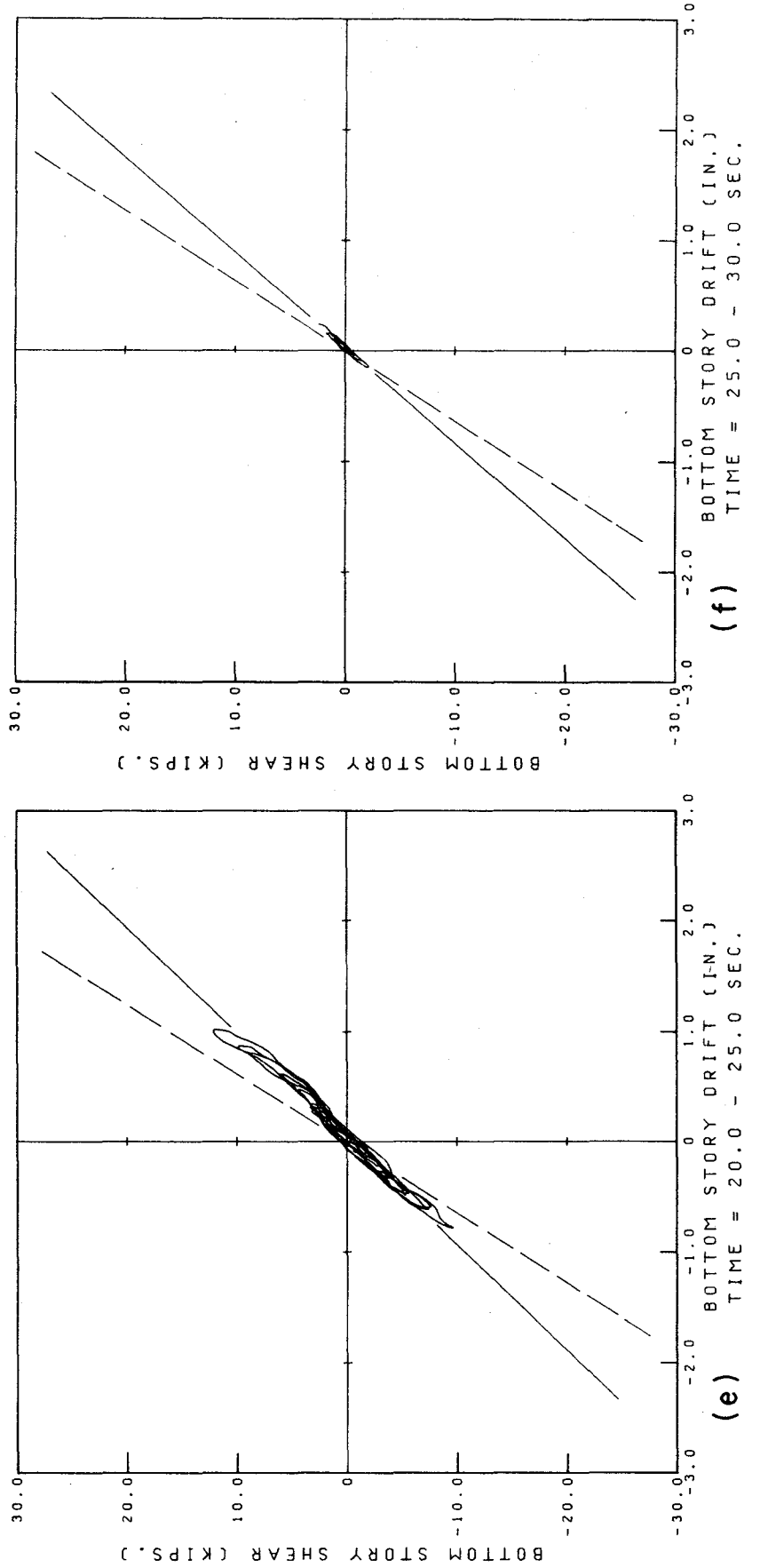

RCF2 RUN W3 TAFT 850(2)

Fig. 3.17 (CONT.)

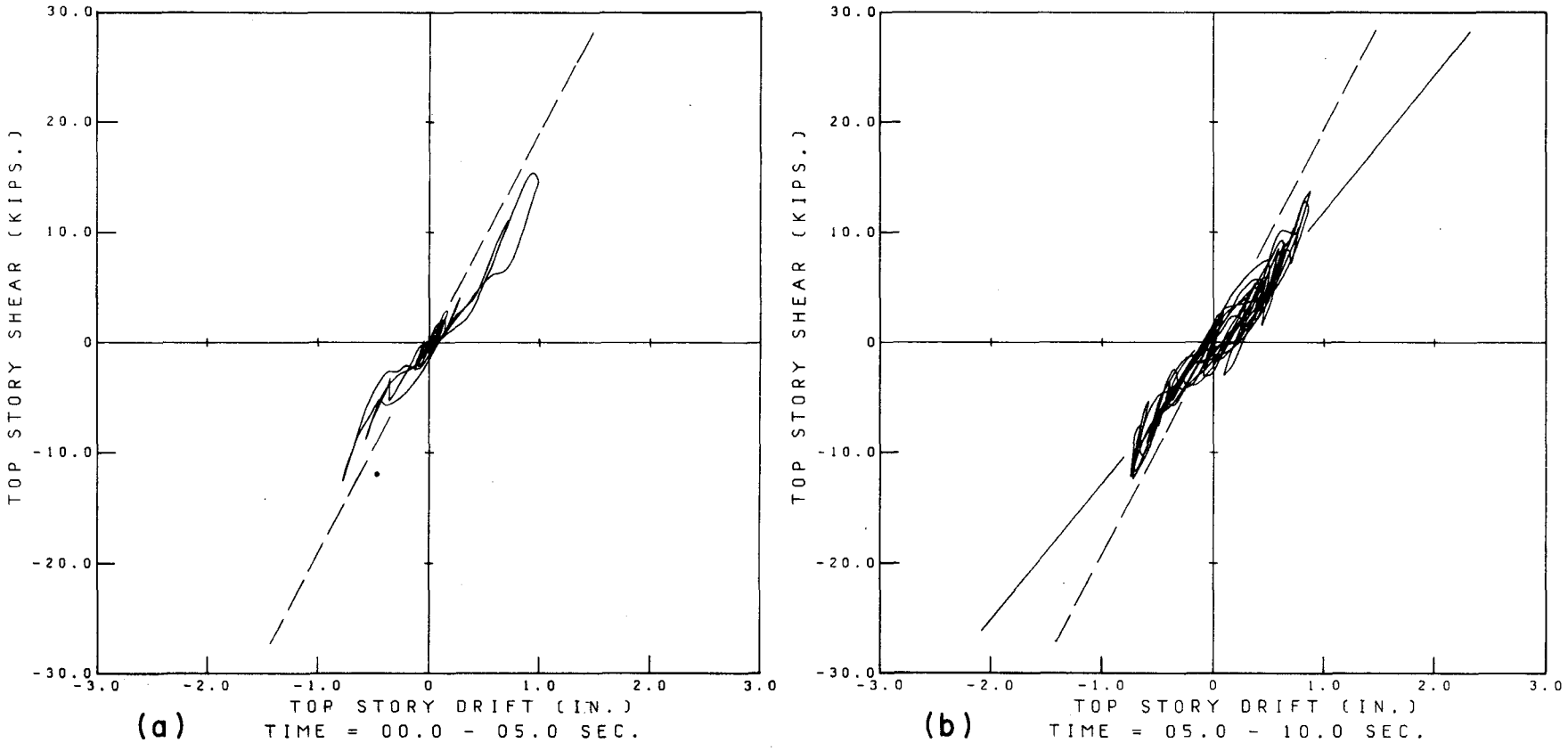

Fig. 3.18 TOP STORY SHEAR - DRIFT RELATIONSHIP DURING 5 SEC. INTERVALS. RUN W3.

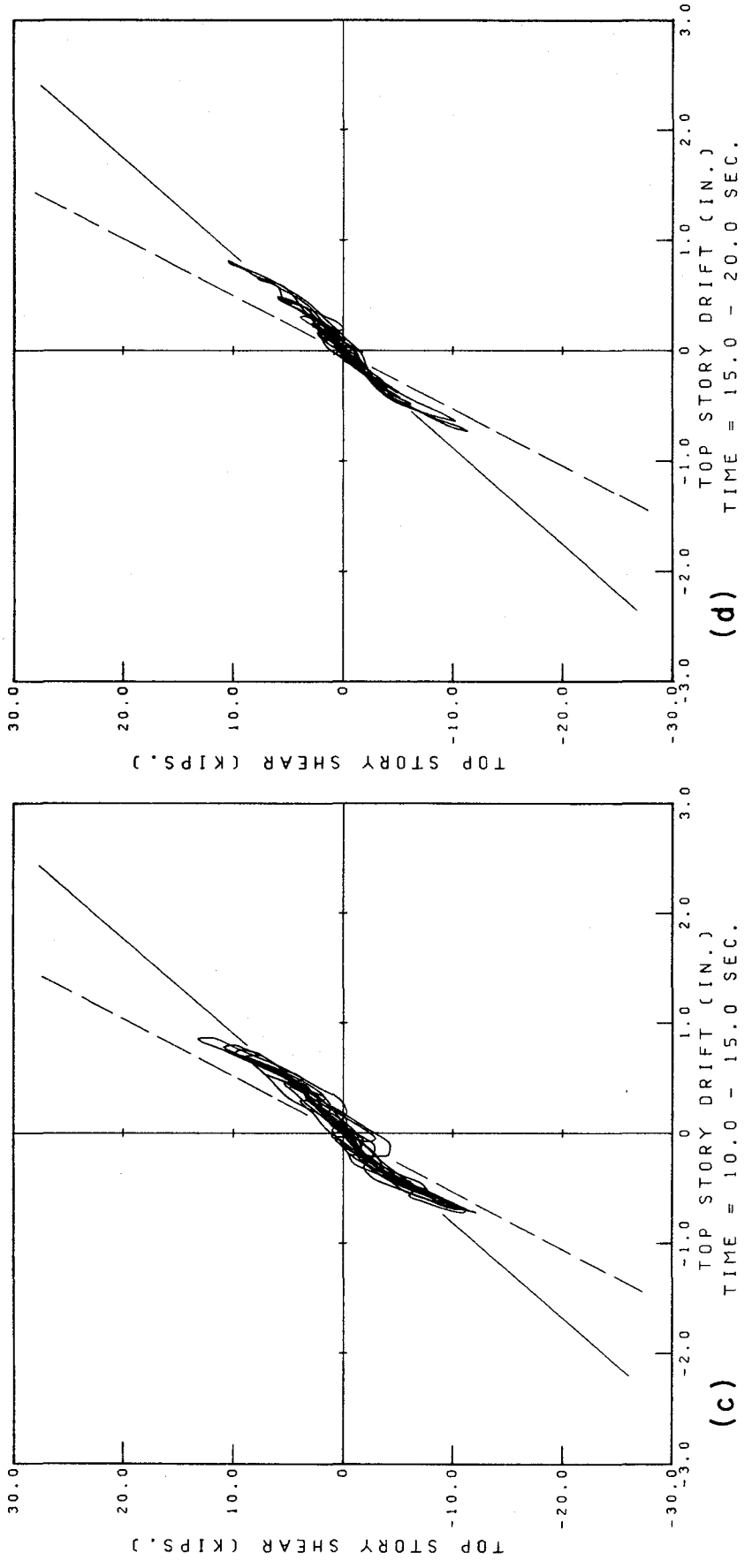
TOP STORY SHEAR (KIPS.)
30.0
20.0
10.0
0
-10.0
-20.0
-30.0
-3.0
-2.0
-1.0
0
1.0
2.0
3.0
TOP STORY DRIFT (IN.)
(c)
TIME = 10.0 - 15.0 SEC.
(d)
TIME = 15.0 - 20.0 SEC.
RCF2 RUN W3 TAFT 850(2)

Fig. 3.18 (CONT.)

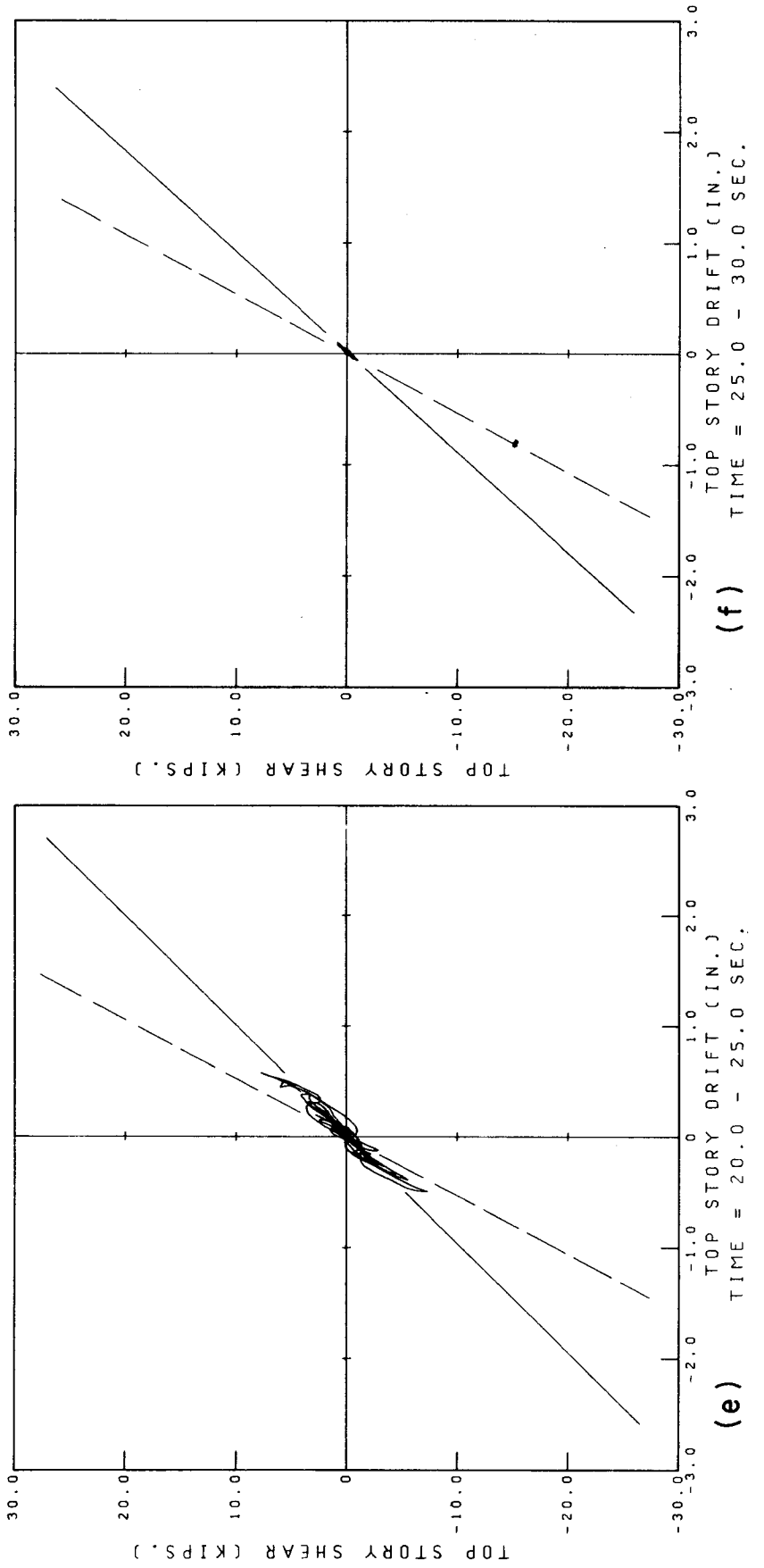
TOP STORY SHEAR (KIPS.)
30.0
20.0
10.0
0
-10.0
-20.0
-30.0
-3.0
-2.0
-1.0
0
1.0
2.0
3.0
TOP STORY DRIFT (IN.)
(e) TIME = 20.0 - 25.0 SEC.
(f) TIME = 25.0 - 30.0 SEC.
RCF2 RUN W3 TAFT 850(2)

Fig. 3.18 (CONT.)

4) EVOLUTION OF THE RESPONSE

4.1 Initial Considerations

The approach used to study the variation of the test structure's vibration period during shaking was based on the assumption that the dominant frequency of the displacement response during a relatively short period of time (which included perhaps a few oscillations) was equal to the natural frequency of the structure during that interval. This is equivalent to assuming that the response of the test structure during a short interval could be considered as essentially linear.

A "running window FFT (Fast Fourier Transform)" technique was used to identify the dominant frequency of the displacement response for several intervals during the tests. This consisted basically of analyzing a number of segments of the time-history (sometimes called "windows", since only a portion of the signal is considered at a time). The dominant frequency, found using the FFT algorithm, was then associated with the time corresponding to the center of each segment. The complete time-history was analyzed by moving the time window along the whole duration of the test.

It was necessary to consider some limitations of the running FFT technique before implementing it. In the first place is the fact that the outcome of the FFT analysis is not exactly the Fourier transform of the signal being processed. The ability of the FFT to represent the frequency spectrum of the input signal depends very heavily on the number of data points being processed. In order to have an acceptable frequency resolution in the FFT it seemed thus necessary to select a large time window (since the time interval between data points was fixed). This constraint was, however, in conflict with the desire of analyzing relatively short segments of the response, during which the behavior of the structure could be considered linear in a global sense.

After some trials, a time window consisting of 256 data samples was selected, taking into account the constraints mentioned above, and the fact that the FFT algorithm which was implemented could handle only data with a number of samples equal to an integer power of two. Since the time interval between data points was about 0.02 seconds, the resulting duration of the window was about 5 seconds. The frequency resolution in the FFT was therefore approximately 1/5, or 0.2 hertz.

In order to perceive the evolution of the vibration frequency during the shaking, it was decided to move the

time window along the time-history at intervals of 128 data samples (about 2.5 seconds) during the main part of the record, and to have, if convenient, a last segment during the free vibrations after the table motion stopped.

4.2 Variation of Vibration Frequency during Shaking

A short summary of the results of the FFT frequency analysis of the bottom story lateral displacement response of RCF2 follows.

Figures 4.1, 4.2 and 4.3 show the bottom story displacement time-history during runs W1, W2, and W3, the time window in three positions during each run, and plots of the FFT of these windows in the frequency range 0.0 to 10.0 hertz. The frequency spectra have been normalized to unit peak amplitude, since only their shape is important to determine the dominant frequency during the time segment being examined. As expected, the frequency analysis revealed that during each time interval, the structure oscillated with essentially one frequency, or within a narrow frequency band. Some other features of the displacement response are also apparent in the frequency spectra, such as the negligible effect of higher vibration modes (even in the "elastic" run W1) and the prescence of the permanent offset during run W2, which appears as the zero frequency component.

The numerical information obtained during each table run and for each time segment analyzed is presented in Tables 4.1, 4.2 and 4.3; they contain the time interval spanned, the position of the center of the time window ,the peak displacement reached, the number of oscillations (cycles) undergone by the structure and the dominant frequency (and period) of vibration during the time interval under study.

The evolution of the vibration frequency during the complete test sequence is presented in Fig. 4.4, in which the values measured during free vibration tests are also shown. Figure 4.5 presents the inverse quantities: the change of the vibration period during the test history. Both figures depict in a global way the response behavior of RCF2 during the tests: during run W1 the structure remained essentially elastic, after having suffered a minor decrease in stiffness due to cracking; run W2, on the contrary, was a severe test during which the specimen suffered noticeable damage, as attested by the dramatic changes in its structural characteristics; finally, the last test was performed on a specimen already damaged, which behaved in an almost uniform way.

An interesting feature observed in Fig. 4.4 is that the frequency measurements made during the free vibration tests were consistently higher than those computed from the

FFT of time intervals at the beginning and end of the tests. This could be due to the very small displacement amplitude at which the free vibration tests were performed, which was not sufficient to allow the cracks to open completely; thus the section and global stiffness corresponded to a less cracked state.

4.3 Response Characterization

The results obtained from the frequency analysis of the response of RCF2 were used to study other aspects of the structural behavior, such as the lateral stiffness degradation and the displacement ductility developed by the test specimen. To perform such studies, a mathematical model was devised to relate the variation of the vibration frequency of the structure with the variation of its mechanical characteristics.

Figure 4.6 shows the simple stiffness degrading model used to characterize the test structure's force-deformation relationship during any time interval. It is defined by its yield resistance, R_y , its initial elastic stiffness, K_o and the maximum displacement, δ_{max} (not necesarily the maximum displacement during the interval under consideration). The linearization of the response is achieved by defining an average stiffness, K , which depends on the maximum displacement.

If $\delta_{max} \leq \delta_y$ then

$$K = K_o \qquad (4.1)$$

and the structure is in the elastic condition; otherwise,

$$K = R_y / \delta_{max} \qquad (4.2)$$

where δ_y is the "yield" displacement, defined by

$$\delta_y = R_y / K_o \qquad (4.3)$$

A displacement ductility factor, μ , measures the maximum inelastic deformation suffered by the test structure in terms of its linear elastic deformation limit, δ_y ; it is, in consequence, a measure of damage. It is defined by

$$\delta_{max} = \mu \delta_y \qquad (4.4)$$

Combining expressions (4.3) and (4.4) into (4.2) yields

$$K = K_o \delta_y / \mu \delta_y$$

or

$$K = K_o / \mu \qquad (4.5)$$

If the structure is considered as a single degree of freedom system with mass M and lateral stiffness K , its vibration frequency f is

$$f = \frac{1}{2\pi}\sqrt{\frac{K}{M}} \qquad (4.6)$$

therefore, if the vibration frequency during a certain time interval is known, the corresponding average stiffness is given by

$$K = M (2\pi f)^2 \qquad (4.7)$$

The initial elastic stiffness can therefore be evaluated as

$$K_o = M (2\pi f_o)^2 \qquad (4.8)$$

where f_o is the frequency of vibration measured under linear elastic conditions.

Expressions (4.7) and (4.8) can be combined to give

$$K = K_o (f/f_o)^2 \qquad (4.9)$$

which, recalling (4.5) yields

$$\mu = (f/f_o)^2 \qquad (4.10)$$

The degrading model used to characterize the structure can therefore be completely defined in terms of its mass M , its initial and average vibration frequencies, f_o and f , and its resistance, R_y . All the other parameters can be computed with the formulas:

$$K_o = (2\pi f_o)^2 M \qquad (4.11)$$

$$K = K_o (f/f_o)^2 \qquad (4.12)$$

$$\mu = (f_o/f)^2 \qquad (4.13)$$

$$\delta_y = R_y / K_o \qquad (4.14)$$

$$\delta_{max} = \mu \delta_y \qquad (4.15)$$

The following numerical values were used to

characterize the response of RCF2:

R_y = 27.7 kips

(maximum base shear measured during run W2)

M = 0.0924 kips-sec/in

(total mass of the structure)

f_o = 3 hertz

(dominant frequency during "elastic" run,W1)

which give the following values for the initial elastic stiffness and yield displacement:

$$K_o = 4\pi^2 . 3^2 . 0924 = 33 \text{ k-in}$$

and

$$\delta_y = 27.7/33 = 0.84 \text{ in}$$

The ability of the mathematical model to represent the response of RCF2 was then evaluated with respect to the experimental measurements. Figure 4.7 a) shows the force-deformation relationship developed during run W1, along with the lateral stiffness K_o predicted above, which slightly underestimates the actual stiffness. This is probably due to the low precision in the computation of the dominant vibration frequency (of about ± 0.1 hertz) using the FFT algorithm, and to the assumption of M being the total translational mass of the structure. Since the error is small, this value of K_o was adopted for the computations that follow.

The response during the "strongest" part of run W2 is depicted in Fig. 4.7 b). The degrading model simulates satisfactorily the average lateral stiffness, but fails to predict the displacement corresponding to the maximum shear, since it occurred during an isolated cycle of significantly large inelastic deformation.

Two comparable segments of runs W2 and W3 are shown in Figs. 4.7 c) and d); again, the average lateral stiffness is identified with reasonable accuracy. In both cases, however, the peak displacement is noticeably smaller than that predicted by the model. In the first case, this effect agrees with the model's assumptions, since a displacement of comparable magnitude occurred previously. This is not true for the second segment, which points out that plastic deformation is not the only source for stiffness degradation, as assumed in creating the mathematical model. The permanent deformation suffered by the bottom story during run W2, clearly observed in Fig. 4.7c), is obviously not detected by the model.

The variation in lateral stiffness through the test history computed using the frequency analysis results (via formula 4.12) is presented in Fig. 4.8. According to the previous observations, this graph offers a realistic representation of the damage inflicted upon the structure during each shaking table run. The stiffness values have

been normalized with respect to the "elastic" cracked stiffness obtained during run W1, to facilitate comparisons.

The displacement ductility developed by RCF2 during the dynamic tests is shown in Fig. 4.9, in which the predictions using formula (4.13) are compared with values computed using the experimental measurements. The predicted ductility requirements are acceptable for run W1, for which elastic behavior is anticipated; for run W2 they are, in general, larger than those actually developed by the structure but they are satisfactory approximations since the "actual" values were computed using a sligthly overestimated value for δ_y of 0.84 inches for consistency with the stiffness computations. The degrading model, however, fails dramatically in run W3, for which it predicts unacceptably large ductility values.

It is necesary to be aware of the limitations of the formulation of the ideal degrading model to interpret the results obtained by its application. For instance, displacement ductility and lateral stiffness are correlated by formula (4.5). This correlation is tested against the experimental values in Fig. 4.10. It is clear that the model is only capable of following the general trend of the structural behavior. Another limitation is that it does not take into account the influence of the number of cycles of

deformation on the stiffness degradation process. Figure 4.11 presents this correlation. For runs W1 and W3 the number of cycles do not seem to influence the value of the lateral stiffness; however, for run W2 there seems to be a strong correlation between the cyclic response and the change of stiffness. Regarding the ductility prediction, formula (4.13) tends to overestimate the displacement ductility requirements imposed on the structure by the seismic motion, probably because δ_{max} is usually much larger than the actual peak displacement (as shown in Figs. 4.7 c) and d).

4.4 Conclusions

The results presented in the preceding sections showed that it is possible to study in a realistic way the evolution of the response of reinforced concrete structures subjected to strong seismic loading using the data measured during shaking table experimentation.

By means of a well known frequency analysis tool, the FFT algorithm, and by modelling the structure as a very simple stiffness degrading system, it was possible to observe the variation in frequency of vibration, in the lateral stiffness, and to a lesser extent, in the displacement ductility developed by RCF2 during the shaking table tests.

The influence of the seismic input characteristics on the evolution of the structural response was not, however, included in that study. As a consequence, it was decided to attempt to correlate the changes in the structural response with characteristic aspects of the base excitation. This investigation and the results obtained are presented in the next Chapter.

segment	time interval (sec.)	average time (sec.)	dominant freq. (hertz)	period (sec.)	peak displ. (in.)	# of cycles
1	2.9-8.0	5.45	3.2	0.31	0.21	15
2	5.5-10.5	8.00	3.0	0.33	0.27	15
3	8.0-13.0	10.50	3.0	0.33	0.27	15
4	10.5-15.6	13.05	3.0	0.33	0.20	15
5	13.1-18.1	15.60	3.0	0.33	0.20	13
6	15.6-20.6	18.10	2.8	0.36	0.10	13
7	18.1-23.2	20.65	3.0	0.33	0.08	15

TABLE 4.1 Frequency Analysis of Run W1 Taft 100

segment	time interval (sec.)	average time (sec.)	dominant freq. (hertz)	period (sec.)	peak displ. (in.)	# of cycles
1	0.0-5.0	2.50	2.4	0.42	1.20	12.5
2	2.5-7.6	5.05	2.2	0.45	2.00	11
3	5.1-10.1	7.60	2.2	0.45	2.00	10.5
4	7.6-12.6	10.10	1.6	0.63	1.32	9
5	10.1-15.2	12.65	1.8	0.56	1.48	9
6	12.6-17.7	15.15	2.0	0.50	1.48	9.5
7	15.2-20.2	17.70	1.8	0.56	1.35	9
8	20.2-25.3	22.75	1.8	0.56	0.88	9

TABLE 4.2 Frequency Analysis of Run W2 Taft 850(1)

segment	time interval (sec.)	average time (sec.)	dominant freq. (hertz)	period (sec.)	peak displ. (in.)	# of cycles
1	0.0-5.0	2.50	1.6	0.63	1.58	8
2	2.5-7.6	5.05	1.6	0.63	1.79	8
3	5.1-10.1	7.60	1.8	0.56	1.79	10
4	7.6-12.6	10.10	1.6	0.63	1.71	8
5	10.1-15.2	12.65	1.6	0.63	1.56	8
6	12.6-17.7	15.15	1.6	0.63	1.64	9
7	15.2-20.2	17.70	1.4	0.71	1.59	7.5
8	21.5-26.5	24.00	1.6	0.63	1.02	8

TABLE 4.3 Frequency Analysis of Run W3 Taft 850(2)

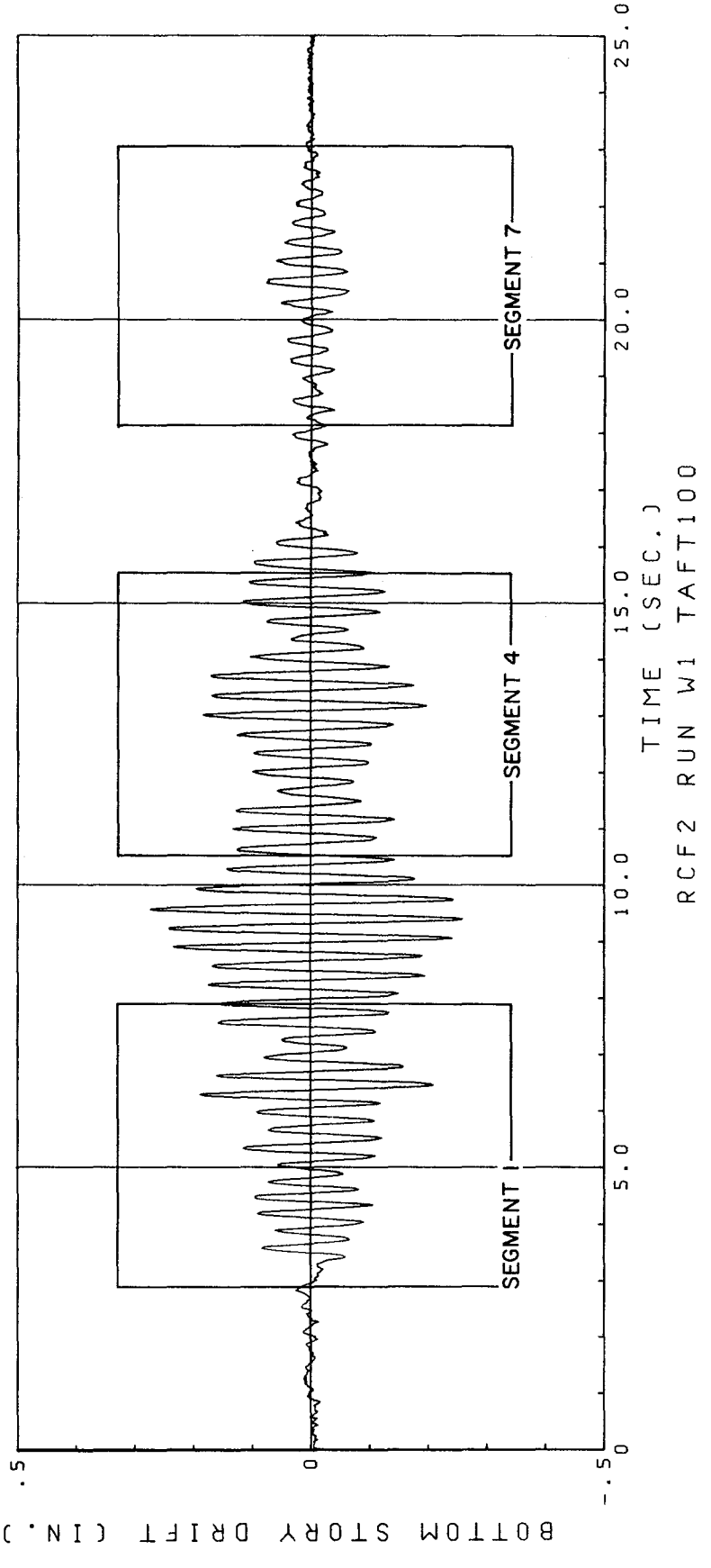

Fig. 4.1a) FFT FREQUENCY ANALYSIS
OF BOTTOM STORY DISPLACEMENT. RUN W1.

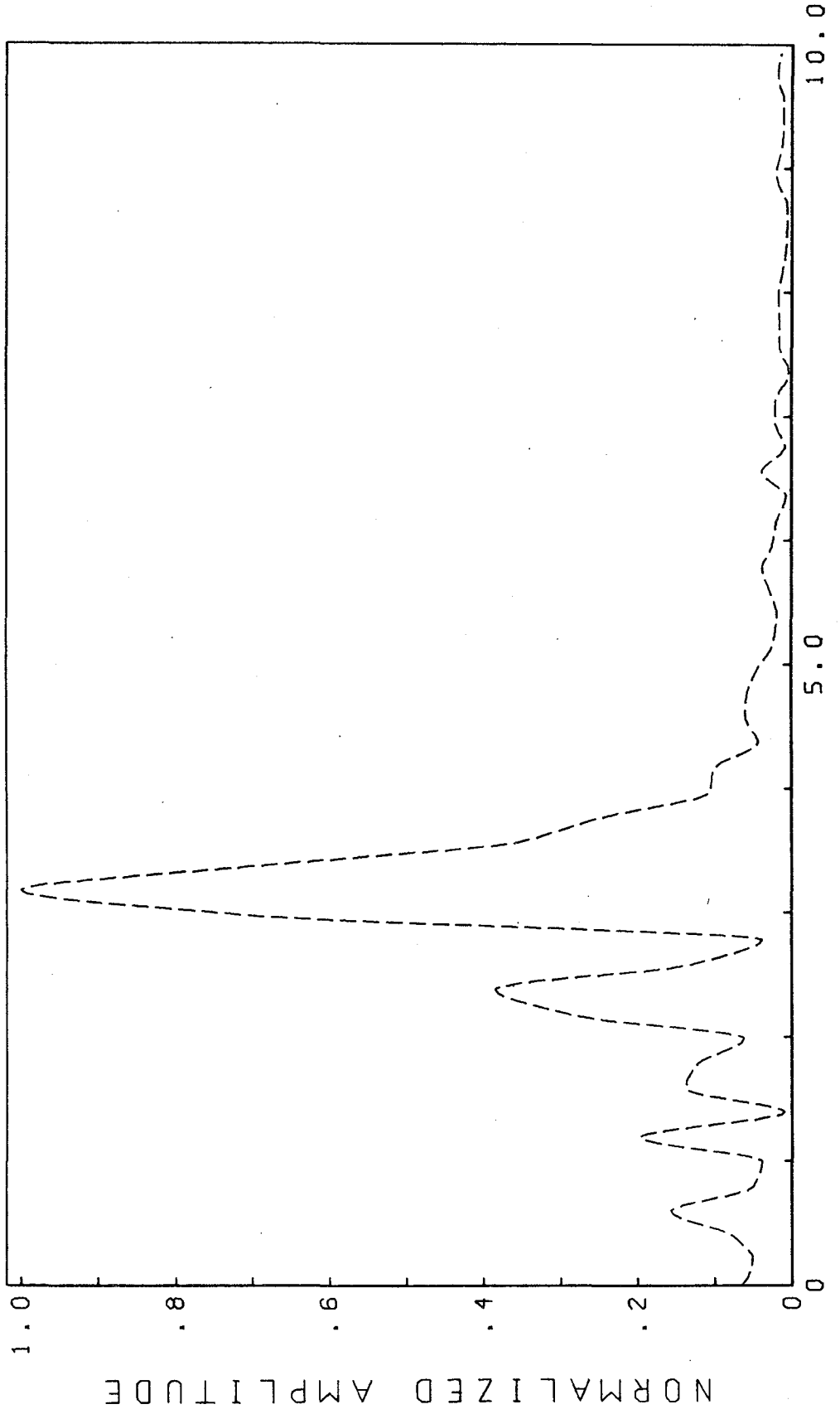

Fig. 4.1b) FFT OF SEGMENT 1 OF BOTTOM STORY DISPLACEMENT. RUN W1.

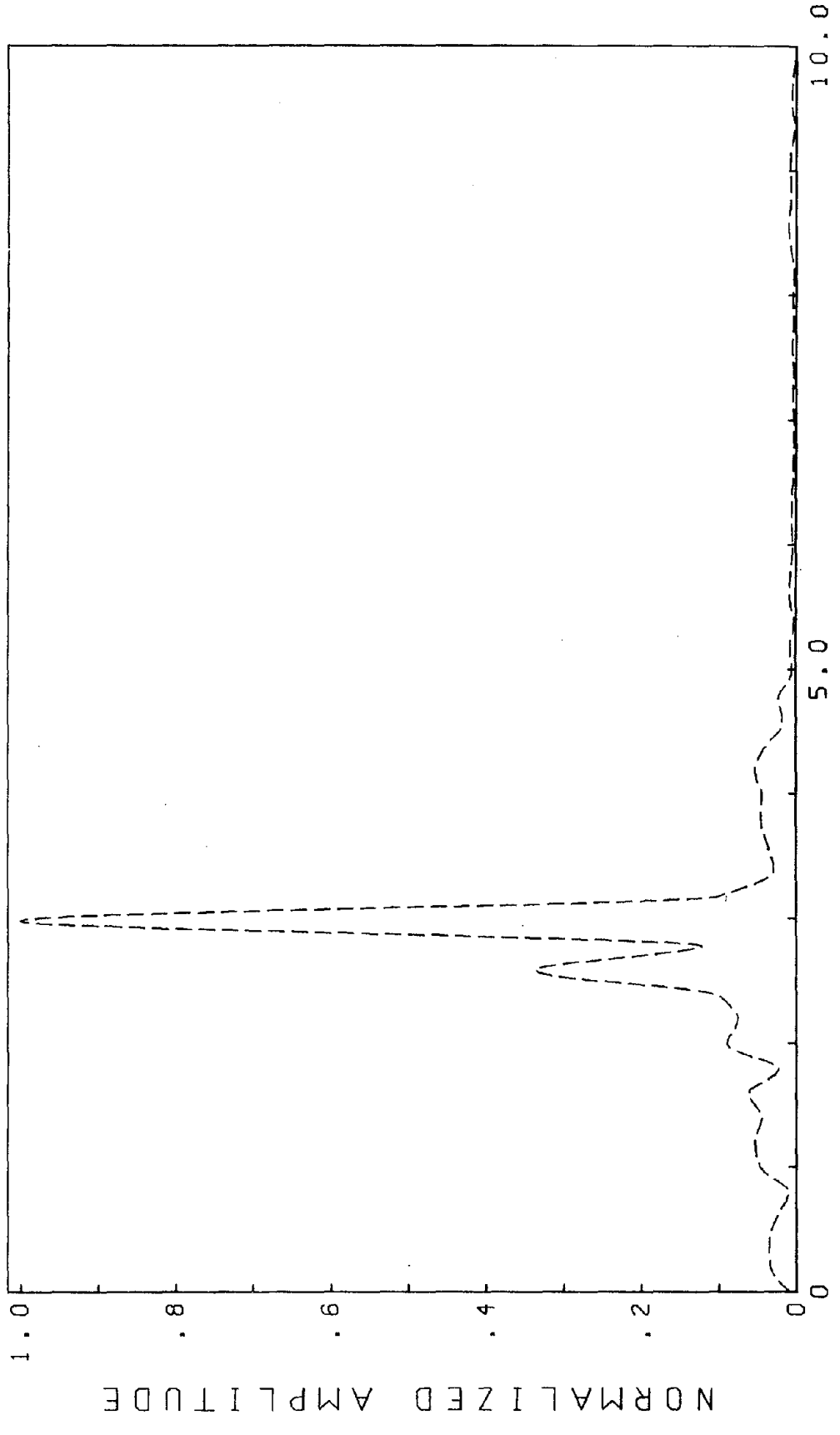

Fig. 4.1c) FFT OF SEGMENT 4 OF BOTTOM STORY DISPLACEMENT. RUN W1.

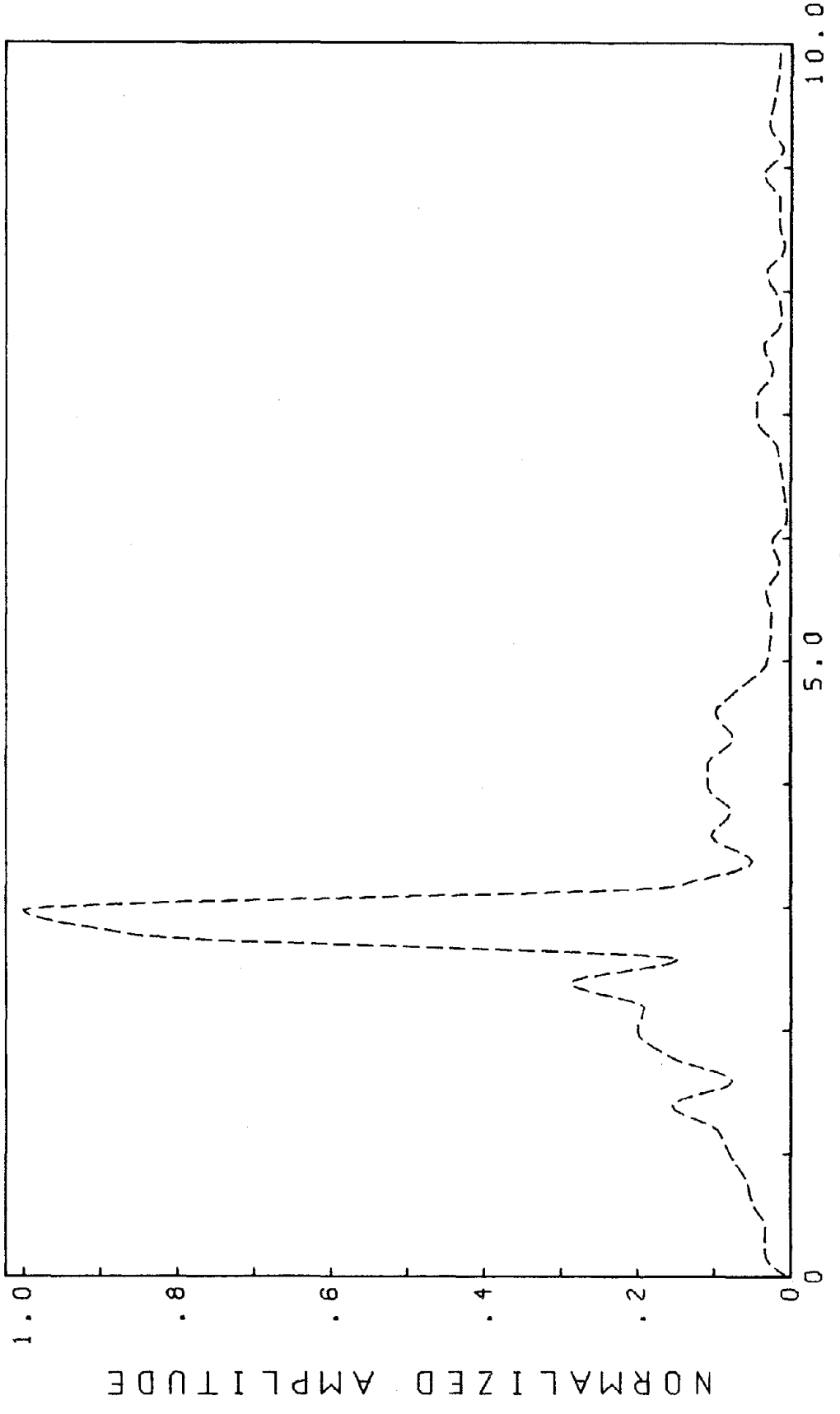

Fig. 4.1d) FFT OF SEGMENT 7 OF BOTTOM STORY DISPLACEMENT. RUN W1.

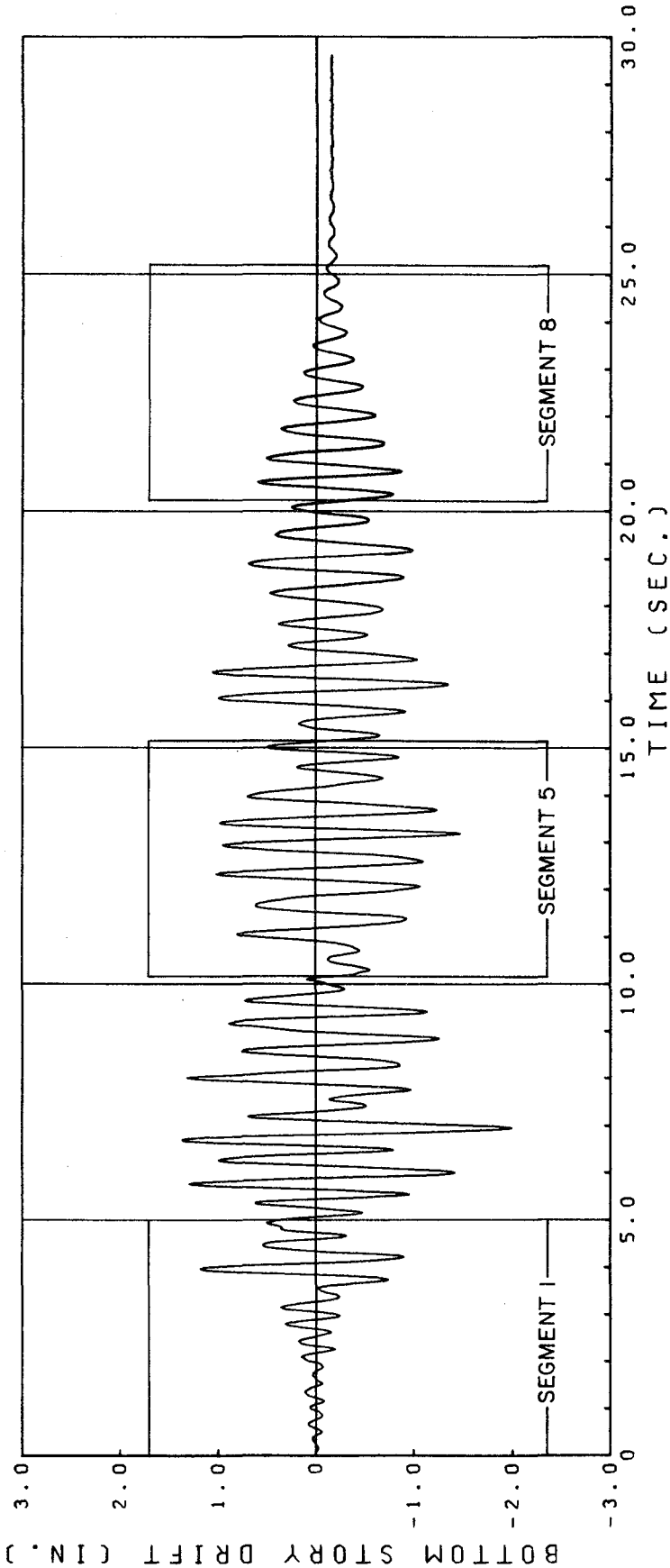

Fig. 4.2a) FFT FREQUENCY ANALYSIS
OF BOTTOM STORY DISPLACEMENT. RUN W2.

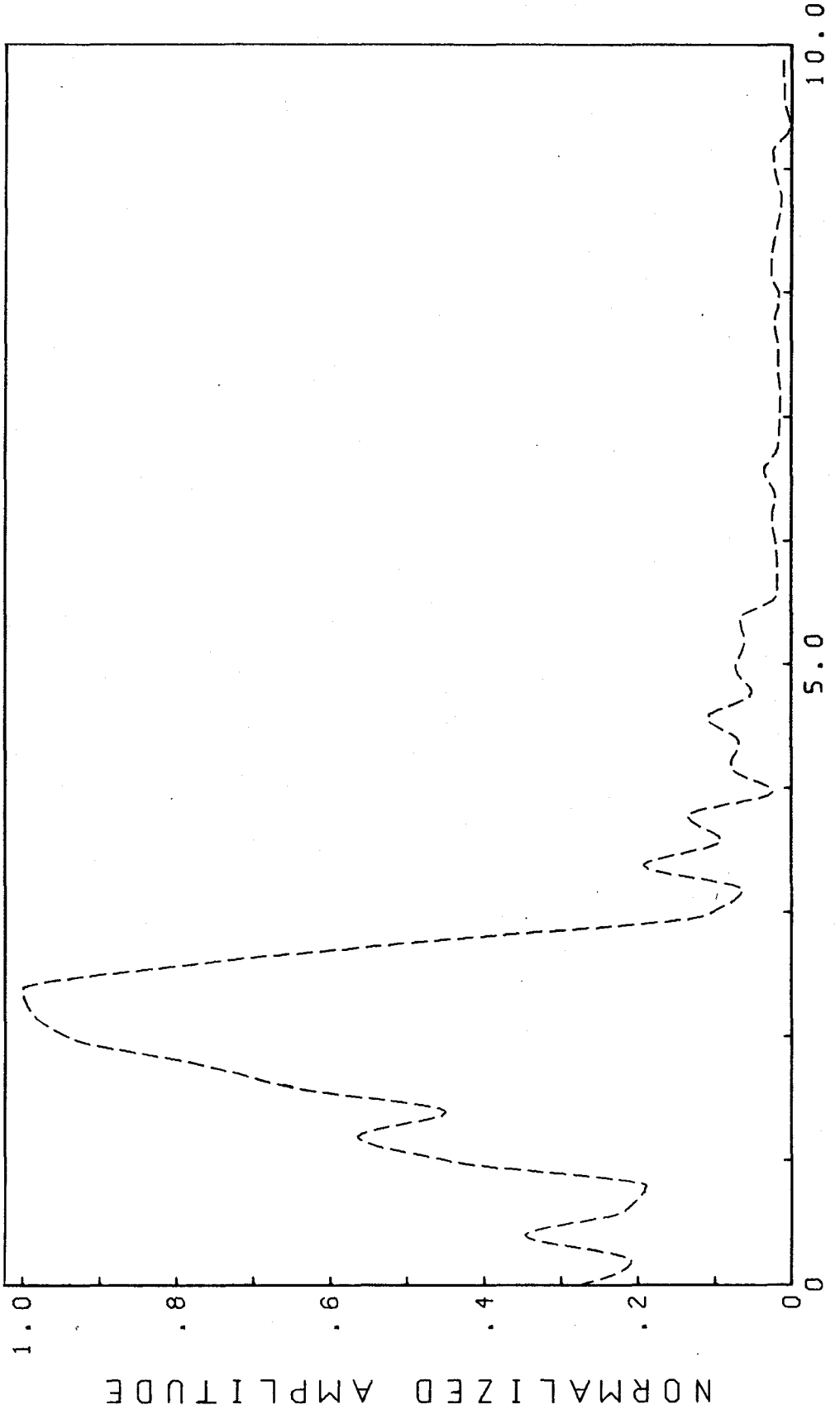

Fig. 4.2b) FFT OF SEGMENT 1 OF BOTTOM STORY DISPLACEMENT. RUN W2.

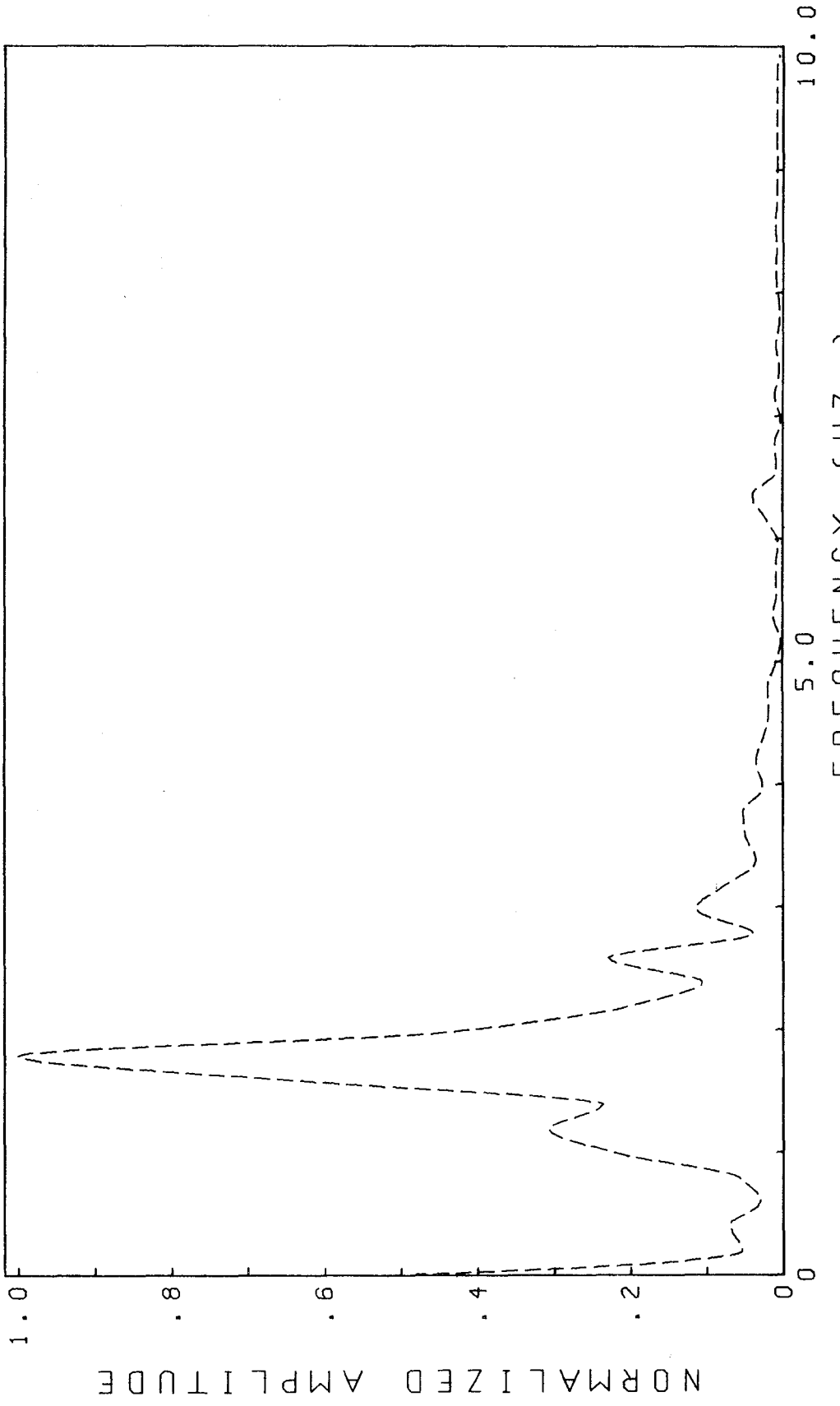

Fig. 4.2c) FFT OF SEGMENT 5 OF BOTTOM STORY DISPLACEMENT. RUN W2.

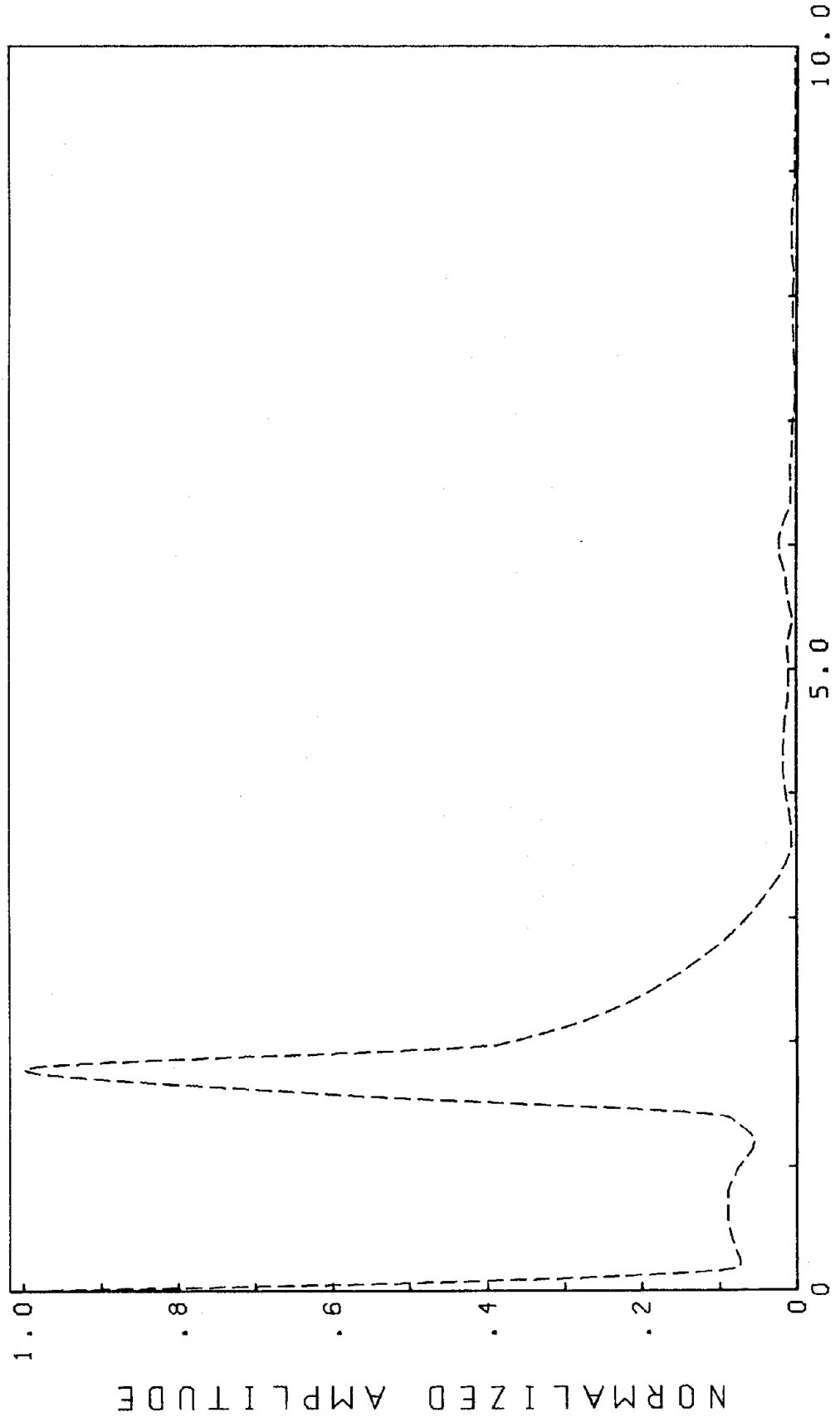

Fig. 4.2d) FFT OF SEGMENT 8 OF BOTTOM STORY DISPLACEMENT. RUN W2.

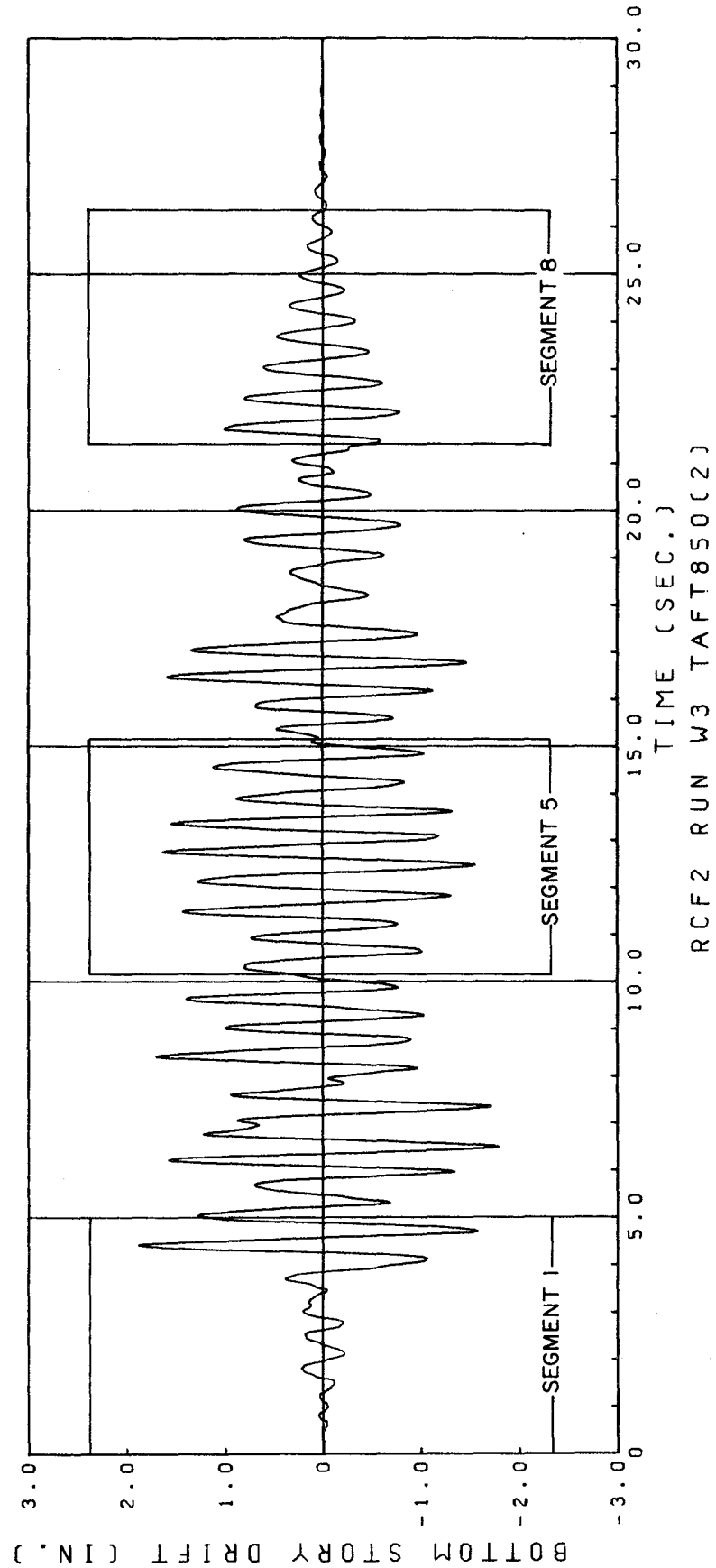

Fig 4.3a) FFT FREQUENCY ANALYISIS
OF BOTTOM STORY DISPLACEMENT. RUN W3.

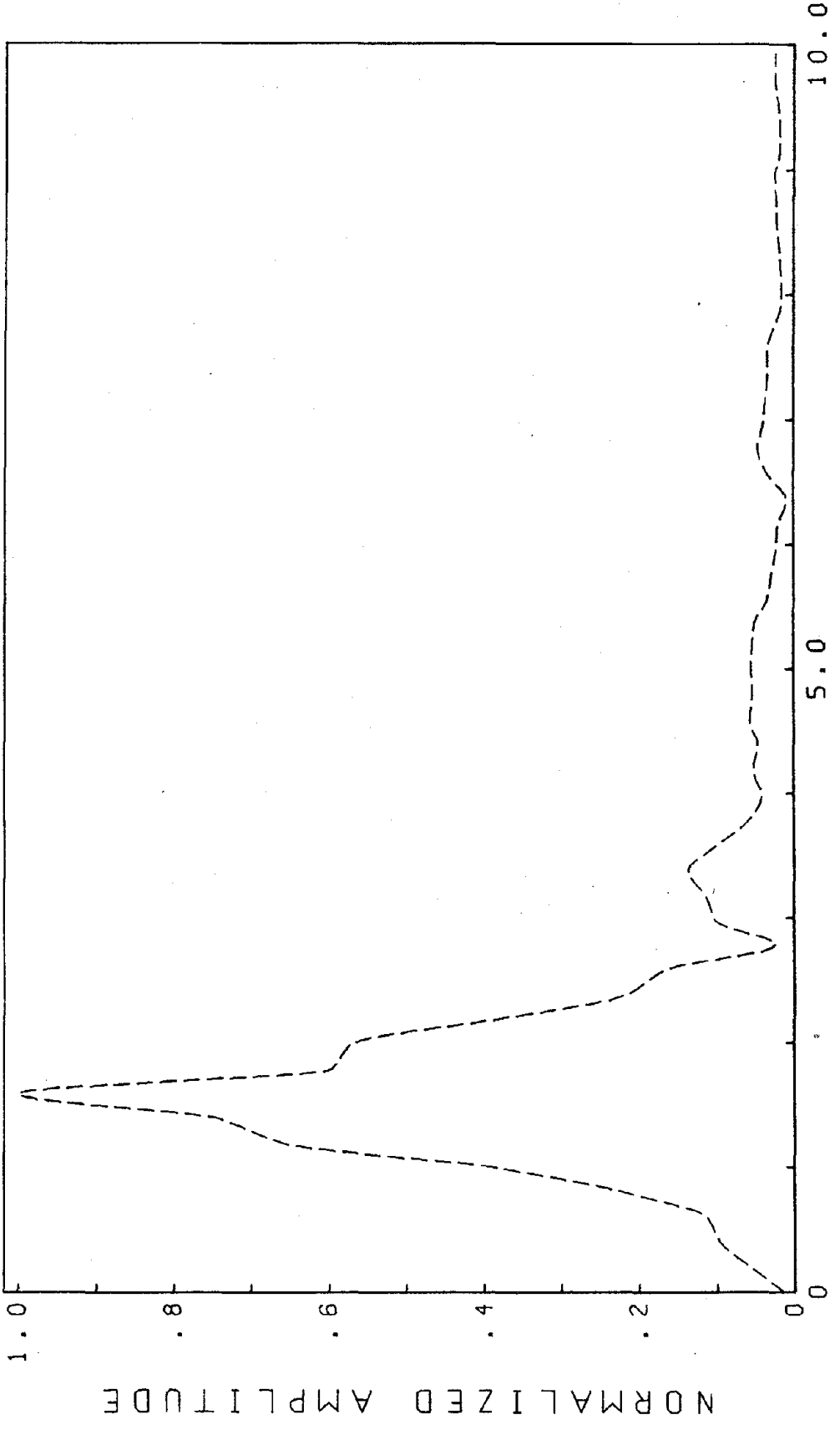

Fig. 4.3b) FFT OF SEGMENT 1 OF BOTTOM STORY DISPLACEMENT. RUN W3.

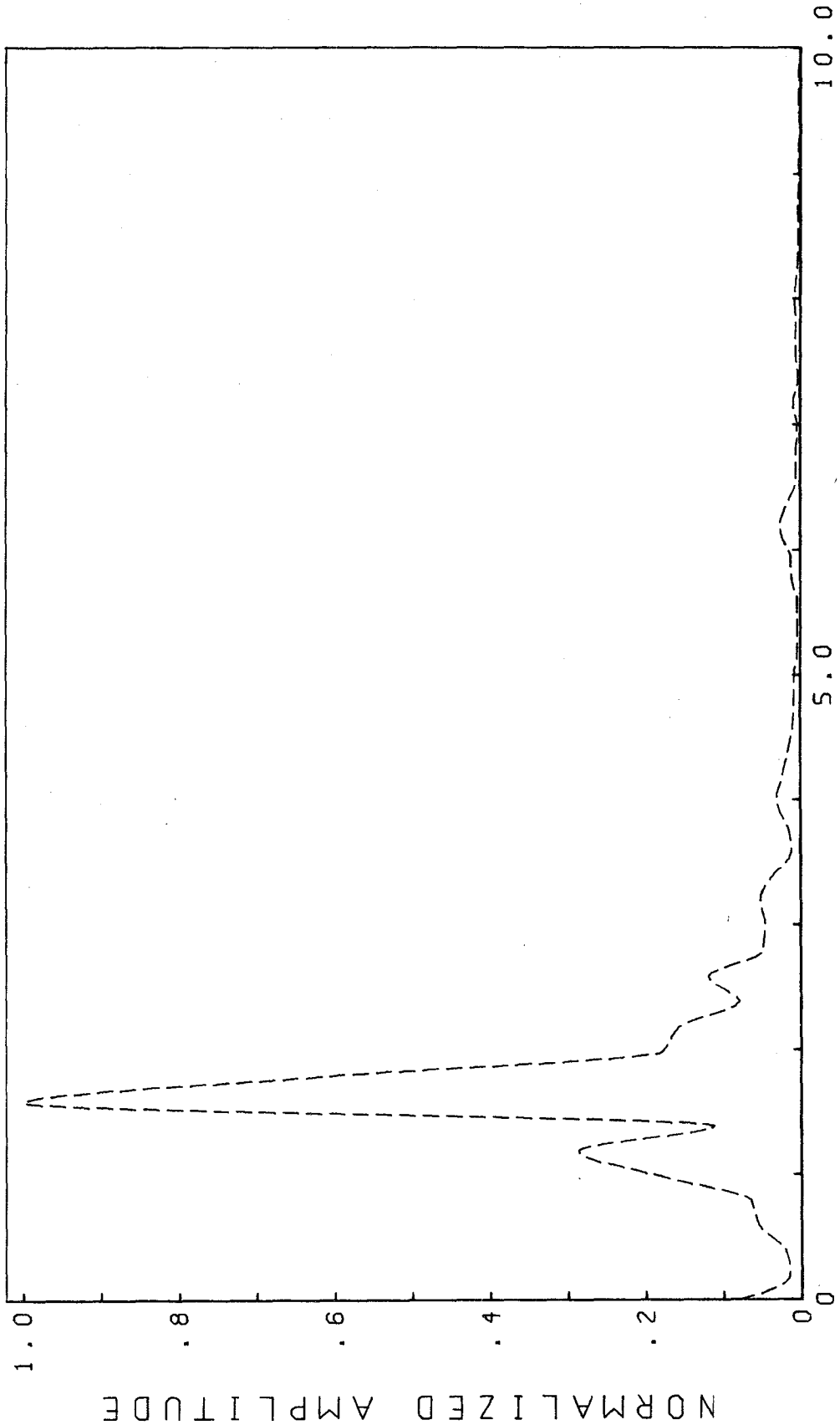

Fig. 4.3c) FFT OF SEGMENT 5 OF BOTTOM STORY DISPLACEMENT. RUN W3.

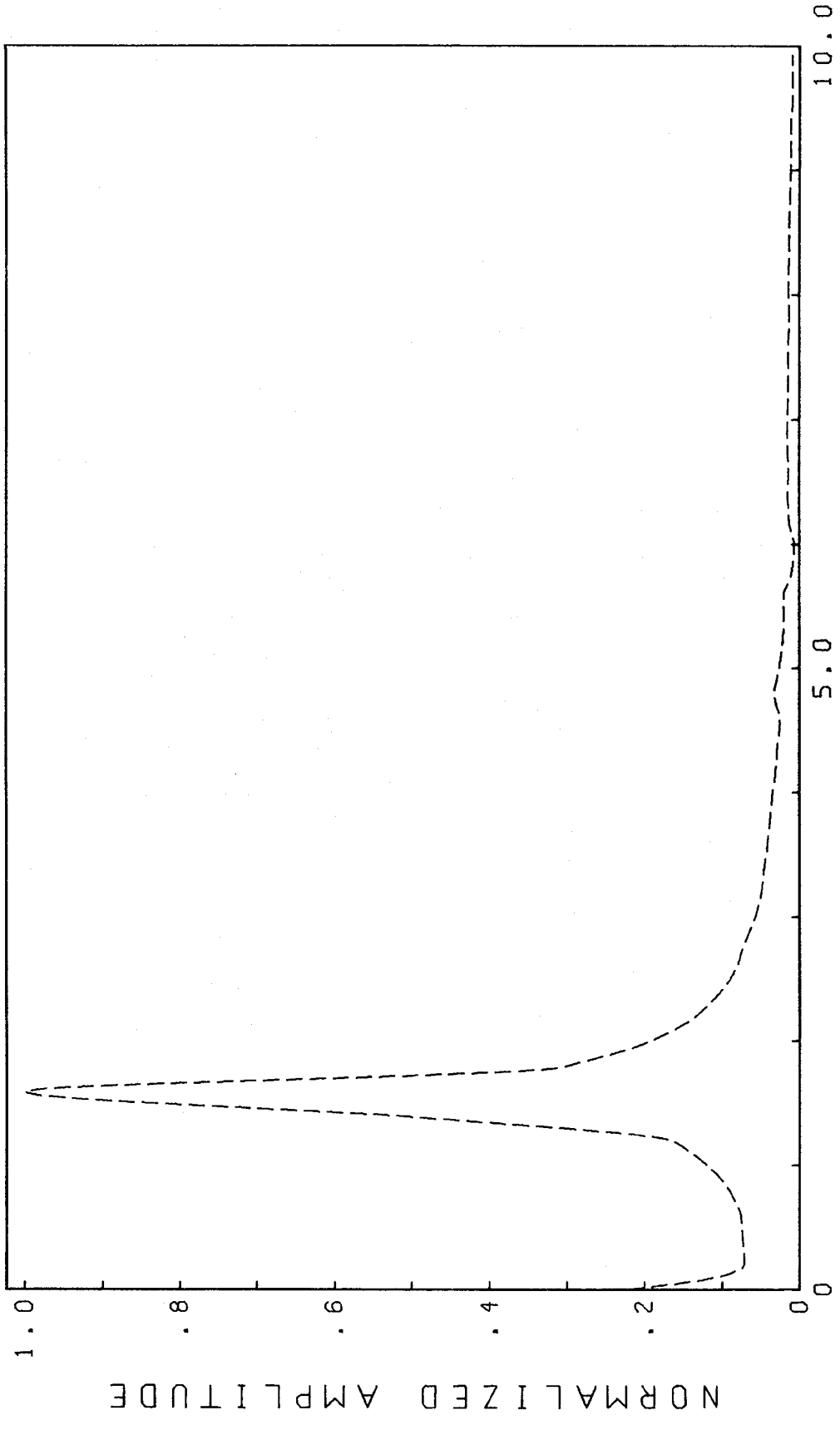

Fig. 4.3d) FFT OF SEGMENT 8 OF BOTTOM STORY DISPLACEMENT. RUN W3.

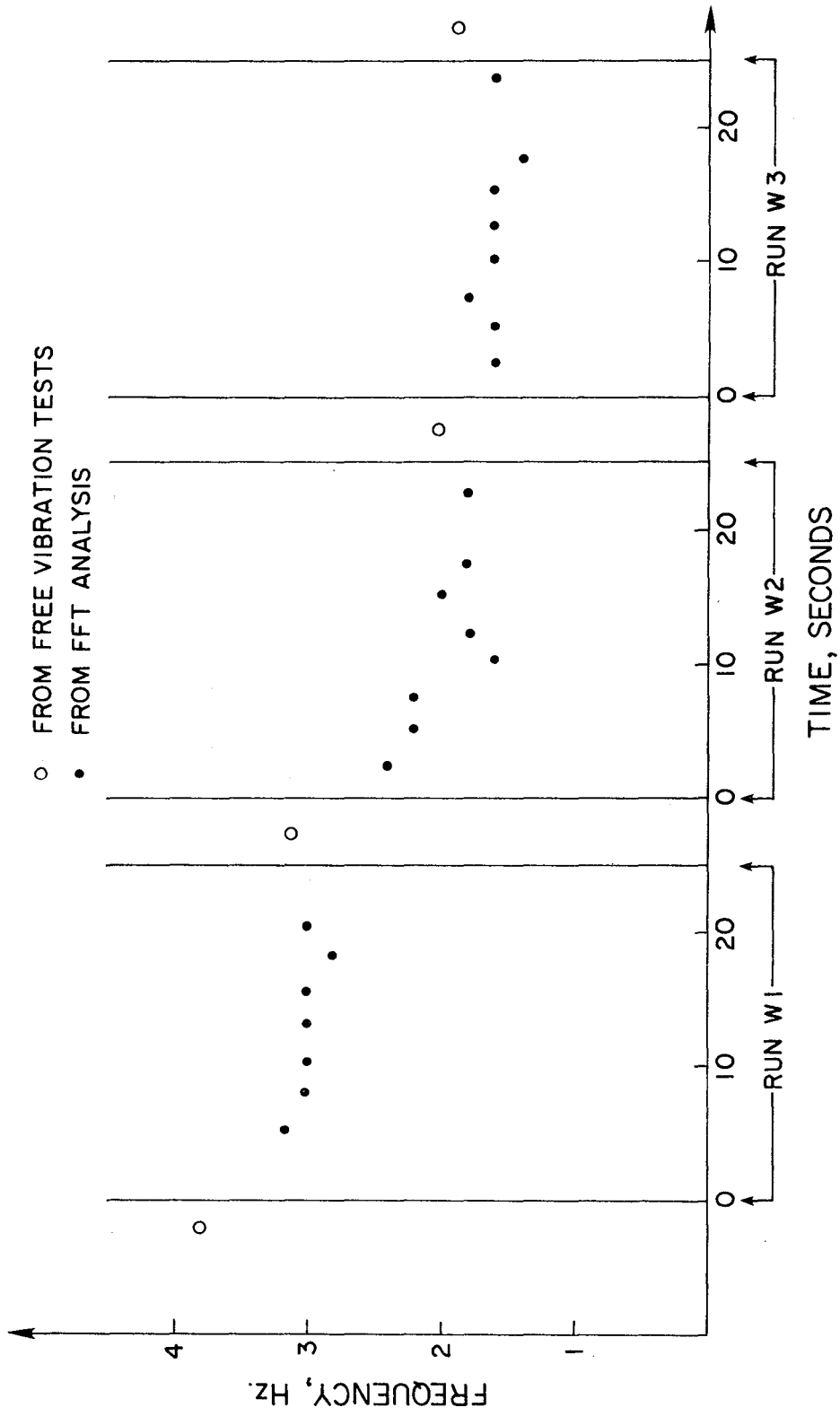

Fig. 4.4 VARIATION OF FUNDAMENTAL FREQUENCY ALONG TEST PROGRAM. (RCF2 - UNREPAIRED)

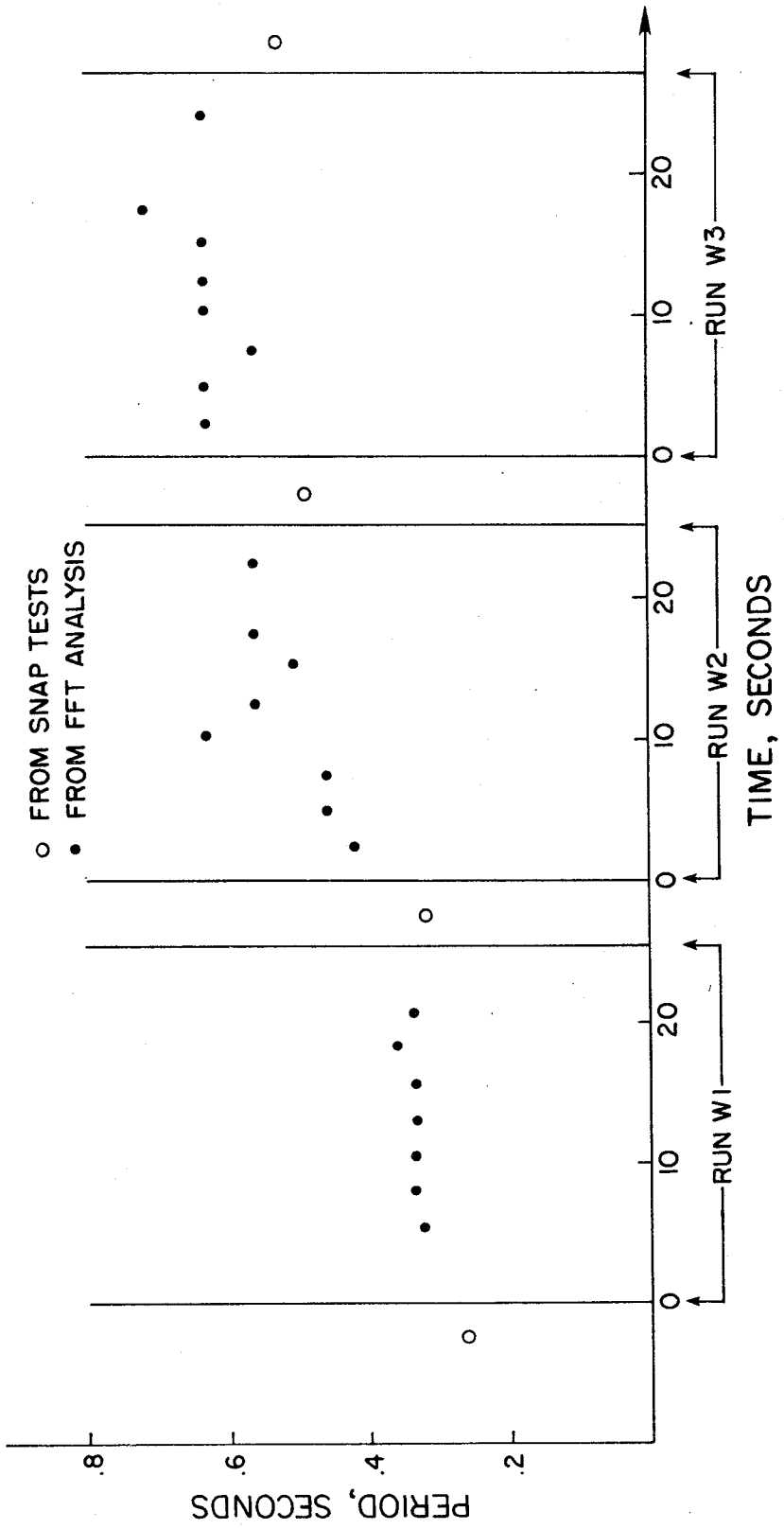

Fig. 4.5 VARIATION OF FUNDAMENTAL PERIOD ALONG TEST PROGRAM.

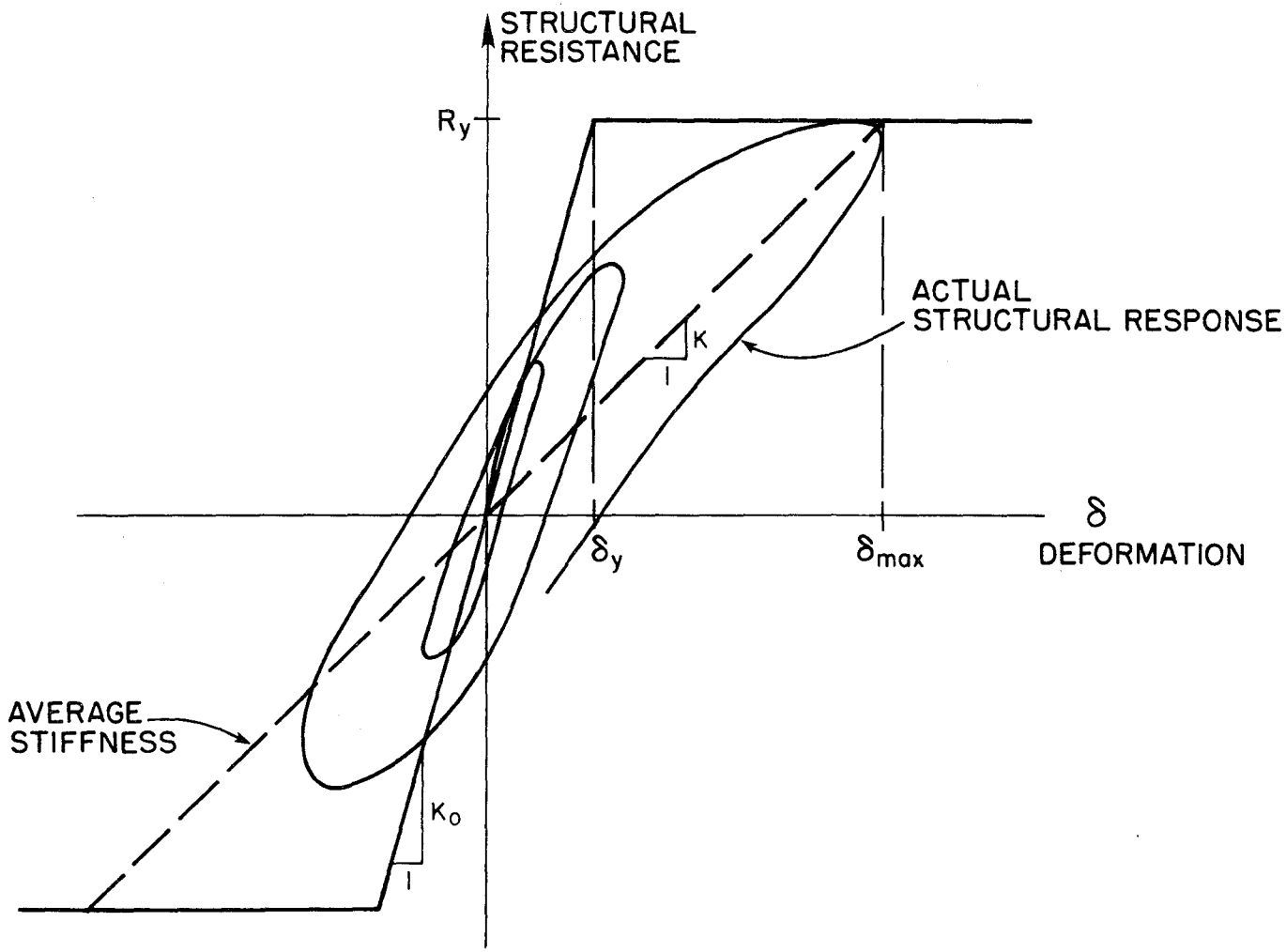

Fig. 4.6 LINEARIZATION OF RESPONSE FOR A GIVEN TIME INTERVAL. (IDEAL DEGRADING MODEL)

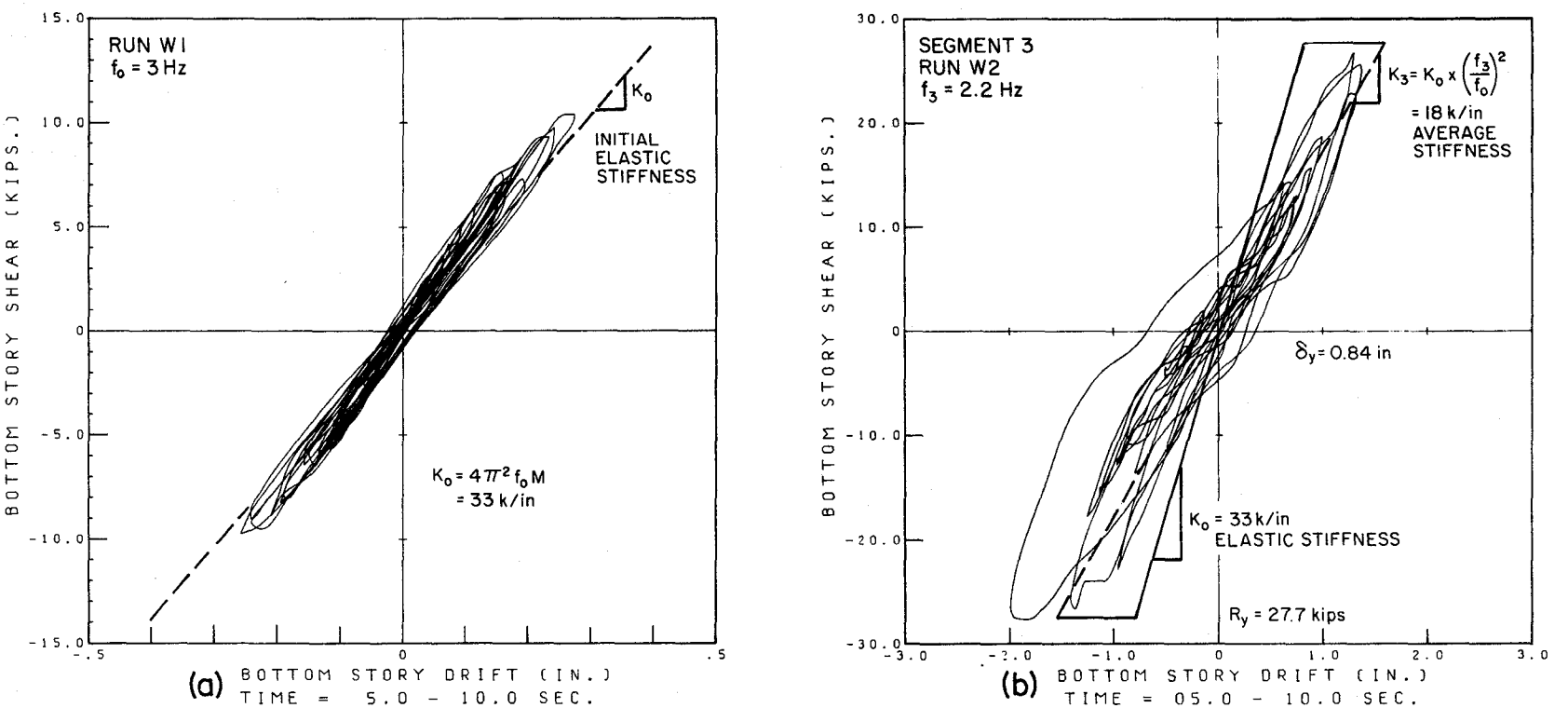

Fig. 4.7 COMPARISON OF PERFORMANCE OF IDEAL DEGRADING MODEL WITH EXPERIMENTAL RESULTS.

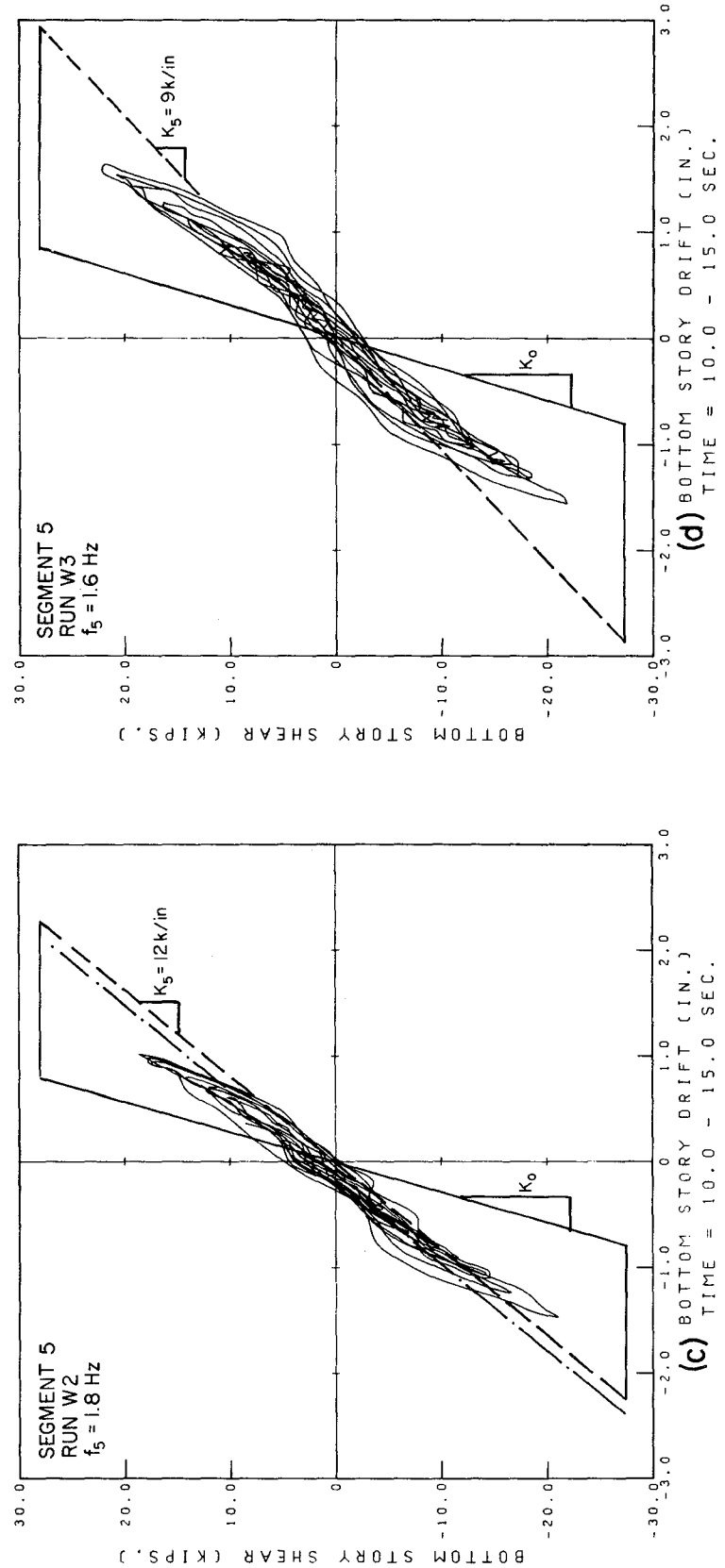
SEGMENT 5
RUN W2
f_5 = 1.8 Hz
K_5 = 12k/in
K_o
BOTTOM STORY SHEAR (KIPS.)
30.0
20.0
10.0
0
-10.0
-20.0
-30.0
-3.0
-2.0
-1.0
0
1.0
2.0
3.0
(c) BOTTOM STORY DRIFT (IN.)
TIME = 10.0 - 15.0 SEC.
SEGMENT 5
RUN W3
f_5 = 1.6 Hz
K_5 = 9k/in
K_o
BOTTOM STORY SHEAR (KIPS.)
(d) BOTTOM STORY DRIFT (IN.)
TIME = 10.0 - 15.0 SEC.

Fig. 4.7 (CONT.)

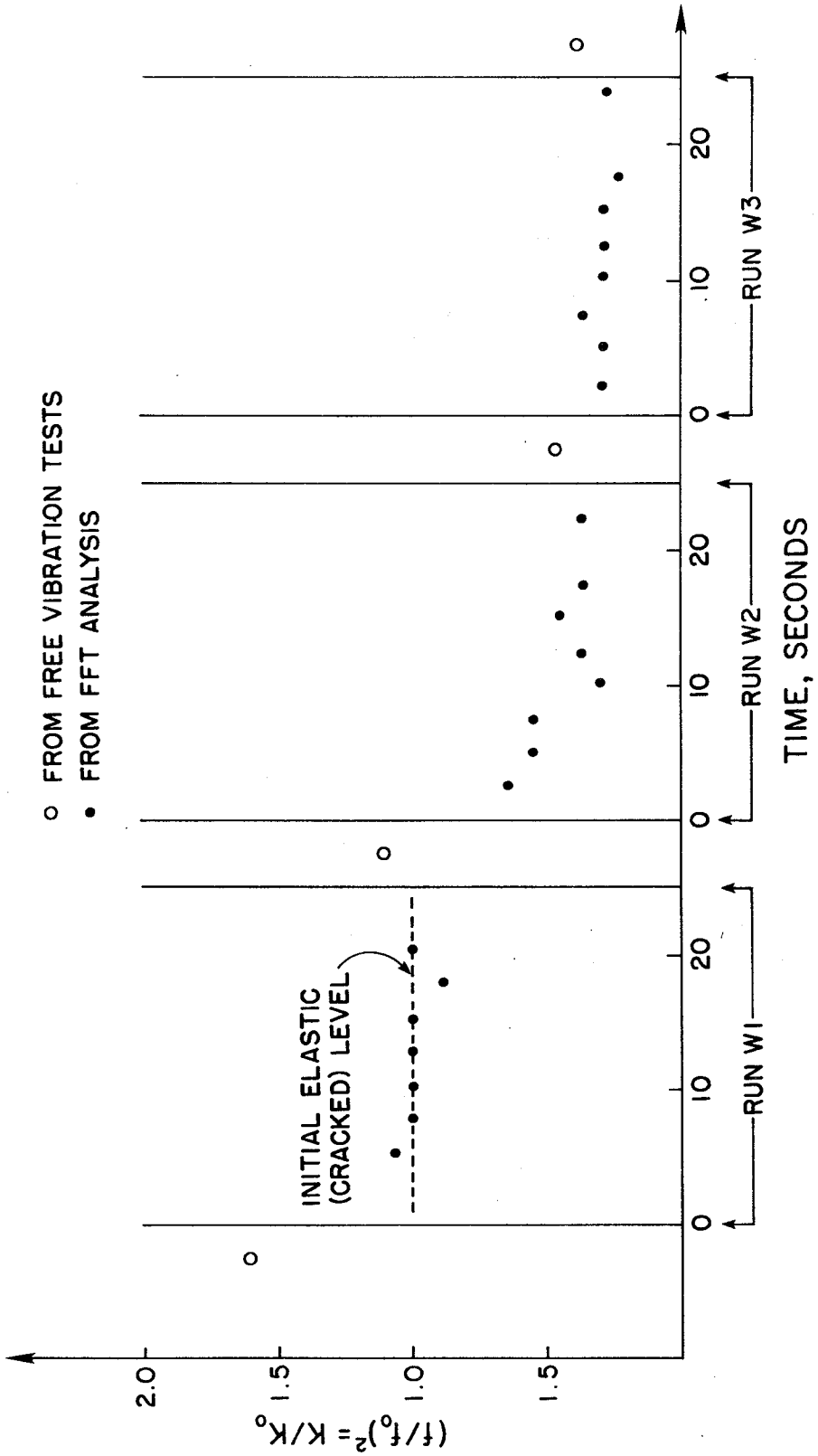

Fig. 4.8 VARIATION OF AVERAGE STIFFNESS ALONG TEST PROGRAM.

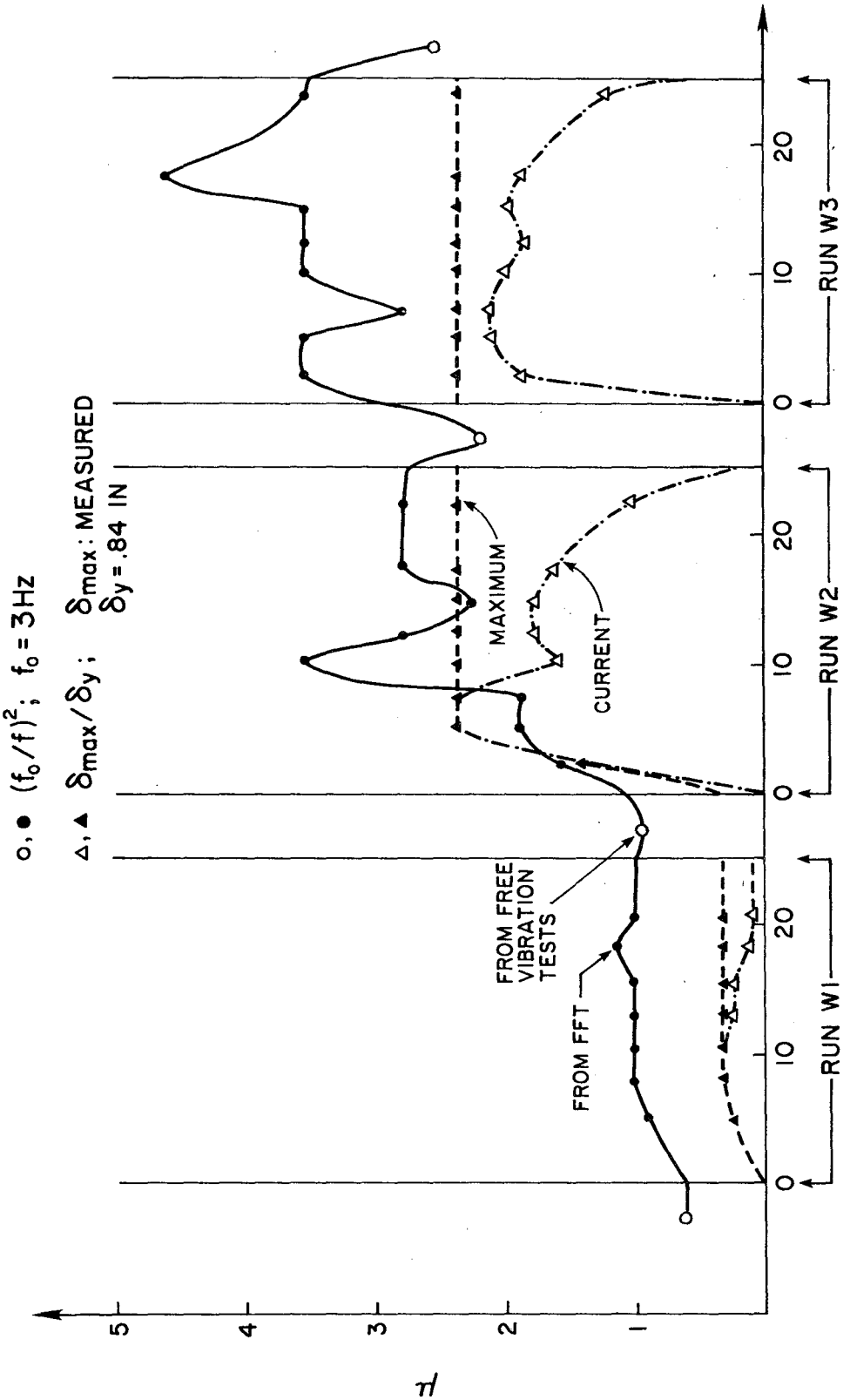

Fig. 4.9 VARIATION OF DISPLACEMENT DUCTILITY ALONG TEST PROGRAM.

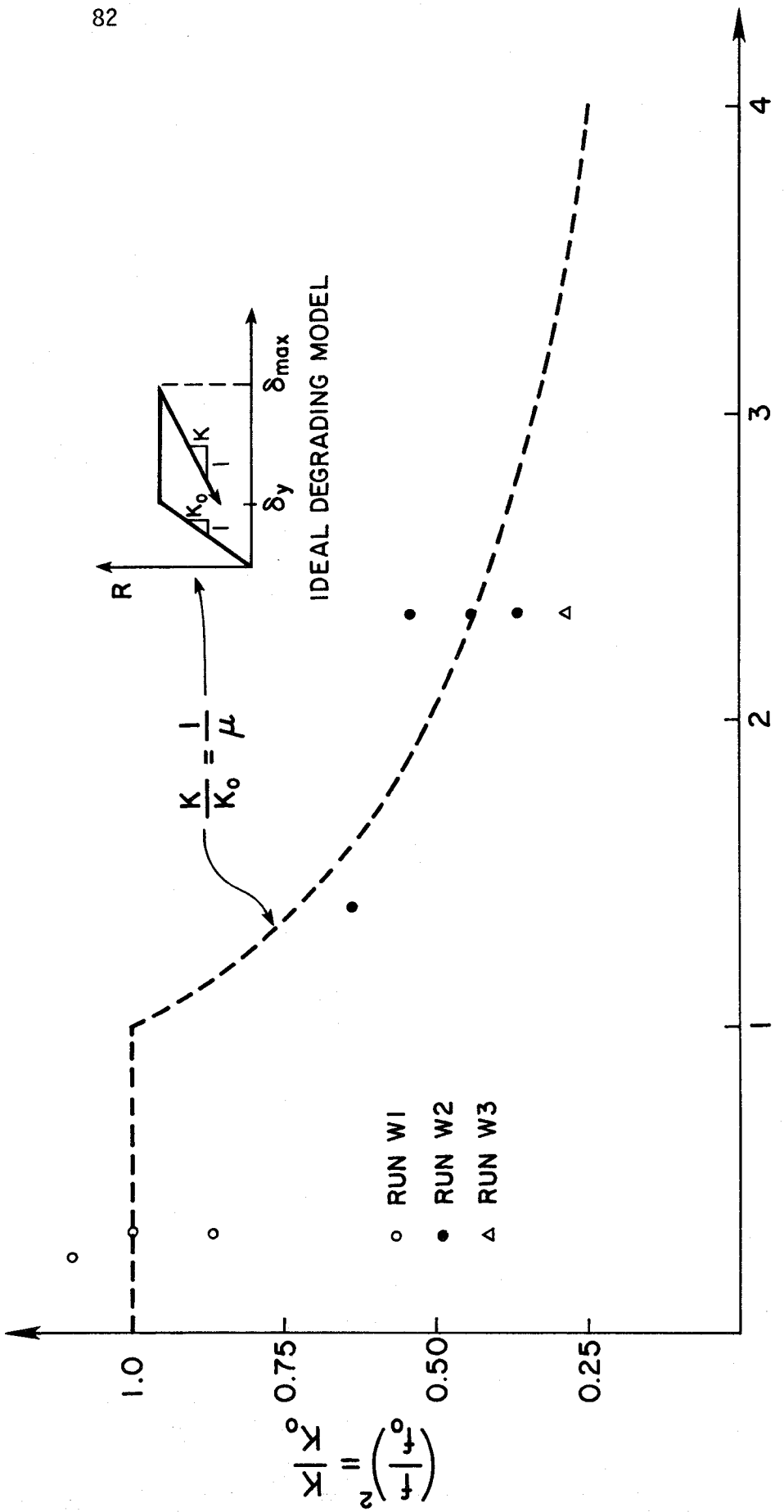

Fig. 4.10 CORRELATION BETWEEN STIFFNESS DEGRADATION AND DISPLACEMENT DUCTILITY (IDEAL AND EXPERIMENTAL)

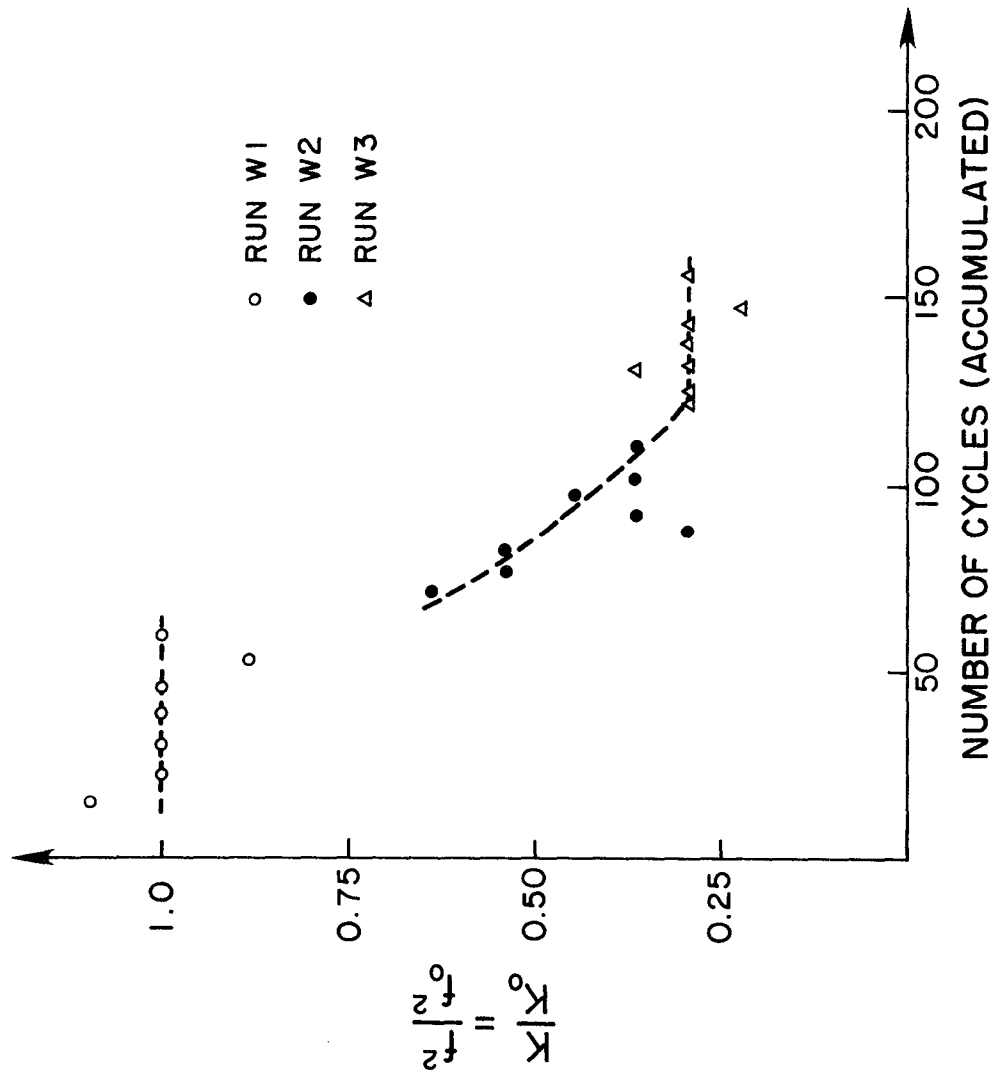

Fig. 4.11 CORRELATION BETWEEN AVERAGE STIFFNESS AND TOTAL NUMBER OF CYCLES OF DEFORMATION.

5)SEISMIC EXCITATION AND STRUCTURAL RESPONSE

5.1 Basic Ideas

The following sections describe some attempts to correlate the response behavior of the test structure to the characteristics of its seismic input. The approach followed was to describe both the input signal and the structural response by means of related, comparable parameters.

One of the most widely accepted measures used to characterize a seismic ground motion is its elastic response spectrum [5]. In particular, the pseudoacceleration (PSA) response spectrum provides a means to compute the maximum lateral force that the base motion would impose on a structure if it remained in elastic condition for the whole duration of the shaking. If the structure does not have the strength to withstand that force, its response to the seismic excitation will entail nonlinear behavior.

A direct comparison of the structural resistance and the PSA spectrum of the ground motion is therefore sufficient to determine whether the structure will remain elastic or behave in a nonlinear way. Starting from that

observation, the results from the previous studies and the experimental measurements were used to determine a way to visualize the extent of the nonlinear behavior imposed on the system due to its strength limitations.

Another concept briefly studied is the temporal distribution of the energy input into the structural system through the ground motion, and the manner in which this energy is absorbed and dissipated by the structure.

5.2 Pseudoacceleration Response Spectrum and Seismic Resistance Coefficient

The correlation of the overall response of RCF2 and the characteristics of its base input was based in the following assumptions:

1) It is possible to globally describe the test structure as a single degree of freedom system characterized by its mass M, its average vibration period T, its resistance R_y, and a viscous damping coefficient ξ. The force-deformation relationship follows approximately the model defined in Fig. 4.6.

2) The seismic input can be characterized by its pseudoacceleration linear elastic response spectrum, $PSA(\xi,T)$. For a lightly damped single degree of freedom

system, this is an approximate measure of the maximum base shear per unit mass (or per unit weight if expressed in "g" units) developed by any linear elastic oscillator with period T and damping coefficient ξ.

3) The overall effect of shaking on a ductile structure is manifested as an increase in the average vibration period and in the viscous damping coefficient ξ.

If the above characteristics of the structure and the base motion are known, it is possible to determine the type of response the system will develop when subjected to the seismic input.

The structure will remain elastic if its yield resistance R_y is never exceeded, or

$$R_y \geq PSA(\xi, T) \cdot W \qquad (5.1)$$

where W is the total weight, and PSA is expressed in g's.

This is equivalent to stating that

$$C_y \geq PSA(\xi, T) \qquad (5.2)$$

where

$$C_y = R_y / W \qquad (5.3)$$

C_y, called the seismic resistant coefficient, is the maximum base shear (per unit weight) that the structure can resist. It also may be interpreted as the maximum pseudoacceleration (in g's) that a seismic excitation can impose on the structure.

In the case where condition (5.2) is not met, or when

$$c_y < PSA(\xi, T) \qquad (5.4)$$

the structural resistance is smaller that the maximum base shear that the ground motion would impose on a linear system with similar period and damping. Therefore, at some point during the shaking the structure will be forced to behave in a nonlinear way, through the occurrence of plastic deformation. As a consequence, its average period, and damping coefficient will change.

From the point of view of seismic resistant design philosophy, a structure is rarely expected to remain elastic during a relatively strong shaking of an intensity likely to occur only a few times during its service life; thus, its seismic resistance coefficient is usually chosen to be smaller than the peak PSA corresponding to these seismic inputs.

In the case of RCF2, the seismic resistance coefficient is

$$c_y = R_y / Mg$$
$$= 27.7 / (0.0924 \times 386.4)$$
$$= 0.78$$

Figure 5.1 shows how this quantity determines a period value, T_y (of about 0.53 seconds) that approximately divides the PSA spectrum corresponding to run W2, (computed for a damping value of about 5%, which was the average

first mode damping coefficient of RCF2 during that run) in nonlinear and linear response period ranges.

This graph defines the type of behavior that any structure with the same seismic resistance and damping as RCF2 would develop if subjected to a base motion similar to the table input in run W2. If the structure has a vibration period smaller than T_y , it will be forced to respond in a nonlinear fashion since its strength level will not be sufficient to withstand the seismic demand. Conversely, if the structural period is larger than T_y , the structure will most probably remain elastic.

Since its initial vibration period was smaller than T_y , RCF2 was in the spectrum region where $PSA > C_y$. As a consequence, it suffered significant nonlinear behavior (it would have had to be able to withstand a pseudoacceleration larger than 1.4 g in order to remain elastic) which caused a noticeable increase in its vibration period (as also shown in figure 5.1) and of its damping coefficient (presented in Table 3.2).

The response spectrum concept is limited in the sense that the spectral quantities correspond to extreme response values which, in general, occur at a different times during the seismic event; therefore, it is difficcult to ascertain when the nonlinear response is going to occur. For this

reason, the concepts of pseudoacceleration response spectrum and seismic resistance coefficient need to be extended to include the temporal evolution of the input and the response.

5.3 Pseudoacceleration Response Surface and Effective Acceleration

The pseudoacceleration response spectrum of a given seismic ground motion is usually computed by evaluating the displacement response of linear elastic oscillators with constant damping factor ξ, and period T, taking the peak displacement during the response, D_{max}, and defining

$$PSA(\xi, T) = \omega^2 \cdot |D_{max}| \qquad (5.5)$$

where

$$\omega = 2\pi / T \qquad (5.6)$$

It is customary to fix the value of the damping factor, ξ and to plot the spectral values as a function of period only, as in Fig. 5.1 for run W2.

In order to observe the evolution of the response of the linear oscillators during shaking, the response spectrum concept can be extended by defining

$$PSA(\xi, T, t) = \omega^2 \cdot D(t) \qquad (5.7)$$

where $D(t)$ is the envelope of the absolute value of the displacement response of a linear elastic oscillator

with damping ξ and period T to the given base motion. For a fixed value of damping, this expression defines a surface, the envelope of the pseudoacceleration response as a function of period and time.

This quantity was evaluated for run W2 and for 5% damping using the standard program SPECEQ [6]; the resulting surface was plotted using the Surface Display Library programs [7] available at the Computer Center at UCB. Figure 5.2 shows a contour map where the elevations represent the PSA (in g's) for the period range of 0.1 to 0.9 seconds, for the whole duration of the test. Figure 5.3 presents a contour view, and figure 5.4 a "mesh view" of the response surface observed from the same viewpoint.

Clearly, these graphs contain more information about the table input signal than the standard PSA response spectrum (Fig. 5.1), which is the projection of the surface on the PSA -Period plane.

The intersection of the surface with a plane perpendicular to the period axis at a value T is the envelope of the pseudoacceleration response of any linear oscillator with that vibration period (and 5% viscous damping) as a function of time; therefore it gives approximately the envelope of the base shear per unit weight (in absolute value) imposed on such systems by the

input excitation. This curve can be clearly observed in Figs. 5.3 and 5.4, for a period value of 0.9 seconds.

Figure 5.5 depicts the variation of the fundamental period that RCF2 suffered during run W2, with respect to the contour map of the PSA response surface of the table input. The shaded areas represent zones for which the pseudoacceleration level is larger than the seismic resistant coefficient (about 0.8 g). Very interesting observations can be made by analyzing the relationship between input base motion and the structural response along the course of the test, as follows.

The structure suffered an initial loss of stiffness at the very beginning of the test, due probably to the opening of the concrete cracks during the first few seconds of shaking. As a consequence,its vibration period increased from 0.32 to 0.45 seconds, which corresponds to the elastic, cracked state. If the strength of the structure had been very large, this period would have remained fairly constant during the whole duration of the test, and the structure would have to absorb a pseudoacceleration level larger than 1.4 g at about 8 seconds. However, the strength of the structure, measured by its seismic resistance coefficient was only of about 0.8 g. Consequently, the structure had to undergo inelastic deformation, thus changing its vibration period.

This modification can be interpreted as the structure changing its mechanical properties to remain within a less demanding region of the surface.

To study the effect of the base motion, characterized by its response surface, on the actual response of test structure, it was necessary to introduce a response quantity similar to pseudoacceleration but applicable to nonlinear structures, such as RCF2. The base shear per unit mass developed on the structure, named effective acceleration, seemed to be an appropiate parameter, since it is dimensionally similar , and for a single degree of freedom oscillator, perfectly elastic and undamped, it is identical to the pseudoacceleration response.

The response of a structure during shaking can therefore be characterized by the evolution of the effective acceleration, a measure of the seismic force absorbed, (the seismic resistance coefficient, C_y , is also the maximum effective acceleration the structure is capable to develop) and the average vibration period, which describes the effect of that force on the system.

Figures 5.6 and 5.7 show the correlation between the response surface and the effective acceleration for the case of run W2. The dashed line represents the effective acceleration developed by the structure as a function of

its vibration period and of the time during the test. The PSA response surface has been "cut" for periods larger than the current structural period, to enhance the comparison between PSA and the effective acceleration.

The relationship between the input, the table shaking, and its effect on the structure can be easily observed in these two figures, which show in a very visual way the basic phenomena occurring during the test.

5.4 Energy Considerations

To complement the findings presented in the previous sections, it was decided to study the experimental results from the energy distribution point of view.

The input energy was computed as the work done by the base shear force acting on the the table displacement. The accumulated energy imposed on the structure as a function of time is shown in Fig. 5.8 for run W2. It can be seen that there are several instants when the table supplies large amounts of energy to the structure in very short time intervals. This effect essentially starts at about 3.5 seconds after the beginning of the test, and is especially apparent during the time interval from 5 to 8 seconds, when about 40% of the total input energy is delivered to the structure. These sudden bursts of energy input probably can

account for the significant damage the structure suffered during those intervals.

In order to visualize the distribution of the input energy within the test structure, the work done by the story shears over their respective interstory drifts was computed and plotted in Fig. 5.9. This graph confirms the observation that most of the damage occurred in the bottom story members; they absorbed more than 5 times the energy of those on the second story. It also shows when most of the damage occurred. The oscillations of the work curves are the result of the interchange between elastic and kinetic energy during the oscillations of the floors around their equilibrium positions. The accumulating values represent the irrecoverable energy dissipated through hysteretic behavior and damping effects.

The total energy input to the structure was computed to be 194.2 kip-in. The work done by the story shears acting over the interstory drift was evaluated at 173.2 kip-in for the bottom story and at 30.0 kip-in for the top story, giving a total of 203.2 kip-in, which is about 5% higher than the input energy. This obviously is an indication of some errors in the evaluation of the forces acting on the structure, or in the measured displacements (assuming that the numerical algorithm used is not responsible for the discrepancy).

A troublesome aspect of this problem was that the story shears were derived from the measured floor accelerations, therefore the discrepancy could be the result of inconsistent measurements of the floor displacements and accelerations. This problem led the research effort to the verification of the quality of the measured data. Part B of this report describes the studies performed, which indicate that the displacement and acceleration records are satisfactorily consistent with each other. The error in the energy computation therefore can be due to a miscalculation of the mass distribution of the structure , or to the numerical algorithm used to compute the work done by the shear forces (some of the difficulties that arise in numerical integration are also hinted at in part B). Fortunately the error is small, and the results can be used in a qualitative way, to roughly describe the energy aspects of the simulated seismic event.

5.5 Practical Implications

The studies on the PSA response surface show that it is a useful description of a seismic ground motion from the point of view of its capability to induce damage in structures. The response surface can be seen as the "fingerprint" of the earthquake, since it not only presents the response for all linear systems (with a given damping coefficient and within a prescribed vibration period

range), but, as in the case of RCF2, it clearly indicates the nature of the behavior that can be expected in a structure with limited seismic resistance.

The results obtained for RCF2 suggest that it is possible to estimate the total change of vibration period a structure would suffer when subjected to a given base excitation using the usual response spectrum concept, if the structural characteristics (initial vibration period, seismic resistance and damping coefficient) are known.

If the initial vibration period, T, is smaller than the "yield" period T_y, then the structure will behave inelastically, as in the case of RCF2. The final vibration period will be close to T_y, since this is the minimum period for which the pseudoacceleration is smaller than or equal to the resistance coefficient of the structure.

If the force deformation of the system is modelled as shown in Fig. 4.6, the change in vibration period can be correlated with the maximum displacement the structure would undergo under the seismic input being considered, and thus with the displacement ductility that will be demanded from the structure.

Conversely, this idea can be used to determine the resistance a structure will need to withstand a certain

seismic input, if the acceptable level of displacement ductility is defined. This idea has been formulated by Sozen and Gulkan [8], from results obtained from shaking table tests performed on a reinforced concrete frame model.

This idea is very simple and appealing, at least for preliminary design, since by merely using the standard linear elastic response spectrum concept it is possible to roughly predict the level of nonlinear behavior that can be expected in a ductile structure, when subjected to a given seismic input.

Regarding the energy aspects of the seismic behavior of reinforced concrete structures, the experimental results were used to verify the adequacy of a measure developed by Housner and Jennings [9] to represent the capacity of a ground motion to supply energy to linear structures of all frequencies. It is called the frequency ensemble work and is defined by

$$W_f = \frac{\pi}{2} \int_{-\infty}^{\infty} a^2(t)\, dt \qquad (5.8)$$

Figure 5.10 shows the integral of acceleration squared as a function of time for run W2. The value corresponding to the end of the test is about 587 ft^2/sec^3. This quantity exceeds the threshold value of 500 ft^2/sec^3 defined by Housner and Jennings, corresponding to ground motions capable of inflicting significant structural damage, with

even some likelihood of collapse. The experimental results are therefore in accordance with the Housner and Jennings criterion, since RCF2 suffered a considerable amount of damage under run W2.

Since the experimental data available is still limited, these results should be used with care, until more information about their reliability is obtained. For example, the correlation between vibration period and ductility demand show that, in general, the predicted ductility is larger than the actual value, due to the simplicity of the mathematical model used. Perhaps with a slightly more refined model this result could be obtained in a more realistic way which would enable it to be used with confidence for earthquake-resistant design purposes.

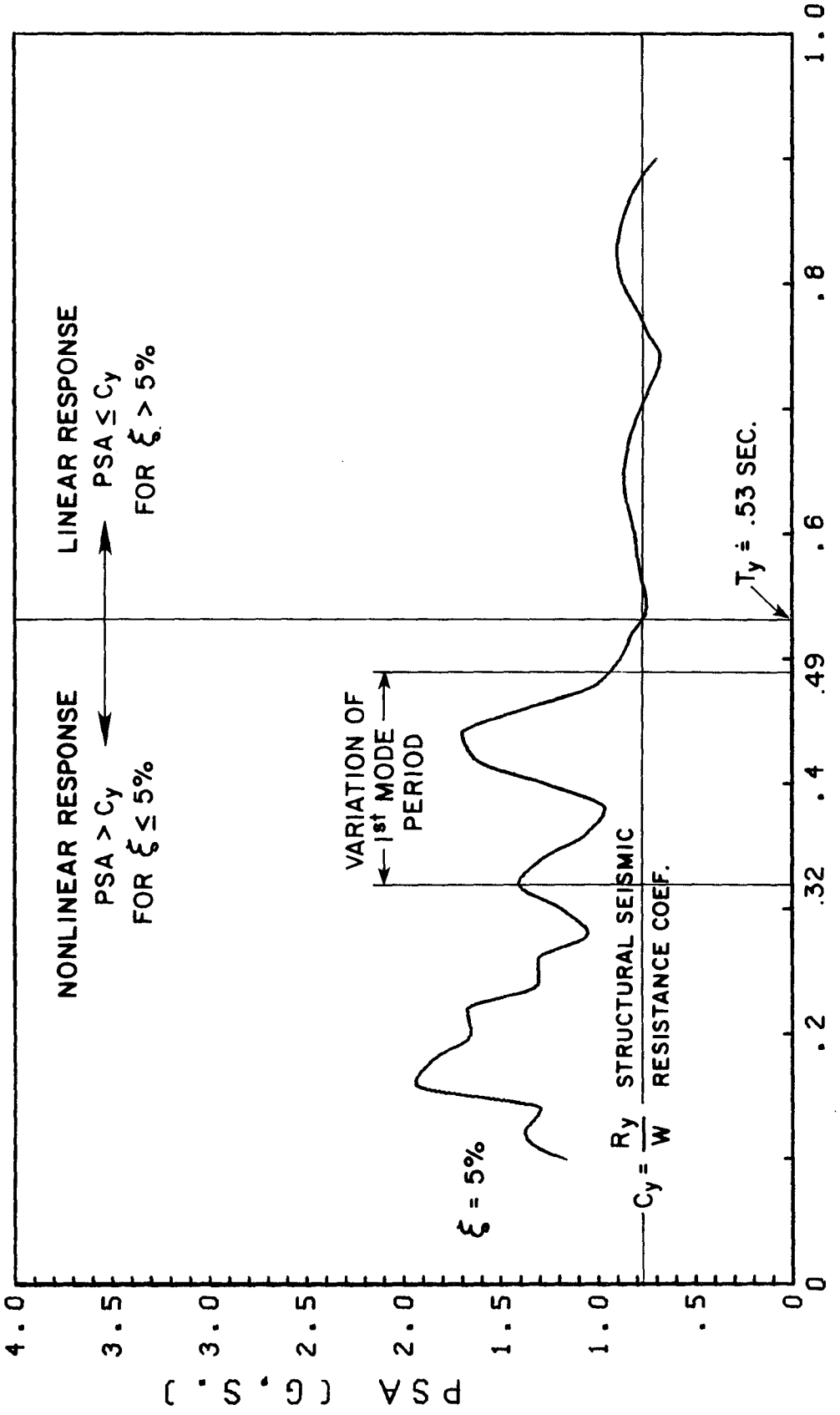

Fig 5.1 PSEUDOACCELERATION RESPONSE SPECTRUM AND SEISMIC RESISTANCE COEFFICIENT. RUN W2.

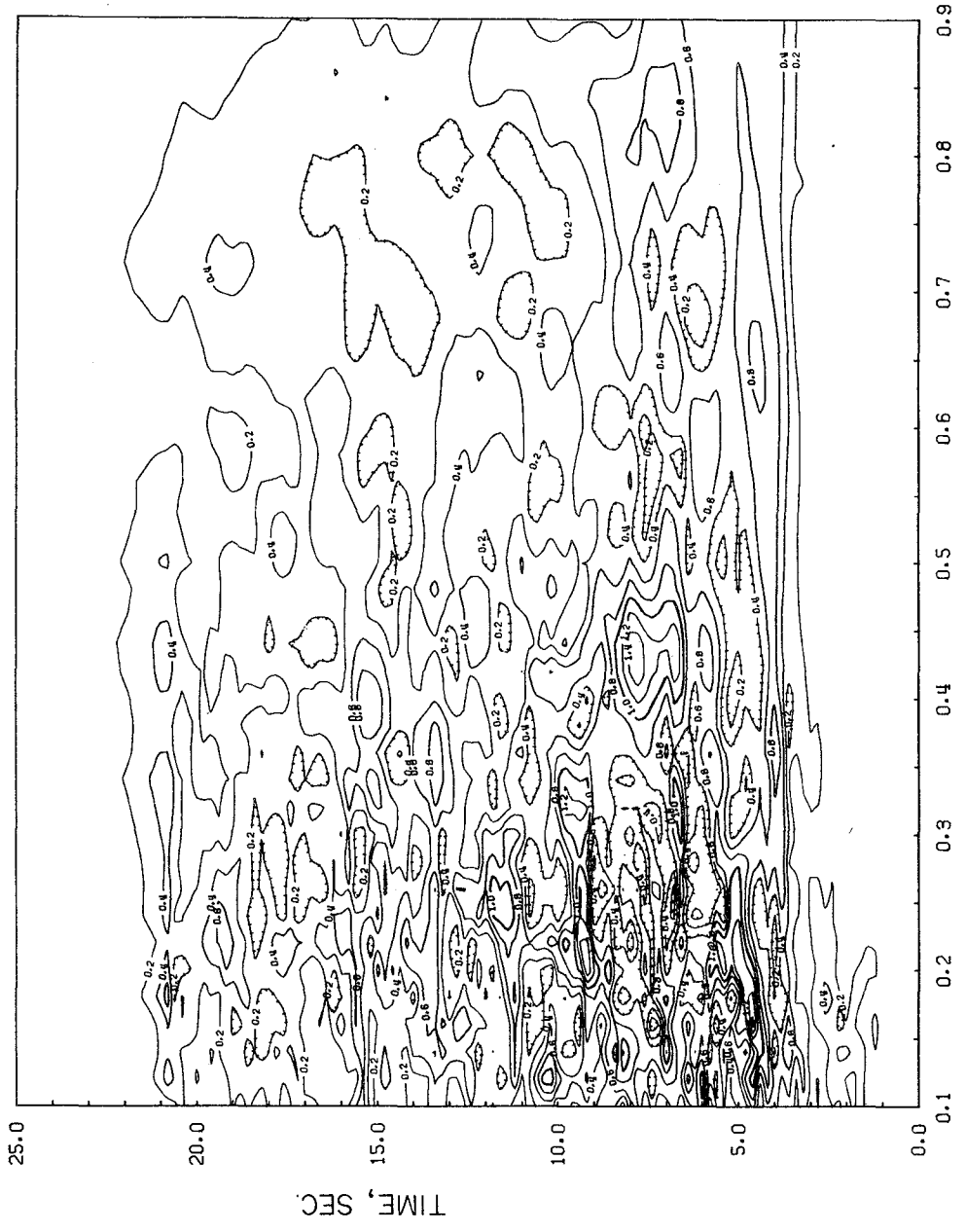

Fig. 5.2 PSEUDOACCELERATION RESPONSE SURFACE.
CONTOUR MAP. RUN W2.

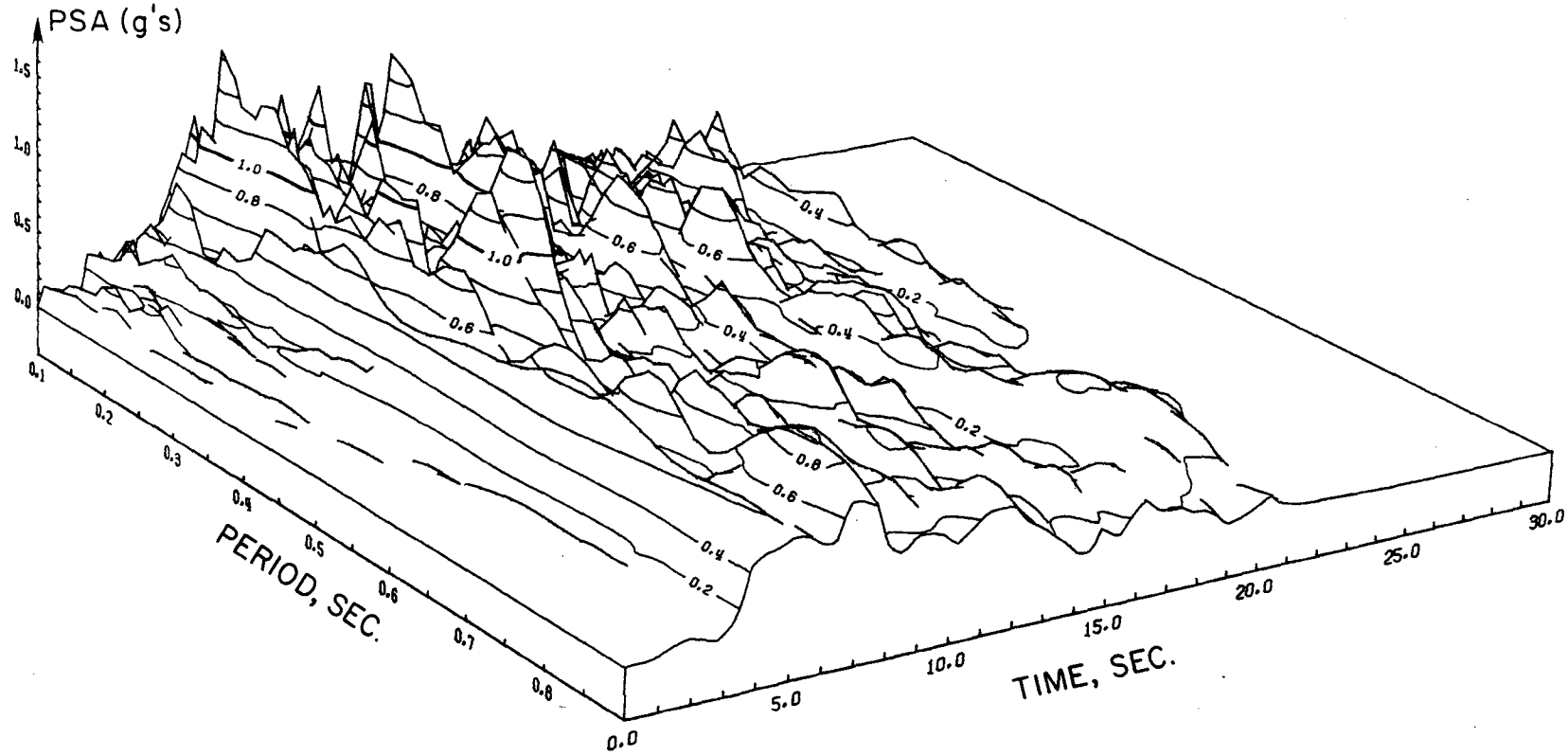

Fig. 5.3 PSEUDOACCELERATION RESPONSE SURFACE.
CONTOUR VIEW. RUN W2.

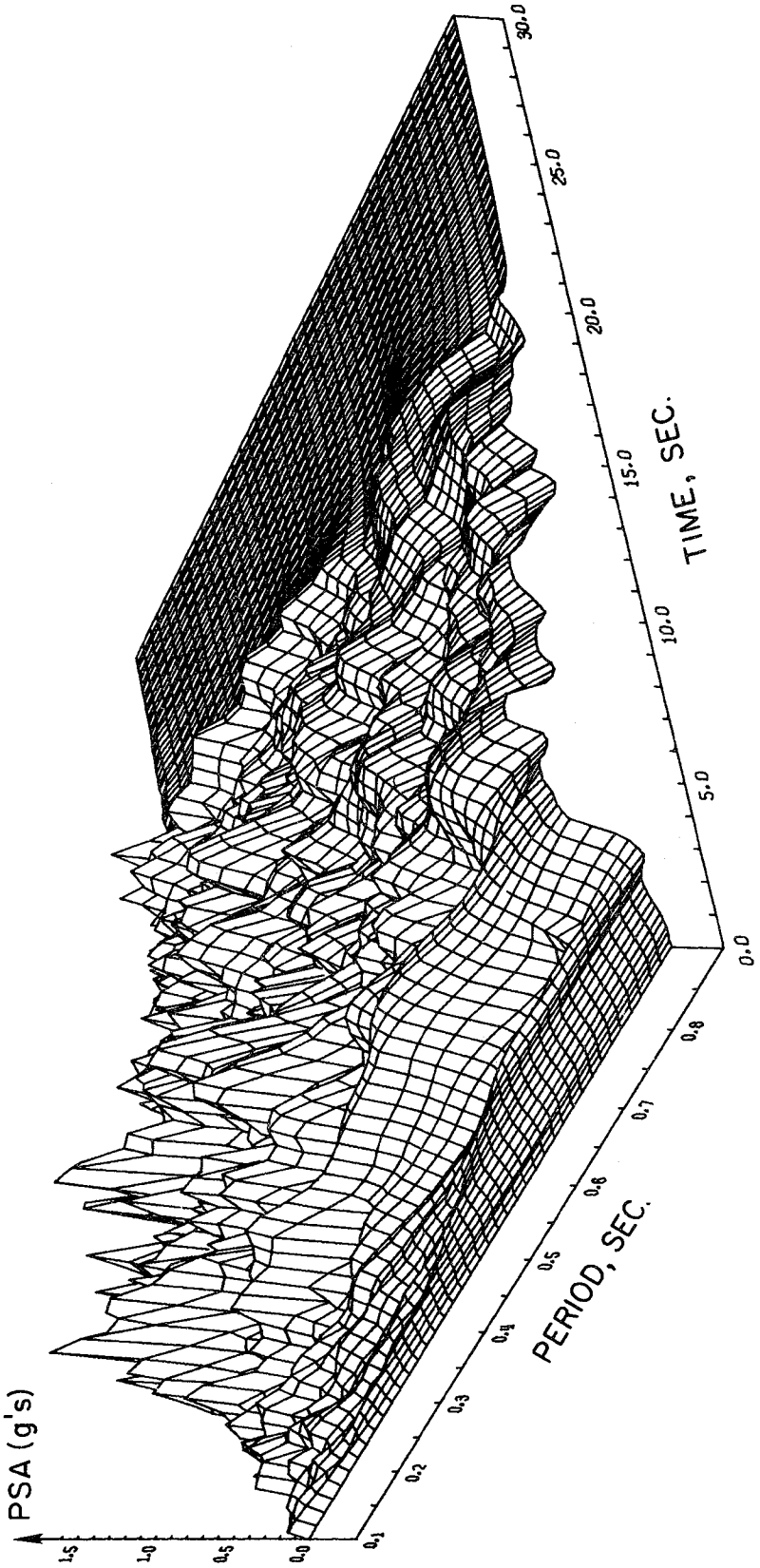

Fig. 5.4 PSEUDOACCELERATION RESPONSE SURFACE.
MESH VIEW. RUN W2.

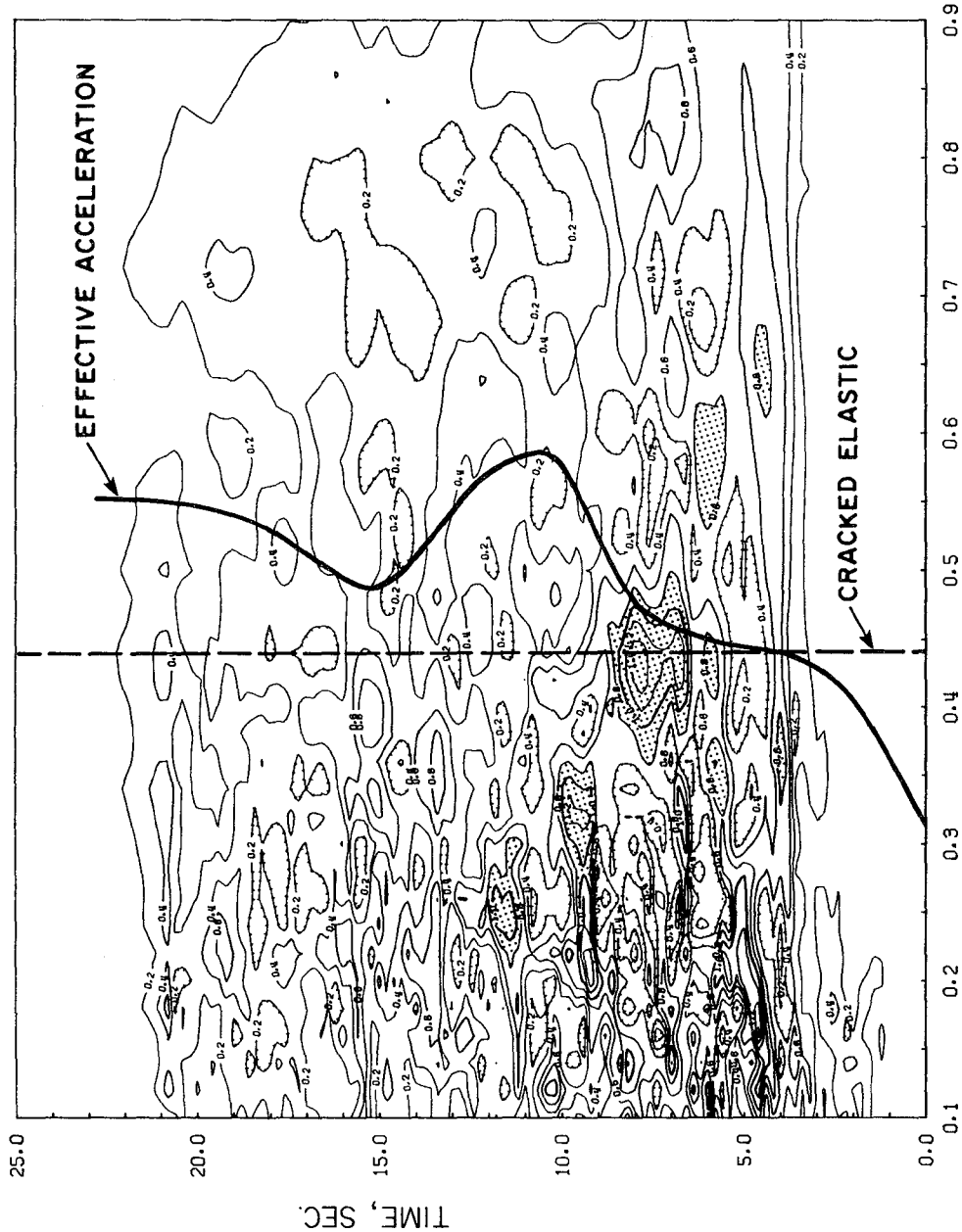

Fig. 5.5 PSEUDOACCELERATION RESPONSE SURFACE AND EFFECTIVE ACCELERATION. CONTOUR MAP. RUN W2.

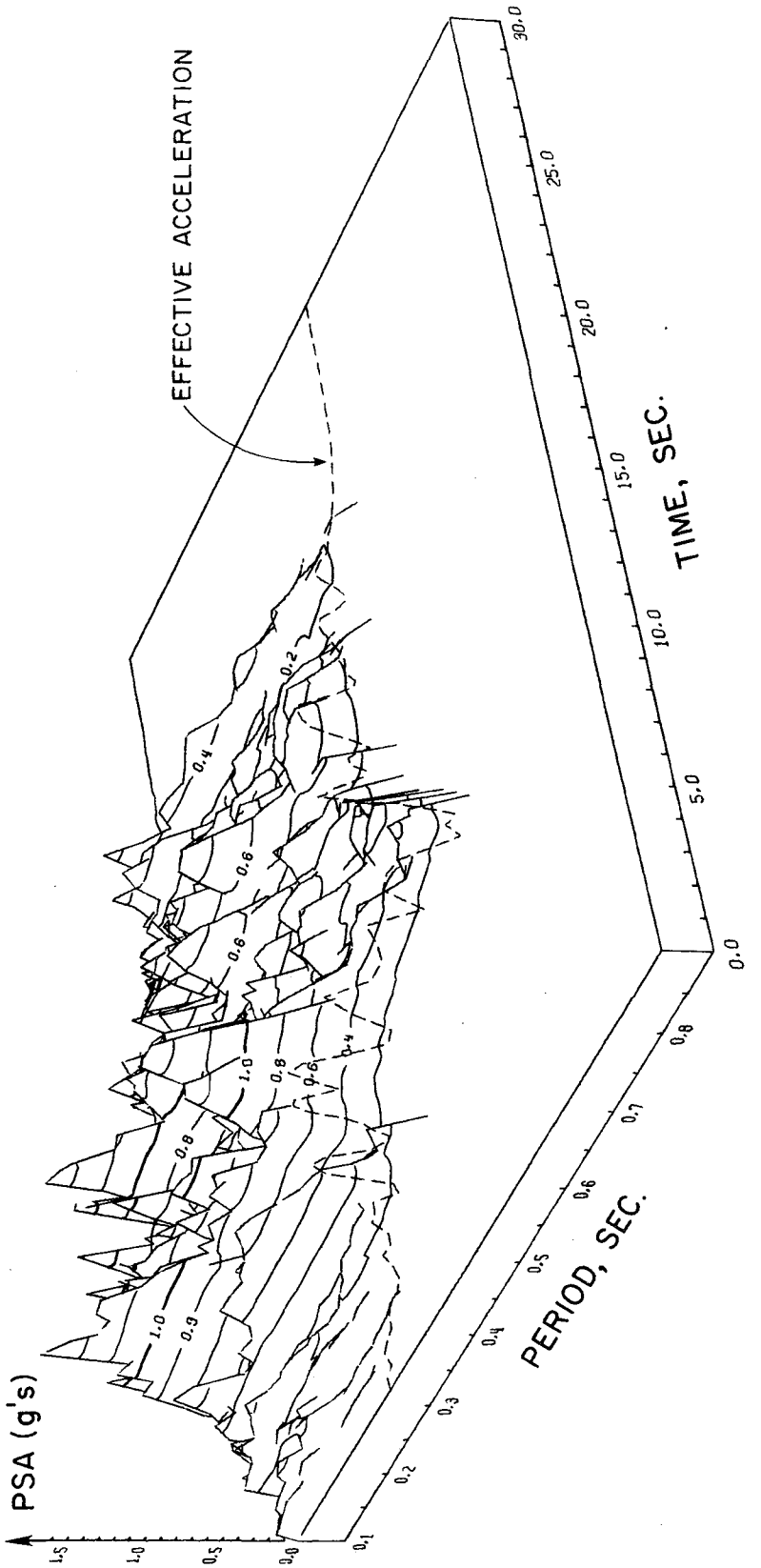

Fig. 5.6 PSEUDOACCELERATION RESPONSE SURFACE AND EFFECTIVE ACCELERATION. CONTOUR VIEW. RUN W2.

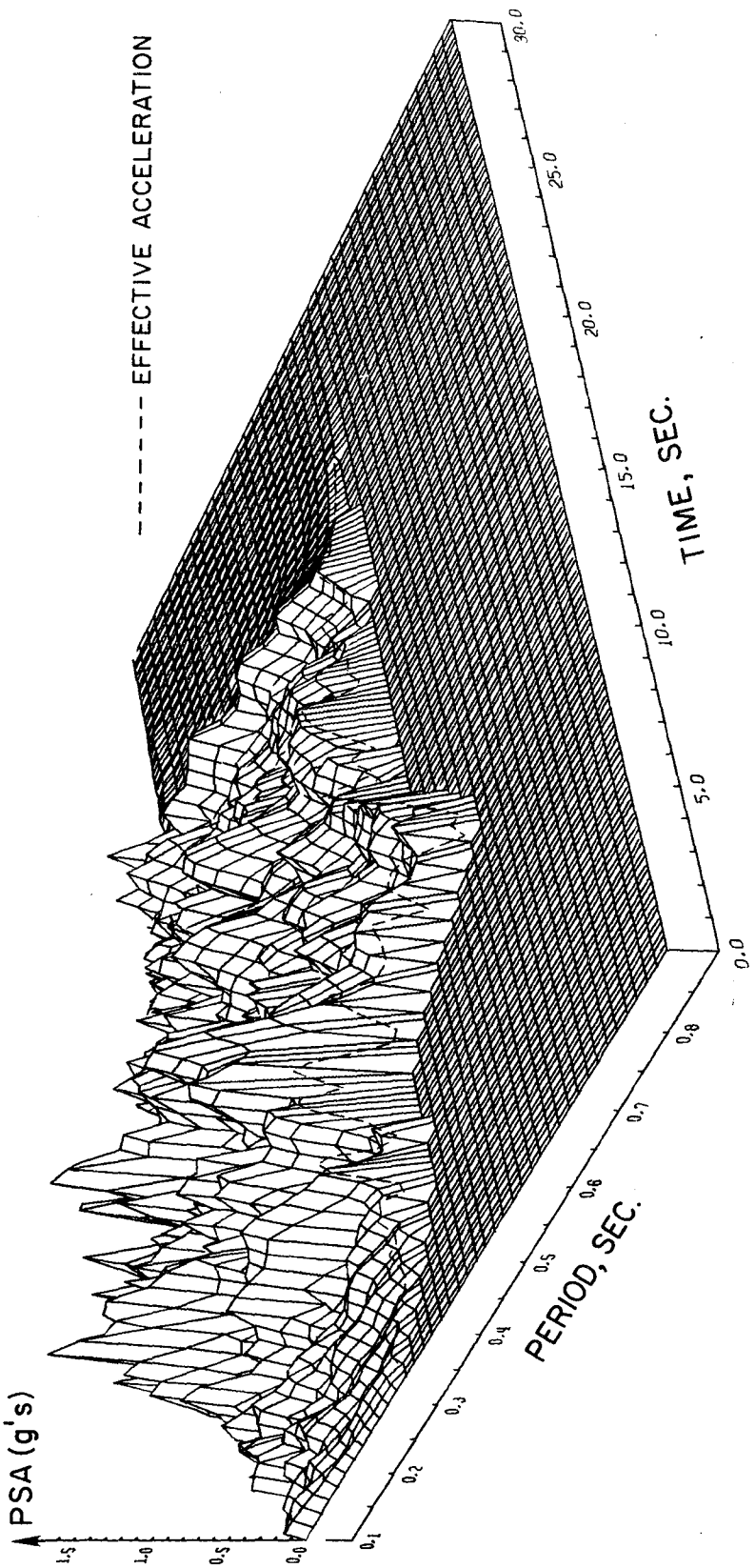

Fig. 5.7 PSEUDOACCELERATION RESPONSE SURFACE AND EFFECTIVE ACCELERATION. MESH VIEW. RUN W2.

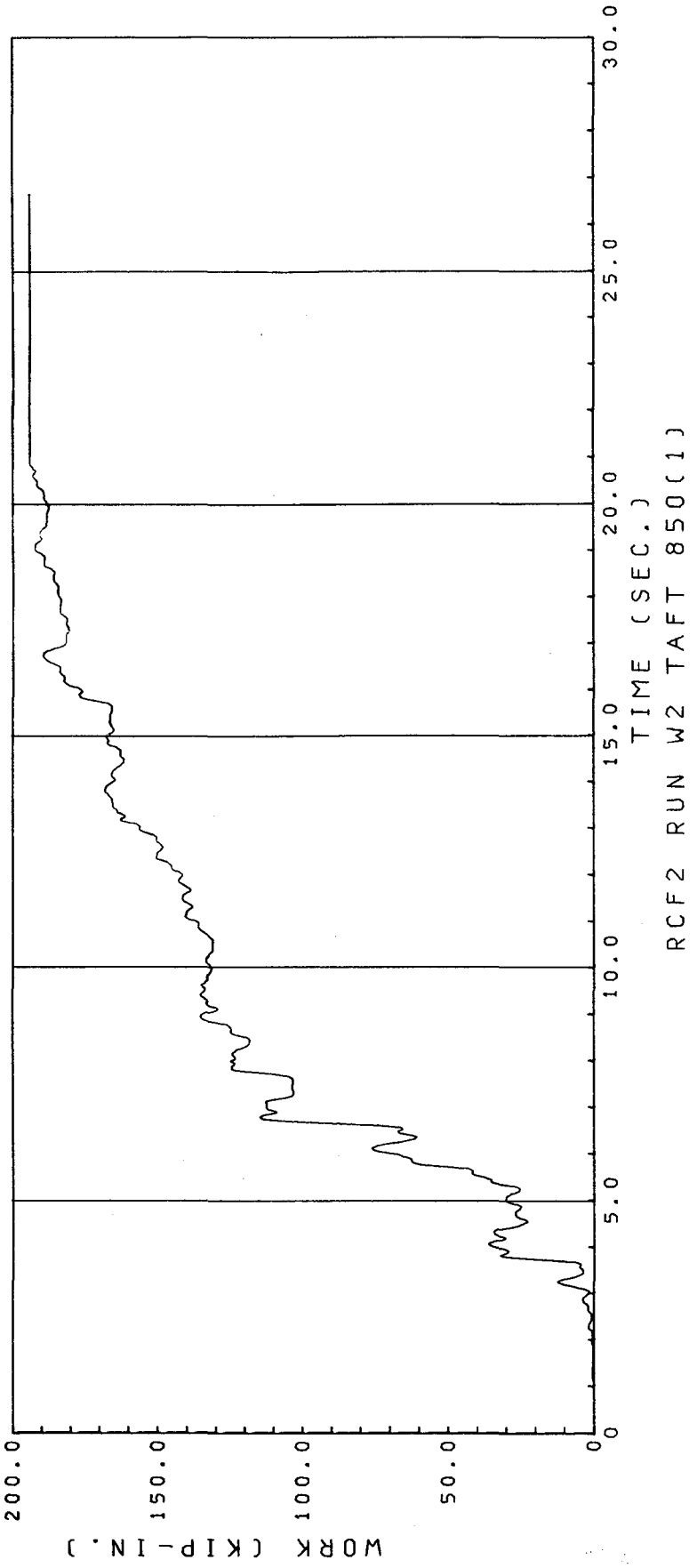

Fig. 5.8 ENERGY INPUT TO RCF2 BY THE SHAKING TABLE. RUN W2.

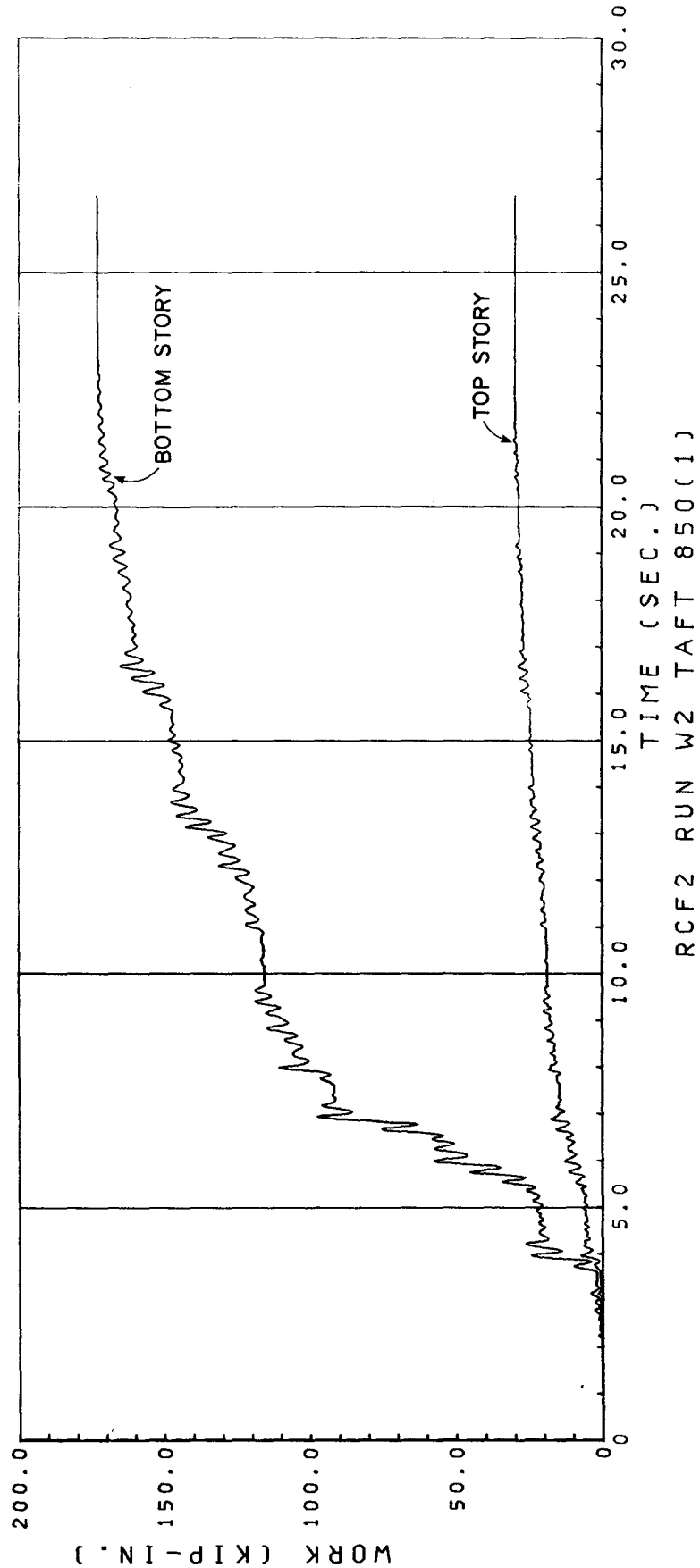

Fig. 5.9 WORK DONE BY THE INTERSTORY SHEARS OVER THE INTERSTORY DRIFTS. RUN W2.

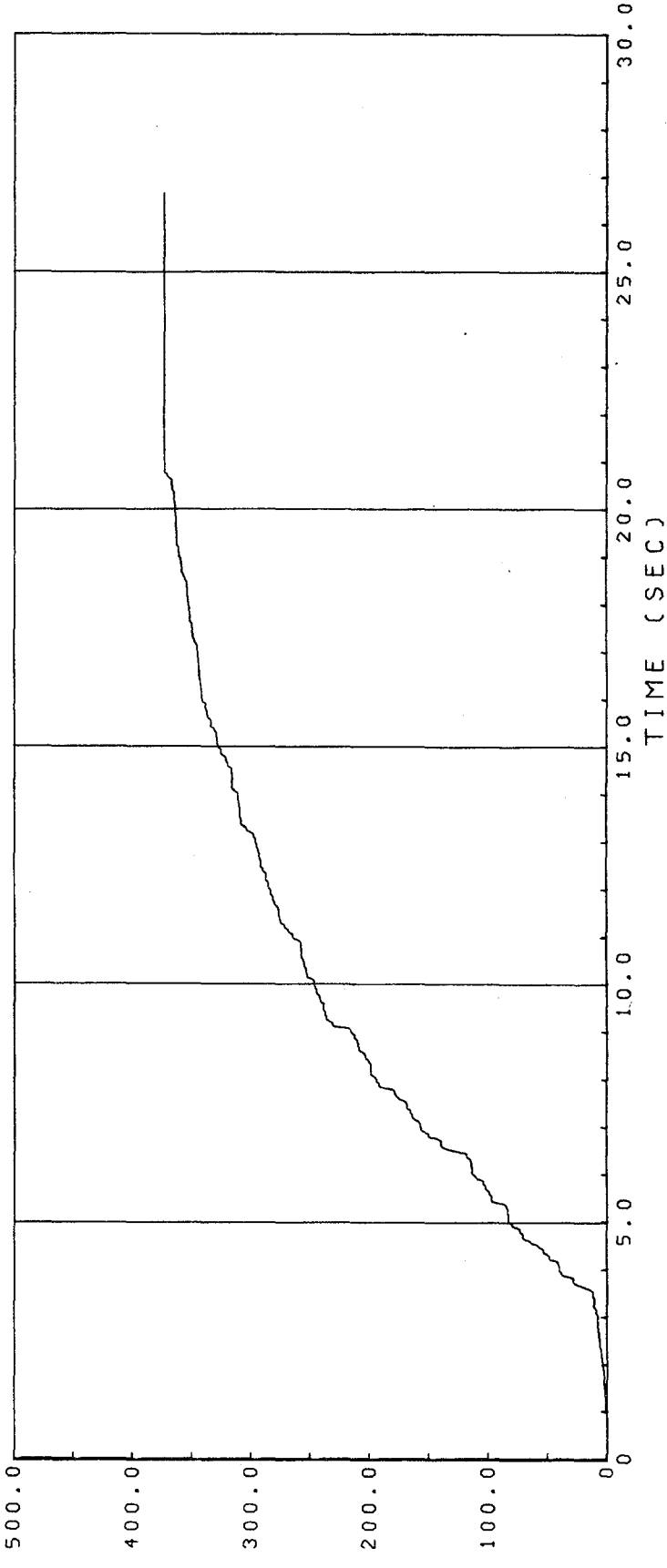

Fig. 5.10 INTEGRAL OF THE SQUARE OF THE SHAKING TABLE ACCELERATION (FT2/SEC3). RUN W2.

6)FINAL REMARKS

The previous sections describe some studies performed using the information gathered during seismic experimentation with a reinforced concrete frame model. Since they were applied basically to only one of the various tests performed, the findings presented are by no means complete, and the generalization of the results obtained to other cases is not an easy task.

The results obtained demonstrate, however, the enormous potential of shaking table testing to provide useful information, and the diversity of ways that the information can be processed to better understand the different aspects involved in the seismic performance of structural systems.

It is also clear that there are many areas where more research effort would be particularly rewarding, not only from the academic point of view, but also from a practical perspective. For instance, it seems urgent to investigate different possibilities for describing the seismic input, both with regard to its capacity to inflict damage upon structures, as well as to the manner in which this damage is manifested for different types of structures.

The concepts of the PSA response surface and the structural effective acceleration have been developed for that purpose. However, they have to be further explored. The next step could be to perform similar studies with data obtained from other experimental tests and from actual field measurements, in order to consolidate the findings presented here. For example, it would seem useful to make a statistical study of the response surface for several different earthquake records, obtained for similar conditions (distance to fault, geological and local soil conditions) in order to generate average, smoothed surfaces that could be used for design purposes.

Another interesting area that deserves to be carefully explored is the evolutionary nature of the response of a reinforced concrete structure to dynamic excitations. It seems crucial to have a better understanding of how and when the changes in the structural properties take place during the shaking, and the effects of these changes on the serviceability of the structure.

PART B

SHAKING TABLE SIGNAL PROCESSING

7)MOTIVATION: MEASUREMENTS = INFORMATION + NOISE

The apparently trivial task of determining the consistency of corresponding acceleration and displacement measurements obtained during the RCF2 testing program proved to be a frustrating endeavor, as demonstrated by the unsuccsesful results obtained by a straightforward implementation of well known numerical schemes.

Figures 7.1 and 7.2 show the displacement and acceleration time-histories of the first floor level during run W2; the corresponding floor velocity, computed from both records is presented in Fig. 7.3; the solid line represents the result of integrating the acceleration using Simpson's rule and the dashed line was obtained by differentiating the displacement record via a second order central difference formula. Both records were smoothed before processing and a linear baseline correction was performed over the first few seconds of the records. The two results agree quite reasonably during the first eigth seconds, but then the integrated acceleration suffers an increasing drift. That version of the velocity is, under a practical point of view, totally unacceptable.

It is apparent that there are only two possible sources for the drift in the integrated acceleration: the

experimental data and the numerical scheme used. It can be shown that Simpson's rule is more accurate for the low frequency components than for those corresponding to high frequencies [10]. Considering that the drift can be described as a very low frequency error, it can be concluded that the problem does not lie in the numerical method, but in the experimental data.

A simple analysis reveals that if a signal contains a certain amount of noise, and is integrated exactly, the low frequency noise content will be amplified [11]. In order to integrate succesfully a given signal, it is therefore necessary to eliminate (filter out) the low frequency noise. This operation is "per se" problematic, since it is generally extremely difficult to distinguish data from noise within the measured values, which requires that both components must be eliminated altogether. It is thus necessary to compromise between the desire to integrate and the need to have the information contained in the low frequency range of the spectrum. In most cases this decision implies giving up important information, such as, for example, the permanent (final) ground displacement [10].

All of the above discussion applies in a converse way to the operation of numerical differentiation of digital signals in the prescence of high frequency noise. This

problem did not occur in the case shown in Fig. 7.3, since the displacement record did not contain significant high frequency components, and furthermore, a smoothing procedure was performed in both signals. This operation (in fact, a filtering procedure) practically eliminated the high frequency noise, facilitating thus the numerical differentiation process.

A number of computer programs are currently available, in which numerical filtering procedures have been implemented for the processing of seismic data (References 12, 13 and 14). However, these programs are very specific, and their modification for processing of shaking table signals seemed to be a more difficult task than designing a new computer program, tailored to perform most of the operations required in shaking table experimentation.

In view of the mentioned considerations, it was decided to perform a study of some methods for numerical filtering of digital signals and to implement them in a program suitable for the manipulation of experimental data. The literature about such methods is abundant, therefore the investigation was necessarily limited to methods which are currently implemented in the accepted "standard" programs [11] [12] and to relatively simple modifications of those procedures. The results of this study and their application to several cases of shaking table and seismic signals are presented in the following Chapters.

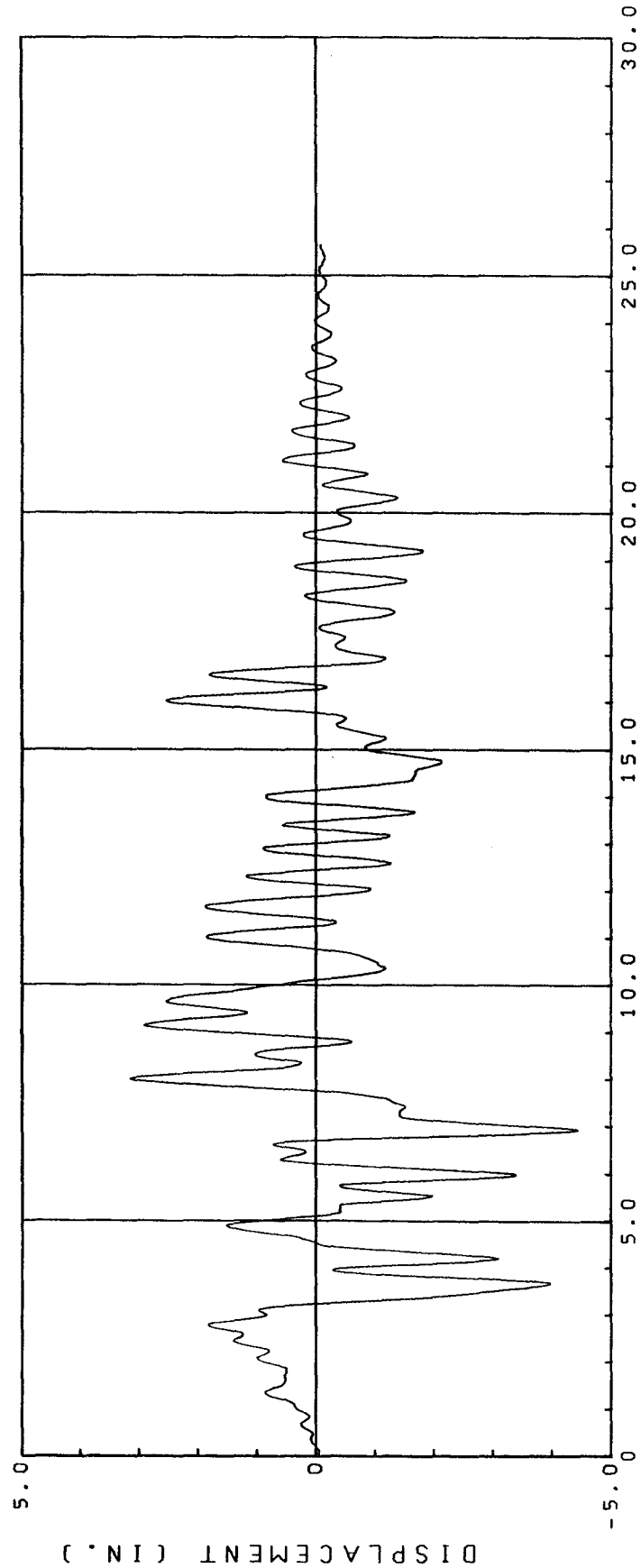

Fig. 7.1 BOTTOM STORY DISPLACEMENT RESPONSE. RUN W2.

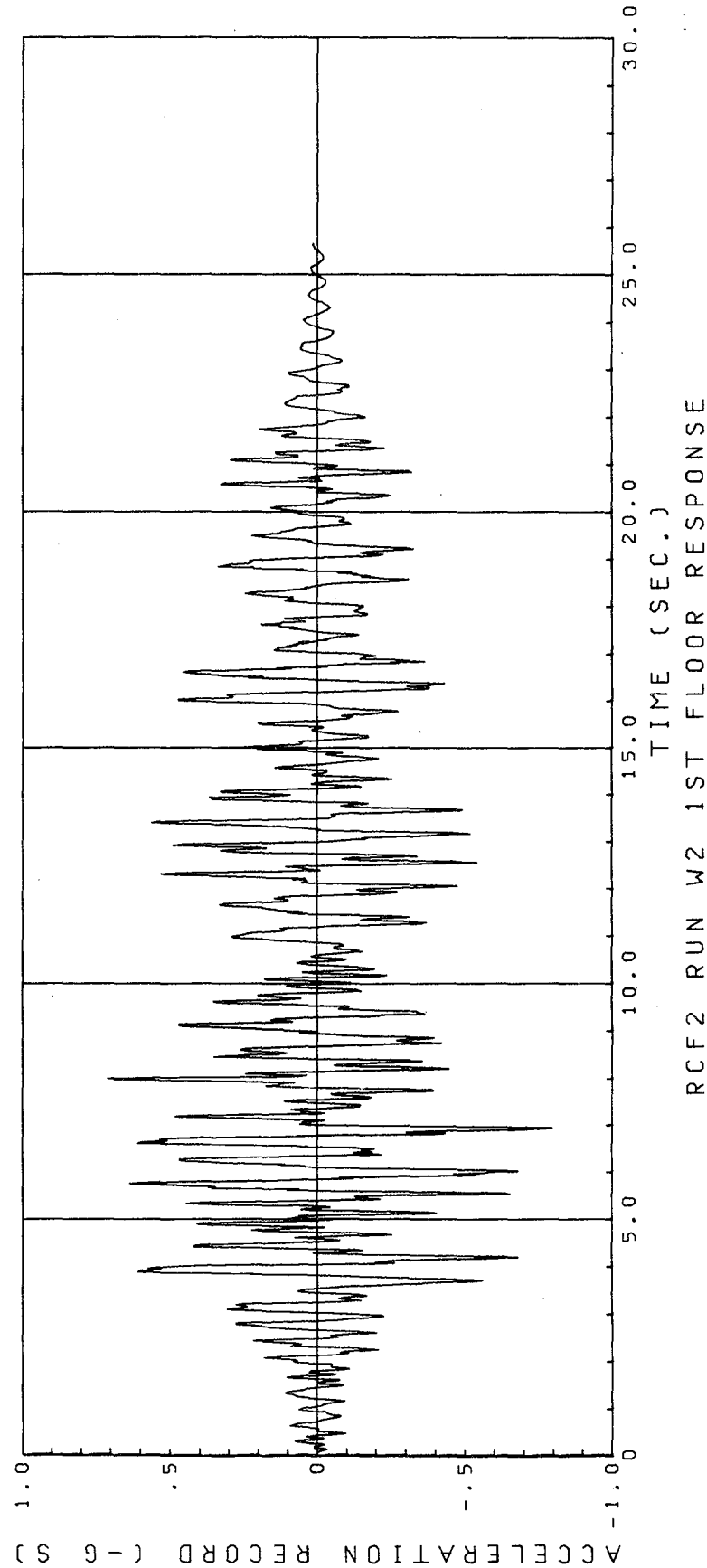

Fig. 7.2 BOTTOM STORY ACCELERATION RESPONSE. RUN W2.

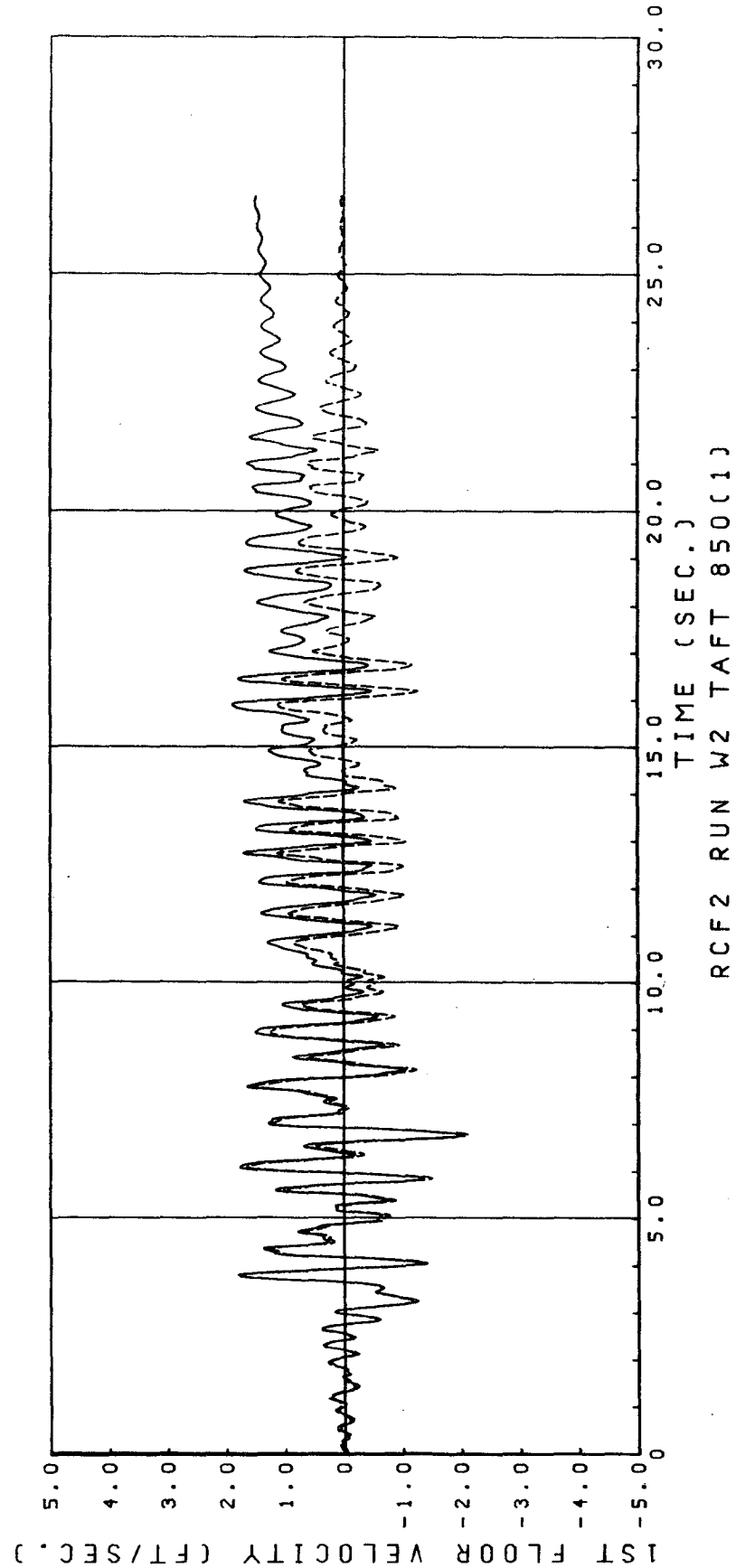

Fig. 7.3 EVALUATION OF BOTTOM STORY VELOCITY.
SOLID LINE: INTEGRATED ACCELERATION;
DASHED LINE: DIFFERENTIATED DISPLACEMENT. RUN W2.

8) CONCEPTS OF NUMERICAL FILTERING

8.1 Preliminary Remarks

This chapter briefly presents some basic concepts of digital signal processing, and of numerical filtering techniques. It includes only the essential information for the development of the techniques presented here. References 10, 11, 15, 16 and 17 provided the necessary background.

The following notation is used: If $h(t)$ is a function of time t; its Fourier transform is denoted by $H(f)$, where f is frequency. The formulation of the transform pair is:

$$h(t) = \int_{-\infty}^{\infty} H(f)\, e^{i2\pi ft}\, df$$

$$H(f) = \int_{-\infty}^{\infty} h(t)\, e^{-i2\pi ft}\, dt \qquad (8.1)$$

In the case where the function $h(t)$ is sampled at regular intervals, equispaced Δt, the sampled values,

$$h(t_n) = h(n\Delta t)\ ;$$
$$n = \ldots, -2, -1, 0, 1, 2 \ldots \qquad (8.2)$$

are denoted by h_n. A similar notation is used for sampled functions in the frequency domain.

Most of the derivations presented in the following sections make use (generally in a pictorial way) of important theorems of Fourier analysis. These can be found within a more formal context in References 18 and 19.

8.2 Description of The Filtering Process

The purpose of filtering a given signal is (in most cases) to modify its frequency spectrum, by eliminating or attenuating some frequency components, probably those with an unacceptable level of noise, and leaving others unaltered, generally those which contain most of the information.

Figure 8.1 represents a typical band-pass filtering process. The filtered signal contains only frequency components within the pass-band, those on the stop-bands being eliminated.

The filtering process can then be described in the frequency domain as a multiplication of the Fourier Transform of the original signal by a certain "shape" function. Thus,

$$\tilde{Y}(f) = Y(f)\,H(f) \qquad (8.3)$$

where $\tilde{Y}(f)$ is the Fourier Transform of the filterd signal and $H(f)$ is called the transfer function of the filter. In the time domain, the filtering procedure is equivalent to a

convolution of the original signal, $y(t)$ with the inverse transform of the transfer function of the filter, $h(t)$; therefore,

$$\tilde{y}(t) = \int_{-\infty}^{\infty} y(\tau)\, h(t-\tau)\, d\tau \qquad (8.4)$$

The convolution operation will be denoted, for convenience as

$$\tilde{y}(t) = y(t) * h(t) \qquad (8.5)$$

$h(t)$ is called the impulse response, or the weighting function of the filter (since convolution can be regarded as a running weighted average).

The filtering process can be accomplished in practice by performing a multiplication in the frequency domain or a convolution in the time domain. It was decided to explore methods based on the latter procedure.

8.3 Sampled vs Continuous Data

Data obtained from shaking table tests consist of sequences of numerical values which are samples of the continuous quantities being measured. In general, data are sampled at a certain fixed time interval, within a certain precision, and during a limited time. It is assumed that the measurements are made with a satisfactory degree of precision.

Figure 8.2 (adapted from Reference 18) shows the effect of sampling in the frequency spectrum of a band limited signal, $g(t)$, sampled at a time interval Δt. This process is equivalent to the multiplication of $g(t)$ with the Dirac comb $s(t)$. In the frequency domain, the process implies the convolution of the transforms of the two functions, $G(f)$ and $S(f)$. The result of such convolution is a function consisting of replicas of $G(f)$ scaled by a factor of $1/\Delta t$ and separated at frequency intervals of $\Delta f = 1/\Delta t$. The frequency spectrum of $g(t)$, i.e. $G(f)$, is preserved (within a scaling constant) by the sampling process.

Trouble arises when Δt is too large (or the function $g(t)$ is undersampled). In that case, the frequency spacing Δf will be reduced and overlapping will occur between the replicas of $G(f)$. As a consequence, the spectrum of the sampled function will not reproduce the transform of the original function in the overlapped zones. This phenomenon is known as "aliasing", since some high frequency components appear (due to the overlapping) in the low frequency range.

In the cases where aliasing occurs, it is very difficult to reconstruct the information contained on the analog signal from the aliased spectrum. The only effective way to prevent aliasing is to sample at a rate high enough

to represent the highest frequency contained in the signal (or to eliminate from the signal the undesirable, alias prone high frequencies before sampling).

It is clear from Fig. 8.2 that the lowest sampling interval that will prevent aliasing of a band limited signal corresponds to a separation from the frequency sampling function of twice the highest frequency, f_c present in the signal; therefore

$$\Delta f = 1/\Delta t = 2f_c \qquad (8.6a)$$

or

$$\Delta t = 1/2f_c \qquad (8.6b)$$

is the smallest time interval for which aliasing does not occur. Conversely, if the sampling interval Δt is fixed (as in most cases in shaking table experimentation) the highest frequency that can be present in the signals in order to prevent aliasing in their frequency spectrum is

$$f_f = 1/2\Delta t \qquad (8.7)$$

this value is known as the Nyquist or the folding frequency, (the alias effect can also be described as a folding of the frequency domain with respect to the Nyquist frequency).

For the purposes of this study,it was assumed that the sampling rate during testing was sufficiently high as to accurately capture the meaningful frequencies of the signals being measured. Most of the derivations were

performed considering continuous signals (it is most of the time easier to manipulate continuous functions than discretized functions) even when these concepts will be applied for sampled signals. The effect of sampling must be therefore implicitly acknowledeged.

8.4 An Ideal Low-pass Filter

One of the most elementary procedures in signal processing is low-pass filtering, which consists on the removal of all frequency components corresponding to frequencies higher than a certain value (cutoff frequency).

Figure 8.3 shows the transfer function of an ideal low-pass filter with cutoff frequency f_c. The corresponding weighting function, $h(t)$, can be easily evaluated by means of the inverse Fourier transform:

$$h(t) = \int_{-\infty}^{\infty} H(f)\, e^{i2\pi ft}\, df$$

$$= \int_{-f_c}^{f_c} 1 \cdot e^{i2\pi f}\, df$$

or

$$h(t) = \int_{-f_c}^{f_c} \cos(2\pi ft)\, df$$

$$= \frac{1}{\pi t} \sin(2\pi f_c t) \qquad (8.8)$$

which can be written as

$$h(t) = 2f_c \ \mathrm{sinc}\ (2f_c t) \qquad (8.9)$$

where

$$\mathrm{sinc}\,(x) \equiv \frac{\sin(\pi x)}{\pi x} \qquad (8.10)$$

The ideal low-pass filter will be designated as "sinc" filter in the following discussions.

The implementation of the sinc filter for sampled data implies the performance of a numerical convolution between the sampled function to be filtered, $y(t_n)$, and a sampled version of the filter weighting function (at the same time interval, Δt). Therefore,

$$\tilde{y}_m = \sum_{n=-\infty}^{\infty} y_n \, h_{m-n} \qquad (8.11)$$

where a particular filter weight, say h_k is given by

$$\begin{aligned} h_k &= h(t_k)\cdot\Delta t \\ &= h(k\Delta t)\cdot\Delta t \end{aligned} \qquad (8.12)$$

then

$$h_k = 2f_c\Delta t \cdot \mathrm{sinc}\,(2f_c k\Delta t) \qquad (8.13)$$

or

$$h_k = \sin(2\pi f_c k\Delta t)\,/\,\pi k \qquad (8.14)$$

There is a computational problem inherent to the convolution formula, (8.11) since it implies an infinite number of operations; therefore, it is usually computed for

a finite number of terms, as follows,

$$\tilde{y}_m = \sum_{n=-N}^{N} y_n h_{m-n} \qquad (8.15)$$

This decision has as a consequence the imperfect realization of the filtering procedure.

8.5 Effect of Finite Size of Filter

The implication of using a finite number of terms for the numerical convolution can be easily visualized for the continuous case.

The truncation of the filter weighting function can be regarded as the multiplication of the infinite duration weighting function $h(t)$ by a function $w(t)$ of rectangular shape. Time limited functions as $w(t)$ are commonly called "windows". The truncated weighting function, $\tilde{h}(t)$, is given by

$$\tilde{h}(t) = w(t)\, h(t) \qquad (8.16)$$

In the transform domain the process is equivalent to the convolution of the transfer function of the filter $H(f)$ with the Fouriewr transform of the window, $W(f)$, or

$$\tilde{H}(f) = W(f) * H(f) \qquad (8.17)$$

This process is shown in Fig 8.4. The effect of the truncation of the signal in the time domain is to have a

"smeared" version of the the original spectrum, characterized by a series of ripples in the pass and stop bands, and a transition zone around the cutoff frequency.

The shape of the transfer function of the finite duration filter depends on the shape of the Fourier transform of the window function. In particular, the transition zone bandwidth is approximately equal to the main lobe width, and the size of the ripples is proportional to the size of the sidelobes of $W(f)$ (with respect to the main lobe).

The phenomenon described above (sometimes referred to as "leakage") is closely related to the Gibbs phenomenon in Fourier series, produced by the abrupt truncation of the Fourier expansion of a given function. In this case, the oscillations in the transform of the filter are due to the truncation of the time signal $h(t)$. The selection of a larger time window produces a sharper transition zone, but the size of the oscillations is not reduced; they only become more rapid, and concentrate near the cutoff frequency zone, as shown in Fig 8.5.

A possible solution for this problem is therefore to reduce the abruptness of the time window by modifying its shape, reducing its size near the truncation zone. Several shapes have been proposed for this purpose; the desired

characteristics being to have a narrow main lobe to reduce the size of the transition zone and to have small sidelobes, to reduce the size of the ripples. These are usually conflicting requirements and a compromise has to be made between the desire of having a flat pass and stop bands and at the same time a very narrow transition in the cutoff frequency zone.

8.6 The Window Method

The most desirable characteristic in selecting a time window shape to reduce the leakage effect is to have narrow functions for both the window and its transform and that the sidelobes of the transform are as small as possible with respect to the main lobe. It has been shown (for the continuous case) that a class of functions, called the prolate spheroidal wavefunctions, have that property. However, they also have very compicated expressions. Kaiser proposed a relatively simple approximation to these functions [20] which are given, for the continuous case, by

$$w(t) = I_0\left(\alpha\sqrt{1-(t/T_c)^2}\right) / I_0(\alpha) \qquad (8.18)$$

where T_c is the cutoff time or half the window duration, T_w and α is a parameter controlling the shape of the window. $I_0(x)$ represents the modified zeroth order Bessel function.

The Fourier transform of the window is proportional to

$$\sinh\left(\alpha\sqrt{1-(f/f_\alpha)^2}\right) \Big/ \sqrt{1-(f/f_\alpha)^2} \qquad (8.19)$$

where f_α is approximately the width of the central lobe of $W(f)$.

For the discrete case, the window coefficients are

$$w_k = \begin{cases} I_0\left(\alpha\sqrt{1-(k/N)^2}\right) / I_0(\alpha) , & |k| \leq N \\ 0 , & |k| > N \end{cases} \qquad (8.20)$$

Figure 8.6 shows the Kaiser window and its Fourier Transform for a time window of unit duration. An additional plot of the quantity $-20\ \log_{10}[W(f)/W(0)]$ (decibel scale) is given, since the linear scale is not adequate to visualize the small quantities involved.

The rectangular window case corresponds to a zero value of α, which controls the value at both ends of the window.

It is now possible to appreciate the trade-off between the size of the sidelobes, which control the size of the ripples, and the main lobe width, responsible for the transition zone width in the transfer function of the finite duration filter. The rectangular window has a transition bandwidth of about $2/T_w$; it clearly has the

narrowest main lobe, however, the sidelobes are considerably large, being only 13 decibels (dB) below the main lobe (22% of the size). For $\alpha = 5$ the main lobe width is about $4/T_w$; but the sidelobes are now about 40 dB below the main lobe (1%). For $\alpha = 10$, the main lobe width is larger than $6/T_w$ and the sidelobe amplitude is about 70 dB below the main lobe (0.03%).

The effect of the application of a Kaiser window to the sinc filter can be appreciated in Fig. 8.7, for a filter with design cutoff frequency of 1 Hz, and for a time window duration of 4 seconds. The maximum ripple size is of 21 dB (about 9% overshoot) for the rectangular window, and of about 50 and 100 dB (0.3% and 0.001% overshoot) for α equal to 5 and 10, respectively. The price paid for the virtual elimination of the ripples is the increase in the transition zone bandwidth. The only way to gain sharpness in the cutoff zone is to use longer time windows (as in Fig. 8.5).

Kaiser developed empirical formulas to determine the required duration for the time window in order to design a sinc filter with a desired attenuation (maximum ripple size in dB) and for a given transition bandwidth. Using these formulas, taken from Reference 16, the procedure for designing a low-pass filter is:

1. Select acceptable values for the maximum ripple size, δ , and for the transition zone bandwidth, B .

2. Compute the attenuation A in dB

$$A = -20 \log_{10}(\delta) \qquad (8.21)$$

3. Compute the filter shape parameter , using the following empirical formulas

$$\alpha = \begin{cases} 0.1102\,(A-8.7) & , \quad A \geq 50 \\ 0.5842\,(A-21)^{0.4} + 0.07886\,(A-21) & , \quad 21 < A < 50 \\ 0 & , \quad A < 21 \end{cases} \qquad (8.22)$$

4. The required number of window coefficients, $2N+1$, which determine the window duration $T_w = 2N \cdot \Delta t$ is computed using

$$N = (A-7.95)/(28.72)\,B\Delta t \qquad (8.23)$$

These formulas show that it is easier to reduce the size of the ripples than to narrow the transition band, from the point of view of the number of window coefficients required (which is inversely proportional to B , and increases linearly with A , which depends on the logarithm of the ripple size, δ) [16].

8.7 The Ormsby Filter

A numerical filter developed by J. F. Ormsby [20] is currently implemented in the "standard" programs for processing seismic data [12]. It is a low-pass filter in which a linear transition zone is specified. Figure 8.8 a) shows the parameters defining the transfer function of the Ormsby filter. They are the cutoff and roll-off termination frequencies (f_c and f_t) or the average frequency in the transition zone, f_a and the transition bandwidth, B . The derivation of the corresponding weighting function is very simple, considering that the transfer function of the Ormsby filter is the convolution of that of a sinc filter with cutoff frequency f_a, and a rectangular function of base B and unit area. This process and the corresponding time domain phenomenon is shown in Fig 8.8 b).

The resulting weighting function for the Ormsby filter is

$$h(t) = 2f_a \, \mathrm{sinc}(2f_a t) \, \mathrm{sinc}(Bt) \qquad (8.24)$$

It is trivial to show that this expression is equivalent to that developed by Ormsby [20], in terms of the cutoff and rollof frequencies,

$$h(t) = (\cos \omega_c t - \cos \omega_t t) / ((\omega_t - \omega_c)\pi t^2) \qquad (8.25)$$

where $\omega_c = 2\pi f_c$ and $\omega_t = 2\pi f_t$.

The sampled filter weights, to be used in the numerical convolution, are

$$h_k = (\cos(\omega_c k\Delta t) - \cos(\omega_t k\Delta t))/((\omega_t - \omega_c)\pi k^2 \Delta t) \qquad (8.26)$$

The effect of the transition zone is to attenuate the weighting function of the sinc filter with cutoff frequency f_a . As a consequence, when only a finite number of weights are used, the truncation effect is not so important as in the case of the sinc filter, and leakage is thus reduced. Figure 8.9 presents the effect of the transition zone bandwidth on the transfer function of the filter. As in the case of the Kaiser window, there is a trade-off between flatness in the transfer function and transition zone bandwidth.

The Kaiser window and the Ormsby filter can be combined to have more flexibilty in the design of the lowpass filter, as shown in Fig. 8.10. The rectangular window offers poor results (large ripples and it does not even replicate the specified bandwidth of the transition zone). The Ormsby-Kaiser transfer functions offer much better attenuation (again, sacrificing narrowness in the transition zone) than the sinc-Kaiser; with attenuation of about 64 and 117 dB for α equal to 5 and 10, respectively.

8.8 Summary and Test Example

The main problem (in addition to sampling) of the numerical filtering of digital signals is that there is a practical need to perform a limited number of operations in the convolution of the signal to be filtered and the weighting function of the filter. This entails the truncation of the weighting function (the use of a finite number of filter weights) which causes leakage; the transfer function of the finite duration filter is a distorted version of the "design" transfer function.

In this study, the leakage problem was attacked in two ways: by tapering the truncated weighting function (window method) and thus reducing the abruptness of the truncation, and by specifying a transition zone between the pass and stop bands (Ormsby filter). In both approaches, the sharpness of the cutoff zone is compromised with the flatness of the transfer function in the pass and stop bands. Both methods can be combined to have more flexibility in the design parameters and thus obtain a more practical implementation.

Figure 8.11 shows a test example, designed to verify the adequacy of the combined method. A "clean signal" consisting of a sinusoid of variable amplitude (Fig. 8.11 a)) was contaminated with low and high frequency noise and

a random noise component (Fig 8.11 b)). The characteristics of the signal and noise are:

Clean signal: peak amplitude 2.5 units, frequency 0.75 Hz
High freq. noise: amplitude 0.30 units, frequency 15.0 Hz
Low freq. noise: amplitude 0.75 units, frequency 0.05 Hz
Random noise: amplitude 0.25 units.
Sampling time interval: 0.02 seconds.

The low-pass and high-pass Ormsby filters are shown in Fig 8.8 c) (the procedure to generate a high pass filter from a low pass filter is described in the next chapter). The Kaiser window was selected for 80 dB attenuation and a transition zone bandwidth equal to half of that of the Ormsby filter. This implied a time window duration of 2.4 seconds for the low-pass filter and 100 seconds for the high-pass filter. The window coefficients were computed using the procedure shown in Section 8.6.

The effect of the low-pass, high pass and band-pass filtering can be seen in the subsequent figures. The results are satisfactory from a practical point of view. It should be noticed that the band-pass filtered signal of Fig. 8.8 f) contains a certain level of noise, which is the component of the random noise within the passband of the filter used.

These results were obtained using the program DIPS, developed for processing of shaking table signals. This program is described in the next chapter.

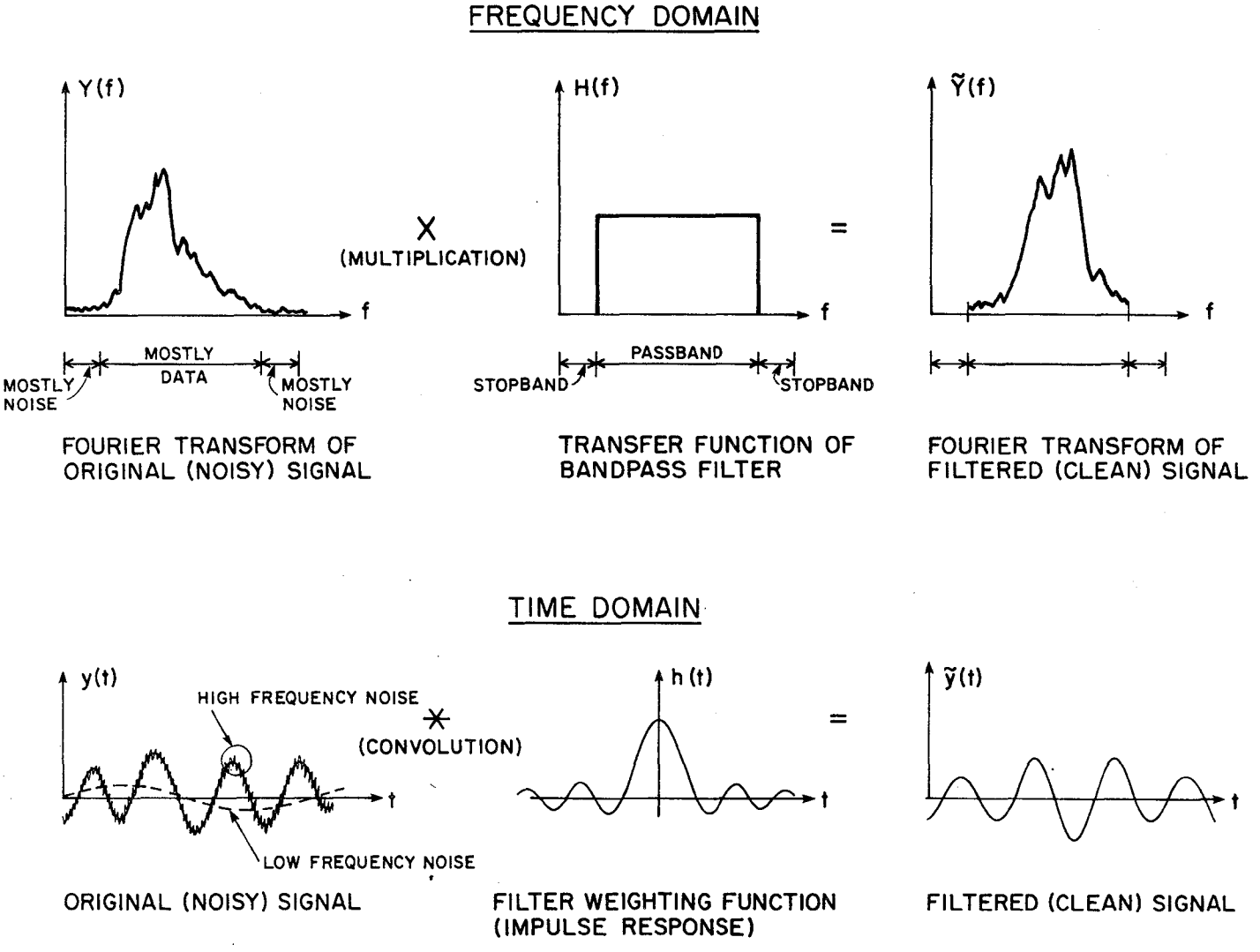

Fig. 8.1 FILTERING PROCESS IN FREQUENCY AND TIME DOMAINS.

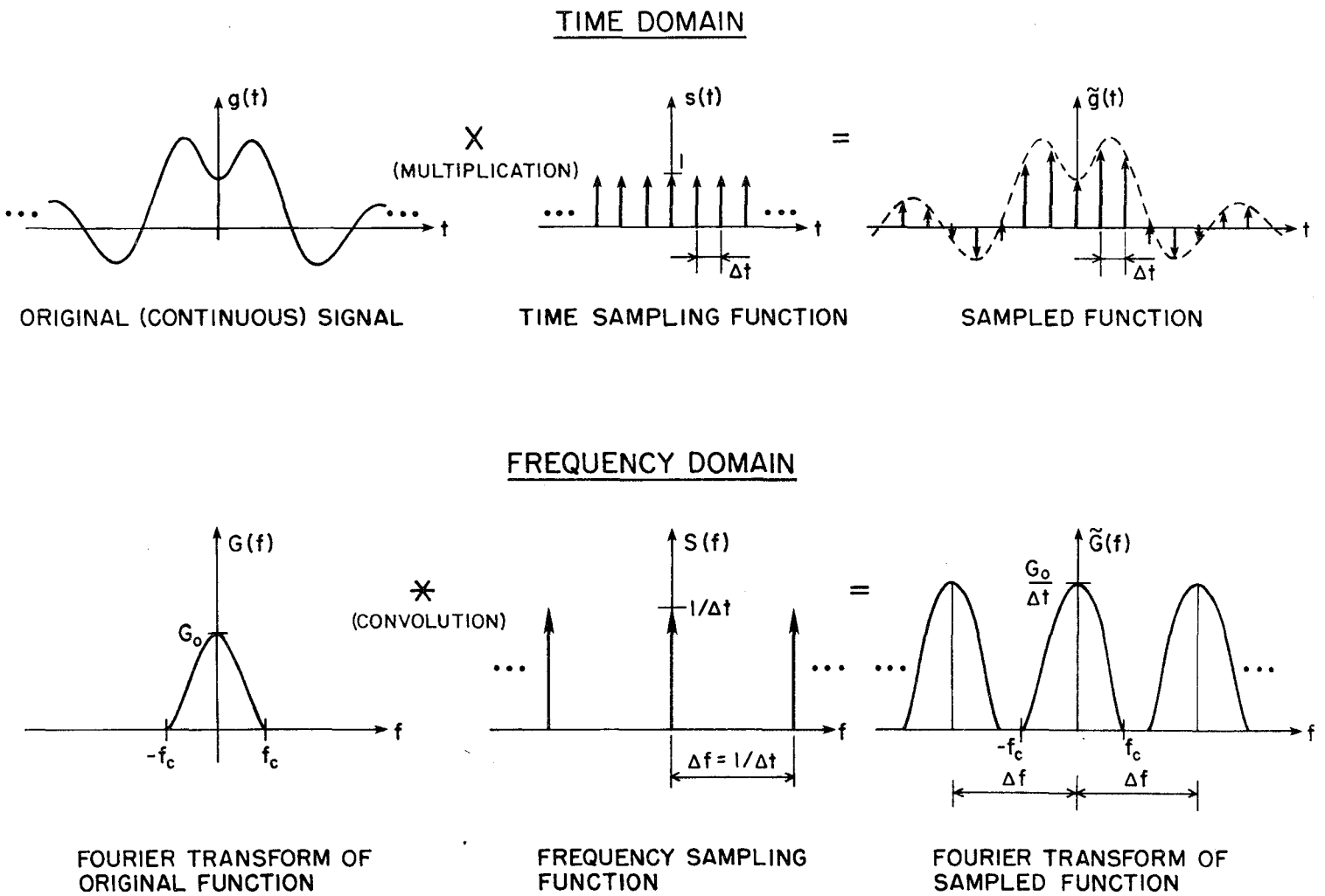

Fig. 8.2 EFFECT OF TIME SAMPLING A BAND LIMITED FUNCTION.

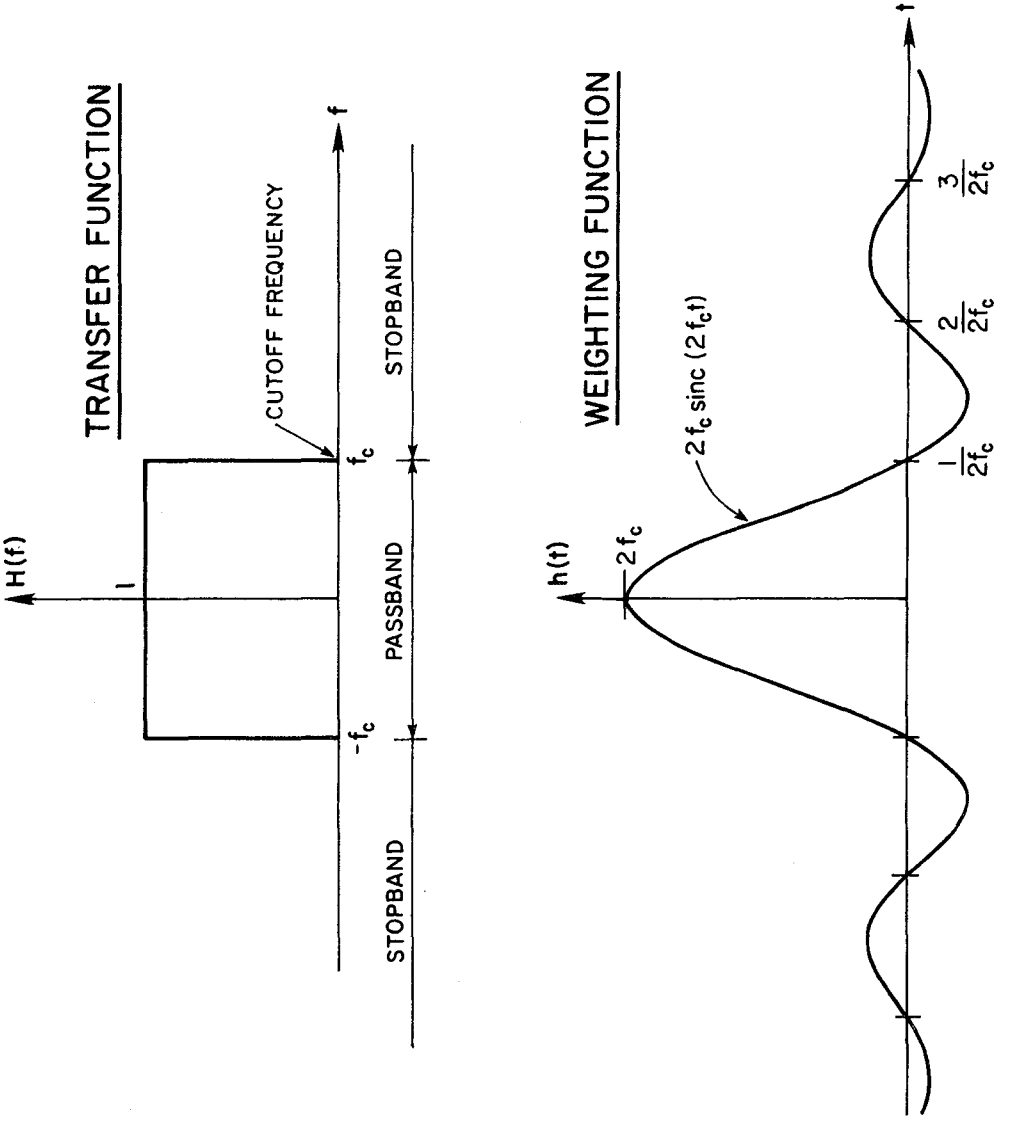

Fig. 8.3 IDEAL LOW PASS FILTER.

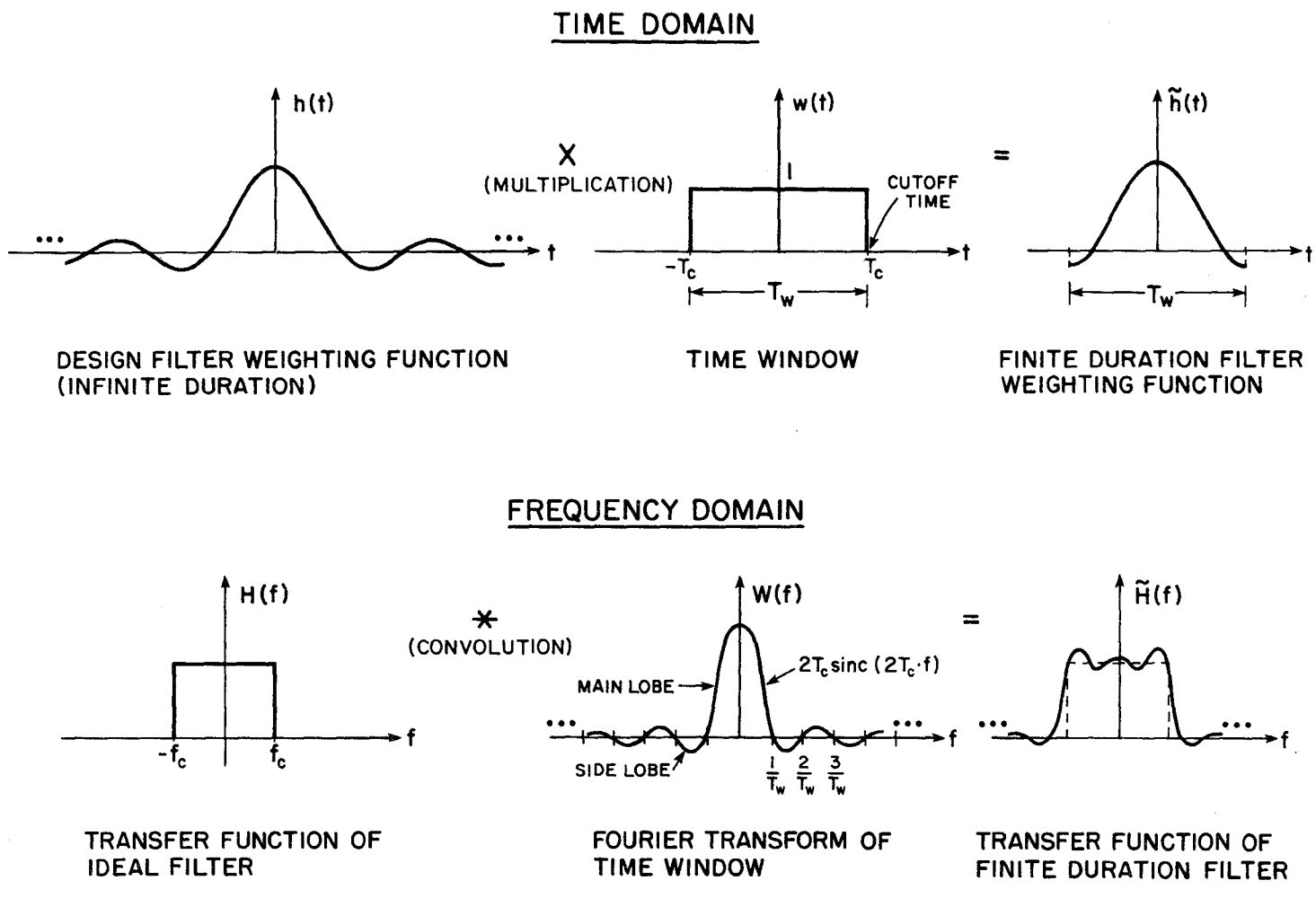

Fig. 8.4 EFFECT OF FINITE DURATION OF FILTER WEIGHTING FUNCTION.

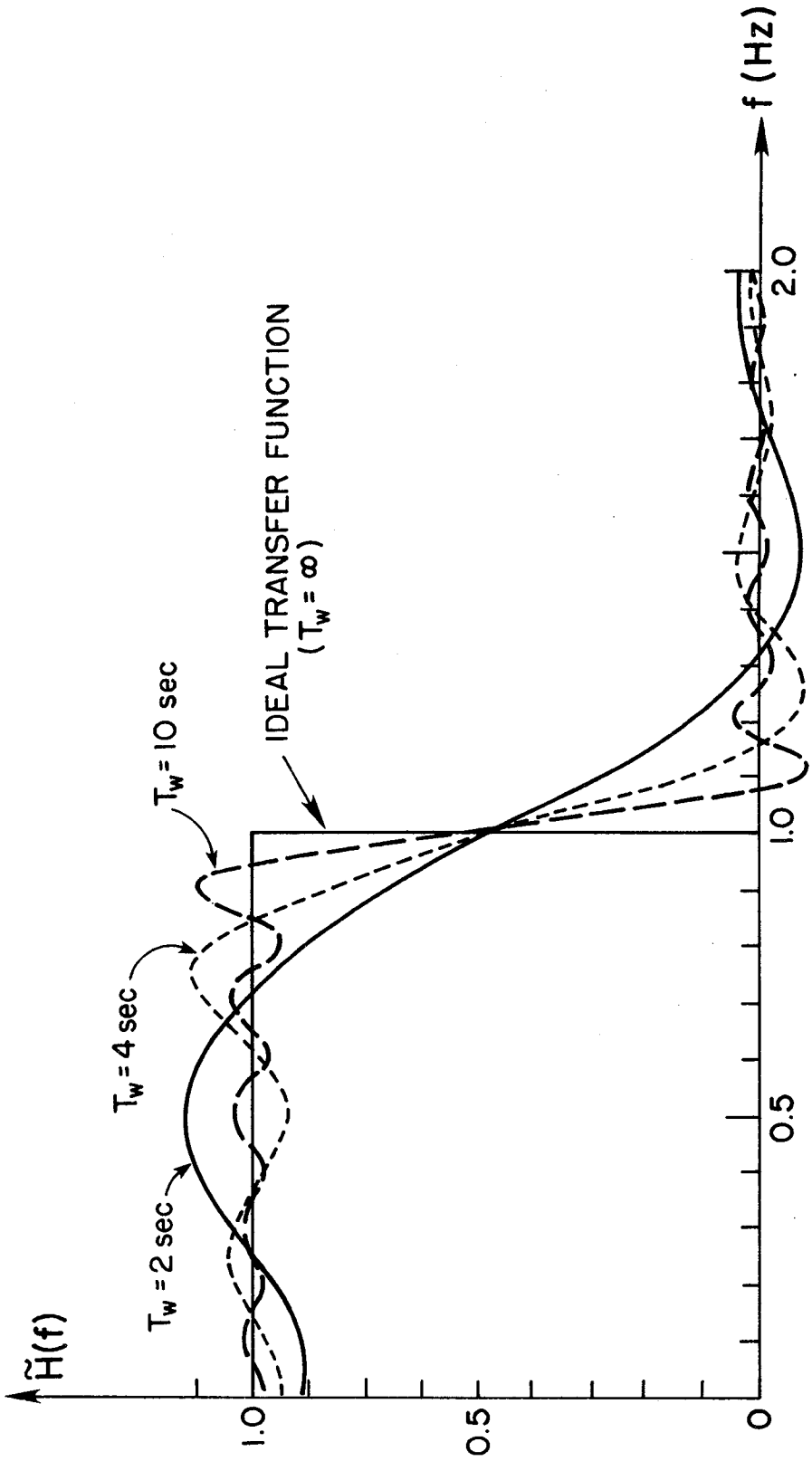

Fig 8.5 EFFECT OF TIME WINDOW DURATION ON TRANSFER FUNCTION OF SINC FILTER. RECTANGULAR WINDOW.

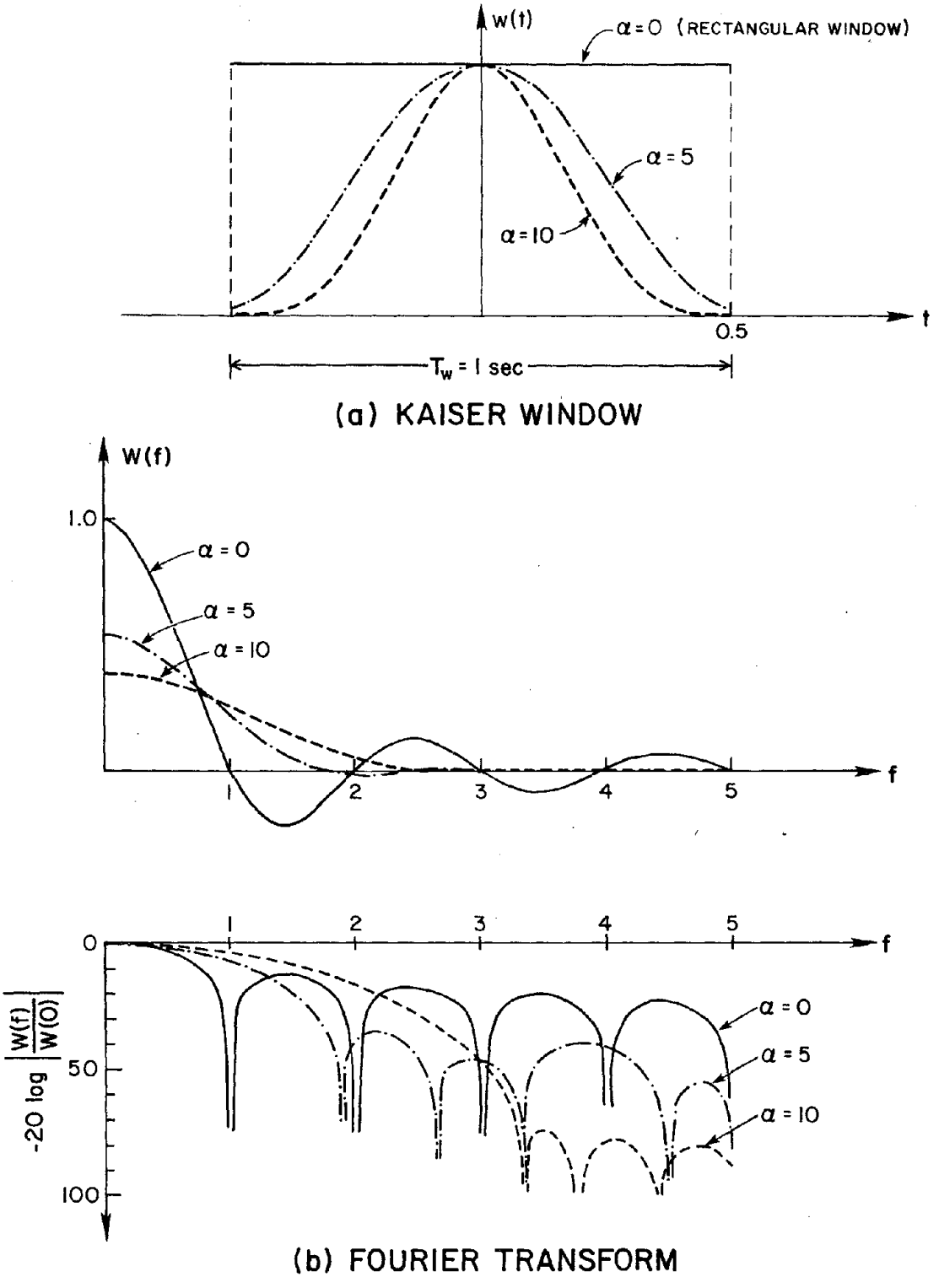

Fig. 8.6 THE KAISER WINDOW AND ITS FOURIER TRANSFORM.

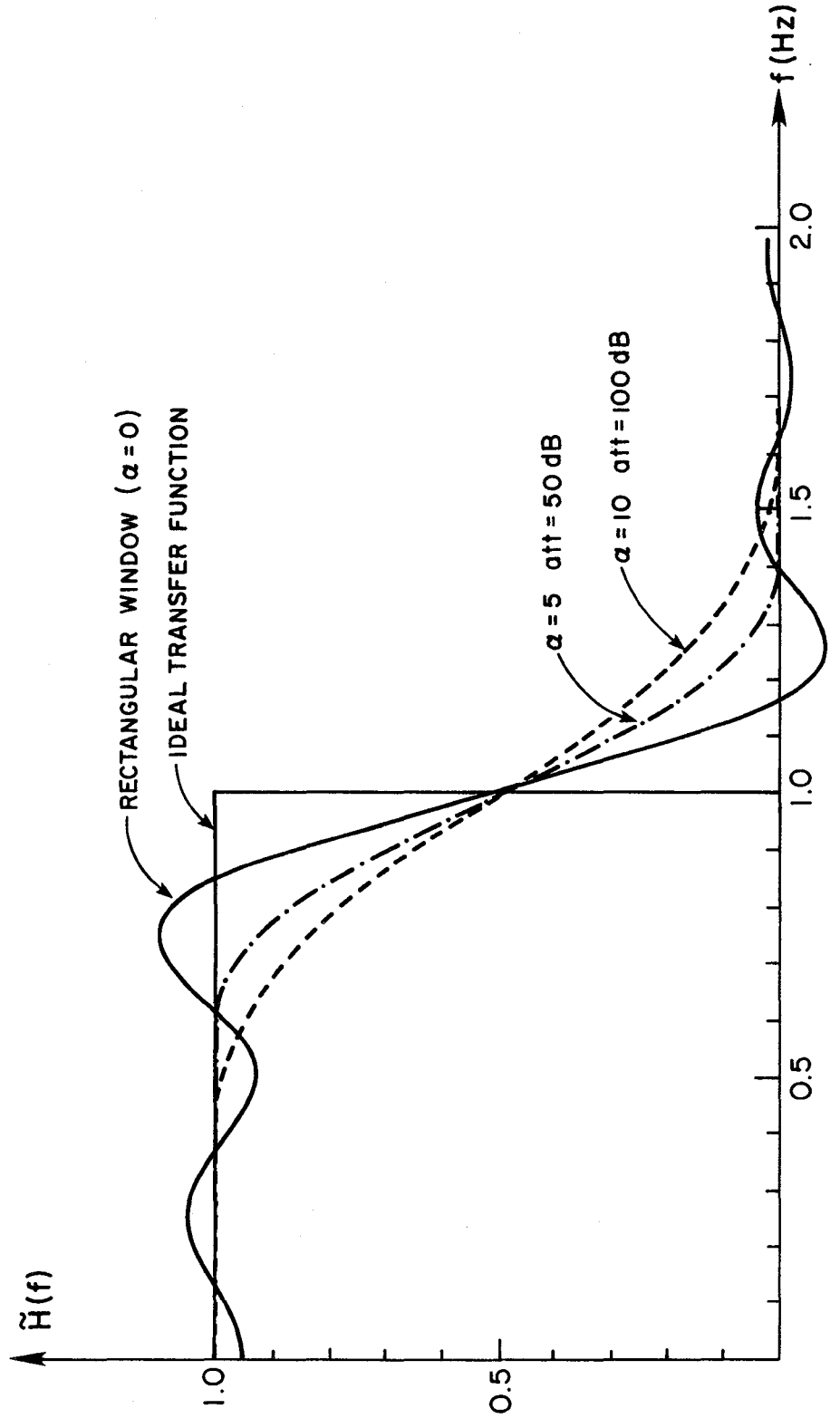

Fig. 8.7 EFFECT OF TIME WINDOW SHAPE ON TRANSFER FUNCTION OF SINC FILTER. f_a = 1 Hz; T_w = 4 sec.

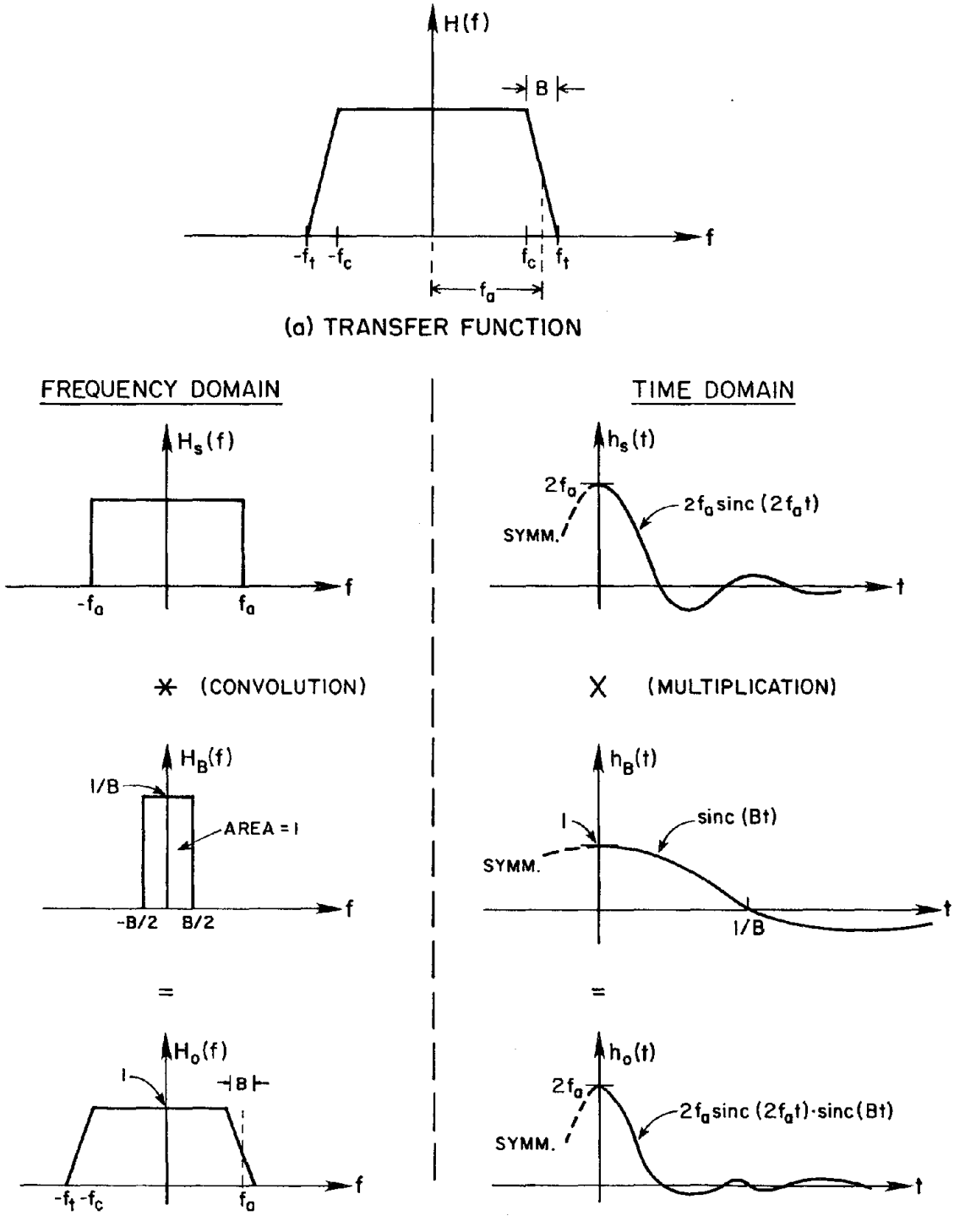

Fig. 8.8 ORMSBY FILTER AND RELATIONSHIP WITH SINC FILTER.

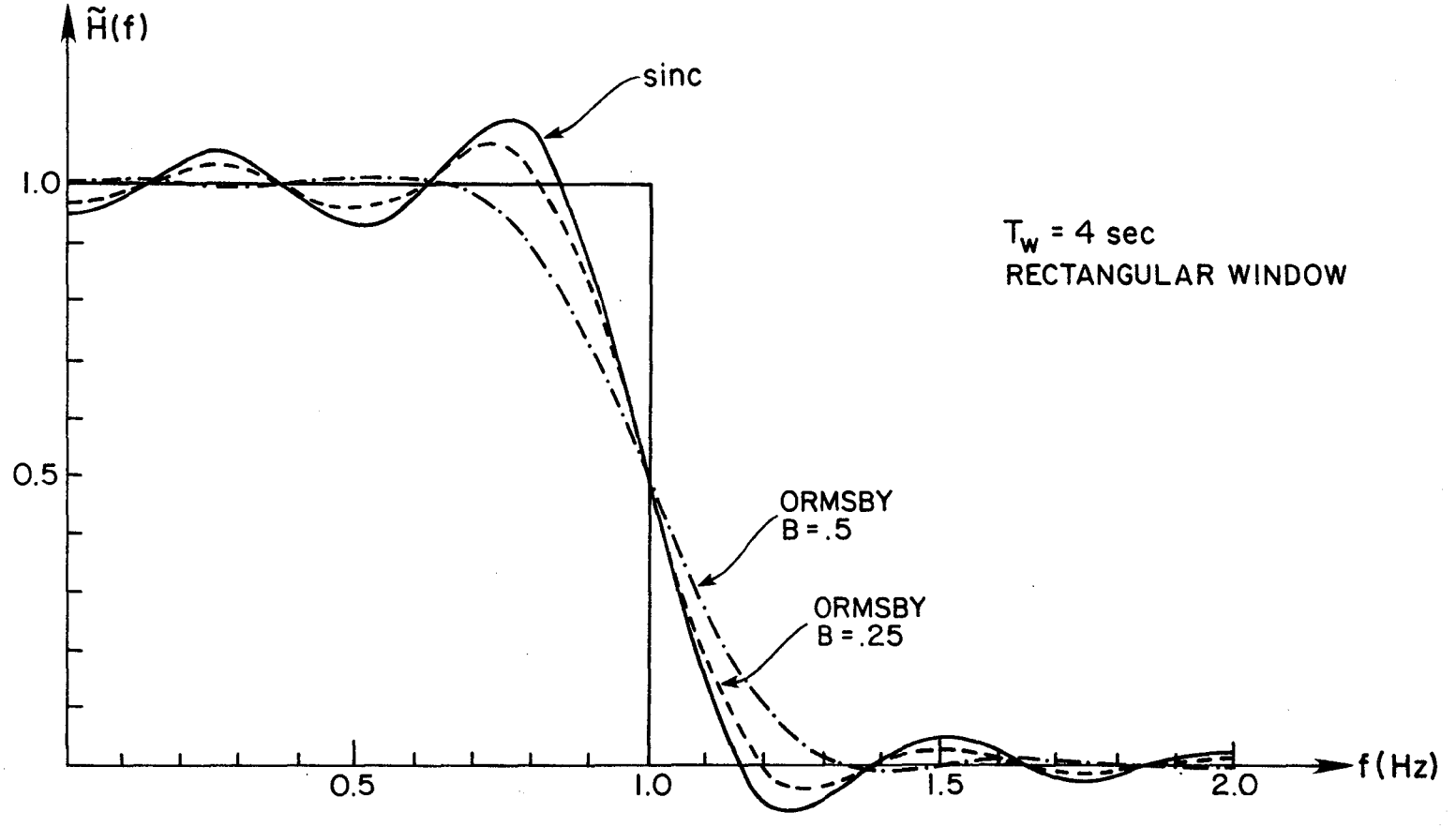

Fig. 8.9 EFFECT OF TRANSITION ZONE BANDWIDTH ON TRANSFER FUNCTION OF ORMSBY FILTER. T_w = 4 SEC.

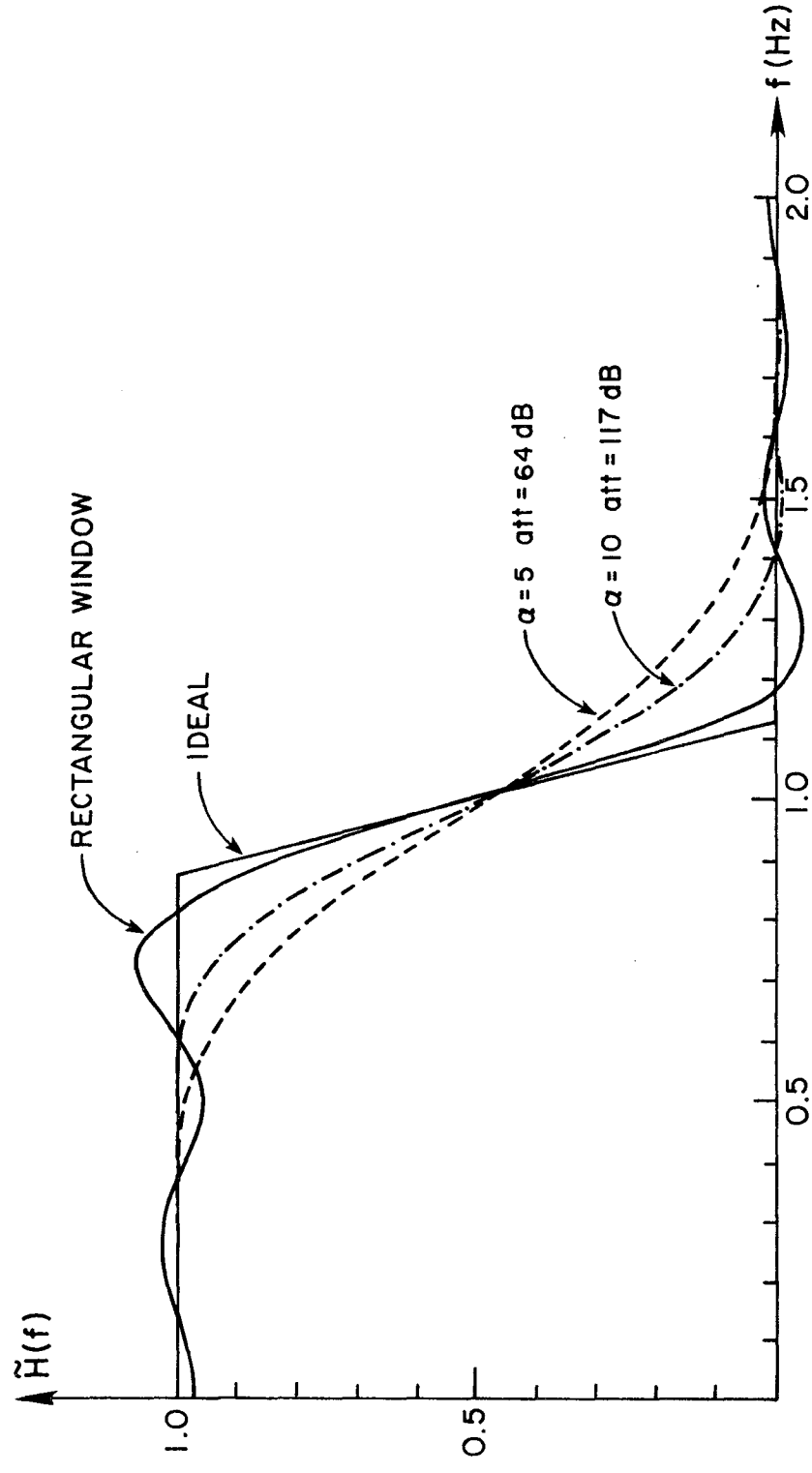

Fig 8.10 EFFECT OF TIME WINDOW SHAPE ON TRANSFER FUNCTION OF ORMSBY FILTER. f_a = 1 Hz.; B = 0.25 Hz.; T_w = 4 sec.

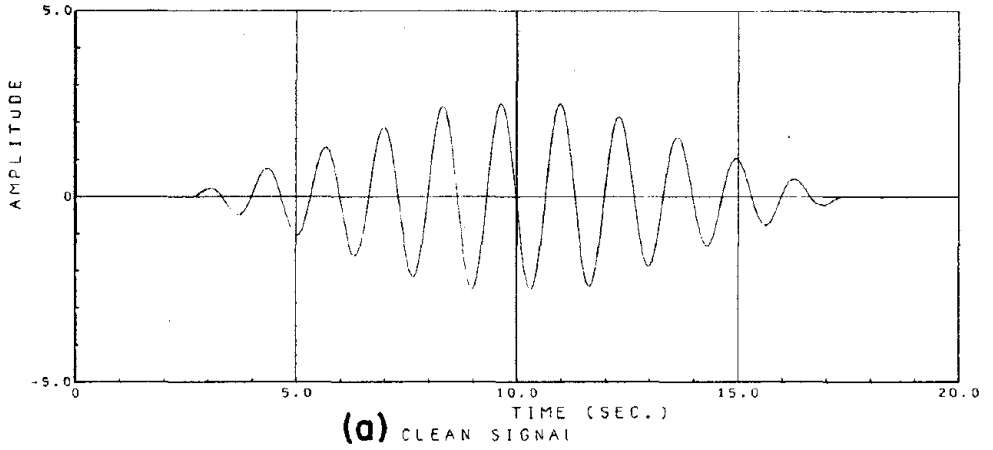

(a) CLEAN SIGNAL

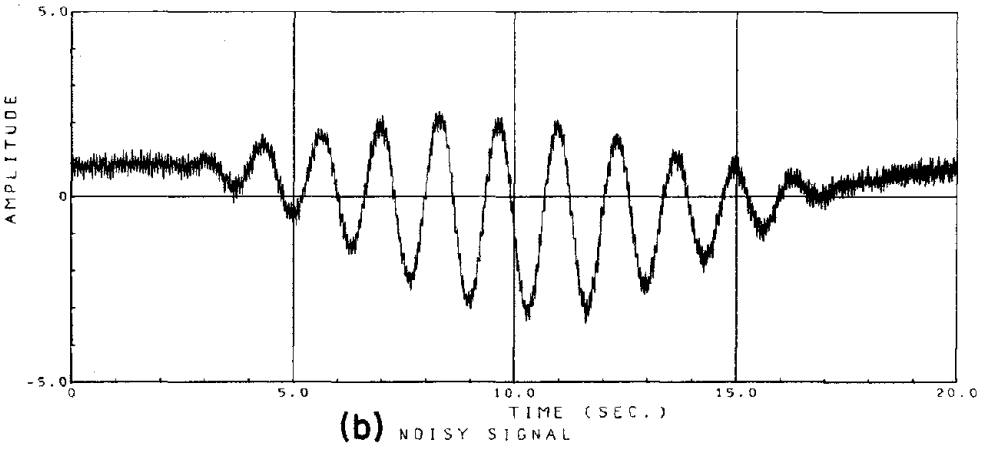

(b) NOISY SIGNAL

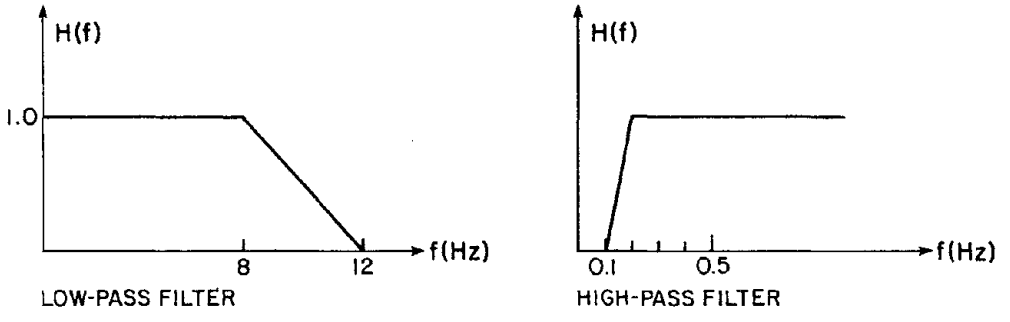

(c) ORMSBY FILTER DESIGN SPECIFICATIONS

Fig. 8.11 TEST OF ORMSBY FILTER + KAISER WINDOW.

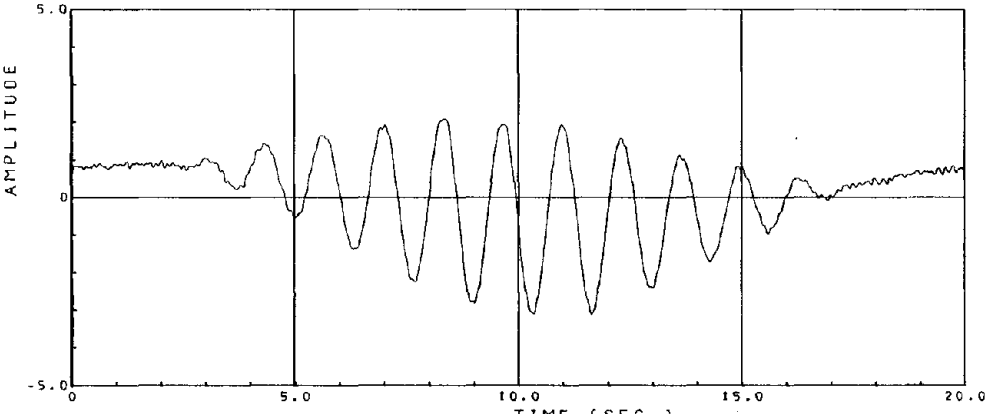

(d) LOW-PASS FILTERED SIGNAL

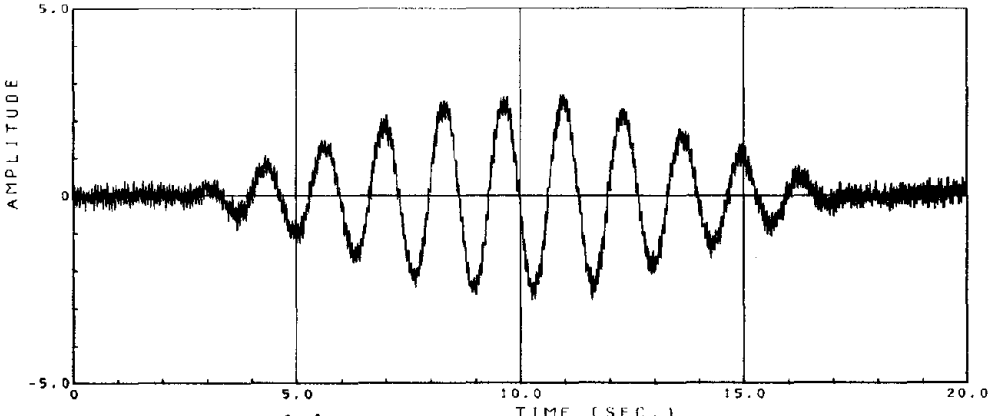

(e) HIGH PASS FILTERED SIGNAL

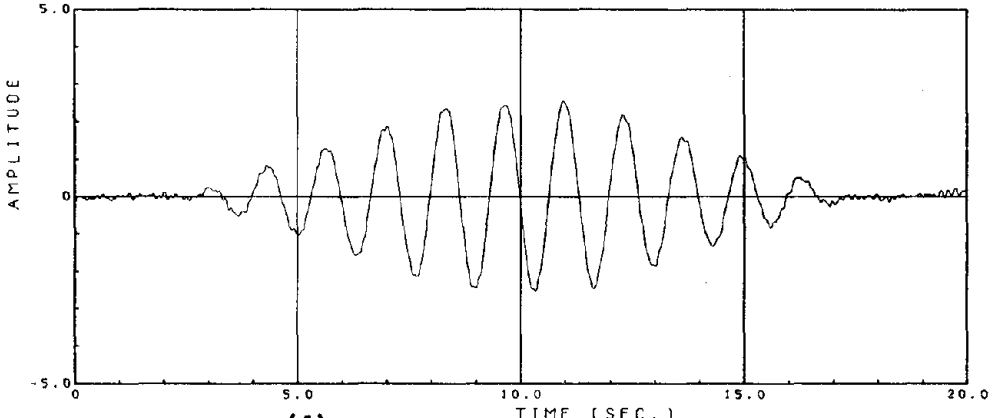

(f) BAND-PASS FILTERED SIGNAL

Fig. 8.11 (CONT.)

9) A PROGRAM FOR DIGITAL PROCESSING OF SHAKING TABLE SIGNALS (DIPS)

9.1 General Characteristics

This chapter describes a general purpose computer program designed specially in this thesis work to perform several tasks for shaking table data processing. The program was coded using the following guidelines:

1) Clarity in the code, to make it easily modifiable and maintained. In certain cases, efficiency in the execution was sacrified for the sake of a more straightforward and intelligible code.

2) Modularity in the structure of the program. Since the program was designed to perform a variety of operations, each of those was programmed as a separate routine, which could be changed or modified independently of the rest of the program. This feature also permits the easy expansion of the program, by the addition of routines to perform new operations.

3) Flexibility of use. Each operation implemented in the program is uniquely identified by a macrocommand. To process a given data record, it is necessary to specify a

sequence of macrocommands, each of them followed by the pertinent input data. This feature was implemented, to give the user the capability of deciding, for each particular case, which operations to perform, and in which order.

The source code was written in FORTRAN. The program is implemented in a CDC 6400 computer. The graphics routines are based on the Graphical Display System available at the Computer Center at UCB, which generates code to drive a Calcomp plotter.

9.2 Program Features and Limitations

The most important limitations in the current version of the program (October 1981) are:

1) The maximum allotted memory size for data records consists of 4000 single precision real numbers. The total number of data points to be processed must be smaller than that value, since some operations require record extensions. The recommended maximum size for any data record is 3800 points.

2) The number of data points must be a multiple of 50.

3) In general, the available operations can be performed in any order. The only exception corresponds to

the instructions START and STOP which must necessarily be the first and last commands.

5) If an unrecognizable macrocommand is specified, the program execution is aborted.

Following is a list of the available operations, and their identifying macrocommands (within parentheses) with a brief description of the input requirements. The limitations corresponding to each command and the numerical techniques employed (if any) are also summarized. The input formats are indicated in the user manual, given in the Appendix.

1) Start the process (START). This command must be the first to be specified, since it invokes an initializing routine. The input required is a general title to identify the process.

2) Input record for processing (READ). This operation requires as input the general characteristics of the data record to be processed: the number of data points, the time interval between them, the number of points at both ends of the record corresponding to the shaking table rest position (at beginning and end of test). The average values of the signals at these zones are used to extend the record for filtering purposes.

There are two possibilities for input data: from punched cards with a user defined format, or from a specified tapefile (in unblocked form).

3) Print record (PRINT). The record in process is output to a printer in a format specified by the user.

4) Punch a deck of cards (PUNCH). A deck of punched cards with the record under process is generated. The format is user specified.

5) Write the record on a tape file (WRITE). The record being processed is copied into a tape file in unblocked form.

6) Plot record (PLOT). This command allows the user to get printer plots of the time history of the signal (using the post processor PRINTR implemented in the CDC 6400 at UCB) and to obtain the code necessary to drive a Calcomp plotter, for high-resolution graphs. The size of the plots is fixed. The input required is the title of the ordinate axis; that of the abscissae axis is "TIME (SEC.)".

7) Perform a baseline correction (BLINE). There are two options for this operation: constant or linear baseline correction. Both corrections are based on the information contained in the NFIRST and NLAST data points (which must

be input by the user). The constant correction is equivalent to subtracting from the signal the average value of those data points. The linear correction is performed by substracting from the original data values corresponding to a straight line obtained by a least squares procedure.

The original record is lost after performing this operation.

8) Low-pass numerical filtering (LOPASS). This operation is performed via a numerical convolution of the data record and the weighting function of an Ormsby low-pass filter, modified with a Kaiser window. The number of points in the filter weighting function is chosen so that the main lobe width of the Fourier transform of the window is approximately equal to one half of the specified transition zone bandwidth in the design Ormsby filter. In order to perform the numerical convolution, the record is extended at both ends with the average of the first and last points specified in the READ command. The user must input the cutoff and rolloff termination frequencies of the filter, as well as the desired attenuation, which must be larger than 50 dB.

The original record is destroyed as a result of performing this operation.

9) High-pass numerical filtering (HIPASS). This operation is also based on the Ormsby-Kaiser low-pass filter. The procedure implemented for high-pass filtering is the following:

a) Generate the filter weights for the Ormsby-Kaiser filter.

b) Perform a low-pass filtering of the signal. The output of this operation is the low frequency noise. Due to the very large number of operations required, the output is specified at every tenth point only (therefore the time interval between output points is ten times larger that in the original signal). This should be taken into account in the specification of the filter coefficients (the low frequency noise should be adequately represented at this sampling rate).

c) Generate the missing values of the low frequency noise, by parabolic interpolation. As a result, the approximation to the low frequency noise is sampled at the same time interval as the original data record.

d) Subtract the low frequency noise from the data. The result is the high pass fitered data.

The original record is destroyed by this operation.

10) Integrate (INTGR) The numerical integration is performed using the trapezoidal rule. The integrated record replaces the original signal.

11) Differentiate (DERIV). The method used is a second order central difference numerical scheme. The original signal is replaced by the differentiated record.

12) Multiply by a constant (SCALE) The record in process is multiplied by a constant, specified by the user.

13) Compute the Fourier Transform (FFT). The implemented version of the FFT algorithm requires a number of data points equal to a power of two. In most of the cases, therefore, it is possible to compute the transform of only a segment of the data. However, this command allows for the use the moving window FFT technique. The size of the window and the interval (in samples) between succesive positions of the window must be specified. The output options include printouts and/or plots of the amplitude or the amplitude squared of the DFT of the record, within a specified frequency band.

14) Stop the process (STOP). This must be the last command specified.

15) Compute record statistics (STAT). The result of specifying this instruction is a printed list of some of the characteristics of the record under process: number of data points,time interval, record duration, peak values and their time of occurrence, and the mean value, the variance and the standard deviation.

16) Specify a label for output (LABEL). A title for output identification purposes must be specified. This command is useful to identify the various phases of the data processing, since the label is included in the printouts and the plots.

17) Replace the record by its square (SQUARE). Each value of the record being processed is replaced by its square.

18) Replace record by square root (SQRT). Each value of the record being processed is is replaced by its positive square root.

19) Compute the response spectrum of record (SPCTR). The record under process is taken as a ground motion accelerogram (in g's). As a result, the displacement, pseudovelocity and pseudoacceleration response spectra are computed and plotted. This command executes a straightforward implementation of the standard program SPECEQ [6].

As an additional option, the peak pseudoacceleration response values and their time of occurrence can be computed, and stored on tapefiles; these results can be used later to generate the pseudoacceleration response surface of the ground motion under process.

The time required to perform each operation, and the total execution time are given in the process printout.

9.3) Application Examples

Two cases of signal processing are presented in this section, to demonstrate the features and capabilities of the program DIPS. The first corresponds to the case that motivated this study: the verification of the consistency of data measured during the RCF2 test program. The second is the application of the program to the processing of a component of the El Centro 1940 accelerogram. The results obtained are compared with those of the program for standard seismic signal processing developed at Caltech [12].

9.3.1 Bottom Story Displacement and Acceleration. RCF2 Run W2.

The numerical results obtained by integrating the acceleration and differentiating the displacement records

measured at the bottom story of RCF2 during run W2 are shown in Figs 9.1 a) and b), respectively. They are identical from a practical point of view. Both records were band-pass filtered in the range 0.08-0.1 to 10.0-15.0 Hertz, and a linear baseline correction was performed as the last step of the process. These figures indicate two basic results: that the displacement and acceleration measurements are essentaially consistent with each other, and that the program DIPS performs satisfactorily.

Taking the verification process one step further, Figs. 9.2 a) and b) present the results of two approximations to the displacement by double integration of the acceleration. The first one corresponds to the sequence LHIBIB, where L stands for low-pass filtering, H for high-pass filtering, I for integration and B for baseline correction. The second one corresponds to the sequence LHIHIH. Both versions of the displacement are acceptable within reasonable limits (The dashed line in both figures corresponds to the measured displacement). Some information is lost in both records, since the low frequency components had to be removed to perform the numerical integration, and they are significantly more important in the displacement time history than in the velocity or acceleration.

The results shown in Fig 9.2 b) seem to be better than those presented in Fig. 9.2 a); however, the former record

is slightly distorted at both ends. This is due to the four numerical convolutions performed to obtain the displacement; each one of these implied an extension of both ends of the signal.

The result of two succesive differentiations on the displacement record is shown in Fig. 9.3. It is very similar to the measured acceleration record (Fig. 7.2). Since the displacement record was filtered and did not contain important information in the high frequencies, the differentiation procedure could take place succesfully.

9.3.2 Processing of El Centro 1940 Acceleration Record

The N-S component of the ground acceleration recorded at El Centro in the 1940 event is shown in Fig 9.4. The versions of the velocity corresponding to the standard Caltech program and DIPS are shown in Figs 9.5a) and b). The band pass filter design parameters were similar to those recommended by Caltech (0.04-0.07 and 20.0-25.0 Hertz). Both versions are practically identical; they differ slightly at both ends of the time histories, due to the distortions caused by the filtering numerical convolution. The Caltech program uses a more refined technique to extend the record for numerical convolution [10, 11]; therefore their results might be more accurate. Since the discrepancy occurs only within the first and last seconds, it does not seem to be of great practical consequence.

Both versions of the ground displacement are shown in Fig. 9.6 a) for the standard program and Fig. 9.6 b) for DIPS. Again, they are very similar; differences appear in the first and last one or two seconds of the record.

To show the great importance of adequately selecting the filter design frequencies, a different version of the El Centro 1940 N-S velocity and displacement is presented in Figs. 9.7 and 9.8. They were obtained using the program DIPS with a bandpasss filter of 0.2-0.3 to 20.0-25.0 Hertz. These design coefficients were proposed by Sunder [12] with the argument that they result in to more "robust" signals for the velocity and displacement. Since the actual values were not measured, it is impossible to say which versions of the ground velocity and displacement are better approximations to the actual quantities.

To finalize this presentation, the frequency spectrum of the El Centro acceleration record is shown in Fig 9.9. Most of the important components lie in the frequency band within 0 to 5 Hertz. The pseudoacceleration, pseudovelocity and displacement response spectra, computed for 2% damping (fraction of critical) are shown in Figs. 9.10 a) b) and c).

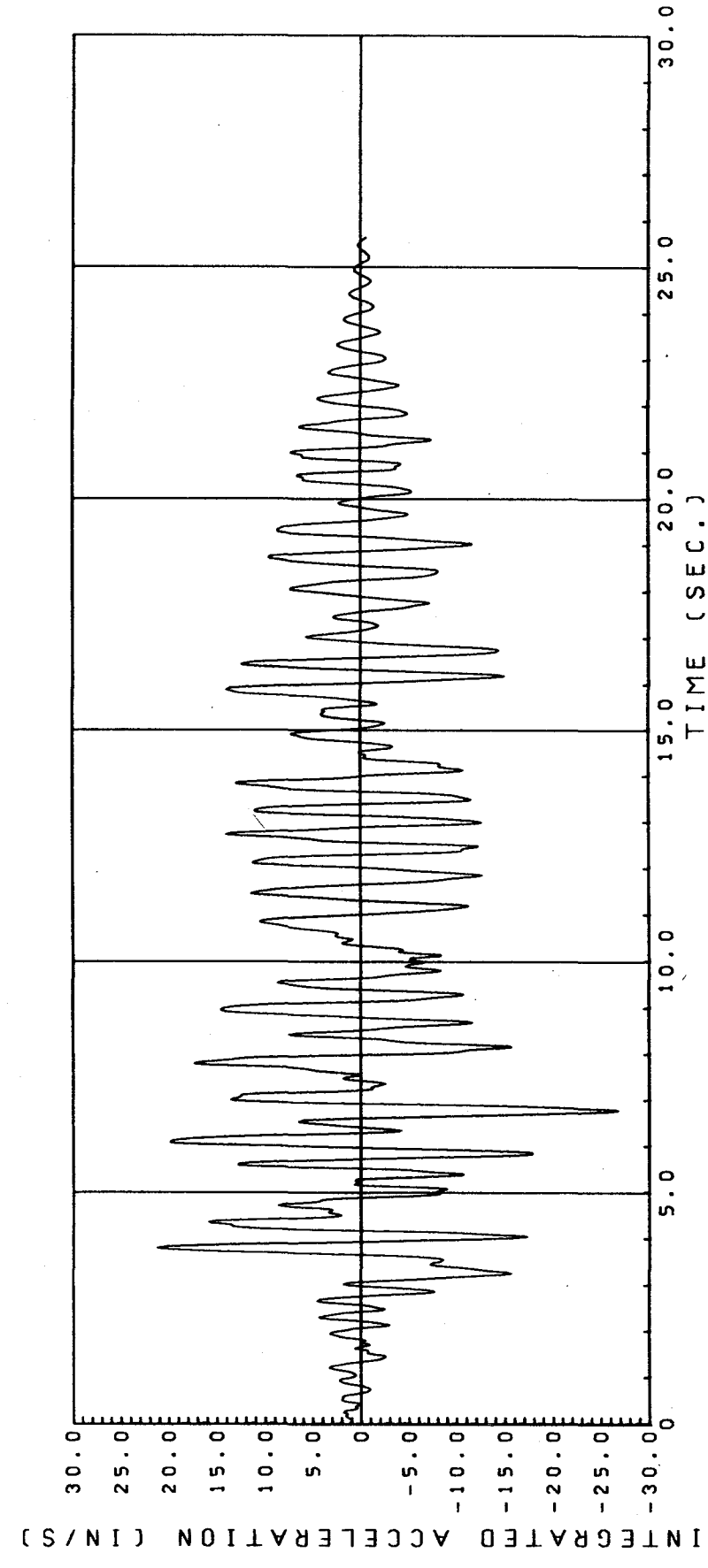

Fig. 9.1a) EVALUATION OF BOTTOM STORY VELOCITY BY INTEGRATION OF THE ACCELERATION RECORD. RCF2 RUN W2.

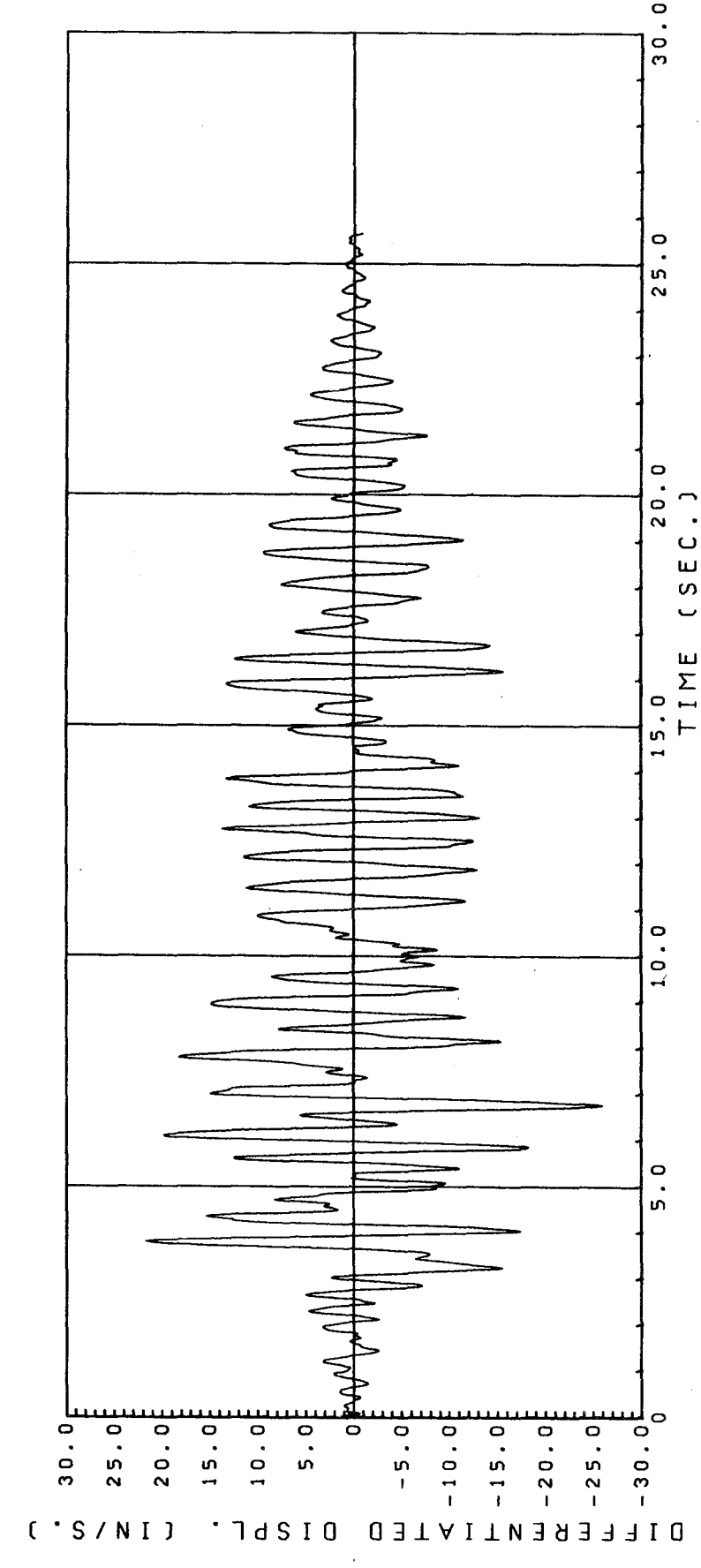

Fig. 9.1b) EVALUATION OF BOTTOM STORY VELOCITY BY DIFFERENTIATION OF THE DISPLACEMENT RECORD.

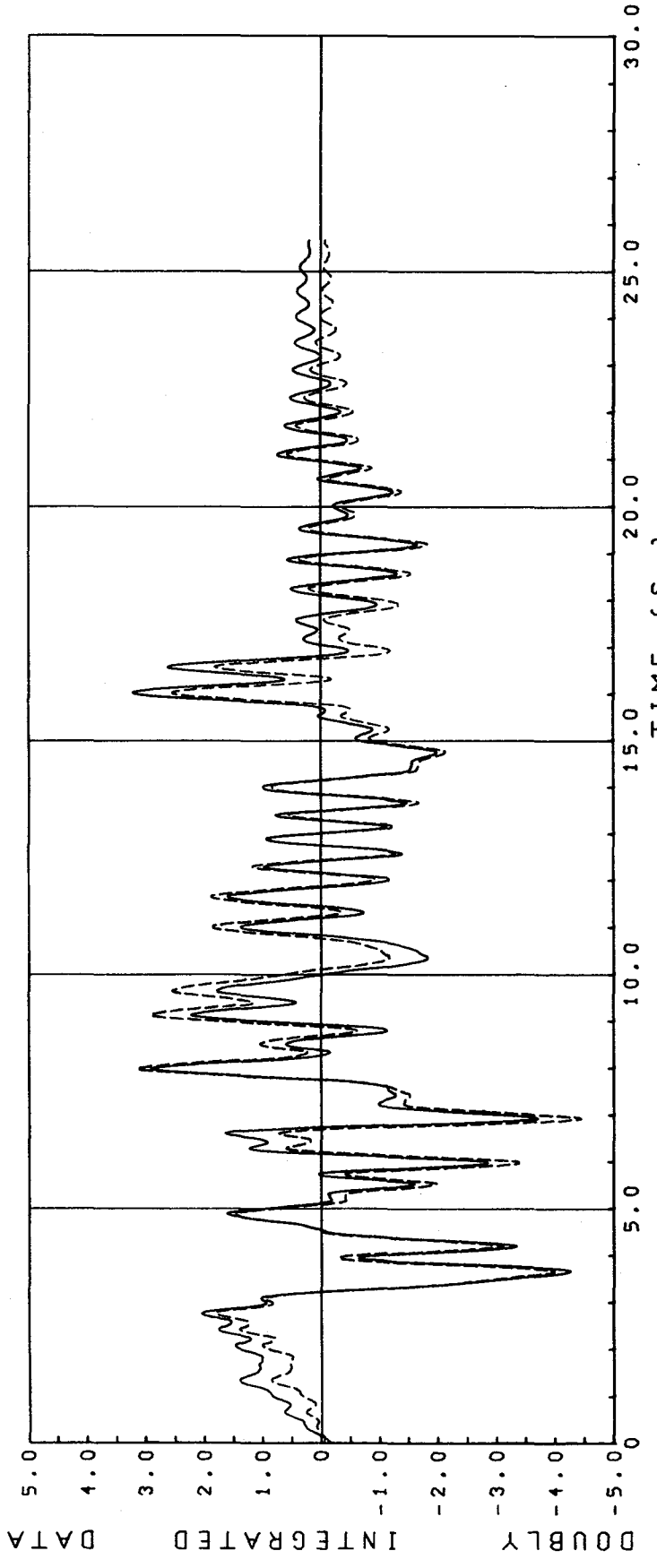

Fig. 9.2a) EVALUATION OF THE BOTTOM STORY DISPLACEMENT BY DOUBLE INTEGRATION OF THE ACCELERATION RECORD. PROCESS: LHIBIB. RCF2 RUN W2.

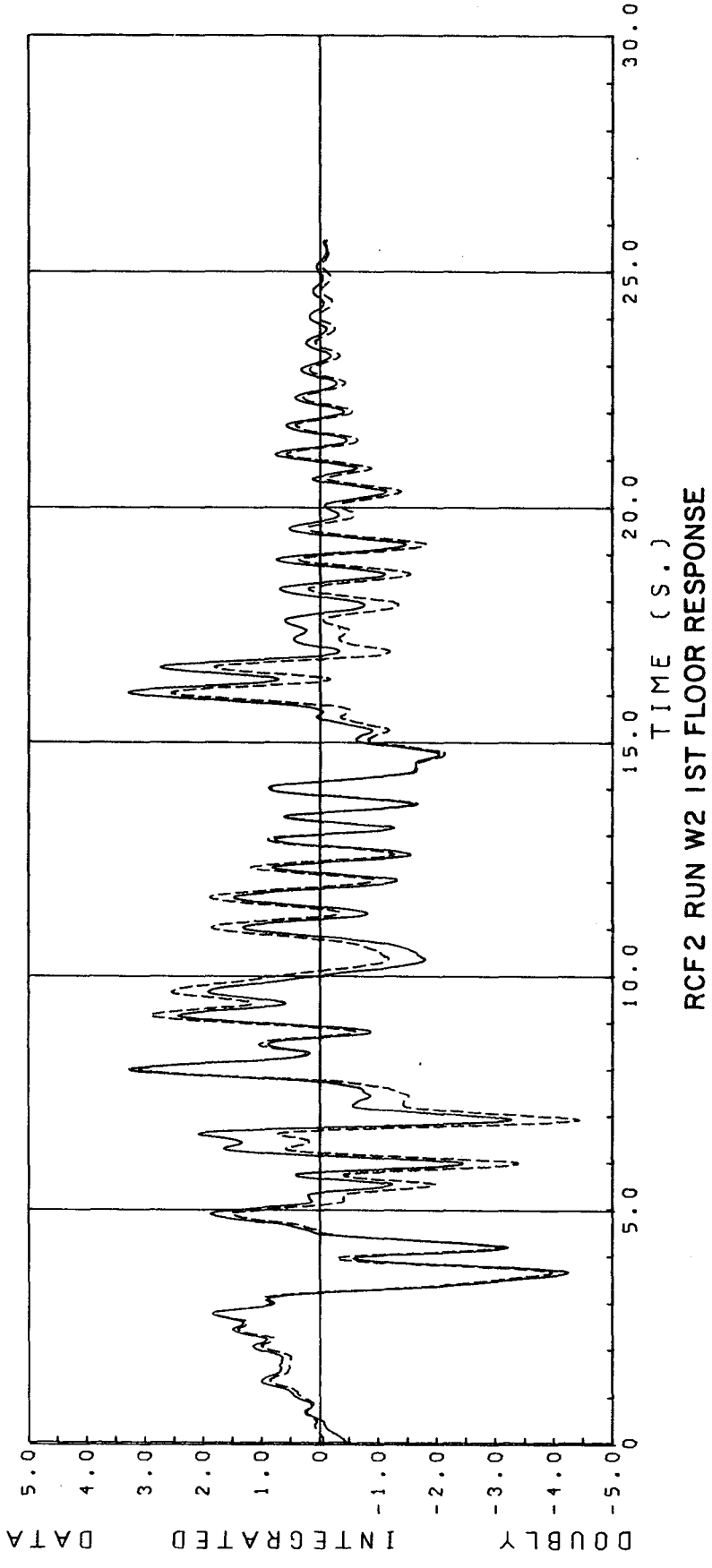

Fig 9.2b) EVALUATION OF THE BOTTOM STORY DISPLACEMENT BY DOUBLE INTEGRATION OF THE ACCELERATION RECORD. PROCESS: LHIHIH. RCF2 RUN W2.

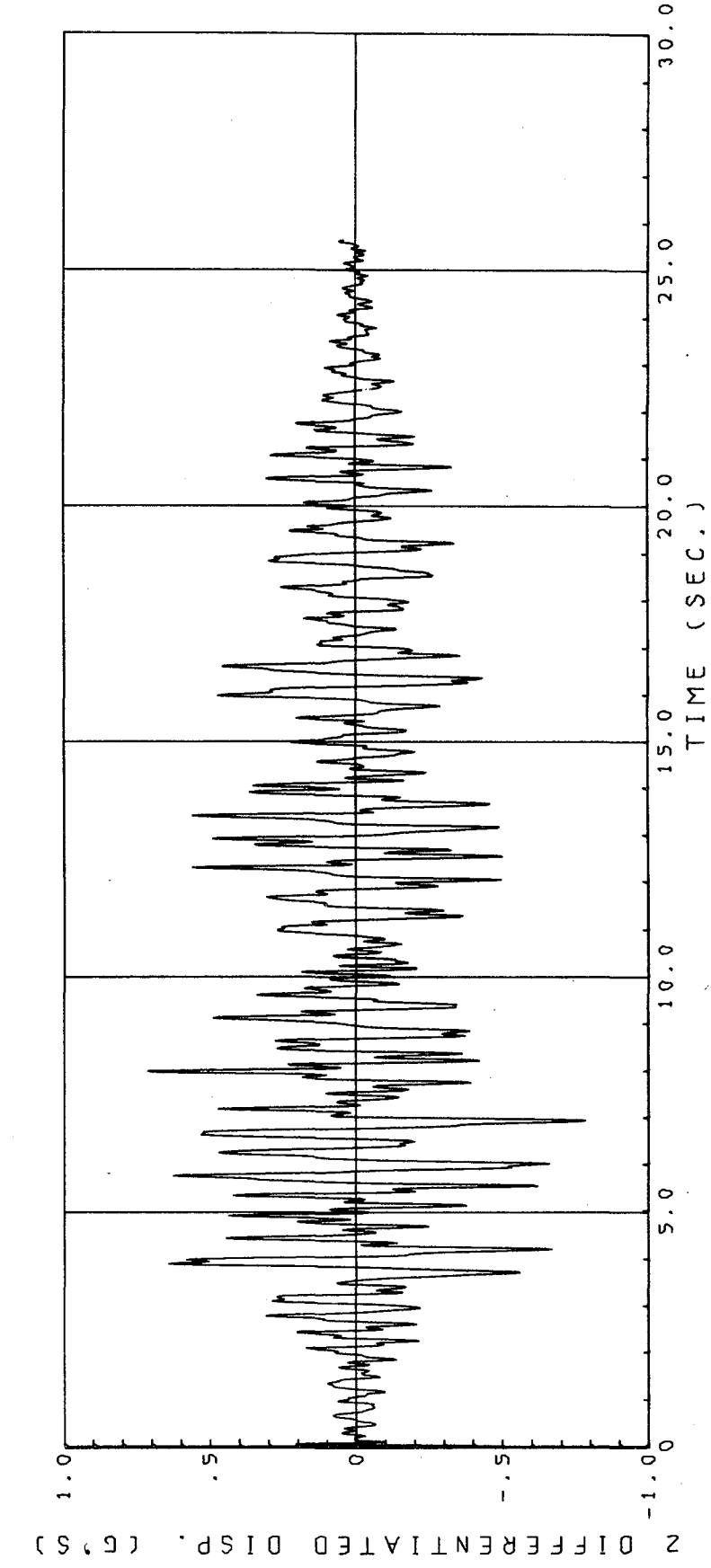

Fig. 9.3 EVALUATION OF THE BOTTOM STORY ACCELERATION BY DOUBLE DIFFERENTIATION OF THE DISPLACEMENT RECORD. RCF2 RUN W2.

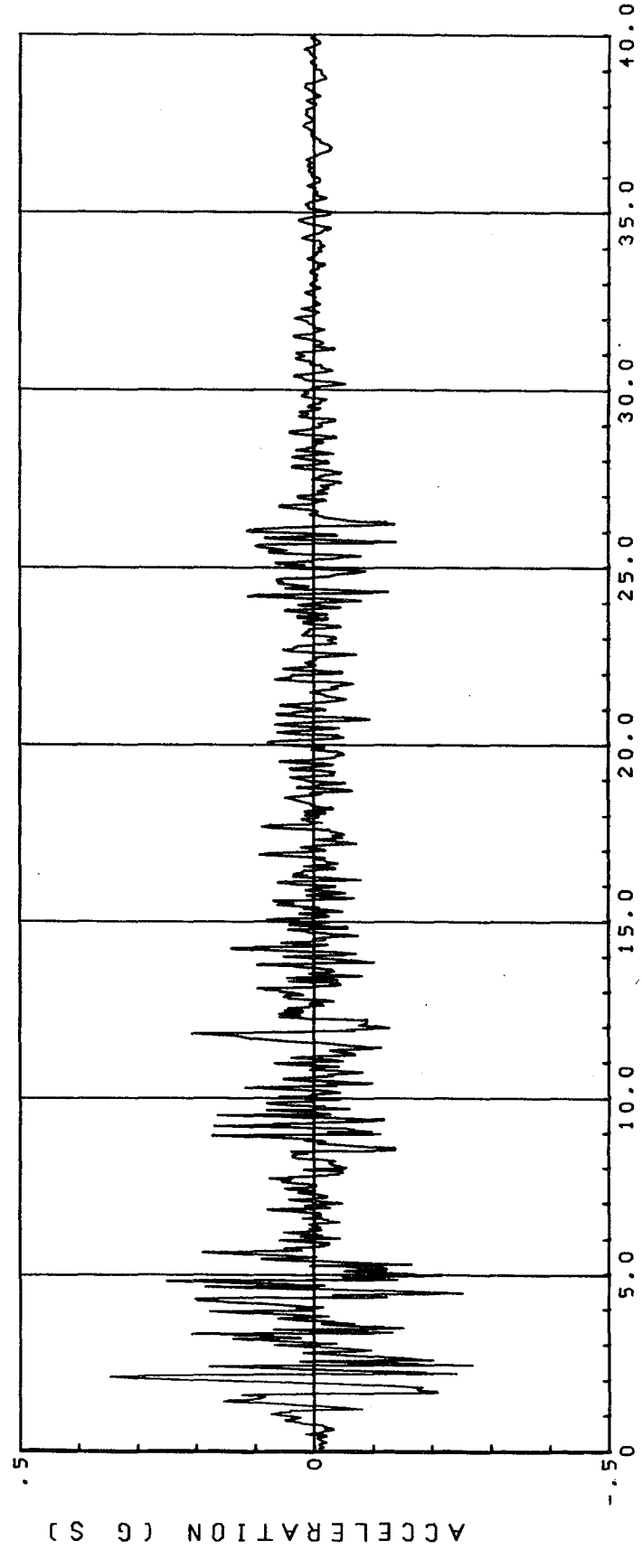

Fig 9.4 EL CENTRO 1940 ACCELERATION RECORD (N-S COMPONENT).

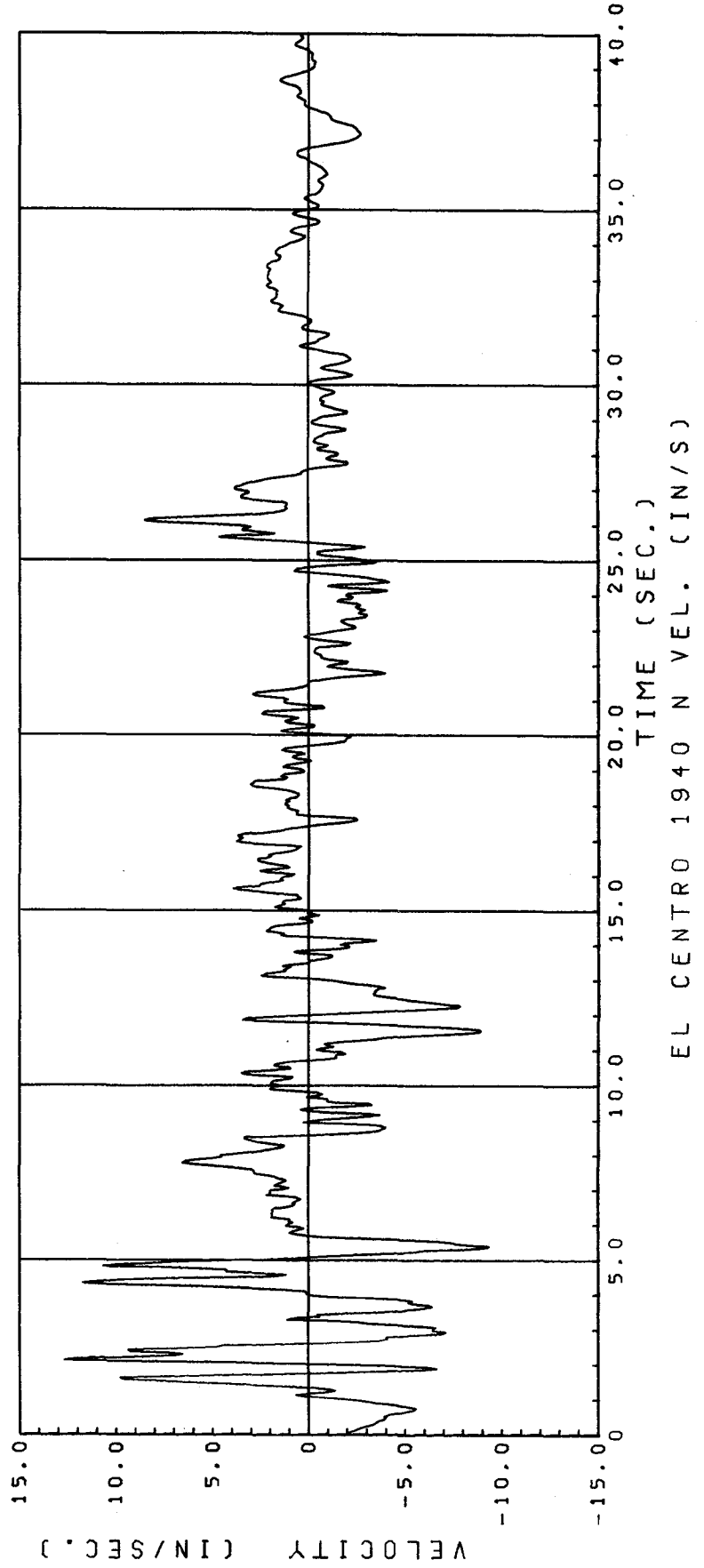

Fig. 9.5a) EL CENTRO 1940 VELOCITY RECORD (N-S COMPONENT). STANDARD PROCESSING.

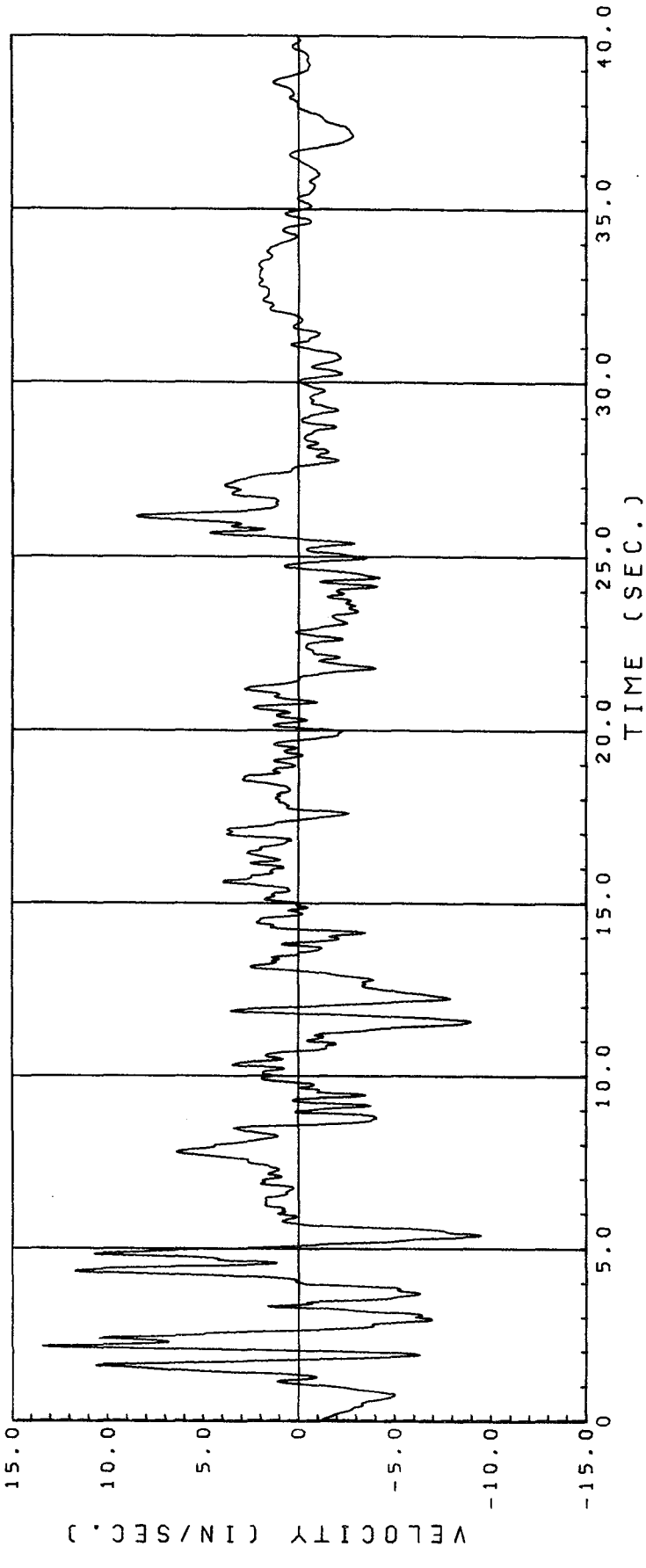

Fig 9.5b) EL CENTRO 1940 VELOCITY RECORD (N-S COMPONENT)
OBTAINED BY INTEGRATION OF THE ACCELERATION RECORD (DIPS).
BPF: 0.04-0.07, 20.-25. HZ.

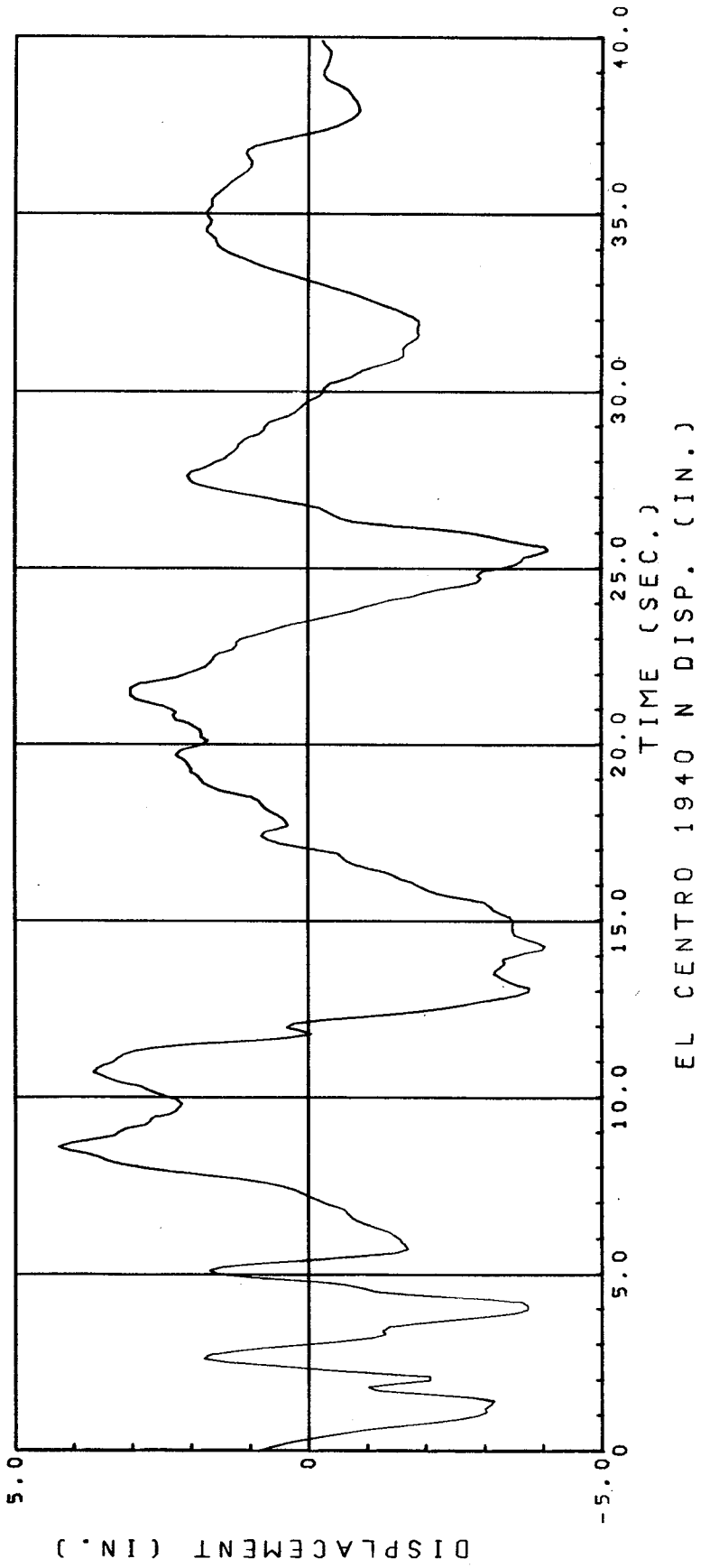

Fig. 9.6a) EL CENTRO 1940 DISPLACEMENT RECORD (N-S COMPONENT). STANDARD PROCESSING.

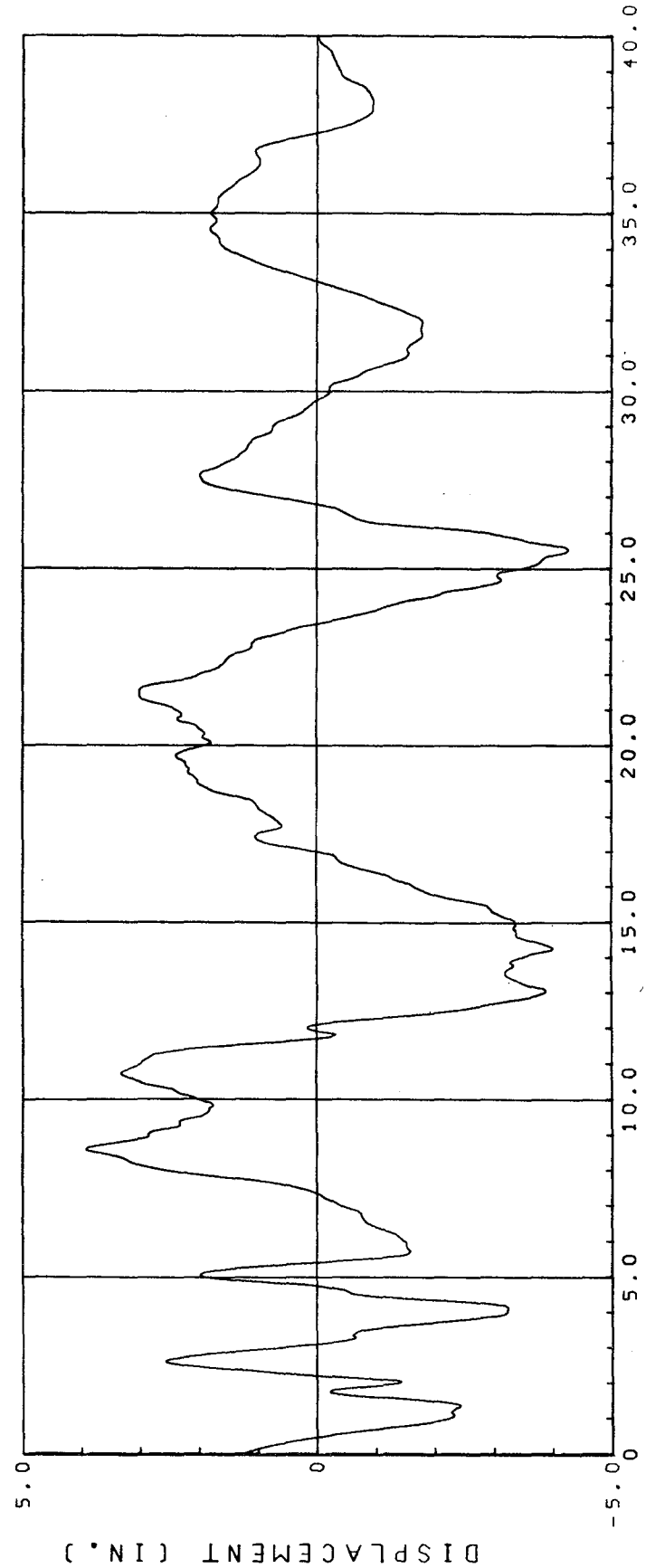

Fig. 9.6b) EL CENTRO 1940 DISPLACEMENT RECORD (N-S COMPONENT)
OBTAINED BY DOUBLE INTEGRATION OF ACCELERATION RECORD (DIPS).
BPF: 0.04-0.07, 20.-25. HZ.

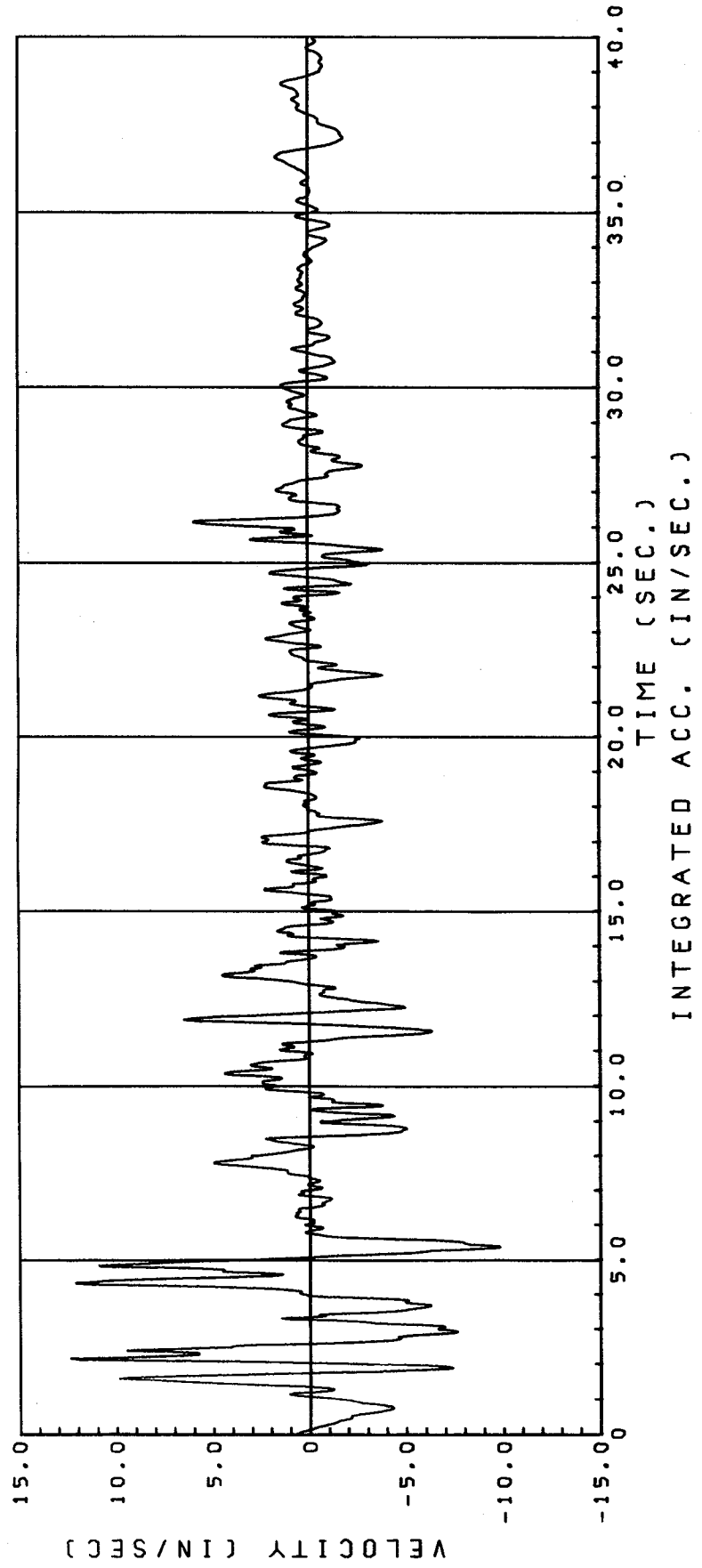

Fig. 9.7 EL CENTRO 1940 VELOCITY RECORD (N-S COMPONENT)
FOR BPF: 0.2-0.3, 20.-25. HZ.
INTEGRATED ACCELERATION USING DIPS.

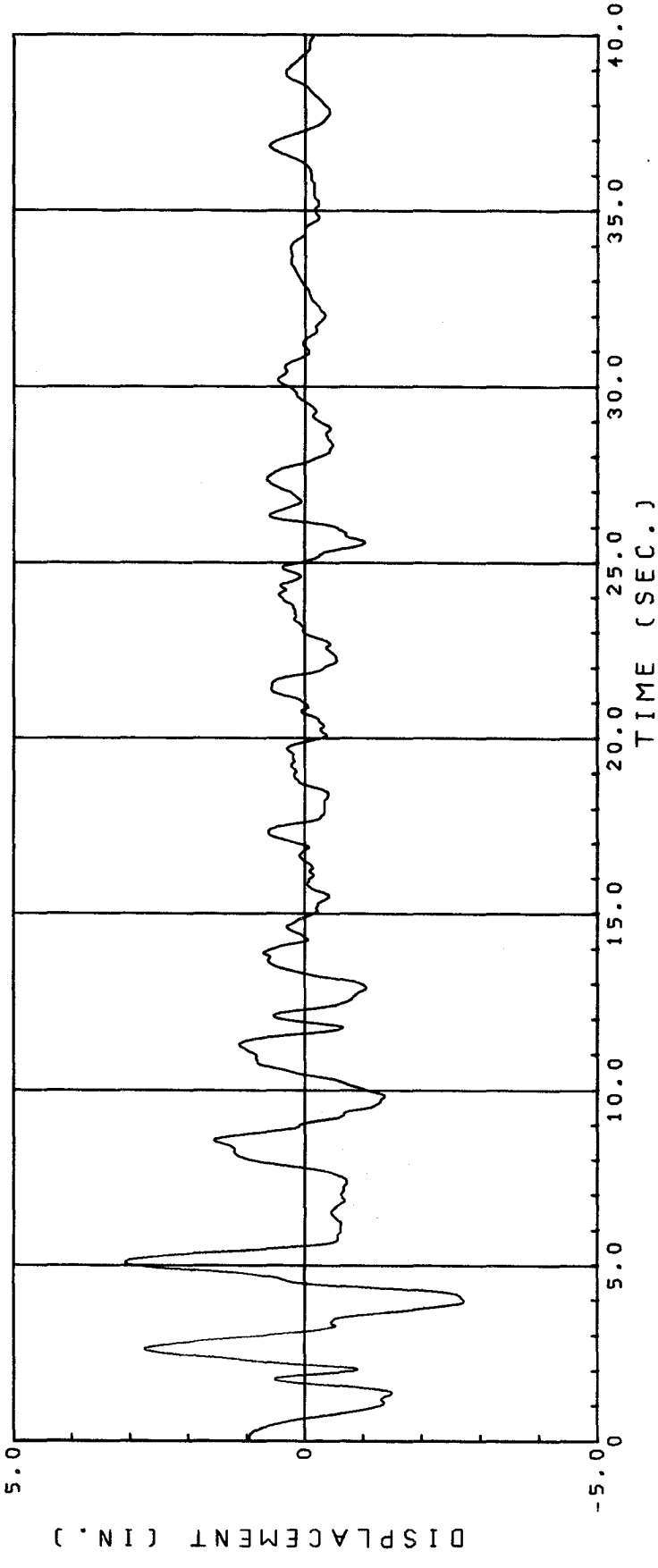

Fig. 9.8 EL CENTRO 1940 DISPLACEMENT RECORD (N-S COMPONENT)
FOR BPF: 0.2-0.3, 20.-25. HZ.
DOUBLY INTEGRATED ACCELERATION USING DIPS.

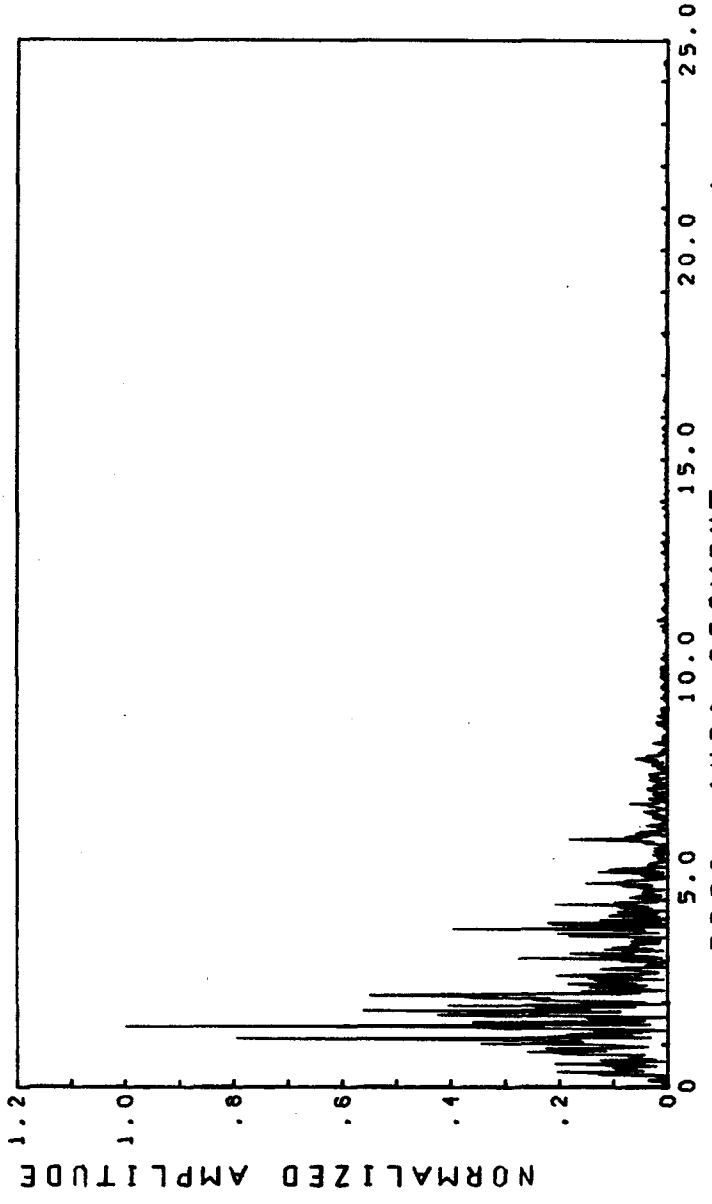

Fig. 9.9 EL CENTRO 1940 (N-S COMPONENT) FOURIER TRANSFORM.

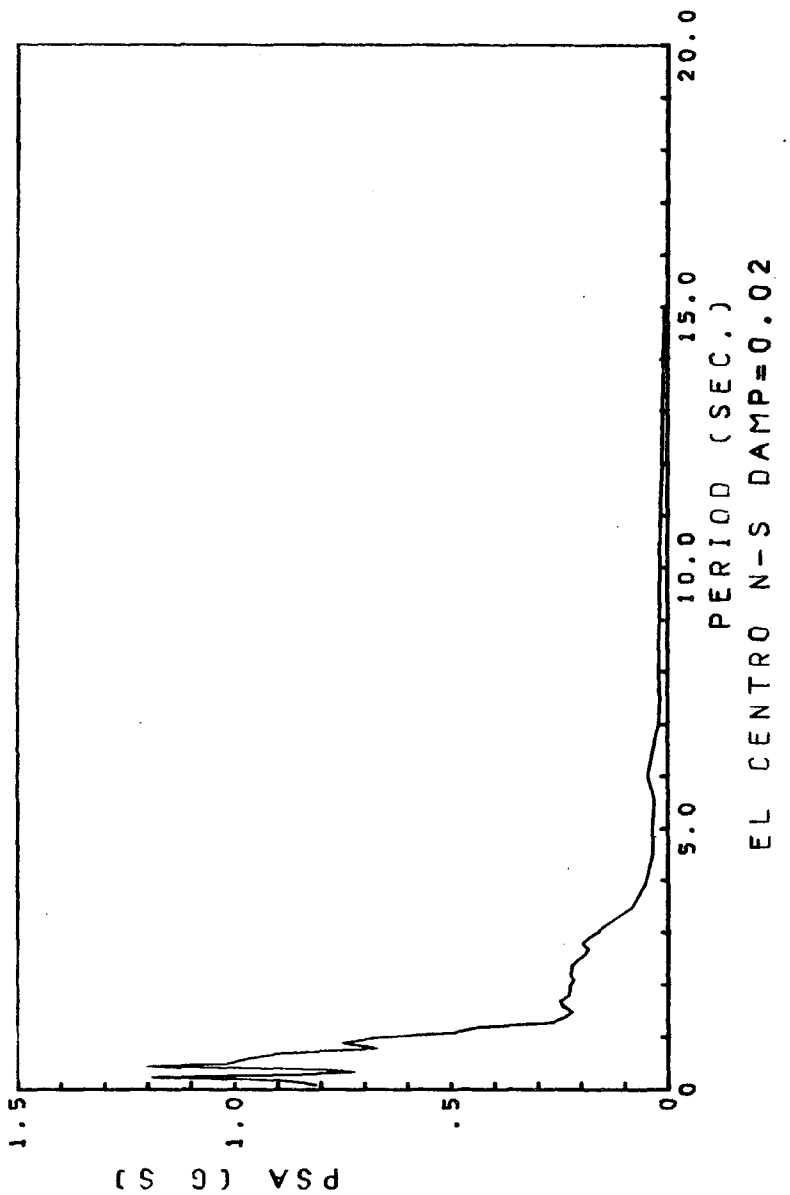

Fig. 9.10a) EL CENTRO 1940 (N-S COMPONENT)
PSEUDOACCELERATION RESPONSE SPECTRUM.
DAMPING: 2% CRIT.

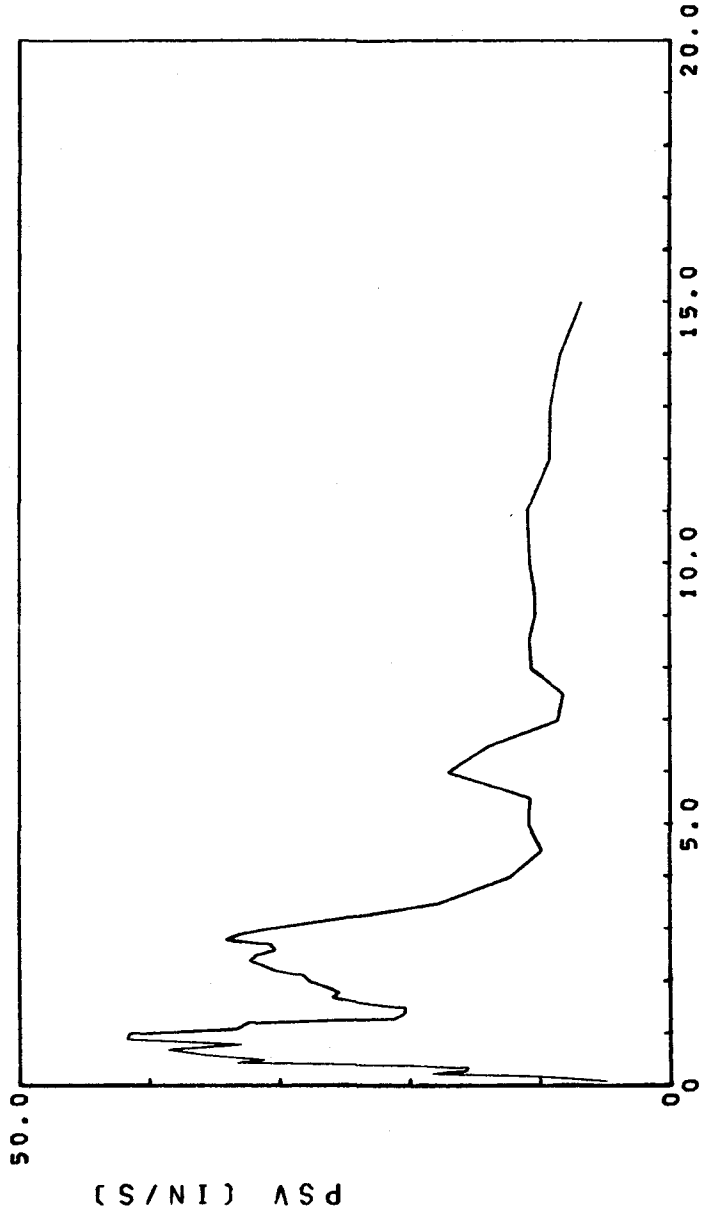

Fig. 9.10b) EL CENTRO 1940 (N-S COMPONENT)
PSEUDOVELOCITY RESPONSE SPECTRUM.
DAMPING: 2% CRIT.

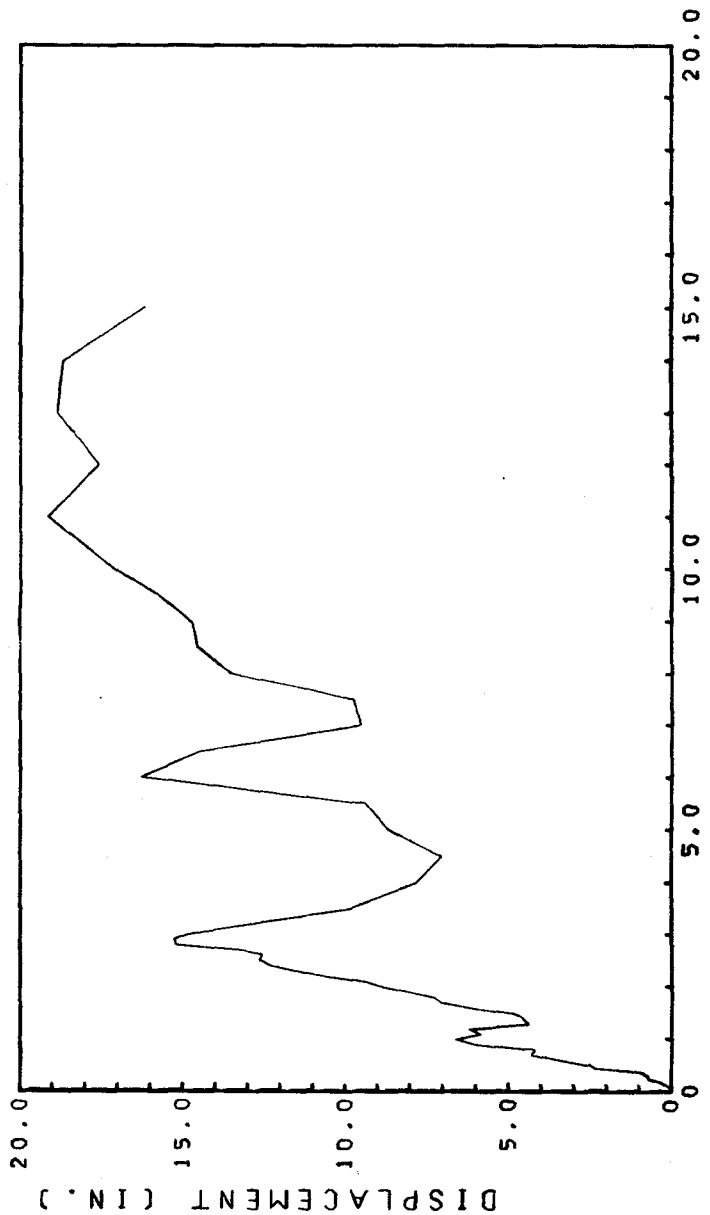

Fig. 9.10c) EL CENTRO 1940 (N-S COMPONENT)
DISPLACEMENT RESPONSE SPECTRUM.
DAMPING: 2% CRIT.

10) FINAL REMARKS

The computer program described in the previous chapter was used in a number of studies of experimental and seismic data (e.g. from the Pacoima dam 1971 record and shaking table tests of a steam generator and a one story steel frame) in which numerical filtering was involved. The experience gained in these studies indicates that the most important aspect in the process is not the sophistication of the numerical techniques employed, but the specification of the filter parameters. These determine how much information is to be preserved for analysis, or further processing, and how much is to be discarded, along with the noise in the data.

In the cases involving the integration of accelerograms to compute the corresponding velocity and displacement, the velocity could be obtained with reasonable accuracy, after adjusting (by trial and error) the filter passband and stopbands. The additional integration to obtain the displacement (combined with filtering and/or baseline correction) was in most cases a risky operation. The results obtained by slightly varying the filter coefficients or the sequence of operations were in general noticeably different.

This situation can have significant repercussions for earthquake resistant design, since the predicted ground displacements can substantially differ according to the specified characteristics of the filter used. It seems probable that the displacement response spectra of seismic ground motions is highly sensitive to the specifications of the filter, especially in the low frequency (long period) range. This remains an invitation for future investigation.

To summarize, a substantial amount of research yet needs to be done to establish meaningful criteria for selecting the transfer function characteristics of the filters to be employed during the processing of real or simulated seismic data.

REFERENCES

1. Blondet, J. M., Clough, R. W. and Mahin, S. A., "Evaluation of a Shaking Table Test Program on Response Behavior of a Two Story Reinforced Concrete Frame," Earthquake Engineering Research Center Report No 80-42, December 1980.

2. Clough, R. W. and Gidwani, J., "Reinforced Concrete Frame 2: Seismic Testing and Analytic Correlation," Earthquake Engineering Reseach Center Report No 76-15, June 1976.

3. Hidalgo, P. and Clough, R. W., "Earthquake Simulator Study of a Reinforced Concrete Frame," Earthquake Engineering Research Center Report No 74-13, December 1974.

4. International Conference of Building Officials, "Uniform Building Code, 1979 Edition," Pasadena, California, 1979.

5. Clough, R. W. and Penzien, J. "Dynamics of Structures," Mc Graw-Hill Book Company, 1975.

6. Nigam, N. C. and Jennings, P. C., "SPECEQ/SPECUQ, Digital Calculation of Response Spectra from Strong-Motion

Earthquake Records," a Computer Program Distributed by NISEE / Computer Applications, California Institute of Technology, Pasadena, California, June 1968.

7. "User Manual for the Surface Display Library," Prepared by the Software Development Group, Dynamic Graphics, Inc., Berkeley, California, 1975.

8. Gulkan, P. and Sozen, M. A., "Inelastic Responses of Reinforced Structures to Earthquake Motions," ACI Journal, Proceedings V. 71, No 12, Dec 1974.

9. Housner, G. W. and Jennings, P. C., "The Capacity of Extreme Earthquake Motions to Damage Structures," in Structural and Geotechnical Mechanics, a Volume Honoring Nathan M. Newmark, edited by J. W. Hall, Prentice Hall, New Jersey, 1977.

10. Hudson, D. E., "Reading and Interpreting Strong Motion Accelerograms," Earthquake Engineering Research Institute, Berkeley, California, 1980.

11. Trifunac, M. D. and Lee, V. "Routine Computer Processing of Strong-Motion Accelerograms," Earthquake Engineering Research Laboratory Report No. 73-03, California Institute of Technology, Pasadena, 1973.

12. Sunder, S. S. "On the Standard Processing of Strong-Motion earthquake Signals," Research Report R80-38, Department of Civil Engineering, Massachusetts Institute of Technology, Cambridge, Massachusetts, September 1980.

13. Shoja-Taheri, J. "Seismological Studies of Strong Motion Records," Earthquake Engineering Research Center Report No. UCB/EERC-77/04, January 1977.

14. Oppenheim, A. V. and Schafer, R. "Digital Signal Processing," Prentice-Hall, Inc, New Jersey, 1975.

15. Hamming, R. W., "Digital Filters," Prentice-Hall, New Jersey, 1979.

16. Rabiner, L. and Gold, B., "Theory and Application of Digital Signal Processing," Prentice-Hall, New Jersey, 1975.

17. Hamming, R. W., "Numerical Methods for Scientists and Engineers," Second Edition, Mc Graw-Hill, Inc., 1973.

18. Brigham, E. O., "The Fast Fourier Transform," Prentice-Hall, New Jersey, 1974.

19. Bracewell, R. N., "The Fourier Transform and its Applications," Second Edition, Mc Graw-Hill Book Company, New York, 1978.

20. Kaiser, J. F., "Digital Filters," Chapter 7 in System Analysis by Digital Computer, by Kuo, F. F. and Kaiser, J. F., John Wiley and Sons, Inc., New York, 1966.

21. Ormsby, J. F., "Design of Numerical Filters with Applications to Missile Data Processing," JACM, 8, 3, July 1961.

APPENDIX

USER'S MANUAL FOR PROGRAM DIPS

This appendix contains a list of the operations currently implemented in the computer program DIPS, for processing of shaking table or seismic signals. The data required to perform each operation, as well as the required input format is also given. The description of these operations, along with their respective limitations, can be found in Chapter Nine of this report.

The general input data sequence is:

Macrocommand (starting in column 1)

Data Card(s)

Blank card (separator, optional).

Macrocommand

Data card(s)

Blank card

ETC.

The operations can be generally specified in any desired order, with the exception of START and STOP, which must be, respectively, the first and last commands.

The available operations and the data required are:

START; one data card (4A10).

Cols

1-40 LINEX3 General Title.

READ

a) Card 1 (3I5,5x,F10.0).

Cols		
1-5	NP	Number of data points (must be a multiple of 50).
6-10	NPT1	Number of points at "quiet zone" at the beginning of record.
11-15	NPT3	Idem, at end of record.
21-30	DT	Time interval between data points.

b) Card 2 (A10,I5).

Cols		
1-10	LFORM	Input data format. If LFORM=TAPE (starting at column 1), then NTAPE, the input file tape number, must be specified. Otherwise, LFORM specifies the format in which data will be input from cards. Example: (10F10.0).
11-15	NTAPE	See above.

c) If LFORM<>TAPE, enough data cards must be provided to input NP data points in the specified (LFORM) format.

LABEL; one data card (3A10).

Cols		
1-30	LINEX2	Title for plot x-axis and for output.

PRINT; one data card (3A10).

Cols

1-30 LFORM Printing format (including control carriage specification).

PUNCH; one data card (3A10).

Cols

1-30 LFORM Punching format.

WRITE; one data card (I5).

Cols

1-5 NTAPE Tape file number where record is to be written (in unblocked form).

PLOT; one data card (3A10)

Cols

1-30 LINEY Title for plot y-axis.

SCALE; one data card (F10.0).

Cols

1-10 AMULT Multiplier.

BLINE; one data card (I5,5X,2I5).

Cols

1-5 IC Indicator for type of correction:

IC=0 Constant baseline correction.

IC=1 Linear baseline correction.

11-15	NFIRST	Number of points at beginning of record to be used for correction.
16-20	NLAST	Number of points at end of record to be used for correction.

LOPASS; one data card (3F10.0).

Cols		
1-10	F3	Cutoff frequency (Hz.).
11-20	F4	Rolloff termination freq. (Hz.).
21-30	ATT	Attenuation (dB.).

HIPASS; one data card (3F10.0).

Cols		
1-10	F1	Rolloff termination freq. (Hz.).
11-20	F2	Cutoff freq. (Hz.).
21-30	ATT	Attenuation (dB.).

INTGR; no data required.

DERIV; no data required.

STAT; no data required

SQUARE; no data required.

SQRT; no data required.

FFT; two data cards.

a) Card 1 (7I5).

Cols		
1-5	NSEG	Number of segments to be processed.
6-10	ISTART	Starting data point number.
11-15	INT	Interval (in data points) between segments.
16-20	M	Power of two. The number of data points in each segment is N=2**M.
21-25	IKIND	Output specification flag: IKIND=0 output is amplitude of DFT. IKIND=1 output is square of amplitude of DFT (proportional to PSDF).
26-30	IPLFT	If nonzero, plots will be generated.
31-35	IPRFT	If nonzero, output will be printed.

b) Card 2 (2F10.0).

Cols		
1-10	FRMIN	Minimum frequency component (Hz.) in output.
11-20	FRMAX	Maximum frequency component in output.

SPCTR

a) Card 1 (F10.0,I5).

Cols		
1-10	DAMP	Damping ratio (fraction of critical).
11-15	NCARDS	Number of cards for period range input .

b) NCARDS data cards (2F10.0,I5).

Cols		
1-10	P1	First period value (sec.)
11-20	P2	Last period value.
21-25	NINT	Number of equal intervals in which the range P1, P2 is to be divided.

c) One data card (4I5).

Cols		
1-5	ISI	If nonzero, the spectral intensity (area under the PSV spectrum) will be computed for the period range TA-TB (specified in the next card).
6-10	IPRSP	If nonzero, the spectral values will be printed.
11-15	IPLSP	If nonzero, the response spectra will be plotted.
16-20	IENV	If nonzero, the envelope of peaks of PSA response and their time of occurrence will be computed and stored for each period value. Output will be written on tapefiles TAPE4 for the peak values and TAPE5 for the corresponding times; in unblocked form. Each record will contain information in the following sequence: period value, number of peaks, data values.

d) Only if ISI<>0. One data card (2F10.0)

Cols

1-10	TA	See above.
11-20	TB	See above.

STOP; no data required.

EARTHQUAKE ENGINEERING RESEARCH CENTER REPORTS

NOTE: Numbers in parenthesis are Accession Numbers assigned by the National Technical Information Service; these are followed by a price code. Copies of the reports may be ordered from the National Technical Information Service, 5285 Port Royal Road, Springfield, Virginia, 22161. Accession Numbers should be quoted on orders for reports (PB --- ---) and remittance must accompany each order. Reports without this information were not available at time of printing. Upon request, EERC will mail inquirers this information when it becomes available.

EERC 67-1 "Feasibility Study Large-Scale Earthquake Simulator Facility," by J. Penzien, J.G. Bouwkamp, R.W. Clough and D. Rea - 1967 (PB 187 905)A07

EERC 68-1 Unassigned

EERC 68-2 "Inelastic Behavior of Beam-to-Column Subassemblages Under Repeated Loading," by V.V. Bertero - 1968 (PB 184 888)A05

EERC 68-3 "A Graphical Method for Solving the Wave Reflection-Refraction Problem," by H.D. McNiven and Y. Mengi - 1968 (PB 187 943)A03

EERC 68-4 "Dynamic Properties of McKinley School Buildings," by D. Rea, J.G. Bouwkamp and R.W. Clough - 1968 (PB 187 902)A07

EERC 68-5 "Characteristics of Rock Motions During Earthquakes," by H.B. Seed, I.M. Idriss and F.W. Kiefer - 1968 (PB 188 338)A03

EERC 69-1 "Earthquake Engineering Research at Berkeley," - 1969 (PB 187 906)All

EERC 69-2 "Nonlinear Seismic Response of Earth Structures," by M. Dibaj and J. Penzien - 1969 (PB 187 904)A08

EERC 69-3 "Probabilistic Study of the Behavior of Structures During Earthquakes," by R. Ruiz and J. Penzien - 1969 (PB 187 886)A06

EERC 69-4 "Numerical Solution of Boundary Value Problems in Structural Mechanics by Reduction to an Initial Value Formulation," by N. Distefano and J. Schujman - 1969 (PB 187 942)A02

EERC 69-5 "Dynamic Programming and the Solution of the Biharmonic Equation," by N. Distefano - 1969 (PB 187 941)A03

EERC 69-6 "Stochastic Analysis of Offshore Tower Structures," by A.K. Malhotra and J. Penzien - 1969 (PB 187 903)A09

EERC 69-7 "Rock Motion Accelerograms for High Magnitude Earthquakes," by H.B. Seed and I.M. Idriss - 1969 (PB 187 940)A02

EERC 69-8 "Structural Dynamics Testing Facilities at the University of California, Berkeley," by R.M. Stephen, J.G. Bouwkamp, R.W. Clough and J. Penzien - 1969 (PB 189 111)A04

EERC 69-9 "Seismic Response of Soil Deposits Underlain by Sloping Rock Boundaries," by H. Dezfulian and H.B. Seed 1969 (PB 189 114)A03

EERC 69-10 "Dynamic Stress Analysis of Axisymmetric Structures Under Arbitrary Loading," by S. Ghosh and E.L. Wilson 1969 (PB 189 026)A10

EERC 69-11 "Seismic Behavior of Multistory Frames Designed by Different Philosophies," by J.C. Anderson and V. V. Bertero - 1969 (PB 190 662)A10

EERC 69-12 "Stiffness Degradation of Reinforcing Concrete Members Subjected to Cyclic Flexural Moments," by V.V. Bertero, B. Bresler and H. Ming Liao - 1969 (PB 202 942)A07

EERC 69-13 "Response of Non-Uniform Soil Deposits to Travelling Seismic Waves," by H. Dezfulian and H.B. Seed - 1969 (PB 191 023)A03

EERC 69-14 "Damping Capacity of a Model Steel Structure," by D. Rea, R.W. Clough and J.G. Bouwkamp - 1969 (PB 190 663)A06

EERC 69-15 "Influence of Local Soil Conditions on Building Damage Potential during Earthquakes," by H.B. Seed and I.M. Idriss - 1969 (PB 191 036)A03

EERC 69-16 "The Behavior of Sands Under Seismic Loading Conditions," by M.L. Silver and H.B. Seed - 1969 (AD 714 982)A07

EERC 70-1 "Earthquake Response of Gravity Dams," by A.K. Chopra - 1970 (AD 709 640)A03

EERC 70-2 "Relationships between Soil Conditions and Building Damage in the Caracas Earthquake of July 29, 1967," by H.B. Seed, I.M. Idriss and H. Dezfulian - 1970 (PB 195 762)A05

EERC 70-3 "Cyclic Loading of Full Size Steel Connections," by E.P. Popov and R.M. Stephen - 1970 (PB 213 545)A04

EERC 70-4 "Seismic Analysis of the Charaima Building, Caraballeda, Venezuela," by Subcommittee of the SEAONC Research Committee: V.V. Bertero, P.F. Fratessa, S.A. Mahin, J.H. Sexton, A.C. Scordelis, E.L. Wilson, L.A. Wyllie, H.B. Seed and J. Penzien, Chairman - 1970 (PB 201 455)A06

EERC 70-5 "A Computer Program for Earthquake Analysis of Dams," by A.K. Chopra and P. Chakrabarti - 1970 (AD 723 994)A05

EERC 70-6 "The Propagation of Love Waves Across Non-Horizontally Layered Structures," by J. Lysmer and L.A. Drake 1970 (PB 197 896)A03

EERC 70-7 "Influence of Base Rock Characteristics on Ground Response," by J. Lysmer, H.B. Seed and P.B. Schnabel 1970 (PB 197 897)A03

EERC 70-8 "Applicability of Laboratory Test Procedures for Measuring Soil Liquefaction Characteristics under Cyclic Loading," by H.B. Seed and W.H. Peacock - 1970 (PB 198 016)A03

EERC 70-9 "A Simplified Procedure for Evaluating Soil Liquefaction Potential," by H.B. Seed and I.M. Idriss - 1970 (PB 198 009)A03

EERC 70-10 "Soil Moduli and Damping Factors for Dynamic Response Analysis," by H.B. Seed and I.M. Idriss - 1970 (PB 197 869)A03

EERC 71-1 "Koyna Earthquake of December 11, 1967 and the Performance of Koyna Dam," by A.K. Chopra and P. Chakrabarti 1971 (AD 731 496)A06

EERC 71-2 "Preliminary In-Situ Measurements of Anelastic Absorption in Soils Using a Prototype Earthquake Simulator," by R.D. Borcherdt and P.W. Rodgers - 1971 (PB 201 454)A03

EERC 71-3 "Static and Dynamic Analysis of Inelastic Frame Structures," by F.L. Porter and G.H. Powell - 1971 (PB 210 135)A06

EERC 71-4 "Research Needs in Limit Design of Reinforced Concrete Structures," by V.V. Bertero - 1971 (PB 202 943)A04

EERC 71-5 "Dynamic Behavior of a High-Rise Diagonally Braced Steel Building," by D. Rea, A.A. Shah and J.G. Bouwkamp 1971 (PB 203 584)A06

EERC 71-6 "Dynamic Stress Analysis of Porous Elastic Solids Saturated with Compressible Fluids," by J. Ghaboussi and E. L. Wilson - 1971 (PB 211 396)A06

EERC 71-7 "Inelastic Behavior of Steel Beam-to-Column Subassemblages," by H. Krawinkler, V.V. Bertero and E.P. Popov 1971 (PB 211 335)A14

EERC 71-8 "Modification of Seismograph Records for Effects of Local Soil Conditions," by P. Schnabel, H.B. Seed and J. Lysmer - 1971 (PB 214 450)A03

EERC 72-1 "Static and Earthquake Analysis of Three Dimensional Frame and Shear Wall Buildings," by E.L. Wilson and H.H. Dovey - 1972 (PB 212 904)A05

EERC 72-2 "Accelerations in Rock for Earthquakes in the Western United States," by P.B. Schnabel and H.B. Seed - 1972 (PB 213 100)A03

EERC 72-3 "Elastic-Plastic Earthquake Response of Soil-Building Systems," by T. Minami - 1972 (PB 214 868)A08

EERC 72-4 "Stochastic Inelastic Response of Offshore Towers to Strong Motion Earthquakes," by M.K. Kaul - 1972 (PB 215 713)A05

EERC 72-5 "Cyclic Behavior of Three Reinforced Concrete Flexural Members with High Shear," by E.P. Popov, V.V. Bertero and H. Krawinkler - 1972 (PB 214 555)A05

EERC 72-6 "Earthquake Response of Gravity Dams Including Reservoir Interaction Effects," by P. Chakrabarti and A.K. Chopra - 1972 (AD 762 330)A08

EERC 72-7 "Dynamic Properties of Pine Flat Dam," by D. Rea, C.Y. Liaw and A.K. Chopra - 1972 (AD 763 928)A05

EERC 72-8 "Three Dimensional Analysis of Building Systems," by E.L. Wilson and H.H. Dovey - 1972 (PB 222 438)A06

EERC 72-9 "Rate of Loading Effects on Uncracked and Repaired Reinforced Concrete Members," by S. Mahin, V.V. Bertero, D. Rea and M. Atalay - 1972 (PB 224 520)A08

EERC 72-10 "Computer Program for Static and Dynamic Analysis of Linear Structural Systems," by E.L. Wilson, K.-J. Bathe, J.E. Peterson and H.H.Dovey - 1972 (PB 220 437)A04

EERC 72-11 "Literature Survey - Seismic Effects on Highway Bridges," by T. Iwasaki, J. Penzien and R.W. Clough - 1972 (PB 215 613)A19

EERC 72-12 "SHAKE-A Computer Program for Earthquake Response Analysis of Horizontally Layered Sites," by P.B. Schnabel and J. Lysmer - 1972 (PB 220 207)A06

EERC 73-1 "Optimal Seismic Design of Multistory Frames," by V.V. Bertero and H. Kamil - 1973

EERC 73-2 "Analysis of the Slides in the San Fernando Dams During the Earthquake of February 9, 1971," by H.B. Seed, K.L. Lee, I.M. Idriss and F. Makdisi - 1973 (PB 223 402)A14

EERC 73-3 "Computer Aided Ultimate Load Design of Unbraced Multistory Steel Frames," by M.B. El-Hafez and G.H. Powell 1973 (PB 248 315)A09

EERC 73-4 "Experimental Investigation into the Seismic Behavior of Critical Regions of Reinforced Concrete Components as Influenced by Moment and Shear," by M. Celebi and J. Penzien - 1973 (PB 215 884)A09

EERC 73-5 "Hysteretic Behavior of Epoxy-Repaired Reinforced Concrete Beams," by M. Celebi and J. Penzien - 1973 (PB 239 568)A03

EERC 73-6 "General Purpose Computer Program for Inelastic Dynamic Response of Plane Structures," by A. Kanaan and G.H. Powell - 1973 (PB 221 260)A08

EERC 73-7 "A Computer Program for Earthquake Analysis of Gravity Dams Including Reservoir Interaction," by P. Chakrabarti and A.K. Chopra - 1973 (AD 766 271)A04

EERC 73-8 "Behavior of Reinforced Concrete Deep Beam-Column Subassemblages Under Cyclic Loads," by O. Küstü and J.G. Bouwkamp - 1973 (PB 246 117)A12

EERC 73-9 "Earthquake Analysis of Structure-Foundation Systems," by A.K. Vaish and A.K. Chopra - 1973 (AD 766 272)A07

EERC 73-10 "Deconvolution of Seismic Response for Linear Systems," by R.B. Reimer - 1973 (PB 227 179)A08

EERC 73-11 "SAP IV: A Structural Analysis Program for Static and Dynamic Response of Linear Systems," by K.-J. Bathe, E.L. Wilson and F.E. Peterson - 1973 (PB 221 967)A09

EERC 73-12 "Analytical Investigations of the Seismic Response of Long, Multiple Span Highway Bridges," by W.S. Tseng and J. Penzien - 1973 (PB 227 816)A10

EERC 73-13 "Earthquake Analysis of Multi-Story Buildings Including Foundation Interaction," by A.K. Chopra and J.A. Gutierrez - 1973 (PB 222 970)A03

EERC 73-14 "ADAP: A Computer Program for Static and Dynamic Analysis of Arch Dams," by R.W. Clough, J.M. Raphael and S. Mojtahedi - 1973 (PB 223 763)A09

EERC 73-15 "Cyclic Plastic Analysis of Structural Steel Joints," by R.B. Pinkney and R.W. Clough - 1973 (PB 226 843)A08

EERC 73-16 "QUAD-4: A Computer Program for Evaluating the Seismic Response of Soil Structures by Variable Damping Finite Element Procedures," by I.M. Idriss, J. Lysmer, R. Hwang and H.B. Seed - 1973 (PB 229 424)A05

EERC 73-17 "Dynamic Behavior of a Multi-Story Pyramid Shaped Building," by R.M. Stephen, J.P. Hollings and J.G. Bouwkamp - 1973 (PB 240 718)A06

EERC 73-18 "Effect of Different Types of Reinforcing on Seismic Behavior of Short Concrete Columns," by V.V. Bertero, J. Hollings, O. Küstü, R.M. Stephen and J.G. Bouwkamp - 1973

EERC 73-19 "Olive View Medical Center Materials Studies, Phase I," by B. Bresler and V.V. Bertero - 1973 (PB 235 986)A06

EERC 73-20 "Linear and Nonlinear Seismic Analysis Computer Programs for Long Multiple-Span Highway Bridges," by W.S. Tseng and J. Penzien - 1973

EERC 73-21 "Constitutive Models for Cyclic Plastic Deformation of Engineering Materials," by J.M. Kelly and P.P. Gillis 1973 (PB 226 024)A03

EERC 73-22 "DRAIN - 2D User's Guide," by G.H. Powell - 1973 (PB 227 016)A05

EERC 73-23 "Earthquake Engineering at Berkeley - 1973," (PB 226 033)A11

EERC 73-24 Unassigned

EERC 73-25 "Earthquake Response of Axisymmetric Tower Structures Surrounded by Water," by C.Y. Liaw and A.K. Chopra 1973 (AD 773 052)A09

EERC 73-26 "Investigation of the Failures of the Olive View Stairtowers During the San Fernando Earthquake and Their Implications on Seismic Design," by V.V. Bertero and R.G. Collins - 1973 (PB 235 106)A13

EERC 73-27 "Further Studies on Seismic Behavior of Steel Beam-Column Subassemblages," by V.V. Bertero, H. Krawinkler and E.P. Popov - 1973 (PB 234 172)A06

EERC 74-1 "Seismic Risk Analysis," by C.S. Oliveira - 1974 (PB 235 920)A06

EERC 74-2 "Settlement and Liquefaction of Sands Under Multi-Directional Shaking," by R. Pyke, C.K. Chan and H.B. Seed 1974

EERC 74-3 "Optimum Design of Earthquake Resistant Shear Buildings," by D. Ray, K.S. Pister and A.K. Chopra - 1974 (PB 231 172)A06

EERC 74-4 "LUSH - A Computer Program for Complex Response Analysis of Soil-Structure Systems," by J. Lysmer, T. Udaka, H.B. Seed and R. Hwang - 1974 (PB 236 796)A05

EERC 74-5 "Sensitivity Analysis for Hysteretic Dynamic Systems: Applications to Earthquake Engineering," by D. Ray 1974 (PB 233 213)A06

EERC 74-6 "Soil Structure Interaction Analyses for Evaluating Seismic Response," by H.B. Seed, J. Lysmer and R. Hwang 1974 (PB 236 519)A04

EERC 74-7 Unassigned

EERC 74-8 "Shaking Table Tests of a Steel Frame - A Progress Report," by R.W. Clough and D. Tang - 1974 (PB 240 869)A03

EERC 74-9 "Hysteretic Behavior of Reinforced Concrete Flexural Members with Special Web Reinforcement," by V.V. Bertero, E.P. Popov and T.Y. Wang - 1974 (PB 236 797)A07

EERC 74-10 "Applications of Reliability-Based, Global Cost Optimization to Design of Earthquake Resistant Structures," by E. Vitiello and K.S. Pister - 1974 (PB 237 231)A06

EERC 74-11 "Liquefaction of Gravelly Soils Under Cyclic Loading Conditions," by R.T. Wong, H.B. Seed and C.K. Chan 1974 (PB 242 042)A03

EERC 74-12 "Site-Dependent Spectra for Earthquake-Resistant Design," by H.B. Seed, C. Ugas and J. Lysmer - 1974 (PB 240 953)A03

EERC 74-13 "Earthquake Simulator Study of a Reinforced Concrete Frame," by P. Hidalgo and R.W. Clough - 1974 (PB 241 944)A13

EERC 74-14 "Nonlinear Earthquake Response of Concrete Gravity Dams," by N. Pal - 1974 (AD/A 006 583)A06

EERC 74-15 "Modeling and Identification in Nonlinear Structural Dynamics - I. One Degree of Freedom Models," by N. Distefano and A. Rath - 1974 (PB 241 548)A06

EERC 75-1 "Determination of Seismic Design Criteria for the Dumbarton Bridge Replacement Structure, Vol. I: Description, Theory and Analytical Modeling of Bridge and Parameters," by F. Baron and S.-H. Pang - 1975 (PB 259 407)A15

EERC 75-2 "Determination of Seismic Design Criteria for the Dumbarton Bridge Replacement Structure, Vol. II: Numerical Studies and Establishment of Seismic Design Criteria," by F. Baron and S.-H. Pang - 1975 (PB 259 408)A11 (For set of EERC 75-1 and 75-2 (PB 259 406))

EERC 75-3 "Seismic Risk Analysis for a Site and a Metropolitan Area," by C.S. Oliveira - 1975 (PB 248 134)A09

EERC 75-4 "Analytical Investigations of Seismic Response of Short, Single or Multiple-Span Highway Bridges," by M.-C. Chen and J. Penzien - 1975 (PB 241 454)A09

EERC 75-5 "An Evaluation of Some Methods for Predicting Seismic Behavior of Reinforced Concrete Buildings," by S.A. Mahin and V.V. Bertero - 1975 (PB 246 306)A16

EERC 75-6 "Earthquake Simulator Study of a Steel Frame Structure, Vol. I: Experimental Results," by R.W. Clough and D.T. Tang - 1975 (PB 243 981)A13

EERC 75-7 "Dynamic Properties of San Bernardino Intake Tower," by D. Rea, C.-Y. Liaw and A.K. Chopra - 1975 (AD/A008 406) A05

EERC 75-8 "Seismic Studies of the Articulation for the Dumbarton Bridge Replacement Structure, Vol. I: Description, Theory and Analytical Modeling of Bridge Components," by F. Baron and R.E. Hamati - 1975 (PB 251 539)A07

EERC 75-9 "Seismic Studies of the Articulation for the Dumbarton Bridge Replacement Structure, Vol. 2: Numerical Studies of Steel and Concrete Girder Alternates," by F. Baron and R.E. Hamati - 1975 (PB 251 540)A10

EERC 75-10 "Static and Dynamic Analysis of Nonlinear Structures," by D.P. Mondkar and G.H. Powell - 1975 (PB 242 434)A08

EERC 75-11 "Hysteretic Behavior of Steel Columns," by E.P. Popov, V.V. Bertero and S. Chandramouli - 1975 (PB 252 365)A11

EERC 75-12 "Earthquake Engineering Research Center Library Printed Catalog," - 1975 (PB 243 711)A26

EERC 75-13 "Three Dimensional Analysis of Building Systems (Extended Version)," by E.L. Wilson, J.P. Hollings and H.H. Dovey - 1975 (PB 243 989)A07

EERC 75-14 "Determination of Soil Liquefaction Characteristics by Large-Scale Laboratory Tests," by P. De Alba, C.K. Chan and H.B. Seed - 1975 (NUREG 0027)A08

EERC 75-15 "A Literature Survey - Compressive, Tensile, Bond and Shear Strength of Masonry," by R.L. Mayes and R.W. Clough - 1975 (PB 246 292)A10

EERC 75-16 "Hysteretic Behavior of Ductile Moment Resisting Reinforced Concrete Frame Components," by V.V. Bertero and E.P. Popov - 1975 (PB 246 388)A05

EERC 75-17 "Relationships Between Maximum Acceleration, Maximum Velocity, Distance from Source, Local Site Conditions for Moderately Strong Earthquakes," by H.B. Seed, R. Murarka, J. Lysmer and I.M. Idriss - 1975 (PB 248 172)A03

EERC 75-18 "The Effects of Method of Sample Preparation on the Cyclic Stress-Strain Behavior of Sands," by J. Mulilis, C.K. Chan and H.B. Seed - 1975 (Summarized in EERC 75-28)

EERC 75-19 "The Seismic Behavior of Critical Regions of Reinforced Concrete Components as Influenced by Moment, Shear and Axial Force," by M.B. Atalay and J. Penzien - 1975 (PB 258 842)A11

EERC 75-20 "Dynamic Properties of an Eleven Story Masonry Building," by R.M. Stephen, J.P. Hollings, J.G. Bouwkamp and D. Jurukovski - 1975 (PB 246 945)A04

EERC 75-21 "State-of-the-Art in Seismic Strength of Masonry - An Evaluation and Review," by R.L. Mayes and R.W. Clough 1975 (PB 249 040)A07

EERC 75-22 "Frequency Dependent Stiffness Matrices for Viscoelastic Half-Plane Foundations," by A.K. Chopra, P. Chakrabarti and G. Dasgupta - 1975 (PB 248 121)A07

EERC 75-23 "Hysteretic Behavior of Reinforced Concrete Framed Walls," by T.Y. Wong, V.V. Bertero and E.P. Popov - 1975

EERC 75-24 "Testing Facility for Subassemblages of Frame-Wall Structural Systems," by V.V. Bertero, E.P. Popov and T. Endo - 1975

EERC 75-25 "Influence of Seismic History on the Liquefaction Characteristics of Sands," by H.B. Seed, K. Mori and C.K. Chan - 1975 (Summarized in EERC 75-28)

EERC 75-26 "The Generation and Dissipation of Pore Water Pressures during Soil Liquefaction," by H.B. Seed, P.P. Martin and J. Lysmer - 1975 (PB 252 648)A03

EERC 75-27 "Identification of Research Needs for Improving Aseismic Design of Building Structures," by V.V. Bertero 1975 (PB 248 136)A05

EERC 75-28 "Evaluation of Soil Liquefaction Potential during Earthquakes," by H.B. Seed, I. Arango and C.K. Chan - 1975 (NUREG 0026)A13

EERC 75-29 "Representation of Irregular Stress Time Histories by Equivalent Uniform Stress Series in Liquefaction Analyses," by H.B. Seed, I.M. Idriss, F. Makdisi and N. Banerjee - 1975 (PB 252 635)A03

EERC 75-30 "FLUSH - A Computer Program for Approximate 3-D Analysis of Soil-Structure Interaction Problems," by J. Lysmer, T. Udaka, C.-F. Tsai and H.B. Seed - 1975 (PB 259 332)A07

EERC 75-31 "ALUSH - A Computer Program for Seismic Response Analysis of Axisymmetric Soil-Structure Systems," by E. Berger, J. Lysmer and H.B. Seed - 1975

EERC 75-32 "TRIP and TRAVEL - Computer Programs for Soil-Structure Interaction Analysis with Horizontally Travelling Waves," by T. Udaka, J. Lysmer and H.B. Seed - 1975

EERC 75-33 "Predicting the Performance of Structures in Regions of High Seismicity," by J. Penzien - 1975 (PB 248 130)A

EERC 75-34 "Efficient Finite Element Analysis of Seismic Structure - Soil - Direction," by J. Lysmer, H.B. Seed, T. Udaka, R.N. Hwang and C.-F. Tsai - 1975 (PB 253 570)A03

EERC 75-35 "The Dynamic Behavior of a First Story Girder of a Three-Story Steel Frame Subjected to Earthquake Loading," by R.W. Clough and L.-Y. Li - 1975 (PB 248 841)A05

EERC 75-36 "Earthquake Simulator Study of a Steel Frame Structure, Volume II - Analytical Results," by D.T. Tang - 1975 (PB 252 926)A10

EERC 75-37 "ANSR-I General Purpose Computer Program for Analysis of Non-Linear Structural Response," by D.P. Mondkar and G.H. Powell - 1975 (PB 252 386)A08

EERC 75-38 "Nonlinear Response Spectra for Probabilistic Seismic Design and Damage Assessment of Reinforced Concrete Structures," by M. Murakami and J. Penzien - 1975 (PB 259 530)A05

EERC 75-39 "Study of a Method of Feasible Directions for Optimal Elastic Design of Frame Structures Subjected to Earthquake Loading," by N.D. Walker and K.S. Pister - 1975 (PB 257 781)A06

EERC 75-40 "An Alternative Representation of the Elastic-Viscoelastic Analogy," by G. Dasgupta and J.L. Sackman - 1975 (PB 252 173)A03

EERC 75-41 "Effect of Multi-Directional Shaking on Liquefaction of Sands," by H.B. Seed, R. Pyke and G.R. Martin - 1975 (PB 258 781)A03

EERC 76-1 "Strength and Ductility Evaluation of Existing Low-Rise Reinforced Concrete Buildings - Screening Method," T. Okada and B. Bresler - 1976 (PB 257 906)A11

EERC 76-2 "Experimental and Analytical Studies on the Hysteretic Behavior of Reinforced Concrete Rectangular and T-Beams," by S.-Y.M. Ma, E.P. Popov and V.V. Bertero - 1976 (PB 260 843)A12

EERC 76-3 "Dynamic Behavior of a Multistory Triangular-Shaped Building," by J. Petrovski, R.M. Stephen, E. Gartenbaum and J.G. Bouwkamp - 1976 (PB 273 279)A07

EERC 76-4 "Earthquake Induced Deformations of Earth Dams," by N. Serff, H.B. Seed, F.I. Makdisi & C.-Y. Chang - 1976 (PB 292 065)A08

EERC 76-5 "Analysis and Design of Tube-Type Tall Building Structures," by H. de Clercq and G.H. Powell - 1976 (PB 252 220) A10

EERC 76-6 "Time and Frequency Domain Analysis of Three-Dimensional Ground Motions, San Fernando Earthquake," by T. Kubo and J. Penzien (PB 260 556)A11

EERC 76-7 "Expected Performance of Uniform Building Code Design Masonry Structures," by R.L. Mayes, Y. Omote, S.W. Chen and R.W. Clough - 1976 (PB 270 098)A05

EERC 76-8 "Cyclic Shear Tests of Masonry Piers, Volume 1 - Test Results," by R.L. Mayes, Y. Omote, R.W. Clough - 1976 (PB 264 424)A06

EERC 76-9 "A Substructure Method for Earthquake Analysis of Structure - Soil Interaction," by J.A. Gutierrez and A.K. Chopra - 1976 (PB 257 783)A08

EERC 76-10 "Stabilization of Potentially Liquefiable Sand Deposits using Gravel Drain Systems," by H.B. Seed and J.R. Booker - 1976 (PB 258 820)A04

EERC 76-11 "Influence of Design and Analysis Assumptions on Computed Inelastic Response of Moderately Tall Frames," by G.H. Powell and D.G. Row - 1976 (PB 271 409)A06

EERC 76-12 "Sensitivity Analysis for Hysteretic Dynamic Systems: Theory and Applications," by D. Ray, K.S. Pister and E. Polak - 1976 (PB 262 859)A04

EERC 76-13 "Coupled Lateral Torsional Response of Buildings to Ground Shaking," by C.L. Kan and A.K. Chopra - 1976 (PB 257 907)A09

EERC 76-14 "Seismic Analyses of the Banco de America," by V.V. Bertero, S.A. Mahin and J.A. Hollings - 1976

EERC 76-15 "Reinforced Concrete Frame 2: Seismic Testing and Analytical Correlation," by R.W. Clough and J. Gidwani - 1976 (PB 261 323)A08

EERC 76-16 "Cyclic Shear Tests of Masonry Piers, Volume 2 - Analysis of Test Results," by R.L. Mayes, Y. Omote and R.W. Clough - 1976

EERC 76-17 "Structural Steel Bracing Systems: Behavior Under Cyclic Loading," by E.P. Popov, K. Takanashi and C.W. Roeder - 1976 (PB 260 715)A05

EERC 76-18 "Experimental Model Studies on Seismic Response of High Curved Overcrossings," by D. Williams and W.G. Godden - 1976 (PB 269 548)A08

EERC 76-19 "Effects of Non-Uniform Seismic Disturbances on the Dumbarton Bridge Replacement Structure," by F. Baron and R.E. Hamati - 1976 (PB 282 981)A16

EERC 76-20 "Investigation of the Inelastic Characteristics of a Single Story Steel Structure Using System Identification and Shaking Table Experiments," by V.C. Matzen and H.D. McNiven - 1976 (PB 258 453)A07

EERC 76-21 "Capacity of Columns with Splice Imperfections," by E.P. Popov, R.M. Stephen and R. Philbrick - 1976 (PB 260 378)A04

EERC 76-22 "Response of the Olive View Hospital Main Building during the San Fernando Earthquake," by S. A. Mahin, V.V. Bertero, A.K. Chopra and R. Collins - 1976 (PB 271 425)A14

EERC 76-23 "A Study on the Major Factors Influencing the Strength of Masonry Prisms," by N.M. Mostaghel, R.L. Mayes, R. W. Clough and S.W. Chen - 1976 (Not published)

EERC 76-24 "GADFLEA - A Computer Program for the Analysis of Pore Pressure Generation and Dissipation during Cyclic or Earthquake Loading," by J.R. Booker, M.S. Rahman and H.B. Seed - 1976 (PB 263 947)A04

EERC 76-25 "Seismic Safety Evaluation of a R/C School Building," by B. Bresler and J. Axley - 1976

EERC 76-26 "Correlative Investigations on Theoretical and Experimental Dynamic Behavior of a Model Bridge Structure," by K. Kawashima and J. Penzien - 1976 (PB 263 388)A11

EERC 76-27 "Earthquake Response of Coupled Shear Wall Buildings," by T. Srichatrapimuk - 1976 (PB 265 157)A07

EERC 76-28 "Tensile Capacity of Partial Penetration Welds," by E.P. Popov and R.M. Stephen - 1976 (PB 262 899)A03

EERC 76-29 "Analysis and Design of Numerical Integration Methods in Structural Dynamics," by H.M. Hilber - 1976 (PB 264 410)A06

EERC 76-30 "Contribution of a Floor System to the Dynamic Characteristics of Reinforced Concrete Buildings," by L.E. Malik and V.V. Bertero - 1976 (PB 272 247)A13

EERC 76-31 "The Effects of Seismic Disturbances on the Golden Gate Bridge," by F. Baron, M. Arikan and R.E. Hamati - 1976 (PB 272 279)A09

EERC 76-32 "Infilled Frames in Earthquake Resistant Construction," by R.E. Klingner and V.V. Bertero - 1976 (PB 265 892)A13

UCB/EERC-77/01 "PLUSH - A Computer Program for Probabilistic Finite Element Analysis of Seismic Soil-Structure Interaction," by M.P. Romo Organista, J. Lysmer and H.B. Seed - 1977

UCB/EERC-77/02 "Soil-Structure Interaction Effects at the Humboldt Bay Power Plant in the Ferndale Earthquake of June 7, 1975," by J.E. Valera, H.B. Seed, C.F. Tsai and J. Lysmer - 1977 (PB 265 795)A04

UCB/EERC-77/03 "Influence of Sample Disturbance on Sand Response to Cyclic Loading," by K. Mori, H.B. Seed and C.K. Chan - 1977 (PB 267 352)A04

UCB/EERC-77/04 "Seismological Studies of Strong Motion Records," by J. Shoja-Taheri - 1977 (PB 269 655)A10

UCB/EERC-77/05 "Testing Facility for Coupled-Shear Walls," by L. Li-Hyung, V.V. Bertero and E.P. Popov - 1977

UCB/EERC-77/06 "Developing Methodologies for Evaluating the Earthquake Safety of Existing Buildings," by No. 1 - B. Bresler; No. 2 - B. Bresler, T. Okada and D. Zisling; No. 3 - T. Okada and B. Bresler; No. 4 - V.V. Bertero and B. Bresler - 1977 (PB 267 354)A08

UCB/EERC-77/07 "A Literature Survey - Transverse Strength of Masonry Walls," by Y. Omote, R.L. Mayes, S.W. Chen and R.W. Clough - 1977 (PB 277 933)A07

UCB/EERC-77/08 "DRAIN-TABS: A Computer Program for Inelastic Earthquake Response of Three Dimensional Buildings," by R. Guendelman-Israel and G.H. Powell - 1977 (PB 270 693)A07

UCB/EERC-77/09 "SUBWALL: A Special Purpose Finite Element Computer Program for Practical Elastic Analysis and Design of Structural Walls with Substructure Option," by D.Q. Le, H. Peterson and E.P. Popov - 1977 (PB 270 567)A05

UCB/EERC-77/10 "Experimental Evaluation of Seismic Design Methods for Broad Cylindrical Tanks," by D.P. Clough (PB 272 280)A13

UCB/EERC-77/11 "Earthquake Engineering Research at Berkeley - 1976," - 1977 (PB 273 507)A09

UCB/EERC-77/12 "Automated Design of Earthquake Resistant Multistory Steel Building Frames," by N.D. Walker, Jr. - 1977 (PB 276 526)A09

UCB/EERC-77/13 "Concrete Confined by Rectangular Hoops Subjected to Axial Loads," by J. Vallenas, V.V. Bertero and E.P. Popov - 1977 (PB 275 165)A06

UCB/EERC-77/14 "Seismic Strain Induced in the Ground During Earthquakes," by Y. Sugimura - 1977 (PB 284 201)A04

UCB/EERC-77/15 "Bond Deterioration under Generalized Loading," by V.V. Bertero, E.P. Popov and S. Viwathanatepa - 1977

UCB/EERC-77/16 "Computer Aided Optimum Design of Ductile Reinforced Concrete Moment Resisting Frames," by S.W. Zagajeski and V.V. Bertero - 1977 (PB 280 137)A07

UCB/EERC-77/17 "Earthquake Simulation Testing of a Stepping Frame with Energy-Absorbing Devices," by J.M. Kelly and D.F. Tsztoo - 1977 (PB 273 506)A04

UCB/EERC-77/18 "Inelastic Behavior of Eccentrically Braced Steel Frames under Cyclic Loadings," by C.W. Roeder and E.P. Popov - 1977 (PB 275 526)A15

UCB/EERC-77/19 "A Simplified Procedure for Estimating Earthquake-Induced Deformations in Dams and Embankments," by F.I. Makdisi and H.B. Seed - 1977 (PB 276 820)A04

UCB/EERC-77/20 "The Performance of Earth Dams during Earthquakes," by H.B. Seed, F.I. Makdisi and P. de Alba - 1977 (PB 276 821)A04

UCB/EERC-77/21 "Dynamic Plastic Analysis Using Stress Resultant Finite Element Formulation," by P. Lukkunapvasit and J.M. Kelly - 1977 (PB 275 453)A04

UCB/EERC-77/22 "Preliminary Experimental Study of Seismic Uplift of a Steel Frame," by R.W. Clough and A.A. Huckelbridge 1977 (PB 278 769)A08

UCB/EERC-77/23 "Earthquake Simulator Tests of a Nine-Story Steel Frame with Columns Allowed to Uplift," by A.A. Huckelbridge - 1977 (PB 277 944)A09

UCB/EERC-77/24 "Nonlinear Soil-Structure Interaction of Skew Highway Bridges," by M.-C. Chen and J. Penzien - 1977 (PB 276 176)A07

UCB/EERC-77/25 "Seismic Analysis of an Offshore Structure Supported on Pile Foundations," by D.D.-N. Liou and J. Penzien 1977 (PB 283 180)A06

UCB/EERC-77/26 "Dynamic Stiffness Matrices for Homogeneous Viscoelastic Half-Planes," by G. Dasgupta and A.K. Chopra - 1977 (PB 279 654)A06

UCB/EERC-77/27 "A Practical Soft Story Earthquake Isolation System," by J.M. Kelly, J.M. Eidinger and C.J. Derham - 1977 (PB 276 814)A07

UCB/EERC-77/28 "Seismic Safety of Existing Buildings and Incentives for Hazard Mitigation in San Francisco: An Exploratory Study," by A.J. Meltsner - 1977 (PB 281 970)A05

UCB/EERC-77/29 "Dynamic Analysis of Electrohydraulic Shaking Tables," by D. Rea, S. Abedi-Hayati and Y. Takahashi 1977 (PB 282 569)A04

UCB/EERC-77/30 "An Approach for Improving Seismic - Resistant Behavior of Reinforced Concrete Interior Joints," by B. Galunic, V.V. Bertero and E.P. Popov - 1977 (PB 290 870)A06

UCB/EERC-78/01 "The Development of Energy-Absorbing Devices for Aseismic Base Isolation Systems," by J.M. Kelly and D.F. Tsztoo - 1978 (PB 284 978)A04

UCB/EERC-78/02 "Effect of Tensile Prestrain on the Cyclic Response of Structural Steel Connections, by J.G. Bouwkamp and A. Mukhopadhyay - 1978

UCB/EERC-78/03 "Experimental Results of an Earthquake Isolation System using Natural Rubber Bearings," by J.M. Eidinger and J.M. Kelly - 1978 (PB 281 686)A04

UCB/EERC-78/04 "Seismic Behavior of Tall Liquid Storage Tanks," by A. Niwa - 1978 (PB 284 017)A14

UCB/EERC-78/05 "Hysteretic Behavior of Reinforced Concrete Columns Subjected to High Axial and Cyclic Shear Forces," by S.W. Zagajeski, V.V. Bertero and J.G. Bouwkamp - 1978 (PB 283 858)A13

UCB/EERC-78/06 "Inelastic Beam-Column Elements for the ANSR-I Program," by A. Riahi, D.G. Row and G.H. Powell - 1978

UCB/EERC-78/07 "Studies of Structural Response to Earthquake Ground Motion," by O.A. Lopez and A.K. Chopra - 1978 (PB 282 790)A05

UCB/EERC-78/08 "A Laboratory Study of the Fluid-Structure Interaction of Submerged Tanks and Caissons in Earthquakes," by R.C. Byrd - 1978 (PB 284 957)A08

UCB/EERC-78/09 "Model for Evaluating Damageability of Structures," by I. Sakamoto and B. Bresler - 1978

UCB/EERC-78/10 "Seismic Performance of Nonstructural and Secondary Structural Elements," by I. Sakamoto - 1978

UCB/EERC-78/11 "Mathematical Modelling of Hysteresis Loops for Reinforced Concrete Columns," by S. Nakata, T. Sproul and J. Penzien - 1978

UCB/EERC-78/12 "Damageability in Existing Buildings," by T. Blejwas and B. Bresler - 1978

UCB/EERC-78/13 "Dynamic Behavior of a Pedestal Base Multistory Building," by R.M. Stephen, E.L. Wilson, J.G. Bouwkamp and M. Button - 1978 (PB 286 650)A08

UCB/EERC-78/14 "Seismic Response of Bridges - Case Studies," by R.A. Imbsen, V. Nutt and J. Penzien - 1978 (PB 286 503)A10

UCB/EERC-78/15 "A Substructure Technique for Nonlinear Static and Dynamic Analysis," by D.G. Row and G.H. Powell - 1978 (PB 288 077)A10

UCB/EERC-78/16 "Seismic Risk Studies for San Francisco and for the Greater San Francisco Bay Area," by C.S. Oliveira - 1978

UCB/EERC-78/17 "Strength of Timber Roof Connections Subjected to Cyclic Loads," by P. Gülkan, R.L. Mayes and R.W. Clough - 1978

UCB/EERC-78/18 "Response of K-Braced Steel Frame Models to Lateral Loads," by J.G. Bouwkamp, R.M. Stephen and E.P. Popov - 1978

UCB/EERC-78/19 "Rational Design Methods for Light Equipment in Structures Subjected to Ground Motion," by J.L. Sackman and J.M. Kelly - 1978 (PB 292 357)A04

UCB/EERC-78/20 "Testing of a Wind Restraint for Aseismic Base Isolation," by J.M. Kelly and D.E. Chitty - 1978 (PB 292 833)A03

UCB/EERC-78/21 "APOLLO - A Computer Program for the Analysis of Pore Pressure Generation and Dissipation in Horizontal Sand Layers During Cyclic or Earthquake Loading," by P.P. Martin and H.B. Seed - 1978 (PB 292 835)A04

UCB/EERC-78/22 "Optimal Design of an Earthquake Isolation System," by M.A. Bhatti, K.S. Pister and E. Polak - 1978 (PB 294 735)A06

UCB/EERC-78/23 "MASH - A Computer Program for the Non-Linear Analysis of Vertically Propagating Shear Waves in Horizontally Layered Deposits," by P.P. Martin and H.B. Seed - 1978 (PB 293 101)A05

UCB/EERC-78/24 "Investigation of the Elastic Characteristics of a Three Story Steel Frame Using System Identification," by I. Kaya and H.D. McNiven - 1978

UCB/EERC-78/25 "Investigation of the Nonlinear Characteristics of a Three-Story Steel Frame Using System Identification," by I. Kaya and H.D. McNiven - 1978

UCB/EERC-78/26 "Studies of Strong Ground Motion in Taiwan," by Y.M. Hsiung, B.A. Bolt and J. Penzien - 1978

UCB/EERC-78/27 "Cyclic Loading Tests of Masonry Single Piers: Volume 1 - Height to Width Ratio of 2," by P.A. Hidalgo, R.L. Mayes, H.D. McNiven and R.W. Clough - 1978

UCB/EERC-78/28 "Cyclic Loading Tests of Masonry Single Piers: Volume 2 - Height to Width Ratio of 1," by S.-W.J. Chen, P.A. Hidalgo, R.L. Mayes, R.W. Clough and H.D. McNiven - 1978

UCB/EERC-78/29 "Analytical Procedures in Soil Dynamics," by J. Lysmer - 1978

UCB/EERC-79/01 "Hysteretic Behavior of Lightweight Reinforced Concrete Beam-Column Subassemblages," by B. Forzani, E.P. Popov and V.V. Bertero - April 1979(PB 298 267)A06

UCB/EERC-79/02 "The Development of a Mathematical Model to Predict the Flexural Response of Reinforced Concrete Beams to Cyclic Loads, Using System Identification," by J. Stanton & H. McNiven - Jan. 1979(PB 295 875)A10

UCB/EERC-79/03 "Linear and Nonlinear Earthquake Response of Simple Torsionally Coupled Systems," by C.L. Kan and A.K. Chopra - Feb. 1979(PB 298 262)A06

UCB/EERC-79/04 "A Mathematical Model of Masonry for Predicting its Linear Seismic Response Characteristics," by Y. Mengi and H.D. McNiven - Feb. 1979(PB 298 266)A06

UCB/EERC-79/05 "Mechanical Behavior of Lightweight Concrete Confined by Different Types of Lateral Reinforcement," by M.A. Manrique, V.V. Bertero and E.P. Popov - May 1979(PB 301 114)A06

UCB/EERC-79/06 "Static Tilt Tests of a Tall Cylindrical Liquid Storage Tank," by R.W. Clough and A. Niwa - Feb. 1979 (PB 301 167)A06

UCB/EERC-79/07 "The Design of Steel Energy Absorbing Restrainers and Their Incorporation into Nuclear Power Plants for Enhanced Safety: Volume 1 - Summary Report," by P.N. Spencer, V.F. Zackay, and E.R. Parker - Feb. 1979(UCB/EERC-79/07)A09

UCB/EERC-79/08 "The Design of Steel Energy Absorbing Restrainers and Their Incorporation into Nuclear Power Plants for Enhanced Safety: Volume 2 - The Development of Analyses for Reactor System Piping,""Simple Systems" by M.C. Lee, J. Penzien, A.K. Chopra and K. Suzuki "Complex Systems" by G.H. Powell, E.L. Wilson, R.W. Clough and D.G. Row - Feb. 1979(UCB/EERC-79/08)A10

UCB/EERC-79/09 "The Design of Steel Energy Absorbing Restrainers and Their Incorporation into Nuclear Power Plants for Enhanced Safety: Volume 3 - Evaluation of Commercial Steels," by W.S. Owen, R.M.N. Pelloux, R.O. Ritchie, M. Faral, T. Ohhashi, J. Toplosky, S.J. Hartman, V.F. Zackay and E.R. Parker - Feb. 1979(UCB/EERC-79/09)A04

UCB/EERC-79/10 "The Design of Steel Energy Absorbing Restrainers and Their Incorporation into Nuclear Power Plants for Enhanced Safety: Volume 4 - A Review of Energy-Absorbing Devices," by J.M. Kelly and M.S. Skinner - Feb. 1979(UCB/EERC-79/10)A04

UCB/EERC-79/11 "Conservatism In Summation Rules for Closely Spaced Modes," by J.M. Kelly and J.L. Sackman - May 1979(PB 301 328)A03

UCB/EERC-79/12 "Cyclic Loading Tests of Masonry Single Piers: Volume 3 - Height to Width Ratio of 0.5," by P.A. Hidalgo, R.L. Mayes, H.D. McNiven and R.W. Clough - May 1979(PB 301 321)A08

UCB/EERC-79/13 "Cyclic Behavior of Dense Course-Grained Materials in Relation to the Seismic Stability of Dams," by N.G. Banerjee, H.B. Seed and C.K. Chan - June 1979(PB 301 373)A13

UCB/EERC-79/14 "Seismic Behavior of Reinforced Concrete Interior Beam-Column Subassemblages," by S. Viwathanatepa, E.P. Popov and V.V. Bertero - June 1979(PB 301 326)A10

UCB/EERC-79/15 "Optimal Design of Localized Nonlinear Systems with Dual Performance Criteria Under Earthquake Excitations," by M.A. Bhatti - July 1979(PB 80 167 109)A06

UCB/EERC-79/16 "OPTDYN - A General Purpose Optimization Program for Problems with or without Dynamic Constraints," by M.A. Bhatti, E. Polak and K.S. Pister - July 1979(PB 80 167 091)A05

UCB/EERC-79/17 "ANSR-II, Analysis of Nonlinear Structural Response, Users Manual," by D.P. Mondkar and G.H. Powell - July 1979(PB 80 113 301)A05

UCB/EERC-79/18 "Soil Structure Interaction in Different Seismic Environments," A. Gomez-Masso, J. Lysmer, J.-C. Chen and H.B. Seed - August 1979(PB 80 101 520)A04

UCB/EERC-79/19 "ARMA Models for Earthquake Ground Motions," by M.K. Chang, J.W. Kwiatkowski, R.F. Nau, R.M. Oliver and K.S. Pister - July 1979(PB 301 166)A05

UCB/EERC-79/20 "Hysteretic Behavior of Reinforced Concrete Structural Walls," by J.M. Vallenas, V.V. Bertero and E.P. Popov - August 1979(PB 80 165 905)A12

UCB/EERC-79/21 "Studies on High-Frequency Vibrations of Buildings - 1: The Column Effect," by J. Lubliner - August 1979 (PB 80 158 553)A03

UCB/EERC-79/22 "Effects of Generalized Loadings on Bond Reinforcing Bars Embedded in Confined Concrete Blocks," by S. Viwathanatepa, E.P. Popov and V.V. Bertero - August 1979

UCB/EERC-79/23 "Shaking Table Study of Single-Story Masonry Houses, Volume 1: Test Structures 1 and 2," by P. Gülkan, R.L. Mayes and R.W. Clough - Sept. 1979

UCB/EERC-79/24 "Shaking Table Study of Single-Story Masonry Houses, Volume 2: Test Structures 3 and 4," by P. Gülkan, R.L. Mayes and R.W. Clough - Sept. 1979

UCB/EERC-79/25 "Shaking Table Study of Single-Story Masonry Houses, Volume 3: Summary, Conclusions and Recommendations," by R.W. Clough, R.L. Mayes and P. Gülkan - Sept. 1979

UCB/EERC-79/26 "Recommendations for a U.S.-Japan Cooperative Research Program Utilizing Large-Scale Testing Facilities," by U.S.-Japan Planning Group - Sept. 1979(PB 301 407)A06

UCB/EERC-79/27 "Earthquake-Induced Liquefaction Near Lake Amatitlan, Guatemala," by H.B. Seed, I. Arango, C.K. Chan, A. Gomez-Masso and R. Grant de Ascoli - Sept. 1979(NUREG-CR1341)A03

UCB/EERC-79/28 "Infill Panels: Their Influence on Seismic Response of Buildings," by J.W. Axley and V.V. Bertero - Sept. 1979(PB 80 163 371)A10

UCB/EERC-79/29 "3D Truss Bar Element (Type 1) for the ANSR-II Program," by D.P. Mondkar and G.H. Powell - Nov. 1979 (PB 80 169 709)A02

UCB/EERC-79/30 "2D Beam-Column Element (Type 5 - Parallel Element Theory) for the ANSR-II Program," by D.G. Row, G.H. Powell and D.P. Mondkar - Dec. 1979(PB 80 167 224)A03

UCB/EERC-79/31 "3D Beam-Column Element (Type 2 - Parallel Element Theory) for the ANSR-II Program," by A. Riahi, G.H. Powell and D.P. Mondkar - Dec. 1979(PB 80 167 216)A03

UCB/EERC-79/32 "On Response of Structures to Stationary Excitation," by A. Der Kiureghian - Dec. 1979(PB 80166 929)A03

UCB/EERC-79/33 "Undisturbed Sampling and Cyclic Load Testing of Sands," by S. Singh, H.B. Seed and C.K. Chan - Dec. 1979(

UCB/EERC-79/34 "Interaction Effects of Simultaneous Torsional and Compressional Cyclic Loading of Sand," by P.M. Griffin and W.N. Houston - Dec. 1979

UCB/EERC-80/01 "Earthquake Response of Concrete Gravity Dams Including Hydrodynamic and Foundation Interaction Effects," by A.K. Chopra, P. Chakrabarti and S. Gupta - Jan. 1980(AD-A087297)A10

UCB/EERC-80/02 "Rocking Response of Rigid Blocks to Earthquakes," by C.S. Yim, A.K. Chopra and J. Penzien - Jan. 1980 (PB80 166 002)A04

UCB/EERC-80/03 "Optimum Inelastic Design of Seismic-Resistant Reinforced Concrete Frame Structures," by S.W. Zagajeski and V.V. Bertero - Jan. 1980(PB80 164 635)A06

UCB/EERC-80/04 "Effects of Amount and Arrangement of Wall-Panel Reinforcement on Hysteretic Behavior of Reinforced Concrete Walls," by R. Iliya and V.V. Bertero - Feb. 1980(PB81 122 525)A09

UCB/EERC-80/05 "Shaking Table Research on Concrete Dam Models," by A. Niwa and R.W. Clough - Sept. 1980(PB81 122 368)A06

UCB/EERC-80/06 "The Design of Steel Energy-Absorbing Restrainers and their Incorporation into Nuclear Power Plants for Enhanced Safety (Vol 1A): Piping with Energy Absorbing Restrainers: Parameter Study on Small Systems," by G.H. Powell, C. Oughourlian and J. Simons - June 1980

UCB/EERC-80/07 "Inelastic Torsional Response of Structures Subjected to Earthquake Ground Motions," by Y. Yamazaki April 1980(PB81 122 327)A08

UCB/EERC-80/08 "Study of X-Braced Steel Frame Structures Under Earthquake Simulation," by Y. Ghanaat - April 1980 (PB81 122 335)A11

UCB/EERC-80/09 "Hybrid Modelling of Soil-Structure Interaction," by S. Gupta, T.W. Lin, J. Penzien and C.S. Yeh May 1980(PB81 122 319)A07

UCB/EERC-80/10 "General Applicability of a Nonlinear Model of a One Story Steel Frame," by B.I. Sveinsson and H.D. McNiven - May 1980(PB81 124 877)A06

UCB/EERC-80/11 "A Green-Function Method for Wave Interaction with a Submerged Body," by W. Kioka - April 1980 (PB81 122 269)A07

UCB/EERC-80/12 "Hydrodynamic Pressure and Added Mass for Axisymmetric Bodies," by F. Nilrat - May 1980(PB81 122 343)A08

UCB/EERC-80/13 "Treatment of Non-Linear Drag Forces Acting on Offshore Platforms," by B.V. Dao and J. Penzien May 1980(PB81 153 413)A07

UCB/EERC-80/14 "2D Plane/Axisymmetric Solid Element (Type 3 - Elastic or Elastic-Perfectly Plastic) for the ANSR-II Program," by D.P. Mondkar and G.H. Powell - July 1980(PB81 122 350)A03

UCB/EERC-80/15 "A Response Spectrum Method for Random Vibrations," by A. Der Kiureghian - June 1980(PB81 122 301)A03

UCB/EERC-80/16 "Cyclic Inelastic Buckling of Tubular Steel Braces," by V.A. Zayas, E.P. Popov and S.A. Mahin June 1980(PB81 124 885)A10

UCB/EERC-80/17 "Dynamic Response of Simple Arch Dams Including Hydrodynamic Interaction," by C.S. Porter and A.K. Chopra - July 1980(PB81 124 000)A13

UCB/EERC-80/18 "Experimental Testing of a Friction Damped Aseismic Base Isolation System with Fail-Safe Characteristics," by J.M. Kelly, K.E. Beucke and M.S. Skinner - July 1980(PB81 148 595)A04

UCB/EERC-80/19 "The Design of Steel Energy-Absorbing Restrainers and their Incorporation into Nuclear Power Plants for Enhanced Safety (Vol 1B): Stochastic Seismic Analyses of Nuclear Power Plant Structures and Piping Systems Subjected to Multiple Support Excitations," by M.C. Lee and J. Penzien - June 1980

UCB/EERC-80/20 "The Design of Steel Energy-Absorbing Restrainers and their Incorporation into Nuclear Power Plants for Enhanced Safety (Vol 1C): Numerical Method for Dynamic Substructure Analysis," by J.M. Dickens and E.L. Wilson - June 1980

UCB/EERC-80/21 "The Design of Steel Energy-Absorbing Restrainers and their Incorporation into Nuclear Power Plants for Enhanced Safety (Vol 2): Development and Testing of Restraints for Nuclear Piping Systems," by J.M. Kelly and M.S. Skinner - June 1980

UCB/EERC-80/22 "3D Solid Element (Type 4-Elastic or Elastic-Perfectly-Plastic) for the ANSR-II Program," by D.P. Mondkar and G.H. Powell - July 1980(PB81 123 242)A03

UCB/EERC-80/23 "Gap-Friction Element (Type 5) for the ANSR-II Program," by D.P. Mondkar and G.H. Powell - July 1980 (PB81 122 285)A03

UCB/EERC-80/24 "U-Bar Restraint Element (Type 11) for the ANSR-II Program," by C. Oughourlian and G.H. Powell July 1980(PB81 122 293)A03

UCB/EERC-80/25 "Testing of a Natural Rubber Base Isolation System by an Explosively Simulated Earthquake," by J.M. Kelly - August 1980

UCB/EERC-80/26 "Input Identification from Structural Vibrational Response," by Y. Hu - August 1980(PB81 152 308)A05

UCB/EERC-80/27 "Cyclic Inelastic Behavior of Steel Offshore Structures," by V.A. Zayas, S.A. Mahin and E.P. Popov August 1980

UCB/EERC-80/28 "Shaking Table Testing of a Reinforced Concrete Frame with Biaxial Response," by M.G. Oliva October 1980(PB81 154 304)A10

UCB/EERC-80/29 "Dynamic Properties of a Twelve-Story Prefabricated Panel Building," by J.G. Bouwkamp, J.P. Kollegger and R.M. Stephen - October 1980

UCB/EERC-80/30 "Dynamic Properties of an Eight-Story Prefabricated Panel Building," by J.G. Bouwkamp, J.P. Kollegger and R.M. Stephen - October 1980

UCB/EERC-80/31 "Predictive Dynamic Response of Panel Type Structures Under Earthquakes," by J.P. Kollegger and J.G. Bouwkamp - October 1980(PB81 152 316)A04

UCB/EERC-80/32 "The Design of Steel Energy-Absorbing Restrainers and their Incorporation into Nuclear Power Plants for Enhanced Safety (Vol 3): Testing of Commercial Steels in Low-Cycle Torsional Fatigue," by P. Spencer, E.R. Parker, E. Jongewaard and M. Drory

UCB/EERC-80/33 "The Design of Steel Energy-Absorbing Restrainers and their Incorporation into Nuclear Power Plants for Enhanced Safety (Vol 4): Shaking Table Tests of Piping Systems with Energy-Absorbing Restrainers," by S.F. Stiemer and W.G. Godden - Sept. 1980

UCB/EERC-80/34 "The Design of Steel Energy-Absorbing Restrainers and their Incorporation into Nuclear Power Plants for Enhanced Safety (Vol 5): Summary Report," by P. Spencer

UCB/EERC-80/35 "Experimental Testing of an Energy-Absorbing Base Isolation System," by J.M. Kelly, M.S. Skinner and K.E. Beucke - October 1980(PB81 154 072)A04

UCB/EERC-80/36 "Simulating and Analyzing Artificial Non-Stationary Earthquake Ground Motions," by R.F. Nau, R.M. Oliver and K.S. Pister - October 1980(PB81 153 397)A04

UCB/EERC-80/37 "Earthquake Engineering at Berkeley - 1980," - Sept. 1980

UCB/EERC-80/38 "Inelastic Seismic Analysis of Large Panel Buildings," by V. Schricker and G.H. Powell - Sept. 1980 (PB81 154 338)A13

UCB/EERC-80/39 "Dynamic Response of Embankment, Concrete-Gravity and Arch Dams Including Hydrodynamic Interaction," by J.F. Hall and A.K. Chopra - October 1980(PB81 152 324)A11

UCB/EERC-80/40 "Inelastic Buckling of Steel Struts Under Cyclic Load Reversal," by R.G. Black, W.A. Wenger and E.P. Popov - October 1980(PB81 154 312)A08

UCB/EERC-80/41 "Influence of Site Characteristics on Building Damage During the October 3, 1974 Lima Earthquake," by P. Repetto, I. Arango and H.B. Seed - Sept. 1980(PB81 161 739)A05

UCB/EERC-80/42 "Evaluation of a Shaking Table Test Program on Response Behavior of a Two Story Reinforced Concrete Frame," by J.M. Blondet, R.W. Clough and S.A. Mahin

UCB/EERC-80/43 "Modelling of Soil-Structure Interaction by Finite and Infinite Elements," by F. Medina

UCB/EERC-81/01 "Control of Seismic Response of Piping Systems and Other Structures by Base Isolation," edited by J.M. Kelly - January 1981 (PB81 200 735)A05

UCB/EERC-81/02 "OPTNSR - An Interactive Software System for Optimal Design of Statically and Dynamically Loaded Structures with Nonlinear Response," by M.A. Bhatti, V. Ciampi and K.S. Pister - January 1981 (PB81 218 851)A09

UCB/EERC-81/03 "Analysis of Local Variations in Free Field Seismic Ground Motion," by J.-C. Chen, J. Lysmer and H.B. Seed - January 1981 (AD-A099508)A13

UCB/EERC-81/04 "Inelastic Structural Modeling of Braced Offshore Platforms for Seismic Loading," by V.A. Zayas, P.-S. B. Shing, S.A. Mahin and E.P. Popov - January 1981 (PB

UCB/EERC-81/05 "Dynamic Response of Light Equipment in Structures," by A. Der Kiureghian, J.L. Sackman and B. Nour-Omid - April 1981 (PB81 218 497)A04

UCB/EERC-81/06 "Preliminary Experimental Investigation of a Broad Base Liquid Storage Tank," by J.G. Bouwkamp, J.P. Kollegger and R.M. Stephen - May 1981

UCB/EERC-81/07 "The Seismic Resistant Design of Reinforced Concrete Coupled Structural Walls," by A.E. Aktan and V.V. Bertero - June 1981 (PB82 113 358)A11

UCB/EERC-81/08 "The Undrained Shearing Resistance of Cohesive Soils at Large Deformation," by M.R. Pyles and H.B. Seed - August 1981

UCB/EERC-81/09 "Experimental Behavior of a Spatial Piping System with Steel Energy Absorbers Subjected to a Simulated Differential Seismic Input," by S.F. Stiemer, W.G. Godden and J.M. Kelly - July 1981

UCB/EERC-81/10 "Evaluation of Seismic Design Provisions for Masonry in the United States," by B.I. Sveinsson, R.L. Mayes and H.D. McNiven - August 1981

UCB/EERC-81/11 "Two-Dimensional Hybrid Modelling of Soil-Structure Interaction," by T.-J Tzong, Sunil Gupta and J. Penzien - August 1981

UCB/EERC-81/12 "Studies on Effects of Infills in Seismic Resistant R/C Construction," by S. Brokken and V.V. Bertero - September 1981

UCB/EERC-81/13 "Linear Models to Predict the Nonlinear Seismic Behavior of a One-Story Steel Frame," by H. Valdimarsson, A.H. Shah and H.D. McNiven - September 1981

UCB/EERC-81/14 "TLUSH: A Computer Program for the Three-Dimensional Dynamic Analysis of Earth Dams," by T. Kagawa, L.H. Mejia, H.B. Seed and J. Lysmer - September 1981

UCB/EERC-81/15 "Three Dimensional Dynamic Response Analysis of Earth Dams," by L.H. Mejia and H.B. Seed - September 1981

UCB/EERC-81/16 "Experimental Study of Lead and Elastomeric Dampers for Base Isolation Systems," by J.M. Kelly and S.B. Hodder - October 1981

UCB/EERC-81/17 "The Influence of Base Isolation on the Seismic Response of Light Secondary Equipment," by J.M. Kelly - April 1981

UCB/EERC-81/18 "Studies on Evaluation of Shaking Table Response Analysis Procedures," by J. Marcial Blondet - November 1981